

DTIC FILE COPY

①

AGARD-CP436

AGARD-CP-436

# AGARD

ADVISORY GROUP FOR AEROSPACE RESEARCH & DEVELOPMENT

7 RUE ANCELLE 92000 NEUILLY SUR SEINE FRANCE

AD-A215 006

AGARD CONFERENCE PROCEEDINGS No.436

## Guidance and Control of Unmanned Air Vehicles

DTIC  
ELECTE  
NOV 22 1989  
S B D

NORTH ATLANTIC TREATY ORGANIZATION



DISTRIBUTION AND AVAILABILITY  
ON BACK COVER

**DISTRIBUTION STATEMENT A**

Approved for public release;  
Distribution Unlimited

89 11 17 003

AGARD-CP-436

NORTH ATLANTIC TREATY ORGANIZATION  
ADVISORY GROUP FOR AEROSPACE RESEARCH AND DEVELOPMENT  
(ORGANISATION DU TRAITE DE L'ATLANTIQUE NORD)

AGARD Conference Proceedings No.436  
GUIDANCE AND CONTROL OF UNMANNED AIR VEHICLES

Papers presented at the Guidance and Control Panel 47th Symposium held at the Letterman Army  
Institute of Research, Presidio of San Francisco, California, USA from 4 to 7 October 1988.

## THE MISSION OF AGARD

According to its Charter, the mission of AGARD is to bring together the leading personalities of the NATO nations in the fields of science and technology relating to aerospace for the following purposes:

- Recommending effective ways for the member nations to use their research and development capabilities for the common benefit of the NATO community;
- Providing scientific and technical advice and assistance to the Military Committee in the field of aerospace research and development (with particular regard to its military application);
- Continuously stimulating advances in the aerospace sciences relevant to strengthening the common defence posture;
- Improving the co-operation among member nations in aerospace research and development;
- Exchange of scientific and technical information;
- Providing assistance to member nations for the purpose of increasing their scientific and technical potential;
- Rendering scientific and technical assistance, as requested, to other NATO bodies and to member nations in connection with research and development problems in the aerospace field.

The highest authority within AGARD is the National Delegates Board consisting of officially appointed senior representatives from each member nation. The mission of AGARD is carried out through the Panels which are composed of experts appointed by the National Delegates, the Consultant and Exchange Programme and the Aerospace Applications Studies Programme. The results of AGARD work are reported to the member nations and the NATO Authorities through the AGARD series of publications of which this is one.

Participation in AGARD activities is by invitation only and is normally limited to citizens of the NATO nations.

The content of this publication has been reproduced directly from material supplied by AGARD or the authors.

Published August 1989

Copyright © AGARD 1989  
All Rights Reserved

ISBN 92-835-0523-9



Printed by Specialised Printing Services Limited  
40 Chigwell Lane, Loughton, Essex IG10 3TZ

## PREFACE

Unmanned Air Vehicles, which include RPVs and autonomous platforms have had a long history in the military field. Recent advances in guidance and control, in sensors and in data processing have led to an upsurge of interest in such systems within NATO. Several new RPVs are under development and there are numerous lessons that are being learned during the development and deployment of these systems.

This symposium intended to examine the state-of-the-art in the unmanned vehicle field covering both short range systems for tactical reconnaissance, target spotting and fire control and the long range systems carrying out surveillance tasks and autonomous platforms.

\* \* \*

Les véhicules non-pilotés, qui comprennent les engins télépilotes (RPV) et les plateformes autonomes, sont connus de longue date dans le domaine militaire. Les progrès réalisés récemment en guidage et pilotage dans le domaine des capteurs et du traitement des données sont à l'origine d'un regain d'intérêt pour de tels systèmes au sein de l'OTAN. Plusieurs engins non-pilotés d'une nouvelle génération sont en cours de développement et nombre d'enseignements sont tirés au travers des réalisations et des déploiements de ces systèmes.

Le but de ce Symposium était de faire le point sur l'état des connaissances dans ce domaine. Ainsi, le programme englobait à la fois les systèmes à courte portée pour la reconnaissance tactique, le repérage d'objectif et la conduite du tir, et les systèmes à longue portée utilisés pour la surveillance et les plateformes autonomes.



<b>Accession For</b>	
NTIS GRA&I	<input checked="" type="checkbox"/>
DTIC TAB	<input type="checkbox"/>
Unannounced	<input type="checkbox"/>
Justification	
By	
Distribution/	
Availability Codes	
Dist	Avail and/or Special
A-1	

#### **GUIDANCE AND CONTROL PANEL OFFICERS**

Chairman: Ir Pieter Ph. van den Broek  
Delft University of Technology  
Department of Aerospace Engineering  
Kluyverweg 1  
2629 HS Delft, The Netherlands

Deputy Chairman: Professor Edwin B. Stear  
Director  
Washington Technology Center  
University of Washington  
376 Loewe Hall — FH 10  
1013 NE 40th Street  
Seattle, WA 98195, USA

#### **TECHNICAL PROGRAMME COMMITTEE**

Chairmen:	Dr J. Niemela	US
	Prof. J. Shepherd	UK
Members	Mr J. B. Senneville	FR
	Dr H. Winter	GE
	Dr B. Mazzetti	IT
	Mr R. Dunn	UK
	Mr D. McIver	US
	Mr J. Ramage	US

#### **PANEL EXECUTIVE**

**From Europe:**  
Commandant M. Mouhamad, FAF  
Executive, GCP  
AGARD-OTAN  
7, rue Ancelle  
92200 Neuilly-sur-Seine, France  
Telephone: (1) 4738 5780 — Telex: 610176 F — Fax: (1) 4738 5799

**From USA and Canada only:**  
AGARD-NATO  
Attention: GCP  
APO New York 09777

#### **HOST PANEL COORDINATOR**

Mr James K. Ramage  
Chief, Advanced Development Branch  
Wright Research and Development Center (WRDS/FIGX)  
Wright Patterson AFB, OH 45433-6553, USA

#### **LOCAL COORDINATOR**

Major Robert V. Barnes  
HQ 6th Army  
AFKC — SGS  
Presidio of San Francisco  
San Francisco, CA 94129, USA

#### **ACKNOWLEDGEMENTS/REMERCIEMENTS**

The Panel wishes to express its thanks to the United States National Delegates to AGARD for the invitation to hold this meeting in their country and for the facilities and personnel which made the meeting possible.

Le Panel tient à remercier les Délégués Nationaux des Etats Unis près l'AGARD de leur invitation à tenir cette réunion dans leur pays et de la mise à disposition de personnel et des installations nécessaires.

## CONTENTS

	Page
PREFACE	iii
PANEL OFFICERS AND PROGRAMME COMMITTEE	iv
	Reference
KEYNOTE ADDRESS by W.C.Bowes	K
<b><u>SESSION I: OPERATIONAL CONCEPTS</u></b> Chairman: Dr J.Niemela (US)	
UNMANNED AIRCRAFT APPLICATIONS: A SUMMARY OF FINDINGS FROM AGARD AEROSPACE APPLICATIONS STUDIES by K.Rumer	11*
OPERATIONAL REQUIREMENTS FOR UNMANNED COMBAT AIRCRAFT by C.H.Hansford	12†
<b><u>SESSION II: REQUIREMENTS AND SYSTEMS</u></b> Chairman: Dr H.Winter (GE)	
OPERATIONAL REQUIREMENTS FOR MULTIPAYLOAD UAV MISSIONS IN SUPPORT OF ENEMY CRITICAL C <sup>3</sup> NODE INTERDICTION OBJECTIVES by M.I.Martin	21
TARGET ACQUISITION IN THE UAV ENVIRONMENT by R.Denaro, R.Kalafus and P.Ciganer	22
COMPARAISON DES TECHNIQUES D'AUTOGUIDAGE ET DE TELEGUIDAGE DES AERONEFS SANS PILOTES COMPARISON BETWEEN SELF AND REMOTE GUIDANCE FOR UNMANNED AIRCRAFT par B.Chaillot	23*
THE PHOENIX REAL TIME BATTLEFIELD SURVEILLANCE SYSTEM by R.W.Dennis and P.T.Jones	24*
ACCURATE DETERMINATION OF TARGET LOCATIONS USING UNMANNED AIR VEHICLES by D.W.Stroud	25
<b><u>SESSION III: VEHICLE GUIDANCE AND CONTROL</u></b> Chairman: Mr J.B.Senneville (FR)	
SYNTHESIS OF CONTROL LAW, ON A RPV, IN ORDER TO MINIMIZE THE NUMBER OF SENSORS by J.L.Boiffier	31
MIRACH 100 FLIGHT CONTROL SYSTEM by A.Sbuelz	32
SUIVI DE LA NAVIGATION DE RPV A L'AIDE DU SYSTEME DE RADIOLOCALISATION TRIDENT IV GROUND CONTROL STATION FOR NAVIGATION OF RECONNAISSANCE RPVs WITH TRIDENT IV RADIOLOCATION SYSTEM par M.Redoutey et D.Dumas	33*

---

\* Printed in classified publication CP436 (Supplement)  
 † Not available at time of printing.

	Reference
NAVIGATION OF AUTONOMOUS AIR VEHICLES BY PASSIVE IMAGING SENSORS by H.Zinner, R.Schmidt and D.Wolf	34
RECALAGE DE NAVIGATION PAR CARTOGRAPHIE RADAR: OPTIMISATION ET VALIDATION PAR OUTIL DE SIMULATION NAVIGATION UP-DATE USING RADAR MAPPING: ASSESSMENT AND OPTIMISATION SIMULATION TOOL par J.P.Guyvarch	35
 <u>SESSION IV: OPTICAL SYSTEMS</u> Chairman: Mr C.W.Bright (CA)	
GUIDANCE AND CONTROL OF ATTACK DRONES by M.Winstone	41†
BEACON NAVIGATION by C.Fry	42†
ELECTRO-OPTIC SENSORS FOR SURVEILLANCE AND TARGET ACQUISITION by J.W.Jack and A.Houston	43
UNMANNED AIR VEHICLES PAYLOADS AND SENSORS by G.S.Amick	44
AUTOMATED SEARCH TECHNIQUES APPLIED TO OPTICAL PAYLOADS IN UNMANNED AIR VEHICLES by R.L.Moody and J.L.Thompson	45
 <u>SESSION V: SYSTEMS EXTERNAL TO THE VEHICLE</u> Chairman: Mr S.Leek (UK)	
PROTECTION DES LIAISONS DE DONNEES DES SYSTEMES RPV FACE AU CONTRE- MESURES ELECTRONIQUES RPVS DATA LINKS PROTECTION AGAINST ELECTRONIC COUNTER-MEASURES par C.Olivier et M.Staron	51*
DIGITAL MAP DISPLAY FOR FLIGHT PLANNING, CONTROL AND TARGET POSITION DETERMINATION by W.Hornfeld	52*
AN INTELLIGENCE-DRIVEN RPV MISSION PLANNER by K.D.Dannenberg, G.M.Barney and C.R.Kirklen	53
ASSESSMENT OF SPOT SATELLITE IMAGERY AS A DATABASE FOR SCENE MATCHING by W.D.McGinn	54*
DISTRIBUTION OF HARDWARE AND SOFTWARE ELEMENTS IN UNMANNED AIR VEHICLE SYSTEMS by L.D.Sauvain	55
 <u>SESSION VI: EVALUATION AND TEST</u> Chairman: Professor J.T.Shepherd (UK)	
TECHNOLOGY AND EVALUATION OF UNMANNED AIR VEHICLES by G.R.Seyfang	61
NAVIGATION AND GUIDANCE TESTING OF THE LOCKHEED/U.S. ARMY AQUILA REMOTELY PILOTED VEHICLE by S.L.Ferguson	62

---

\* Printed in classified publication CP436 (Supplement).  
† Not available at time of printing.

KEYNOTE ADDRESS BY  
 RADM W.C. BONES  
 DIRECTOR, UNMANNED AERIAL VEHICLES JOINT PROJECT  
 NAVAL AIR SYSTEMS COMMAND  
 WASHINGTON, DC 20361-1014

Thank you for inviting me to present the keynote address at the 47th Symposium of the Guidance and Control Panel. It is a particular pleasure to speak this year since the theme of the symposium deals with the renewed interest in unmanned aerial vehicle (UAV) systems as well as with advances and new developments in these systems.

I can confidently state to you today that the requirement for unmanned aerial vehicles in all four of the U.S. Services is solid, and the enthusiasm for the capabilities provided by UAV's is increasing every day. The significant contribution that unmanned systems can make by keeping manned aircraft out of harm's way in a combat environment while providing real or near-real-time data required for battle management decisions is leading to a new era for unmanned aerial vehicles.

UAV's are certainly not a new capability, although their road to acceptance and continued use by the U.S. Services has not been a smooth one. The era of unmanned aerial vehicles was born in the United States soon after the Wright brothers conducted their first manned flight at Kitty Hawk in 1903. In 1917, Glen Curtis and Lawrence Sperry built and successfully tested, a modified Curtis biplane for use as an unmanned aerial torpedo. Concurrent with this Navy development, the Army decided to build the Kettering Bug—a biplane aircraft to deliver a bomb. However, with the end of World War I, and subsequently the economic depression of the 1930s, the era of unmanned aerial vehicle development ended in the United States. This was the first of many stops and starts in UAV system usage.

As a result of World War II, the United States re-entered the unmanned system arena by requiring large numbers of target drones for Navy and Army gunnery practice. In addition, B-17 and B-24 bomber aircraft were modified for remote-control bombing missions (after a pilot had bailed out) to target areas in Europe.

Following World War II, UAV efforts in the United States centered on converting manned aircraft into target drones. With the start of the Korean conflict, standard aircraft were modified to carry explosives by remote control to a chosen target. But the efforts never obtained a strong hold in all of the U.S. Services.

In the 1960s, the role of unmanned aerial vehicle systems changed dramatically. The loss of U-2 reconnaissance aircraft over the Soviet Union and Cuba added the reconnaissance role to the UAV mission set, but the requirement did not stimulate extensive UAV usage.

Once again conflict stimulated the U.S. need for UAV's. The escalation of the Vietnam War required the operational and mission capabilities provided by reconnaissance drones. The need for this capability was readily apparent, and more than 3400 drone missions were flown in Vietnam using many versions of the Firebee built by the Ryan Aeronautical Company.

The UAV missions conducted over Vietnam demonstrated the capability that drones had when operating in a sophisticated, high threat, surface-to-air missile environment that would have placed manned aircraft in high risk conditions. Unfortunately, at the conclusion of the Vietnam conflict the drones were mothballed, and another era ended for unmanned aerial vehicles.

The importance of integrating unmanned aerial vehicles within the battleforce structure was very effectively demonstrated by Israel. In 1973, the Israeli Air Force successfully used unmanned aerial vehicles as decoys to draw Egyptian surface-to-air missile fire in addition to being used for reconnaissance, electronic jamming and target location/weapon delivery missions.

The lessons learned from using UAV's in the 1973 Arab-Israeli War and the June 1982 Israeli use of Scout and Mastiff UAV's in the Bekaa Valley were the impetus for the United States' renewed strong focus on UAV's.

The U.S. Navy has procured Pioneer UAV systems which are now operationally deployed with U.S. Marine Corps units and recently completed a very successful deployment onboard the battleship USS Iowa. The U.S. Army is a very strong advocate for the use of UAV's and is continuing the use of the Aquila systems that have been procured while the U.S. Army anxiously awaits the procurement of the first DOD common UAV system.

The U.S. military services are starting to integrate unmanned systems into their force structure and operational thinking. A new era for unmanned aerial systems is starting. However, for this new era to survive, a concentrated effort must be made to obtain the correct capability that is affordable, reliable, effective, and supportable. The UAV community has a golden opportunity to remain a vital and integral part of our operating forces - but we must deliver what we promise. With that as an introduction let me tell you what the U.S. DOD UAV Joint Project is doing to meet the requirements of the U.S. Services, meet the demands of our Congress, eliminate independent Service UAV Programs, and centrally manage and procure common DOD UAV Systems.

As the Director, Unmanned Aerial Vehicle Joint Project I will share with you the goals and objectives of the Joint Service Project. I will describe how the Services will use UAVs, the systems we will have, our development and procurement strategy, and how we intend to successfully provide and deploy systems to the various Services. In addition, I will describe how recent activities conducted

by the Services with UAVs will interface with the Joint Project. When I have finished, I hope that you will see that the UAV Joint Project is committed to the challenge of providing UAV's that are affordable, effective, suitable, and supportable for use in defended and hostile threat environments.

First, I would like to set the background for establishing the Joint Service Project. The Congress of the United States in the Fiscal Year 1988 Appropriations Act eliminated independent Service UAV Programs and directed the Secretary of Defense to consolidate all programs under centralized management. The Congress also directed that a Master Plan be established for UAVs that would integrate Service needs and requirements as well as eliminate duplication of efforts. In addition, the procurement of a Non-developmental-Item (NDI) short range UAV system to meet multi-service requirements as well as the procurement of four additional Navy Pioneer systems necessary for continued Service evaluation, training or for use in contingency operations was directed.

The DOD UAV Master Plan describes systems required to support Service needs. These systems will consist of air vehicles, payloads, launch and recovery capability, data links, and ground control/mission planning/data exploitation stations. The systems will be developed by utilizing modular building blocks while maintaining maximum commonality between systems and subsystems commensurate with requirements of the Services. The use of modular building blocks provides a cost-effective approach for implementing new changes in a system as block up-grades as new technology and development items evolve.

The Joint Project goal is to provide the battle force commander at all command levels unmanned aerial vehicles that will effectively support reconnaissance and surveillance, target acquisition and spotting, command and control, meteorological data collection, NBC detection, and disruption and deception missions. In order to provide systems that can provide the aforementioned capabilities, Service requirements were harmonized and reconciled among the areas of air vehicle characteristics, payloads, ground stations, launch and recovery, and data link characteristics.

The process of defining Service operational needs and the reconciliation of requirements has defined four categories of unmanned aerial vehicles. The categories evolved during a process to define operational and mission capabilities necessary by the battleforce commander. These categories are close range, short range, medium range and endurance. The radius of action for each category (relative to the Forward Line of the Troops (FLOT)) is approximately 30 Km for close, 150 Km (300 km desired) for short and 700 Km for medium. Endurance requirements are not tied directly to a range limitation but are categorized as having longer flight time requirements than any of the other categories.

The close range UAV system will satisfy lower echelon tactical unit and small surface ship operational requirements. This system will be deployed in large numbers and must be affordable since it will probably be utilized for local area operations that contain heavy enemy activity and the possibility of heavy vehicle losses. The system must be fairly simple and provide capability to the user with a minimum of training. It must be launched, recovered, and operated with a minimum impact on organic assets available to the deployed units. The Sprite, Raven, and AROD are examples of close range UAV systems.

The short range UAV will support a variety of missions for the Service and will provide extended range surveillance capability (150 Km) from the FLOT or a reference point such as a ship. If possible this UAV will have the capability to support Army Corps Operations out to a range of 300 Km. This vehicle will conduct missions at low altitudes and transmit data to a ground control station within line of site or via an airborne or other relay if the vehicle is below the horizon. The vehicles utilized in the short range system may be configured to carry mission specific payloads or have unique survivability characteristics; however, maximum commonality will be maintained for mission planning and control, data exploitation and processing, data links and relay, as well as launch and recovery technique.

The medium range UAV will complement manned strike aircraft when operating in a hostile environment. The system will provide near-real time reconnaissance data necessary for pre-strike and post-strike planning. The UAV will be a high subsonic vehicle, have moderate to high resolution imagery capability, be preprogrammed and have navigational accuracies required to support survivable tactical operations and targeting for weapon delivery. The vehicle will be ground or air launched and will have a radius of action from the launch point to 700 Km. The medium range system will utilize mission planning and control, and data link standards established for the short range system. However, the Advanced Tactical Air Reconnaissance System will be integrated into the vehicle, and the system will have the capability for interface with the Joint Service Imagery Processing System.

The endurance UAV will generally operate within 300 Km of the FLOT or reference point and have the capability for extended flight time periods up to 36 hours and at altitudes above 20,000 feet. The system will provide a capability for wide area surveillance with a single or dual sensors, i.e. imagery, radio relay, and SIGINT. The system will have launch and recovery capabilities for at-sea or land operations and will be interoperable with the mission planning/control/data exploitation system of the short range system.

A critical part of the aforementioned systems is integrated logistics support and adequate training. These areas will be considered early in the system evolution process to ensure that the service user is adequately trained with a system that is fully supportable when deployed.

Commonality between unmanned aerial vehicle systems will be emphasized in the high cost areas of mission planning, command and control, data exploitation, payload packages, training, and logistics support. Any specific subsystems that require unique operational or environmental constraints such as airframes or unique launch and recovery techniques will be developed by assessing the impact on commonality and affordability.

The Joint Project objective, as stated earlier, is to provide the user an affordable and effective family of UAV systems. Initially we will consider the best systems and subsystems available with off-the-shelf technology and utilize all the lessons learned from existing UAV systems. This approach will define the system(s) required to meet harmonized service requirements.

A major near-term activity of the program is to provide an off-the-shelf DoD Short Range RPV system that will be affordable and meet Service requirements. A competition will be conducted in FY 89 and two contractors will be selected to each deliver 2 systems within 12 months after contract award. The systems selected will be evaluated concurrently by development and operational activities. These activities will evaluate system performance and capabilities as well as assess system strengths and weaknesses under operational conditions. After the evaluation there will be a down select to one contractor for follow-on production.

In parallel with the plans to procure the DoD Short Range System, a series of demonstrations are planned to support the requirement definition of the close and endurance UAV.

A NATO Special Working Group, under US Navy leadership, is investigating the use of UAVs for small ships. Under this effort NATO asked industry to participate in studies and demonstrations to define a UAV system capable of operating from small NATO ships. The coordinated efforts of industry and the NATO working group were able to establish and develop UAV characteristics, mission requirements and capabilities, cost-performance trade-offs, and vehicle platform interfaces as well as initiating a demonstration program to launch and recover UAVs on small ships. System supportability and affordability guidelines governed the groups' efforts. As a complement to the NATO trade-off studies, a series of demonstrations are scheduled this fall with three different V/STOL UAV systems. The demonstrations are scheduled with the United Kingdom (Sea Sprite, ML Aviation), Canada (CL-227, Canadair and Texas Instruments) and the United States (Pointer, Bell-Boeing). The UAV systems and technologies demonstrated in the NATO program as well as complementary demonstrations of similar systems by the Foreign Weapons Evaluation (FWE) Program will provide insight for using this class of vehicle for the close/short UAV system requirement.

The concept and configuration of an endurance UAV system are being developed through the AMBER program. This program was a joint DARPA, ARMY, Marine Corps, and Navy Program. However, the program transitioned to the Navy for military utility after DARPA demonstrated the flight capability and concept of the AMBER vehicle. The AMBER vehicle is a multi-payload vehicle that uses state-of-the-art aerodynamics and engine technology. The Navy is concentrating on verification of flight and engine performance as well as integrating various payloads for evaluation. To assist in evaluating military utility of an endurance system, maximum commonality is being maintained between the payloads and ground control station used with the Navy Pioneer System. Flight testing of AMBER with the Pioneer system will be used to verify flight capability, reliability and operational performance necessary for an endurance vehicle. To date we have demonstrated endurance greater than 38 hours and altitudes greater than 27,000 feet.

The Medium Range UAV being developed under the Joint Project will support Navy, Marine Corps and Air Force requirements and will provide near-real time tactical reconnaissance in hostile environments. The vehicle will have a combat radius in excess of 300 nautical miles and moderate to high subsonic speeds. The system will have navigational accuracies required to support survivable tactical operations as well as targeting accuracy for weapon delivery. The Medium Range vehicle developed will support target drone as well as reconnaissance requirements; therefore the air vehicle will be developed with a common aft end (truck) and one of several mission related payload noses. Contractors will conduct the required trade-offs to optimize the operational effectiveness/performance and cost-effectiveness of the system. Commonality and interoperability with the DOD family of UAV systems will be achieved in the particular areas of data link and mission planning and control. Proposals have been received from industry and are presently being evaluated for a competitive full scale engineering effort. Contract award is anticipated for December of this year. The evolution of the DOD family of vehicles will use the lessons learned by the Navy PIONEER system deployed at-sea aboard the Battleship IOWA and with various Marine Corps RPV Companies. In addition, the extensive testing conducted by the Army during the development and the ongoing operation of the Aquila System will augment the lessons learned.

The key to successful use and acceptance of the Navy and Marine Corps Pioneer UAV system was the rapid acquisition and fielding of fully supportable systems under operational conditions. Baseline PIONEER systems were provided concurrently to Navy test and operational activities to evaluate system performance, capabilities and weaknesses; and to fleet users to develop expertise in UAV's while developing operational concepts and tactics. This approach provided an assessment of the system as well as a sufficient quantity of systems to support operational contingencies.

While deployed with operational units the PIONEER system was assessed for its effectiveness and suitability while conducting operational scenarios. Subsequently, the user(s) agreed that short range systems with PIONEER capability, and the PIONEER in particular, are potentially effective and suitable. In addition, as a result of the operational deployment, each user recommended changes to the PIONEER system to enhance effectiveness and suitability. A similar approach will be used for the initial DoD family of UAV systems.

The process of defining UAV systems that can meet mission and affordability criteria requires inputs from a variety of sources. To assist in defining Service UAV systems, the Joint Project Office is coordinating the efforts of a Joint Service Working Group composed of system developer and user personnel. This group develops UAV system concepts, defines system configuration requirements, and assesses force level requirements based upon operational and mission scenarios matrixed with force structure. The JSWG is serving as a vital link between DOD's operational requirements development process and the UAV Joint Project's acquisition process.

In addition to the Joint Service Working Group, the Association for Unmanned Vehicle Systems (AUVS) has established an Industry Support Group (ISG). The ISG will serve as a forum for ensuring that the Joint Project is fully aware of the UAV capabilities that are available from industry to meet the near term DOD UAV joint requirements. Seven committees have been formed to consolidate industry's inputs. These committees cover Mission Definition, Test and Evaluation, System Integration, Mission Planning Control Station, Launch and Recovery, Logistics and Supportability, and Air Vehicle Integration. All are composed of and chaired by industry representatives.

While the family of DoD systems is evolving, PIONEER systems and Aquila systems presently in the service inventory will be used to continue additional evaluations of the effectiveness and suitability of subsystems and components while continuing training, tactics development, and operational support for any potential contingencies.

While existing systems are being used to define and assess the configuration requirements of the family of DoD UAV systems, parallel research and development efforts will evolve new technologies and concepts for UAV platforms, mission planning and control including airborne control of UAVs, engines, data relay capability, sensor packages, launch and recovery methods, and data exploitation and processing techniques. The planned development efforts will solve near-term requirements, such as a heavy fuel engine for shipboard application, and will also provide inputs for potential system block upgrades required to improve system capabilities as technology matures.

The Joint Service Project is faced with many technical and operational challenges. The challenges reflect the multi-mission role of the services---from the at-sea mission to the land-based mission.

Service payloads must be cost-effective and designed within the weight, volume, and power constraints of unmanned vehicles. Technology advances must have improved sensor payload capability for day TV, LLTV, IR scanners, FLIR, and laser designators as well as electronic countermeasure payloads. New sensor miniaturization can provide specialized packages for SIGINT, SAR, bistatic and millimeter wave radars. Advanced navigation and data link payloads can provide wideband secure anti-jam capability as well as accurate platform localization, stabilization, and command and control.

Sensor payload, navigation, and data link advances must include capabilities for all-weather operating conditions.

The development of unmanned aerial vehicle systems must consider multi-service use, attempt to maximize commonality and strive to develop standard interfaces. System engineering and integration efforts must consider common mission planning/data exploitation and control systems for the various categories of vehicles described.

Concurrent with the development of the unmanned systems, logistics and supportability must be major drivers for system definition. UAV systems must consider deployment requirements, training, and common logistics elements for affordable support.

The UAV Joint Project Office, the Services, and Industry must work together to solve the challenges that will provide our forces with unmanned aerial vehicle systems that are affordable, effective, reliable, and supportable.

You, the experts in UAV guidance and control are at a major crossroad for UAV utilization by the U.S. DOD. The challenge is yours to design, develop, produce, and then support the payloads, data links, navigation systems, and ground control stations that are the essence of every UAV system. The challenge is yours - I promise you the support of the DOD UAV Joint Project Office in utilizing the fruits of your efforts.

## OPERATIONAL REQUIREMENTS FOR MULTIPAYLOAD UAV MISSIONS IN SUPPORT OF ENEMY CRITICAL C<sup>3</sup> NODE INTERDICTION OBJECTIVES

MARVIN L. MARTIN

Command Systems Group, Inc.  
23430 Hawthorne Blvd., Suite 150  
Torrance, California 90505  
(213) 373-9819

The AirLand Battle doctrine requires commanders to fight in an extended battlefield, to see deep and to fight deep by identifying and interdicting critical C<sup>3</sup> nodes. Critical node interdiction provides combat power multipliers that offset enemy numerical superiority, thereby enabling commanders to fight outnumbered and win. An operational concept is outlined, providing for the interworking of a family of UAV payloads—SIGINT, SAR and FLIR—in support of a critical node interdiction campaign. Quantitative example shows that the skillful interworking of multiple UAVs equipped with diverse sensor payloads produces the desired combat power multiplier effect, promotes survivability; effectively deals with relocatable targets, and is extraordinarily productive in terms of the number of targets identified and precisely geolocated, without recourse to high-resolution imagery. The skillful interworking of UAV missions requires: 1) the introduction of UAVs in "decisive" numbers, and 2) an innovative, well thought-out concept to integrate multipayload/multi-UAV mission planning and sensor product exploitation into a closed-loop system that emphasizes sensor report fusion and cued payload operations.

### 1. INTRODUCTION

Tactical commanders have always had a basic need to understand as accurately as their enemy's intent, be aware of his most likely and available courses of action and, as accurately as possible, know the strength and disposition of his forces. In early times, this could be achieved only by controlling the high ground or by infiltrating enemy positions. In more recent times, the use of manned aerial platforms has helped to serve this need.

With the emergence of highly sophisticated surface-to-air missile (SAM) air defense systems and their integration with ground controlled intercept (GCI) air-to-air systems, the use of manned airborne platforms for either intelligence collection or for target location and designation has been sharply curtailed, or forced into stand-off type operations. Simultaneously, Air-Land Battle tactics have: 1) increased the need for reconnaissance operations in an extended battlefield, and 2) set forth a requirement for targeting critical nodes in the full tactical depth of enemy forces. The Air-Land Battle doctrine, on one hand, requires that commanders see deep to anticipate the enemy in concentrating force, and thereby facilitate dynamic defense tactics. On the other hand, the Air-Land Battle emphasizes deep interdiction to: 1) disrupt the timing, coordination, and combat readiness with which the enemy commits follow-on forces, and 2) destroy critical C<sup>3</sup> nodes, thereby gaining a combat power multiplier needed to offset enemy numerical advantages in manpower and weapons. Obviously, the need for deep reconnaissance is increasing, and doing so at a time when manned aircraft are forced to operate from disadvantageous stand-off orbits.

With the advent of micro-processor controlled, miniaturized digital electronic systems and the growth in advanced composite structures technology, the feasibility of unmanned airborne systems having good survivability potential, payload flexibility, and navigational accuracy has been established. This UAV technology has been available for several decades. However, for the past 15 years in both the U.S. and abroad, the UAV systems that have been taken through a demonstration phase have not achieved full production and force integration status within NATO. The results of demonstrations to date confirm that the ability to effect productive reconnaissance and targeting through the use of UAVs is not limited by the lack of hardware or technology nearly as much as by the lack of military/operational experience and a lack of understanding of how to use the asset.

It is recognized in the U.S. and elsewhere that the key to productive UAV operations lies in cued, multipayload operations. The focus of this paper is the family of payloads that are in consonance with the presently conceived objective UAV program, and how the capability of this objective system can be best integrated in the interest of target productivity and survivability in a dense air defense environment. Emphasis is placed on the critical C<sup>3</sup> node interdiction mission in the tactical, as opposed to the operational, depth of enemy forces. The material is organized into three related discussions:

- Mission Analysis and Requirements, illustrating the target acquisition and interdiction requirements for a counterfire C<sup>3</sup> node interdiction mission. The mission requirement relates the available combat power multiplier to the rate at which critical nodes are destroyed within an operationally critical time window. This requirement is then related to force structure in terms of: 1) the number of UAVs that can be simultaneously employed to support critical node interdiction, and 2) the efficiency of the combined arms and C<sup>3</sup> concepts that integrate the UAV with fire support means in order to destroy identified critical C<sup>3</sup> nodes.
- Family of Payloads Operational Concept for interworking: 1) SIGINT sensors, capable of coarsely geolocating enemy radioelectronic emitters, 2) active imaging (SAR) sensors, with wide-area surveillance, change detection, and precision target geolocation capability, and 3) FLIR sensors that acquire and identify ground order-of-battle objects that are normally discovered by SIGINT and wide-area surveillance means.
- Family of Payloads Employment Concept, including: 1) need for mini-UAVs with single payloads as opposed to larger, multipayload air vehicles, 2) requirements for multipayload sensor report processing for cueing and target identification, and 3) integrated mission planning for survivability enhancement, mission productivity enhancement, and maximum likelihood of target detection/identification.

## 2. MISSION ANALYSIS AND REQUIREMENTS FOR CRITICAL C<sup>3</sup> NODE INTERDICTION

Critical C<sup>3</sup> nodes are a set of related targets that support a combat-essential function. The set of C<sup>3</sup> nodes are said to be critical because if they are interdicted at a critical time in the battle, the loss of the combat-essential function will force the enemy commander to rethink and alter his intended course of action.

Generally, critical nodes have an additional quality as a target set; their interdiction produces a combat power multiplier, reducing enemy fire and maneuver capability to a much greater extent than would the kill of individual weapons such as tanks or self-propelled howitzer gun mounts.

Critical C<sup>3</sup> nodes are defined, therefore, to be a target set associated with a combat-essential function whose loss at a critical time in battle will produce a combat multiplier effect and force the enemy to alter an intended course of action, i.e., either his mission or scheme of fire and maneuver. The interdiction of fire direction centers within Soviet provisional artillery groups provides a quantifiable example of critical node interdiction requirements and the combat power multiplier effect.

### 2.1 EXAMPLE OF A C<sup>3</sup> NODE

Provisional artillery groups are formed at the combat regiment and division echelons to deliver preparatory fires that precede an attack. These groups are also found in the task organization for Soviet defensive operations. In the offense, the artillery groups provide sufficient firepower (e.g., artillery units resubordinated from army/front echelons) to ensure a 6:1 fire support advantage at a principal axis of (division) attack. Under these conditions, where friendly artillery units are outgunned, a counter battery artillery duel is a poor counterfire tactic, and a combat power multiplier is desired.

Consider the organization and operations concept of a Soviet provisional artillery group. Each artillery group is typically task-organized to include at least three howitzer battalions. The two combat-essential C<sup>3</sup> functions of the group are:

- The command function at the group and battalion echelons, that issues "calls for fire" based upon analysis of the terrain and target acquisition product. The staff at the command observation post (KNP) identifies and locates targets by consolidating reports from sound and flash radar DF, counterbattery radar, and battlefield surveillance radar sensors.
- The fire direction centers (FDCs) respond to calls for fire. FDCs at group and battalion echelons employ automated means and digital data links to compute and disseminate fire solutions to artillery batteries. Battery fire direction centers are a backup, manual means for fire solution computation.

The development of an artillery group is illustrated by Figure 2-1. Command observation posts are deployed near the FLOT on forward slopes where commanders can observe fires. At the higher echelons (group and battalion), FDCs are also deployed near the FLOT, on reverse slope and proximate to their KNPs so as to facilitate: 1) line-of-sight digital data radio communications with battery FDCs that are further to the rear, and 2) wire communications with the command staff.

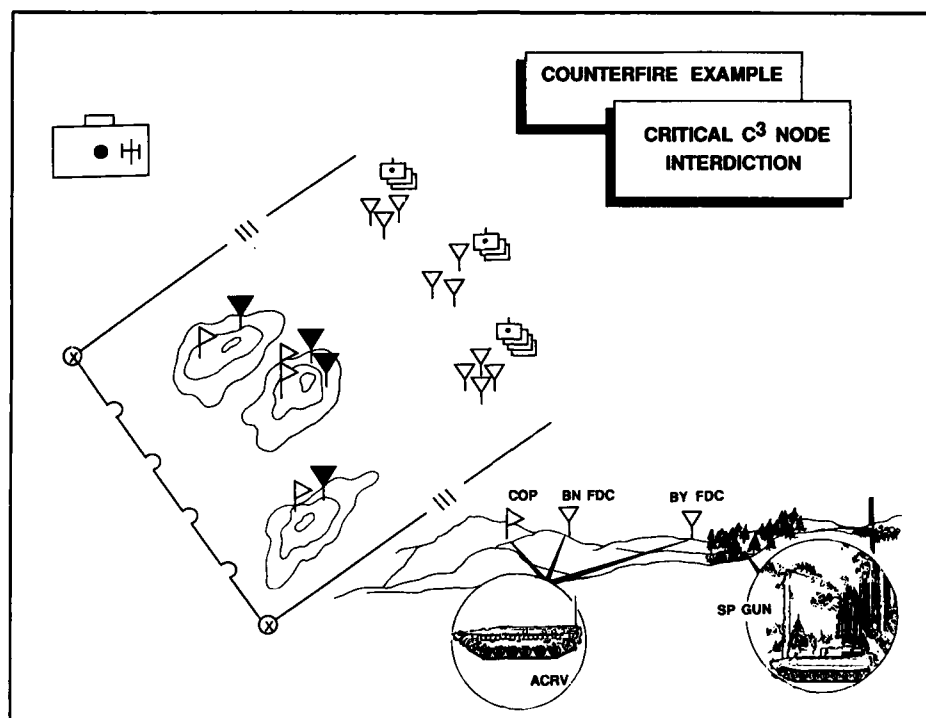


Figure 2-1. Deployment of a Provisional Artillery Group

The collocated fire direction center and command observation post of the self-propelled artillery consist of two ACRV-class armored command vehicles (one vehicle for each function). Therefore, the destruction of a single aim point is tantamount to a fire direction center kill. For the representative provisional artillery group, there are four major (automated) FDCs and nine battery FDCs, thirteen targets in total.

## 2.2 COMBAT POWER MULTIPLIER

Figure 2-2 quantifies the results of a critical C<sup>3</sup> node interdiction campaign directed against enemy fire direction centers, in terms of a reduction in capacity to compute fire solutions and the impact of that reduced capacity on artillery firepower. The initial reduction in fire direction capacity, due to redundancy in the capability to compute fire solutions, has no effect upon fire power. In the firepower drawdown curve, it is assumed that close-in, group and battalion echelon automated fire direction centers are preferentially attacked. With this rule of engagement, the interdiction of eight fire direction centers (eight ACRVs) will have the equivalent impact upon enemy firepower (75 percent reduction) as would the destruction of 40 self-propelled gun mounts. A 5:1 combat power multiplier is therefore achieved.

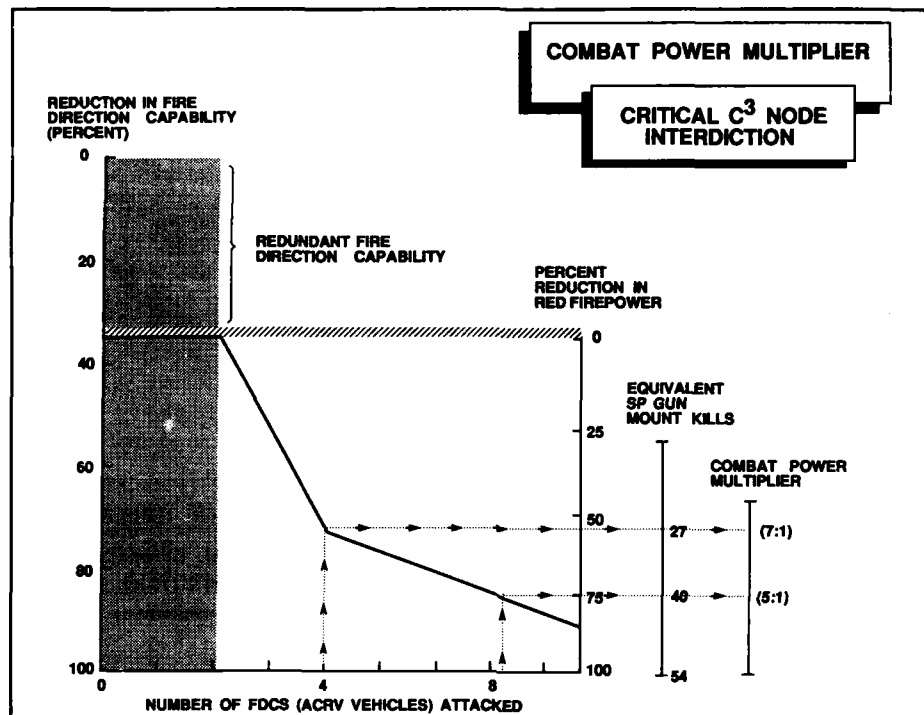


Figure 2-2. Drawdown In Enemy Firepower Resulting from Fire Direction Center Interdiction

### 2.3 PRINCIPLES OF TIMELINESS AND DECISIVENESS

To gain the combat power multiplier associated with the interdiction of critical  $C^3$  nodes, fire direction centers must be destroyed well within a time window defined by the sum of: 1) the time required for artillery groups to occupy firing positions and attain combat readiness (less than one hour), and 2) the time required to deliver the preparatory fire concentrations (also less than one hour). Therefore, the drawdown in enemy firepower is proportional to the number of critical nodes destroyed in a 60 to 90 minute time window. For a given number of RPV sections committed to the counterfire campaign, the rate at which targets can be engaged is maximized if the RPV interworks with a dedicated firing battery and precision guided munitions are employed. As indicated, adjusted fire is far less effective, especially when, in calling for fire, RPVs contend with other target acquisition means such as the Firefinder counter-mortar/counter-battery radar. These contention delays are magnified when slow rise time radios and cumbersome message switching systems are employed, as is the case for the TACFIRE fire support system (which will be product-improved by the AFATDS program). The effect of these time delays on target kills is shown by Figure 2-3.

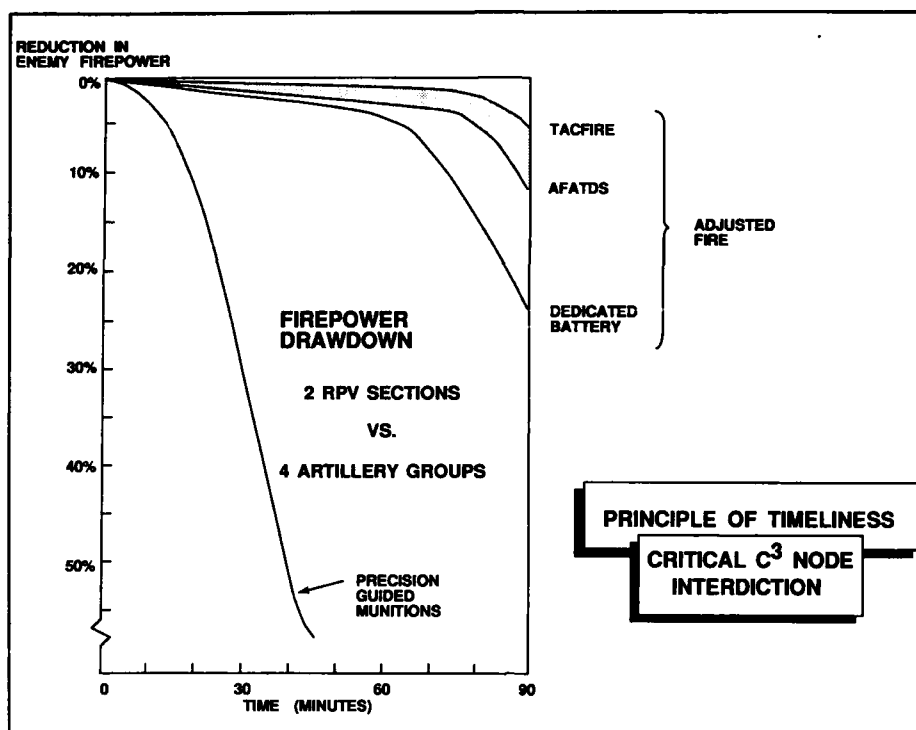


Figure 2-3. Reduction of Enemy Firepower Versus Time and Concept for Interworking RPVs and Counterfire Weapons

The skillful introduction of RPVs into the battlefield requires that RPV sections be introduced in decisive numbers, ensuring that an interdiction capability can be massed to produce a combat power multiplier effect within critical time windows. As stated, enemy doctrine requires at least a 6:1 fire support advantage at principal attack axes. To offset the enemy's numerical fire support advantages, at least seven RPVs must support counterfires against critical C<sup>3</sup> nodes in four provisional artillery groups, given that smart munitions are employed and RPVs interwork with dedicated firing batteries, cued by other RPVs and systems.

### 3. UAV FAMILY OF PAYLOADS

The UAV "family of payloads" includes wide area surveillance and high-resolution imaging systems. For illustration SAR, SIGINT and FLIR payloads are assumed to support the following missions:

- Wide-area signals and active imagery reconnaissance to identify potentially targetable areas
- Follow-up "cued" imagery surveillance to identify critical C<sup>3</sup> nodes and/or refine the location of aimpoints within the potentially targetable areas.

The operational concept for interworking SAR, SIGINT and FLIR sensors is best effected if each payload is integrated into a separate UAV. The operational concept and the argument supporting the employment of multiple, mini-UAVs with single payloads is presented herein.

#### 3.1 MULTISENSOR OPERATIONAL CONCEPT

The missions and operational concept for the "family of UAV payloads" is depicted in Figure 3-1.

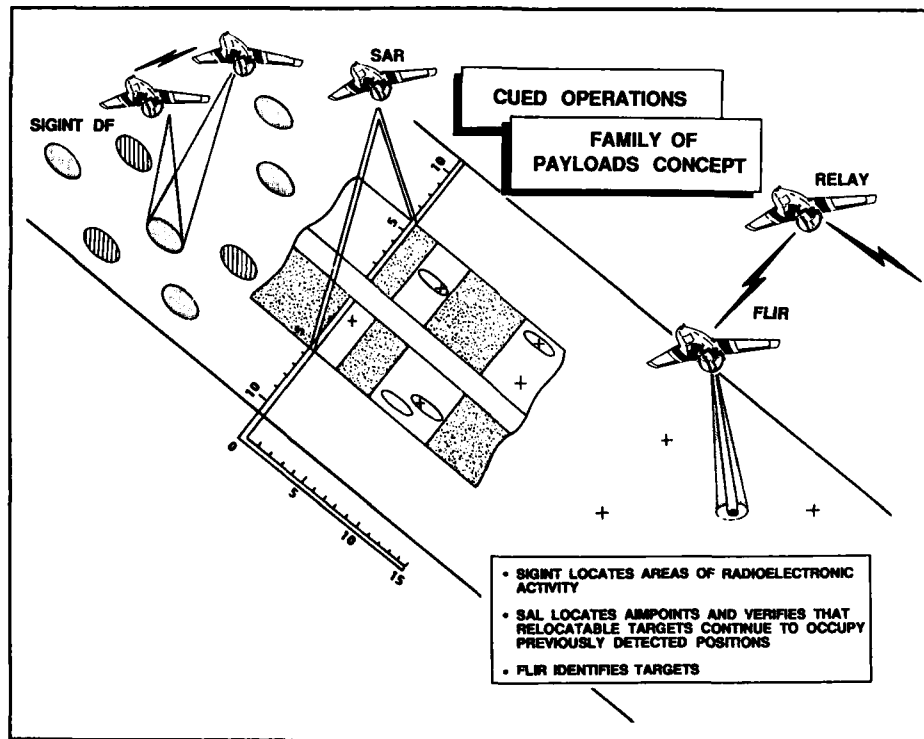


Figure 3-1. Overview of Roles and Missions of SIGINT, SAR and FLIR Sensors within a UAV Family of Payloads

Within an area of interest, UAVs (two) with SIGINT payloads: 1) cooperatively geolocate radioelectronic emitters, and 2) for stations/outstations that are organized into simplex radio networks, establish network relationships among the stations/outstations based upon their transmission at a common radio frequency (RF). Cooperative operations of SIGINT-equipped UAVs are

essential to the geolocation of short time duration (e.g.,  $\leq 30$  second) transmissions. The resulting geolocation of stations/outstations provides sufficient position certainty to:

- Cross-correlate geolocated stations/outstations to associate multiple emitters with individual  $C^3$  nodes or units
- Cue SAR-equipped UAVs to: 1) refine the geolocation of  $C^3$  nodes and 2) confirm or negate the suspicion that relocatable  $C^3$  nodes continue to operate from their previously geolocated positions
- Cue UAVs equipped with high-resolution (FLIR) imaging payloads to conduct a reconnaissance to identify and precisely locate selected  $C^3$  nodes.

The SAR sensor supports the following wide area surveillance objectives:

- Detection of units/nodes that include a large number of ground order-of-battle vehicles, and that also observe EMCON (emissions control) practice and therefore, cannot be detected by SIGINT means
- Cued reconnaissance of areas, designated as potentially targetable by SIGINT means, for the purpose(s) of: 1) precision geolocation of targets/aimpoints within the "SIGINT uncertainty ellipse," and 2) detecting any changes in target deployments.

High-resolution imaging systems support critical  $C^3$  node identification and target exploitation missions.

In a target identification application, UAVs equipped with FLIR sensors are cued to image a carefully selected subset of the potentially targetable areas designated by SIGINT and SAR wide-area surveillance systems. The number of cues derived from SIGINT and SAR operations is large compared to the number of cued areas that can be exploited by an imaging system. For this reason, it is desirable to image only those cued areas that, in the context of all-source intelligence production, will maximize the number of critical  $C^3$  nodes identified. The radio network-node relationships derived from SIGINT sources can be exploited to unambiguously identify a larger number of nodes than can be identified by SIGINT means alone, when a small subset of the nodes are identified by imaging. This concept is explained in Section 4.

Target exploitation, the interworking of imaging systems and weapons, also requires care in target selection. As previously noted, a critical  $C^3$  node interdiction campaign, to succeed in causing a commander to change his intended course of combat action, must:

- Select a subset of the identified nodes that together constitute a combat essential function, and
- Decisively interdict the critical  $C^3$  nodes within the time window during which the function supported by the  $C^3$  nodes is of a combat-essential nature.

Otherwise, combat-essential functions cannot be denied and the enemy commander will be able to follow his intended course of action.

### 3.2 MULTI-UAV OPERATIONAL CONCEPT

SIGINT and FLIR operations are best conducted at low altitude:

- Low-altitude FLIR operations are required to: 1) stay below the cloud cover (e.g., for average European weather the likelihood of a target being occluded is about 33 percent at 2500 feet and 60 percent at 5000 feet altitude), 2) "hide in the ground clutter" (where doppler radars have difficulty extracting low-fliers from the static terrain background), and 3) detect armored fighting vehicles in the FLIR wide field-of-view imaging mode.

- Low altitude SIGINT operations are required to reduce cochannel interference effects, and to maintain a high S/N by limiting the slant range between the UAV and the emitters that are to be cooperatively geolocated.

By contrast, SAR sensors are best operated on UAVs that are flown at higher altitudes where: 1) terrain masking effects do not limit wide field-of-view search operations, and 2) clusters of ground order-of-battle vehicles, concealed within treelines, can be viewed at the high depression angles that can penetrate the canopy.

In addition to being flown at low altitudes, SIGINT and FLIR payloads are also best flown on separate air vehicles. Because of SIGINT receiver antenna patterns and polarization considerations, radioelectronic emitters that are cooperatively geolocated from a UAV will be viewed at shallow depression angles (e.g., for the U.S. Skydancer program at 5 degrees or less), as measured from the UAV local horizontal. Figure 3-2 shows that at shallow depression angles and low altitude: 1) geolocated radioelectronic emitters will be a minimum of 40 km from the air vehicle, and 2) at an army main attack axis, the nadir of the air vehicle will be several divisions away from the area in which geolocated radios are deployed. Therefore, in a multipayload UAV, a SIGINT sensor is inefficient as an on-board cuer for an imaging payload because of the long distances that must be flown to image a cued target.

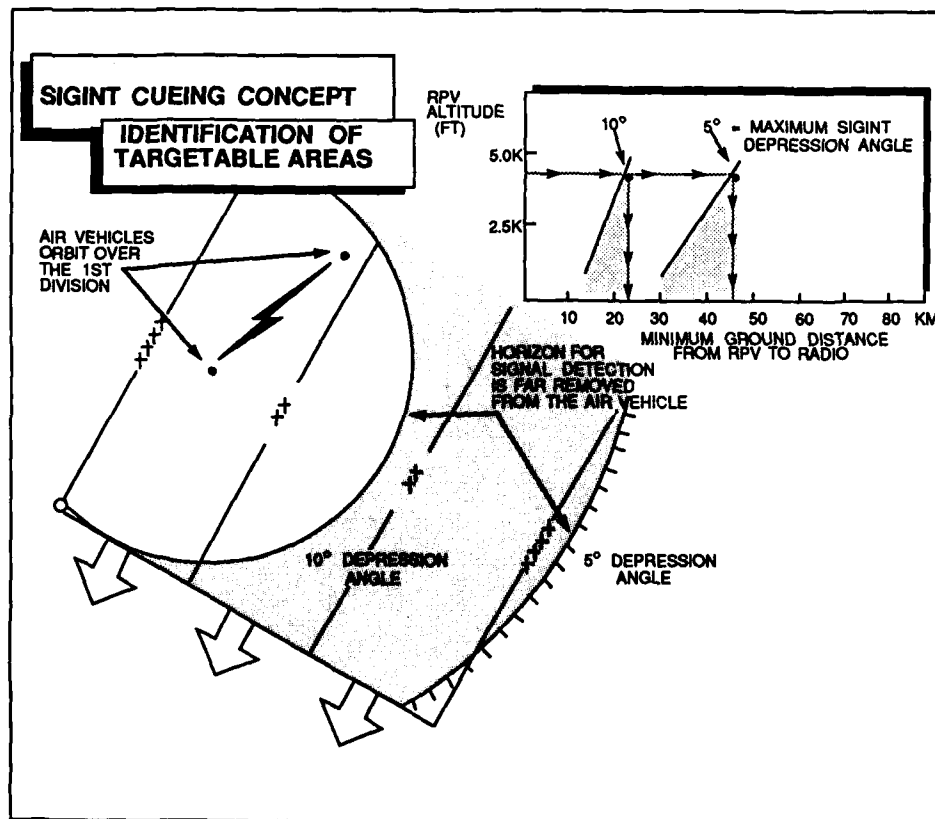


Figure 3-2. Position of Geolocated Radioelectronic Emitters Relative to the UAV

Furthermore, a real-time data relay is needed if ground order-of-battle targets are to be identified from a low-flying, FLIR-equipped UAV. The concept of operations is that cued targets initially be acquired in a wide field-of-view imaging mode. Such an image has a trapezoidal footprint of (typically) 1 km maximum width, within which the two image line pairs needed to detect a target are

available. Subsequently, the imaging payload operator would "zoom" and articulate the payload to stare at and identify detected targets. A video data link is therefore required to provide the real-time control of the imaging payload needed to interwork a wide field-of-view detection mode with a narrow field-of-view target identification mode. In other words, the commander's need for real-time imagery is not the "driver"; for a real-time data link, it is the requirement to control the payload. Further, analysis has shown that the link itself is best closed through a standoff relay air vehicle rather than a UAV orbiting at high-altitude, positioned somewhere between the imaging UAV and its ground control station.

Finally real-time data link for SIGINT operations is also needed to effect multiplatform, cooperative geolocation of short-time duration, radioelectronic emitters. Otherwise, emitters cannot be geolocated based upon the sensor line-of-bearings data because the UAV position does not appreciably change during the period of radio transmission.

#### 4. FAMILY OF PAYLOADS EMPLOYMENT CONCEPT

The efficient identification of critical C<sup>3</sup> nodes is promoted by a "family of payloads" operational concept that emphasizes:

- Cueing of FLIR-equipped UAVs that are otherwise inefficient in searching large areas to detect, locate, and identify high-value targets
- Fusion of SIGINT, SAR and FLIR data in an automated process that maximizes the ratio of targets identified to targets that are imaged by a FLIR-equipped UAV.

The cued operations planning and fusion concepts, essential efficient employment of the family of payloads, is discussed herein.

##### 4.1 MULTIPAYLOAD FUSION CONCEPT

The family of payloads operations concept for critical C<sup>3</sup> node interdiction includes the following precepts:

- SIGINT surveillance systems identify areas that may contain high-value targets.
- SAR, wide-area surveillance systems refine the location of aimpoints in SIGINT-cued areas, and maintain periodic surveillance of the cued areas to detect changes indicating the redeployment of relocatable targets.
- FLIR-equipped UAVs image a subset of the yet-unidentified targets, directly identifying the imaged targets and indirectly identifying the vast majority of targets by means of imagery results with the SIGINT and SAR product, i.e., SIGINT network-node relationships, and SAR count of ground order-of-battle vehicles.

The fusion concept will be described, again with reference to the artillery group counterfire campaign example. The organization of communications within a Soviet provisional artillery group is represented by the network node relationships shown in Figure 4-1. At the group echelon: 1) the command observation post (KNP) is seen to be an outstation on the division CRTA network and the control station in the group command net that includes all artillery battalion command posts, and 2) the collocated group fire direction center (FDC) is the control station in a group fire direction network that includes artillery battalion fire direction centers as outstations. (This collocated group COP/FDC is identified as point A in Figure 4-1. Similarly, command and fire direction networks are organized within artillery battalions with firing batteries as outstations.

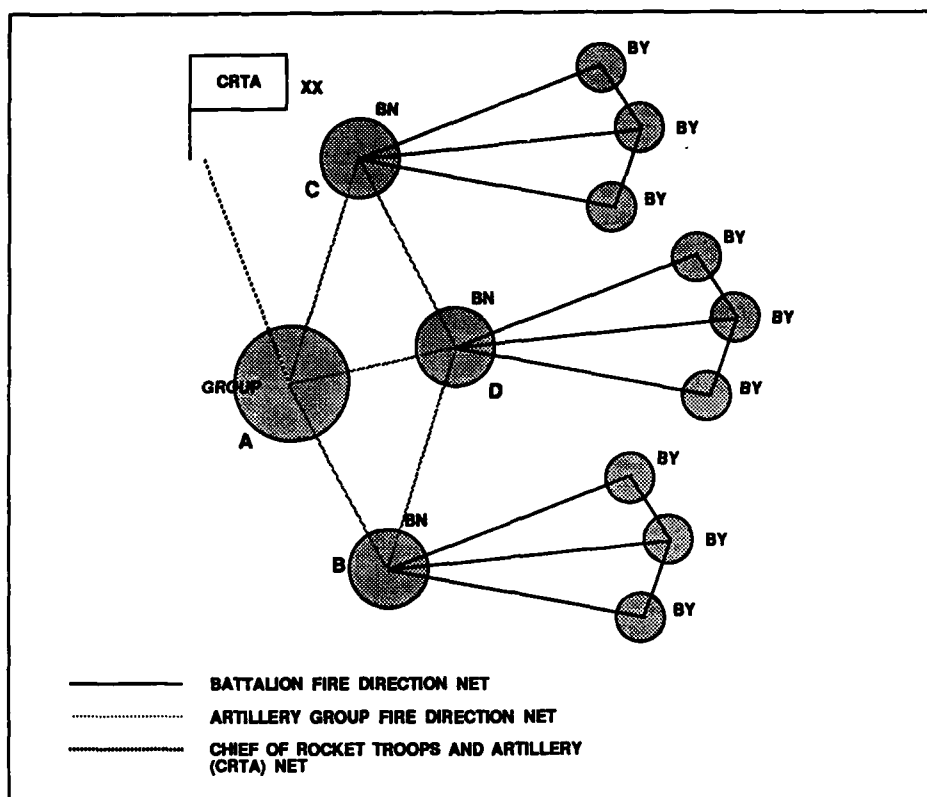


Figure 4-1. Provisional Artillery Group Fire Direction Networks

The organization of enemy communications is analogous to a crossword puzzle where networks, each corresponding to a different radio frequency, are shown in the "down" direction, and  $C^3$  nodes, each corresponding to a geolocation, are shown in the "across" direction. The identification of networks and nodes in the SIGINT puzzle cannot be accomplished unambiguously on the basis of network-node relationships alone. Additional intelligence is required and can be acquired by cueing an RPV to image, and thereby facilitate the identification of a judiciously selected subset of the geolocated  $C^3$  nodes. For example, SIGINT information might reveal the existence and locations of four separate communication points operating on the same radio frequency. SIGINT information does not, however, reveal what these communication points are. A FLIR-equipped UAV is cued to one of these four points (e.g., Point B in Figure 4-1). If the resulting imagery shows two closely positioned ACRV-class armored command vehicles, a collocated command observation post/fire direction center (COP/FDC) is thereby identified. This single point identification automatically identifies the other members of this radio net (points A, C, and D in Figure 4-1) as being COP/FDCs. Thus, the information acquired from a single imaging mission, when used with previously acquired SIGINT information, results in the identification and location of four critical  $C^3$  nodes. In this manner, IMINT and SIGINT data are combined to unambiguously identify the vast number of critical  $C^3$  nodes. An RPV can subsequently be tasked to support interdiction of these critical  $C^3$  nodes. Four software modules support the multisensor cueing scheme:

- Cross-correlation software associates multiple emitters, geolocated with overlapping error ellipses, with a single  $C^3$  node.

- Self correlation software associates emitters with simplex radio networks in a process which distinguishes previously undetected network outstations from previously detected outstations that have shifted position.
- Signal parametrics analysis software is used to analyze the SIGINT puzzle and judiciously select a subset of  $C^3$  nodes to be imaged.
- Fusion software combines imagery reports that identify targets with the SIGINT product to identify critical combat nodes.

The synthetic aperture radar contribution is implicit in the multisensor fusion process. The SAR precision geolocates  $C^3$  nodes that are geolocated by SIGINT means and, employing its change detection capability, supports the radioelectronic emitter correlation process. The relationship among the four software modules used in this analysis process is shown by Figure 4-2.

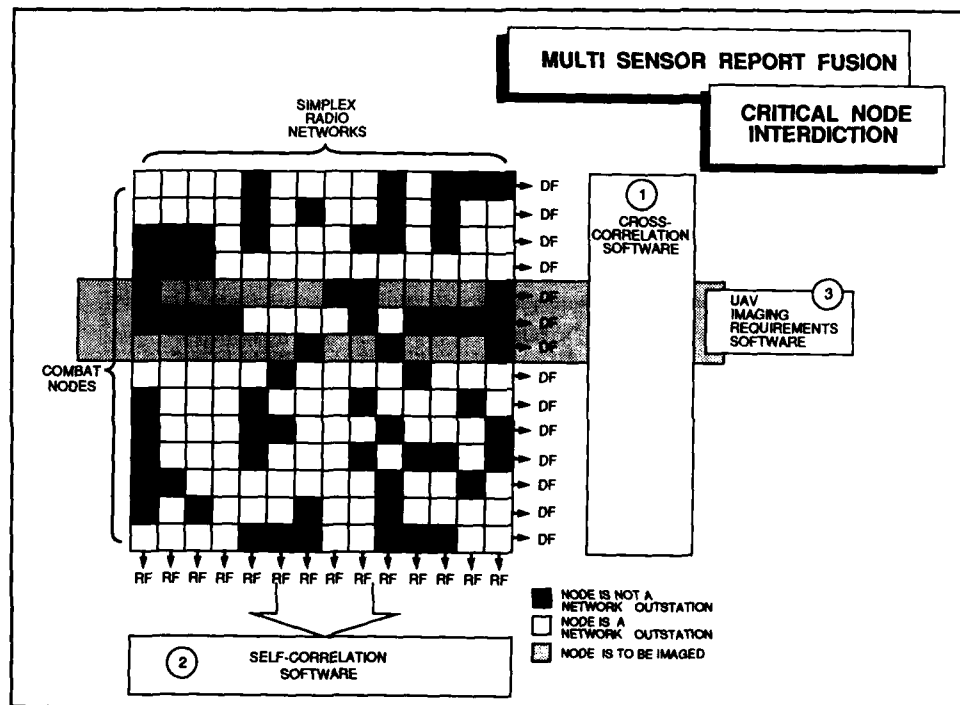


Figure 4-2. Fusion of SAR, SIGINT and IMINT Data, A Crossword Puzzle Analogy

## 4.2 UAV OPERATIONS PLANNER

Within the Ground Control and Processing Station (GCPS), the UAV operations planner is a mission critical element in evolving a critical node interdiction scheme for cued multipayload operations. UAV operations planning is discussed herein in terms of FLIR operations planning. The major building blocks of the system are: 1) A multiple employment planner that identifies conflicts between tasking and available UAV resources, thus allowing planners to reconcile conflicts in a manner that supports both a predictable mission contribution to a combined arms operation and decisive, timely RPV support to each assigned mission, 2) A navigation waypoint selector that efficiently implements the mission plan. This waypoint selector identifies all points on a route at which RPV rate of climb or descent, engine power level, or turn rate must be modified in order to change

UAV heading, altitude or speed (i.e., so as to optimize survivability, mission efficiency, and/or terrain and terrain-masking avoidance), and 3) An imaging operations planner that controls UAV/FLIR sensor operation to maximize likelihood of target detection in a cued area.

The ensuing discussion is based upon Command Systems Group's UAV Operations Planner.

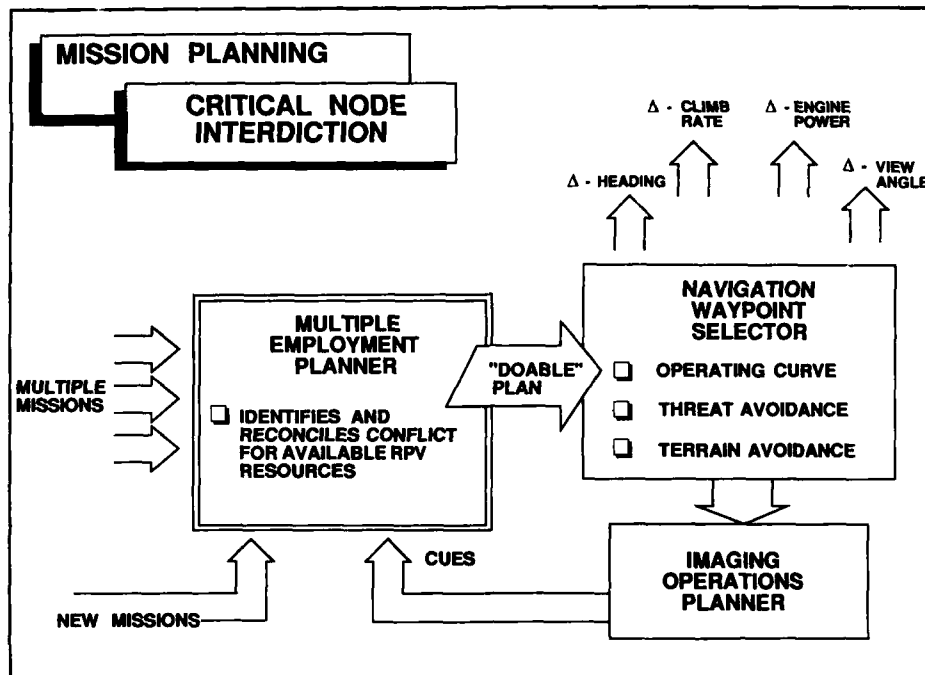


Figure 4-3

#### 4.2.1 Multiple Employment Planning

Multiple employment refers to the use of an aviation asset to perform more than one mission in the course of an overall military operation. Missions must be defined in a tasking protocol. A reasonable tasking protocol includes:

- Definition of areas of interest (AOI)
- Definition of missions in each AOI
- Definition of the target list for each mission
- Mission guidance, including: 1) order in which areas-of-interest are to be addressed, 2) "sampling strategy," the fraction of targets associated with each mission that must be imaged cloudfree during the UAV sortie, and 3) mission priority, a consideration to be employed in reconciling conflicts among missions for available UAV.

Multiple employment planning is effected in two steps: 1) Allocation of UAV system resource (time) among the areas-of-interest (AOI), and 2) apportionment of the time allocated to an AOI among the UAV missions that have been identified within the AOI. For example:

- **Step 1** - Figure 4-4A shows the manner in which the planner allows UAV sortie resource (time) to be allocated among AOI after time for ingress (0.193 hrs), transition between AOI (0.138 hrs), and egress time (0.063 hrs) is accounted for. One hour is then allocated for all missions in the "FROG" AOI and an hour and a half for missions in the "DIV 2ND ECH" AOI. A margin of 0.11 hours remains unused and available for contingencies.
- **Step 2** - Subsequently, the time allocated is compared to the time required to accomplish the missions in each AOI (Figure 4-4B). In the example of Figure 4-4, the FROG AOI time allocation is exceeded by 0.36 hours. The operator can accommodate the shortfall by: 1) reallocating UAV sortie time among AOIs, 2) reducing the "target sampling" requirement for one or more mission in the AOI, and/or 3) eliminating AOIs or missions.

The benefit of multiple employment planning is that commanders can predict, control, and thereafter rely upon UAV sortie accomplishment because the mission requirements are inherently "doable."

#### 4.2.2 Navigation Waypoint Selection

Navigation waypoint selection employs dynamic mathematical programming to select an optimum set of targets to be imaged in an AOI based upon a value function that is simply (and appropriately) the ratio of time allocated to a given mission within an AOI to the total time allocated to the AOI. As stated, in addition to selecting an efficient sequence in flying among targets, terrain avoidance and threat avoidance are important facets of navigation waypoint selection. This is illustrated in Figure 4-5 and described below.

**Figure A.** In a 3-hour UAV sortie, 0.39 hours are wasted in ingress, egress and transition between two AOI: (1) FROG, allocated 1 hour of mission time, and (2) DIV 2ND ECH, allocated 1.5 hours.

Plan	InterAOI Resource Req'd	IntraAOI Resource Left
NEWPLAN	0.39	0.11

AOI	InterAOI Resource Req'd	IntraAOI Resource Left
FROG	0.193	1.0
DIV 2ND ECH	0.138	1.5
HOME	0.063	

3.0	Total Available	Total Expended	2.89
-----	-----------------	----------------	------

Area of Interest	Allocation
FROG	1.0

Active Missions	% Req'd	Time	Expected Return %
DZ/LZ	100.0	0.66	80
TAI	100.0	0.7	80

1.36
------

**Figure B.** For the FROG AOI, the two missions: (1) Drop Zone = DZ and (2) target areas of interest = TAI, require 1.36 hours of UAV sortie time, 0.36 hours more than was initially allocated.

Figure 4-4. Multiple Employment Planning Screens for Operator Interaction

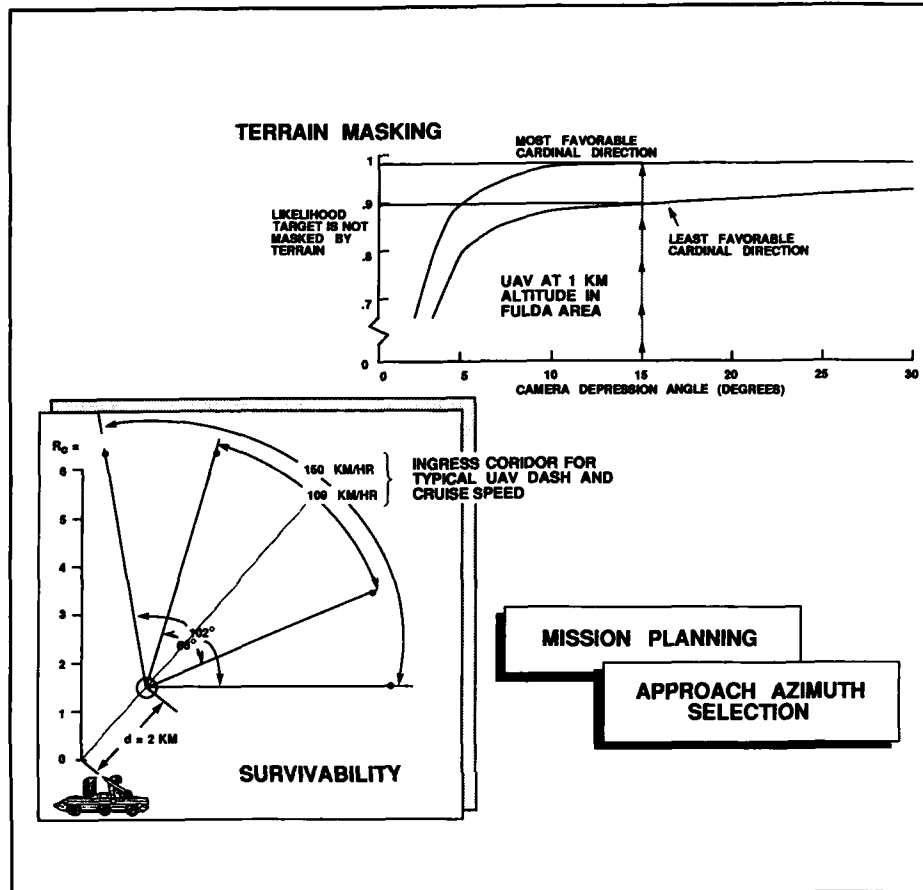


Figure 4-5. Threat and Terrain Avoidance Considerations

As a UAV approaches a target to conduct a high-resolution imaging operation at low altitude, the selection of an approach azimuth can be critical to both the likelihood of target detection and to survivability. As indicated for the Fulda region of Germany, the choice of the best and worst cardinal direction of target approach will, on the average, reduce likelihood of target detection by 15 percent. Furthermore, the direction of approach against a SAM-defended target will influence the likelihood of target detection and engagement. The indicated (Figure 4-5) safe approach corridor is a function of air vehicle speed and heading since control of the component of air vehicle velocity presented to the defending radar will affect the radar's ability to employ doppler to "pull" low, slow flying RPVs out of the background clutter.

#### 4.2.3 Imaging Operations Planning

Cueing of an RPV to image a target significantly improves the likelihood that the target will be detected. Improved detection during a cued mission arises from two sources: 1) alerted performance of operators during a cued mission is greater than in an uncued mission, and 2) imagery of small, cued areas can be captured in freeze-frames for follow-up, near real-time level-II exploitation. A condition precedent to operator exploitation of cued targets is that the combination of RPV

speed, heading, altitude and camera depression angle be selected in a manner that facilitates target detection in a scene. The presence of an "optimum" is illustrated by the "operating curve" for imaging operations shown in Figure 4-6.

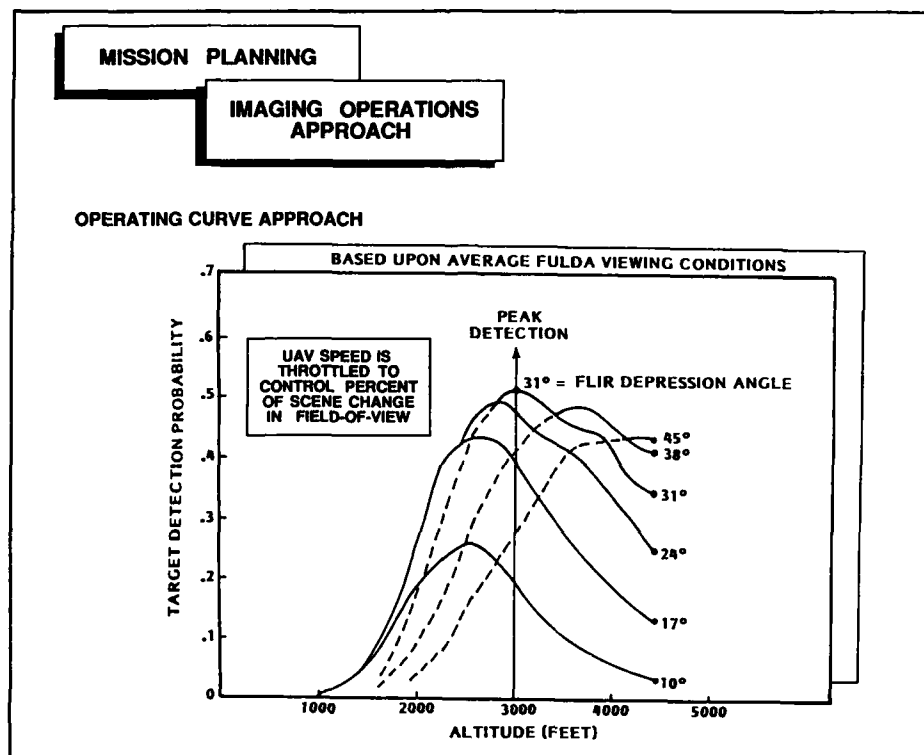


Figure 4-6. Operating Curve

The operating curve approach to planning imaging operations allows terrain, weather, target, background, sensor resolution, field-of-view, frame rate, and rate of scene change within the sensor field-of-view to be systematically considered in optimizing imaging operations. The two-dimensional operating curve indicates how the combination of RPV altitude and sensor depression angle affect target detection likelihood for average terrain and weather conditions in the Fulda region of Germany, given that RPV speed is throttled back to ensure that no more than 15 percent of the scene in the sensor field-of-view changes each second. As indicated, selection of a non-optimum altitude and camera depression angle will materially impact likelihood of target detection.

## TARGET ACQUISITION IN THE UAV ENVIRONMENT

by

R. Denaro, R. Kalafus, P. Ciganer  
TAU Corporation  
485 Alberto Way, Bldg D  
Los Gatos, California 95032, USA

### ABSTRACT

Large-scale tactical use of Unmanned Air Vehicles (UAVs) in the expected high intensity Air/Land battle environment is currently possible. This is due to recent advances which have made available mature technologies at low cost. These key technologies include semi-autonomous guidance and control, real-time image acquisition, and advanced navigation capabilities.

For good reasons, most of the R&D efforts to date have been concentrated on platform design and evaluation. Now that performance requirements have been firmed up and defined, it is now possible to focus attention on the development of system concepts which achieve the operational objectives of the current battle management doctrine.

This paper specifically addresses the emerging Target Acquisition objective of UAVs (beyond former objective of target designation) relevant in the Army's UAV program. A system concept is described which supports Target Acquisition by UAVs in a tactical environment. The concept rests on three critical enabling technologies: (1) Image exploitation for target detection and identification, (2) Pre-flight and real-time mission planning to support image analysis with dissimilar levels of tactical information (therefore fused by the operator), and (3) highly precise vehicle positioning and attitude determination, along with photogrammetric algorithms, for target localization of sufficient accuracy to authorize standoff weapon firing.

### INTRODUCTION

Unmanned Air Vehicles (UAVs) are the subject of increased attention for operational development. Concentrating on the U.S. Army mission, UAVs represent a major future resource for battlefield surveillance, data acquisition, target designation, target acquisition, and even defense suppression.

Developments in recent years have yielded a variety of potentially effective airframes for the various missions envisioned for UAVs. Due to the UAVs necessarily limited payload, the challenges are great in avionics design to achieve required mission capability within size, weight, power, and complexity/reliability constraints. Fortunately, technology advances in sensors and computers may now be ready for more intense integration development to meet these mission requirements within vehicle constraints. Small, lightweight sensors with early digital conversion are available, enabling the power of multispectral imaging. The advent of powerful 32-bit microprocessors and parallel architectures makes the required intensive computational power within reach. Adequate navigation and positioning are made possible with small Navstar GPS receivers and advances in solid-state inertial components. Finally, ground workstations are now available which can properly integrate automatic functions with expert operators to achieve mission goals.

A significant and tangible recognition of these new avionics and sensor capabilities is in the extension of the mission objectives for UAVs. Formerly, surveillance was the goal. To aid the battlefield commander more directly in strike missions, target designation was proposed as the mission objective. However, it is now possible to consider complete target acquisition, including target detection, target identification and classification, and target location. The latter delivers accurate target coordinates of an identified target to the commander.

To achieve this goal, none of the targeting components can be missing. Image processing must be able to aid isolation and identification of a target. Positioning must be precise enough to meet location specifications in all axes. The groundstation must be flexible enough to give the operator full situation awareness and accurate data for fast analysis. And this three-legged stool must be realized with small, lightweight components to keep vehicle size, weight, and complexity (cost) within desired limits.

Current UAV airframes are diverse in their design and mission objectives. The table below outlines some of the foreign and domestic platforms which have been developed over the past five years [1]. An overview of each one of those systems is beyond the scope of this paper, but the table provides a reference of their diverse applications.

Design efforts have been focused on developing a compact and efficient airframe which can accommodate various mission payloads. To date, less time has been spent on integrating the airframe design and its support structure into an operational environment concept. The various UAV programs are following traditional development patterns in which new autonomous airborne systems are initially engineered to maximize platform performance, versatility and efficiency and then, once the platform design has been fixed, focus their attention to operator interaction and asset network integration.

### IMAGE EXPLOITATION TECHNIQUES

Image exploitation is not a panacea for solving the target detection and identification problem. Much time has been spent on automation of complex image processing functions to achieve object recognition, but the science is still young, and the scope of applications with reasonable probabilities of success is small. Programs such as the Advanced Digital Reconnaissance Imagery Exploitation System (ADRIES) and the Advanced Target Acquisition Reconnaissance System (ATARS) are making significant advances in target recognition for these applications.

However, image processing can play an important role as a decision aid for the operator at the ground control station. Image enhancement can certainly improve the quality of most images for operator interpretation.

Table 1. The RPV Spectrum

<u>Vehicle Name</u>	<u>Prime Manufacturer</u>	<u>Objective/Program</u>	<u>Range</u>	<u>Sponsor/User</u>
Skyeye R4E-40	Developmental Sciences	UAV/MP	Short	Army
CM-30, CM-44	California Microwave	UAV/MP	Short	Army
Heron 26	Pacific Aerosystems	UAV/MP	Short	Army
Altair	Lockheed	EW/Recon	Medium	IR&D/Army
Pioneer	AAI	Recon/Spotting Damage Assmt	Short	Navy
Mirach 100 Mizar	Meteor	IMINT	Medium	Navy/AF/USMC
	Martin Marietta	IMINT	Medium	Navy/AF
	Aerodyne Systems Engineering	IMINT	Medium	Navy/AF
Design 754	Grumman	Early Warning	Medium	Navy
	Goodyear Aerospace	AEW	Medium	Navy
	Westinghouse	AEW	Medium	Navy
Skydancer	---	COMINT/ELINT	Long	USMC
BQM-34A Firebee	Teledyne Ryan	ELINT/IMINT	Medium	AF
AGM-81A Firebolt	Teledyne Ryan	ELINT/IMINT	Long	AF
Brave 200	Boeing Military	Seek Spinner	Medium	AF
Pave Cricket	Aircraft	Pave Tiger		
Tacit Rainbow	Northrop	ARM	Medium	AF/Navy
RAV	Texas Instruments	Reconnaissance	Long	DARPA
Amber	---	ELINT/SIGINT/ COMINT	Short	Army/Navy
D-340 Pointer	Bell Textron	IMINT/COMINT	Short	IR&D
Mastiff	Mazlat	Targeting	Short	USMC
Scout	Mazlat	Sigint	Short	IDF/USMC
Phoenix	BAe	ASW	Medium	UK
CL-289	Canadair/MATRA/ MBB	IMINT/SIGINT	Medium	FRG
CL-227 Sentinel	Canadair	IMINT	Short	IR&D
BQM-1BR	Brazil	Targeting	Short	BR AF
MQ-2	Guimar	Targeting	Medium	ARG/AF
Eyrie	National Dynamics	IMINT	Short	SA Army
B-2	PRC	Targeting	Short	PRC Army

Image object recognition is of questionable value in an operational UAV environment with current technology, but can aid in gross isolation of areas of interest. On the other hand, image manipulation and comparison techniques can be used by the operator to investigate imagery in a methodical manner. As such, the groundstation becomes a true imagery workstation for maximizing the speed and amount of information extracted from the data.

There are several image processing algorithms which are clear candidates for the UAV image processing workstation application. These algorithms fall generally into the categories of:

- Intelligent Enhancement
- Contrast Stretching
- Filtering (e.g., local mean removal, high pass)
- Edge Detection
- Thresholding
- Image Segmentation and Blob Analysis
- Morphological Processing
- Feature Detection/Measurement, Matched Filtering

Image enhancement begins with those functions that can be mathematically derived from the known error characteristics of the image data collected, defined earlier as intelligent enhancement. Examples are deblurring, image warp (actually dewarp in this case), and selective filtering based on available known parameters such as vehicle speed.

Contrast enhancement is a common function in image processing that increases the dynamic range of the pixel intensity values according to defined end points and a polynomial function between them. It can be applied to the entire image or to selected regions, with various functions on the image or region histogram (including clipped adaptive histogram equalization). Regions and the parameters of the new intensity range can be automatically keyed to measurements in the image, as well.

Filtering is performed to remove noise in the image, a strong need in typical FLIR images. The key to successful filtering is to improve signal-to-noise ratio without decreasing signal at all, that is, to remove noise without degrading the recognizability of significant features. Local mean removal, convolution and low pass filtering are typical applications for this function. As with contrast enhancement, filtering parameters can be functions of measurements in the image to automate the process.

While contrast enhancement and filtering improved the quality of the image, it is edge detection that begins the significant sharpening of the specific objects of interest in the image. A number of edge and feature detection algorithms are available. Normal functions such as Sobel and Robert's edge detectors are useful for preliminary edge detection. Ramp detectors can be used to find less distinct edges. The Hough transform is a very fast technique to identify linear features in an image, such as edges of man-made objects. It transfers the x-y image into a rho-theta domain which compresses the very wide bandwidth image data (e.g., 512 X 512 pixels by 8 bits intensity) to a single point in the Hough domain. The payoff is extremely fast identification of such features. This function is also useful for image-to-image registration, by the way, as registration in the Hough domain (given the presence of linear features) is extremely fast and accurate compared to registration in the image domain.

Since all edge detection schemes result in (in the general case) a discontinuous edge, continuity functions can be applied after edge detection to close in the detected object. After such processing the detected object can be superimposed back on the original image to truly sharpen the image. This is also a useful operator-in-the-loop function in that he can judge whether the computer-identified feature of interest in fact appears to be of strategic importance. This overlaying capability can also be applied at later stages in the processing described later.

Thresholding is important in separating potential objects out from those of improbable interest. "Blobs" of approximately the right dimensions are detected if their intensity exceeds a threshold. It is best used in conjunction with the operations discussed earlier, for example, iterative thresholding and filtering to distill out the objects of interest (low pass filtering is usually applied before thresholding). The threshold is typically set (high) to achieve a high probability of detection at the possible cost of too many false detections (the unavoidable tradeoff in this operation). Any such false detections will be removed later by more sophisticated means, but those more complex functions need only be applied to a small subset (the detected blobs) of the original data, thus again a large processing load saver. Using efficient algorithms for this function, a microprocessor-based image processor can detect about 10 blobs per image per second.

Obviously, thresholding is the beginning of the next class of image processing called image segmentation and blob analysis. This general function is important for two reasons. First, segmentation allows concentration of the algorithms on a "region of interest," thus increasing the performance of the algorithm by eliminating unnecessary and perhaps corrupting or confusing data. Second, such focus vastly increases the speed of processing. Some of the blob analysis functions will work best on a binary image, where the image or region has been reduced to only two contrasting intensity values.

Morphological processing is really the start of object recognition in the image. Morphological processing is typically performed on binary (thresholded) images in order to detect certain binary neighborhood patterns which can be used in the analysis. In addition, the binary image is grown or eroded (a type of boundary-less fill or delete function) to reconstruct the probable extent of the object that is otherwise attenuated or blurred in the original image. Obviously, this is a very powerful sharpening tool that is particularly relevant to target detection in the image.

Feature detection and recognition is the ultimate goal of the target identification problem. From the morphological processing, the features of the object can be extracted, such as the size (area), perimeter, centroid, and first and second moments (for orientation).

Finally, it is important to note that sensor size and power are coming down significantly to make real-time, on-board UAV image acquisition and transmission a real possibility. Of course, much of the image processing would be performed on the ground at the UAV control station, but an important tradeoff exists with the amount of data sent over the datalink. It may be wise to carry on board some preliminary image compression capability, or image segmentation and selection, to minimize the amount of data transmitted continuously.

#### **REAL-TIME MISSION PLANNING AND INTELLIGENT WORKSTATIONS**

The ground control unit of the UAV system is the critical link between the operator responsible for mission success and the remote vehicle. This implies a need for adequate volume of information, information processing to make the operator's workload acceptable, and flexible displays to maintain situation awareness and control. Two features are provided by the control station. First, real mission performance enhancement is a possibility. Second, increase in vehicle survivability is an important goal.

Survivability of the UAV can be accomplished through a combination of both internal and external means. Internal means include projecting a low radar cross-section (RCS), employing as many passive sensors as possible, using infrequent, high speed, high data rates communications and giving agile flight characteristics to the platform. External means include planning a flight path taking advantage of both artificial (ECM) and natural (terrain masking) shields against detection. A low altitude flight plan in a dense threat environment, 500 feet or lower, helps meet several of those requirements. Mission planning using terrain masking, especially in a central European theater, can be quite advantageous for both penetration and egress. It will also help test the relative advantages of candidate waypoints for active sensor employment and data transmission. TAU Corporation has successfully implemented this planning function using DMA digital data and other sources, (whenever DTED or DFAD are either incomplete or unavailable), in a microprocessor environment suitable for real-time planning/replanning.

The advantage of such an approach is the ability for the aircraft to automatically perform terrain avoidance in addition to terrain following. Terrain following capabilities have been with us for a long time. The problem of such a method resides in its limitation to the vertical axis. As Figure 1 indicates, in some cases flying over a ridge is less desirable than going around the hill, on the opposite side of a threat.

It is important to note that terrain avoidance is only possible through in-flight/on-board access to prestored terrain elevation data. Current Random Access Memory devices allow the storage of a 20,000 square nautical miles map (100x200) of DMA's Level 1 data on a single chip. TAU has developed algorithms which allow the access and replanning of route segments 30 seconds ahead in time, at a velocity of 100 knots and altitude of 50 feet, which require very fast initialization of corrections to the flight path if the characteristics of the aircraft (in one scenario, we use a reasonably maneuverable generic drone model with a wingspan of 10 feet, a 30 HP engine, a gross weight of 300 pounds, and a payload of 120 pounds including fuel) are to be taken into consideration.

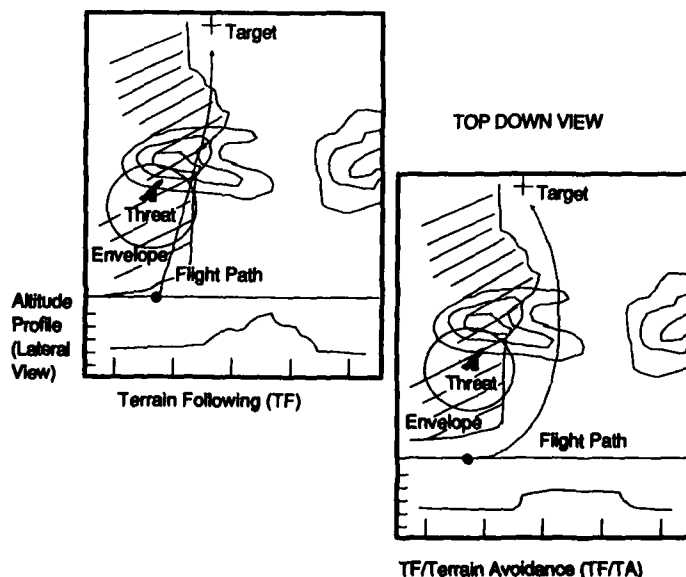


Figure 1. Terrain Following (TF) Versus Blended Terrain Following/Terrain Avoidance (TF/TA)

### Ground Control

System operations can be divided into three phases:

- a) Prelaunch including mission definition, scheduling and planning.
- b) Mission execution including launch, penetration, data reception, analysis and dissemination, egress and recovery.
- c) Post mission debriefing including additional data correlation, formatting and distribution.

Additionally, the ground crew responsibilities during the flight are shared between guidance and control of the platform and storage, analysis and possibly dissemination of collection data to the customers. The tactical deployment of UAVs at division, and eventually battalion, level requires a ground station to be reasonably transportable, possibly in a specially fitted HUMMER, reliable and flexible (not all missions are like in either profile, goals or duration).

The core of the ground station is the central processor which will support, in parallel, vehicle guidance and control, reception, processing and storage of collection data and communications with the platform and other nodes in the network including customers and other relevant users.

The current generation of superminicomputers (e.g., Sun Microsystems), through a flexible bus architecture, supports the real-time distribution and support of multiple tasks. Footprint, and power requirements have also been reduced enough in some instances to consider potential field deployment. Finally, both ruggedization and "Tempesting" are available for several NDI computers.

Software and firmware developments have made windowing (splitting a display into several screens showing different processes) an acceptable method to show and control parallel events such as displaying real-time imagery in one corner of the screen, a "bird's eye" view of the flight path on a digital map in another and flight control gauges in a third area (see Figure 2 below).

The complexity and performance characteristics of advanced airborne systems developed over the past ten years have required focusing on improved and stable operator efficiency throughout the mission cycle by reducing workload through enhanced selection and training on the one hand and automation of as many flight control functions as possible without degrading overall system performance or flexibility on the other.

If the qualification process and training of UAV operators is not as selectively focused as, for example, helicopter pilots, then the enhancements to system operation efficiency have to concentrate on designing a robust and forgiving man-machine interface. Current trends in this area seem to indicate a paradox between past years efforts to support complex vehicle operation through funding research in exploring the design of very advanced aids (Pilot's Associate, Automated Wingman, Battle Management Expert Systems, Intelligent Analytical Aid) and considering a direct control, albeit via extremely complex and sophisticated subsystems, over the vehicle by the ground based operator. Multiple, computer enhanced, joystick and/or trackball controlled, windows providing a bird's eye, perspective and bottom-up view of the aircraft are going to help but will still require a very skilled individual capable of taking-off, flying and landing the vehicle in usually less than ideal conditions (Central Germany in winter and spring is not known for its clear skies and stable weather), while at the same time performing traditional intelligence activities in reconnaissance, surveillance and targeting.

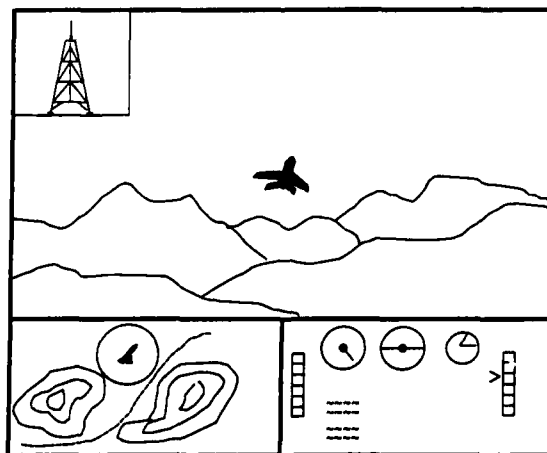


Figure 2. 19-Inch Bit Mapped or High Resolution (1k x 1k) Sample Display Layout

One possible ground-control architecture could move the operator in a supervisory position for flight control operations, allowing him to focus his attention on collection and coordination activities. This approach would be based on a fast and realistic mission planning capability, in which flight path selections would be interactively tested and ATO's generated, and an automated transfer of this flight plan along with an on-board replanning capacity addressing pop-up threats or revisiting requirements. Figure 3 describes the interaction and role of the traditional vs supervisory man-in-the-loop functions in sensor management, avionics interface and mission planning/replanning.

Finally, current flight test results have indicated a potential problem in system recovery even under controlled conditions. If traditional frontline pressures are added to operator performance forecasts, the rate of recovery might fall below acceptable levels sooner than anticipated, potentially depriving the commander of one of its most valuable tactical reconnaissance assets at the time he needs it most, i.e., during the first few days of the battle when the FLOT is still quite fluid and optimal resource allocation is most critical.

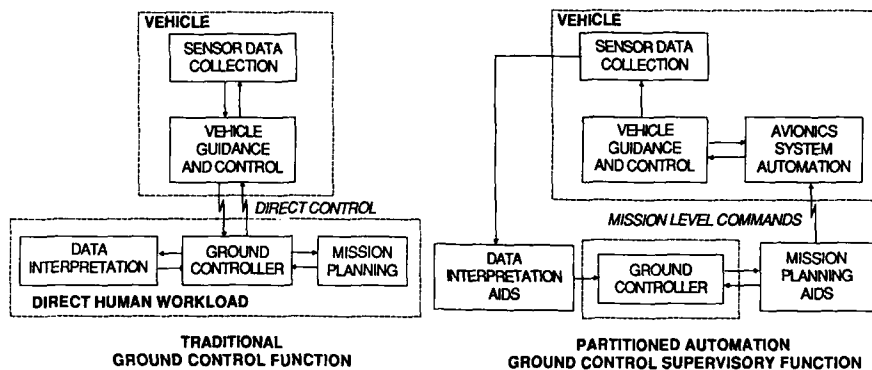


Figure 3. Alternative Control System Architectures

An added benefit to this supervisory approach is found in a closer internetting of the UAV operation with other assets and units through a decreased flight control workload, allowing interoperability requirements to be considered for both in-flight route replanning and real-time product analysis and distribution above and beyond the direct customer needs.

Along with deployability and flexibility, interoperability is one of the three major system requirements in the UAV operational environment. In addition to possible interoperability for higher level product dissemination through JTIDS and possibly JSIPS, tactical considerations have yet to be addressed such as integration of UAV flights into both air defense and close air support plans. If you add to this scene multiple and initially unidentified and unplanned UAV track files, the workload on the air defense component is unnecessarily increased and might impact overall system performance. Besides IFF, a pre-flight, time critical, UAV corridor indication would minimize this potential problem.

From a direct vehicle operation standpoint, in case of temporary or permanent loss of contact with the primary ground control station (GCS) operators, a graceful degradation or secondary network reacquisition capability as a complement to self-destruction could be built into the platform. Although unitary cost objectives are low, a direct loss correlation between the ground station and the platform might be unnecessarily rigid and avoidable. This could be achieved through a combination of an autonomous Return To Base (RTB) capability and reacquisition interrogation from the platform should loss of contact exceed either preset time lines or GCS link be non-available at predetermined waypoints.

#### **ACTIVE TARGET LOCATION USING INTEGRATED GPS WITH PHOTOTARGETING TECHNIQUES**

Navigation is elevated to critical importance in the UAV, not only because of the need for reliable, autonomous, remote performance, but for the task of target location as well. Inertial systems are attractive because of their extreme short-term precision and availability of attitude as well as position data. Unfortunately, vehicle size constraints the use of very small units whose drift characteristics are excessive for mission requirements. The solution is to add GPS to the architecture which provides the long-term stability as well as dissimilar redundancy to meet reliability requirements.

The Navstar Global Positioning System has demonstrated impressive absolute accuracy in tests and operational use. Most applications will benefit from the increased accuracy afforded by GPS over conventional systems. However, UAV applications may require even better accuracy than GPS can provide in the standalone mode.

Differential GPS is a concept that eliminates some of the common, bias errors experienced by conventional GPS. Differential GPS derives its potential from the fact that the measurement errors are highly correlated between different users (as well as highly autocorrelated). By employing a second GPS receiver with comparison to truth, slowly varying, correlated errors can be isolated and eliminated. In addition, depending on the relative rates, Selective Availability (SA), intentional degradation of the C/A signal, may be eliminated by differential GPS as well [2]. Measurement errors are also highly correlated between satellites for any

particular user, but such common errors are removed by the conventional GPS solution as they are indistinguishable from user clock bias, hence corrupt only that estimate.

Differential GPS is a practical solution in many situations, providing few-meter level accuracy under dynamic conditions. It has been noted that the majority of error sources are related to the satellites and the propagation environment. With the satellites at approximately 20,000 kilometer altitude, the relative geometry between two close terrestrial sites is very similar, so the range errors tend to be highly correlated in a local geographic area. Conclusive data are not yet available, but the "local" area appears to be as large as 300-600 kilometer before significant spatial decorrelation of the range errors occurs. This area more than adequately covers many applications, such as offshore oil survey, harbor control and navigation, aircraft landing approach, and local military missions.

In differential GPS, a receiver reference station is located in the local area where greater accuracy is desired, as illustrated in Figure 4. The correlated errors that a receiver experiences (such as satellite ephemeris errors) should be common to all users in a relatively close geographical area. If the reference station can obtain a reliable estimate of its actual error and transmit that to dynamic users, the dynamic users may be able to compensate for a large portion of their errors. In the UAV case, the vehicle downlinks its measurements and the differential solution is computed in the groundstation.

The basic task of target location involves the concepts of photogrammetry or phototargeting accomplished free of fiducial landmarks. In this process, the basic collinearity equation of photogrammetry is used to relate the image plane to the terrain plane [3]. The geometry of the problem requires that the object (target) of interest be located in two images taken from different locations. An error budget analysis of the process reveals that the position location accuracy of the vehicle when the image is acquired as well as the angular separation of the two points of image acquisition affect target location accuracy. As an example, for a 5-degree separation in image angles, each meter of position error results in 11 meters of target location error; for a 1-degree separation, the result is 57 meters per meter of vehicle position error.

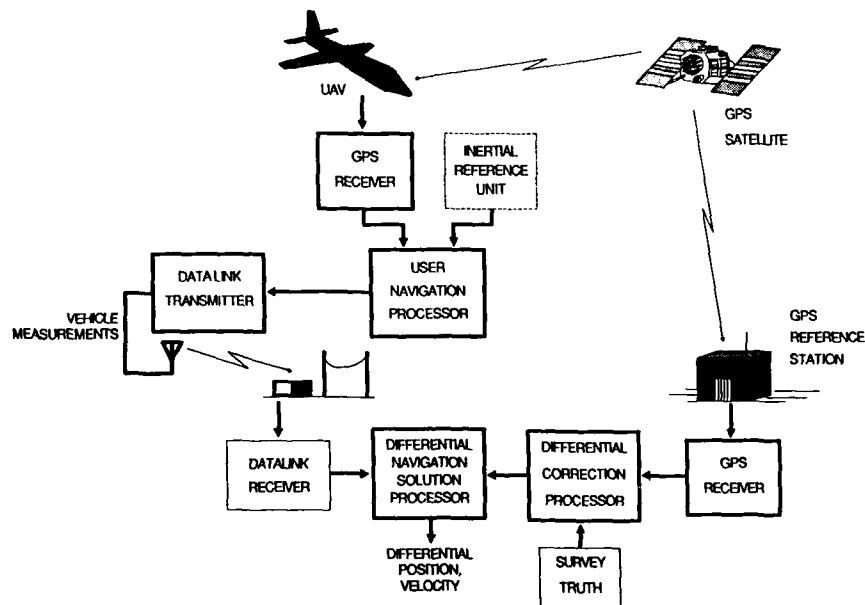


Figure 4. High-Accuracy UAV Positioning with Differential GPS

Some sensors may have ranging capability so that the measurements are azimuth, elevation and range, such that only one image is required (although multiple observations will improve accuracy). For passive (e.g., FLIR) operation, multiple views are required as illustrated in Figure 5.

Aircraft attitude is assumed available from the GPS-calibrated inertial. However, it is possible to determine attitude passively using the photogrammetric method. For images with no known-location landmarks, this attitude can be determined only in a relative sense, however [3]. This requires three common points in two images to accomplish mathematically.

Development of representative mission scenarios for the range of vehicles for which the proposed system might serve as core reference system is an important preliminary design step. Table 2 lists some of the critical mission aspects and their corresponding impact on system design or component specification.

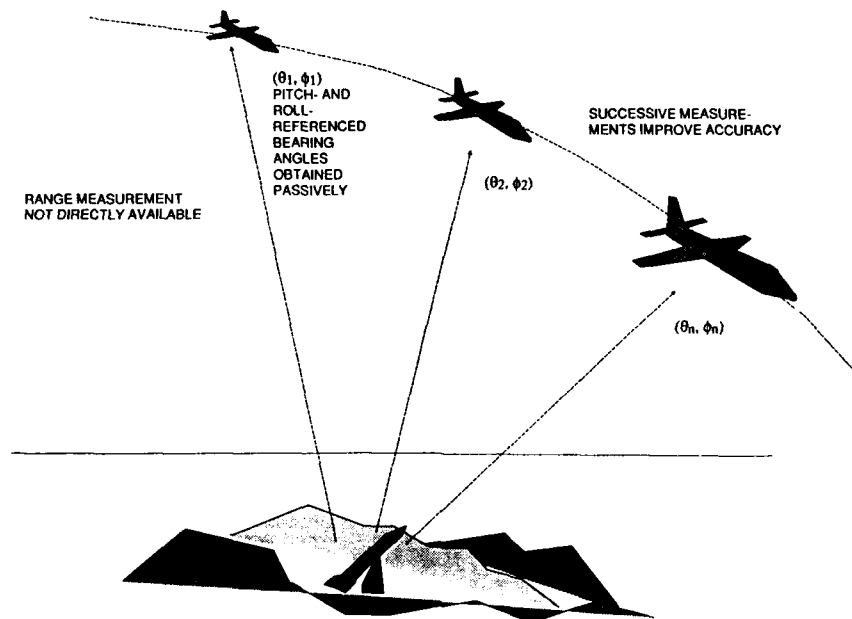


Figure 5. Target Location with Passive Sensing

Table 2. Example Mission Characteristics and System Design Impact

<u>Mission Characteristic</u>	<u>Design Impact</u>
Duration	Reliability, drift linearity
Dynamics	GPS loss-of-lock, g-sensitive drifts, attitude requirements
Targeting	Attitude precision, altitude, nav accuracy
Expendability	Cost, classification
Landing Technique	Autopilot precision, feedback parameters, rate

The missions should be described in terms of their primary objective, and any requirements that those objectives place on the core reference system, and in terms of their spatial and event profiles. The threat environment is defined because of its importance to the GPS jamming performance which is a critical aspect in assuming adequate GPS calibration for the inertial components.

#### Hardware Selection

Selection of an integrated navigation system involves derivation of specifications for the system components and integrated system algorithms. Of particular interest is the performance of the inertial components, since their combined solution provides the essential "process" for the linear and rotational solution. It is important to note that the specifications required for the integrated system are not necessarily those typically reported for inertial components. For example, turn-on to turn-on bias of the inertial instruments is not particularly of interest since the GPS can very precisely estimate and calibrate this bias. Rather, it is the randomness, or higher order terms, of this bias that determines how quickly the component diverges from its compensated estimate when GPS is lost. In other words, in an integrated system, the stability of the error characteristics is of greatest interest.

This characteristic, stability of error characteristics even when their absolute magnitude is large, is the attractive feature of lower cost, solid-state gyros that are applicable to this application. These gyros have large drift characteristics that change each time they are started (turn-on to turn-on). For this reason, they are undesirable for any long-term, uncalibrated application. However, their solid-state nature makes them quite stable for relatively short periods of stand-alone operation. Low-cost gyros have been largely ignored for stand-alone navigation, but there appears to be evidence that their use with GPS is an exploitable innovation.

The accelerometers are somewhat less of a concern. On one hand, their performance is just as critical, or nearly so, as the gyros. Worse yet, there are no easy solutions to improved accelerometer performance. On the other hand, the accelerometers are not big cost drivers to the system, even if significantly more precise instruments are used. Therefore, there are few tradeoffs in hardware selection here, and the task is one of adequate integration software design to adequately compensate the accelerometers.

#### Algorithm Selection

The significant technical issues which drive the design of an algorithm to integrate a core reference system for a UAV can be summarized as follows:

- Minimization of the effect of the expected jamming environment upon navigation and tracking loop performance;
- Filter state design for reference system error estimation and calibration;
- Tolerance to both GPS and IMU hardware failures;
- Adaptability to hardware changes or upgrades.

The algorithm designed to integrate GPS and the inertial components must provide robustness to failures in both of these subsystems. GPS "outages" can be induced by antenna masking, loss of satellite visibility, and high dynamics and/or noise, in addition to receiver hardware failures. Certain "soft failure" mechanisms within GPS must also be tolerated; e.g., in a heavy jamming state, the receiver may not know when code lock has been lost, and pass suspect measurements to the navigation filter. The integrated system must therefore support an inertial-only mode. Inertial component hardware failures, if not accommodated through redundant hardware, dictate that a GPS-only navigation algorithm be utilized. Finally, the algorithm, to the greatest extent possible, should be adaptable to hardware upgrades, e.g., an upgraded inertial system or a GPS receiver with added channels. The algorithm should be designed so that hardware changes can be accommodated by simply changing algorithm parameters.

Common to all integration approaches under consideration is the use of a Kalman filter for optimally blending of the GPS and IMU measurement data, and IMU aiding of the GPS receiver tracking loops. In addition, a barometric altimeter is assumed available for stabilizing the inertial system's vertical channel. Specific, integrated designs which can be considered differ with respect to the following issues:

- IMU error source calibration;
- Estimation of receiver clock frequency error g-sensitivities;
- Use of multiple correlation, extended range detection receivers;
- Use of carrier tracking loop aiding;
- Method of code loop aiding: "partitioned" or "integrated" [4];
- GPS and IMU failure tolerance;
- Utilization of barometric altimeter data.

Ability to estimate IMU error sources is dependent upon the dynamic environment. As a minimum, the Kalman filter should estimate the basic (nine) error states associated with inertial component error propagation, including three position errors, three velocity errors, and three attitude error components. In addition, gyro drift errors must be included due to their effect upon navigation performance in the absence of GPS measurements. Other elements of the state vector are accelerometer biases, scale factor errors, and misalignments (random mounting errors). The accelerometer biases and attitude error will only be jointly observable unless there is in-flight calibration during maneuvers. Observability of accelerometer scale factor errors is strongly dependent upon the dynamic environment; for UAV applications, their estimation is possibly not feasible. Note that g-sensitive gyro drifts must be included if conventional, electro-mechanical gyros are to be considered for the guidance package.

Rate aiding of the code loop when carrier lock has been lost is beneficial for a number of reasons. Since the code loop can tolerate tracking errors up to roughly fifteen meters (P-Code, much larger for C/A-Code), the accuracy requirements on inertial derived velocity are much less stringent. The code loop aiding can be of two general forms: the classical "partitioned" or "integrated" approach. The so-called partitioned approach basically attempts to separate the signal tracking and navigation functions, rather than considering them as a single integrated function. Inertially derived velocity, corrected by Kalman filter estimates, is summed with the outputs of the code loop filter (simply a time varying gain), and used to drive the numerically controlled oscillator. The integrated approach closes the code loop entirely through the Kalman filter, offering some immediate advantages over the partitioned approach. The Kalman filter is able to adjust the code loop bandwidth as a function of both the noise and dynamics environment of the receiver, whereas the partitioned design's bandwidth (proportional to  $k$ ) is adjusted only as a function of the sensed noise environment.

Failure tolerance can generally be enhanced through hardware and/or analytic redundancy. Redundant inertial systems, e.g., a "dual quad" arrangement of gyros and accelerometers, are attractive, together with a parity checking algorithm to enable detection, identification, and removal of failed instruments. Generally, to detect and isolate  $k$  failures requires  $2k + 3$  instruments sensing a three dimensional quantity, e.g., angular velocity. Thus, five gyros are required to detect and remove the effects of a single failure. The "dual quad" mechanization, where two physically separated clusters of inertial instruments (with three input axes along the edges of a cube, and the fourth along the diagonal), is motivated by the potential loss of a single cluster. At any time, only one cluster is used for navigation. Detection of a failure in the active cluster (which requires only 4 gyros) activates the second cluster. The low cost of the sensors and their multi-function application encourages consideration of such architectures and the concomitant rise in reliability.

In addition to detecting "hard" failures, where the instrument produces no useful output, it may also be desirable to compensate for "soft" failures (corresponding to degraded instrument operation). Statistical tests on Kalman filter residuals, coupled with hypothesis testing for the failure mode is generally used, and can provide some measure of analytic redundancy.

If redundant inertial hardware is not available, a backup capability should be supplied, i.e., a GPS only navigation mode. Transitioning to this mode is triggered by Built-In-Test (BIT) detection of a gyro and/or accelerometer failure, and involves a redefinition and restructuring of the Kalman filter. The Kalman filter, up to the downmoding, has been estimating errors in the inertial solution. These states must therefore be redefined to represent errors in the current best estimates of vehicle state; the Kalman filter must operate as an extended Kalman filter following the detected inertial component failure.

Generally speaking, GPS failures are more easily accommodated than inertial failures. The lock detection schemes are fairly reliable, and the integrated navigation solution will degrade gracefully to a calibrated inertial system when GPS measurements are unavailable. There is a specific, possible soft failure mechanism for GPS worthy of specific attention. In a sufficiently heavy jamming state, it is generally very difficult for a GPS receiver to determine if code lock has been maintained with reasonable confidence. Thus, it is possible that invalid pseudorange measurements can be passed to the Kalman filter. As a minimum, the Kalman filter should be made insensitive to this; in addition, with the integrated code loop aiding scheme proposed, the Kalman filter can be utilized in determining the receiver lock status. Several methods can be used to desensitize the filter to suspect pseudoranges, including delaying the correction of the filter state until lock can be determined with certainty, maintaining two parallel Kalman filters (with one filter avoiding the suspect measurements) until lock is determined with some certainty, and delaying measurement updates. Of these three alternatives, the last approach is preferred due to its simplicity: no additional computations are required; rather, the filter needs only to accommodate a variable update interval.

Two basic options exist for using the barometric altimeter data:

- Conventional, constant gain damping of the inertial vertical channel;
- Processing the barometric altimeter as a measurement to the Kalman filter.

The second option is becoming preferred, since the vertical channel is effectively stabilized through the "optimal" Kalman filter gains, rather than a set of "ad hoc" fixed gains. In addition, the barometric altimeter measurement will only be processed when GPS satellite coverage is incomplete (as determined from the covariance matrix). Otherwise, the barometric altimeter bias error is calibrated using an offline filter, such that calibrated barometric altimeter data is available for measurement processing.

Figure 6 represents a high level block diagram for the integrated GPS/inertial navigation system and its interaction with the navigation sensors. As illustrated, the algorithm receives estimated vehicle position, velocity, and attitude from inertial components, and may supply certain moding commands, e.g., those dictating either alignment or navigation. Note that it is assumed that the inertial subsystem includes the (perhaps) redundant set of accelerometers and gyros and any required Failure Detection and Isolation (FDI) software (i.e., parity testing), and the necessary software for calculating vehicle position, velocity, and attitude (in the form of the quaternion or direction cosine matrix between body and geographic frames) from the accelerometer-sensed delta velocity increments and the incremental rotations output by the gyros. The barometric altimeter simply inputs measured altitude to the integration algorithm.

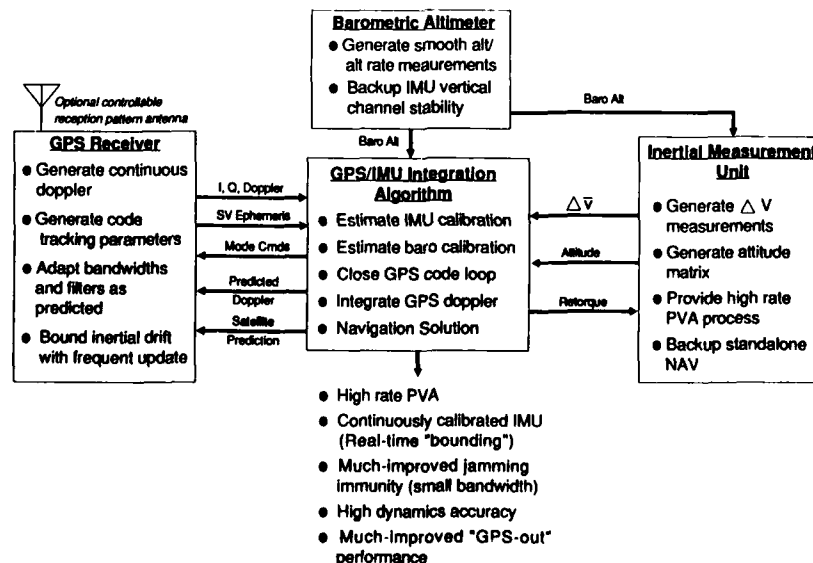


Figure 6. Block Diagram of Integrated Navigation System

The GPS receiver provides measured pseudo and deltarange to the algorithm, in addition to demodulated ephemeris data for each satellite tracked. Software exists in the receiver for code and carrier loop tracking and satellite data demodulation; note that it must be designed to provide open loop detector outputs to the integration algorithm when carrier tracking has been lost, since the Kalman filter closes the code loop. It receives NCO and moding commands from the integration algorithm, providing position and velocity information for signal acquisition and reacquisition, and channel assignment and control information.

#### SUMMARY

Target location in the UAV environment is now feasible due to advances in small, lightweight sensors and advances processing techniques. Combinations of technologies in image processing for target detection and identification, ground control and mission planning, and precise navigation enable this mission capability, but not without significant architectural design and processing challenges. However, with the maturing of some very effective airframe designs, the UAV community is ready for intensive efforts in avionics design and development to achieve these objectives.

#### REFERENCES

1. Ciganer, P., and Denaro, R., "RPVs in the Airland Environment: Technology and Operational Issues," AFCPA Intelligence Symposium, Dalgren, VA, October 1987.
2. Kalafus, R. Vilcans, J., and Knable, N., "Differential Operation of Navstar GPS," NAVIGATION, Volume II, The Institute of Navigation, Washington, DC, March 1983.
3. Moffitt, F.H., and Mikhail, E.M., Photogrammetry, Harper and Row, New York, 1980.
4. Copps, E.M., Geter, G.J., Fidler, W.C., and Grundy, P.A., "Optimal Processing of GPS Signals," Journal of the Institute of Navigation, Vol. 27, No. 3, Fall 1980.

## ACCURATE DETERMINATION OF TARGET LOCATIONS USING UNMANNED AIR VEHICLES

David W. Stroud  
Research Engineer, Sr.  
Lockheed Missiles & Space Company, Inc.  
O/T7-40, B/312  
6800 Burleson Rd.  
Austin, Texas 78744-1016

*Summary. The Aquila unmanned air vehicle system is particularly suited to the problem of accurately locating targets. This paper discusses how the overall system is designed to minimize error sources in the target location calculation. The different targeting algorithms are discussed as well as the means provided in the system for correcting survey errors. Sources are identified which contribute to the error in target location. The ability of Aquila to locate targets accurately and rapidly is discussed as well as the conditions under which the system's capability was demonstrated.*

### Introduction

One of the most useful applications of unmanned air vehicles is providing real-time target location information from the battlefield. Knowledge of what lies over the next hill is invaluable to the maneuver commander. Precise location of targets is an added bonus which can be used to minimize the number of rounds expended to engage a particular target, redeploy forces to meet a changing threat, or avoid areas containing a high concentration of threats.

Accurate automatic target location in unmanned air vehicle systems requires knowledge of the position of the airborne sensor and determination of the target location relative to the airborne sensor. The Aquila system accomplishes this by combining precision navigation information with sensor line-of-sight information.

The Aquila system is particularly well-suited to the task of target location since the system was originally conceived and designed as a target locator/designator for field artillery. The entire system is built to military specifications and capable of deployment and utilization anywhere in the world.

### Aquila System Description

The Aquila system comprises an air vehicle with a choice of electro-optical payloads, a ground control station, an anti-jam datalink, a launch subsystem, a recovery subsystem, a maintenance shelter, and related ground support equipment. The system is built entirely to military specifications and has undergone extensive environmental testing. High reliability, maintainability, and transportability have been demonstrated throughout the full scale engineering development program.

The air vehicle is built of Kevlar epoxy laminates with graphite/epoxy laminates added for strength. Power is provided by a Herbrandson two-cycle, two-cylinder engine. On-board electronics include the flight control computer, attitude reference assembly, recovery guidance beacon, and air data sensors. The flight control computer handles all navigation, flight control, guidance, data link control, and payload sensor control functions. Body attitude and inertial data are provided via the Singer-Kearfott attitude reference assembly. The air data sensors provide true airspeed and barometric altitude measurements to the flight control computer. The recovery guidance beacon is used to guide the air vehicle automatically into the center of the recovery net.

The Aquila air vehicle is designed to accept a variety of payloads. Both a forward looking infra-red (FLIR) sensor and a daylight television sensor have been flown. Aquila is currently fielded with a daylight sensor package manufactured by Westinghouse Electric Corporation. The package consists of an inertially-stabilized platform equipped with a low-light-level, high-resolution optical sensor with laser designation/rangefinder capabilities. The payload operator has control of sensor field-of-view, laser arm/fire designation codes and pulse repetition rates, automatic payload pointing, and automatic payload search patterns. In addition, the operator can manually position the payload line-of-sight with a joystick. The FLIR sensor is produced by Ford Aerospace and is still undergoing integration flight testing, but will be available in late 1988. The Ford FLIR performs the same functions as the Westinghouse payload and is controlled from the same operator's console.

The ground control station is contained inside an S-280 shelter mounted on a 5-ton truck. There are three operator positions: air vehicle operator, mission payload operator, and mission commander. There is room for an additional crew member. The main ground computer is a militarized Norden 11/34 computer with hard disk storage. A ruggedized commercial PDP 11/84 computer will soon replace the 11/34 to expand computing power. Primary operator interface is through the control consoles. Additional interface in the form of mission plan entry, edit, and update is provided through

a standard teletype terminal. Command and control of the datalink is accomplished through an additional control panel mounted on the front of the ground communication equipment.

Harris Corporation provides the anti-jam datalink in the form of their Modular Integrated Communications and Navigation System (MICNS). MICNS is a J-band system which provides a command uplink, a telemetry link (downlink), and a video link. All of these are anti-jam and provide positive command, control, and telemetry in hostile environments. The high level of anti-jam is achieved by spread-spectrum techniques, a highly directional uplink beam, and steerable airborne antennas. In addition, the ground tracker is used as the navigation reference point. Azimuth and range of the air vehicle from the ground tracker are used to update the airborne Kalman filter.

The launch subsystem is manufactured by All American Engineering and comprises a 5-ton, truck-mounted hydraulic rail launcher. The launcher provides ground power and initialization and accelerates the air vehicle to flight speed. A remote initializer is built into the launcher. This initializer is used to initiate the air vehicle power-up sequence and to provide a reference frequency and initial antenna pointing angles to the airborne data terminal.

The recovery subsystem is built by Dornier and consists of a 5-ton, truck-mounted vertical ribbon net and hydraulic braking system. The automatic recovery guidance aid corrects the air vehicle final approach flight path to the center of the net. The braking mechanism decelerates the air vehicle from a flight speed of 130 kilometers per hour to rest in approximately 0.7 seconds. Damage at recovery is rare, and the air vehicle can be readied for launch less than 30 minutes after it is recovered.

The maintenance shelter is an S-280 5-ton, truck-mounted shelter. Automatic test equipment for the air vehicle is contained inside the shelter. The entire fuselage can be mounted inside the shelter for maintenance and trouble-shooting. The maintenance shelter is designed to operate anywhere the ground control station will operate and provides on-site maintenance facilities for all subsystems.

### Locating Targets

Target locations are constructed in the Aquila system from two vectors: the vector from the navigation reference point to the air vehicle (long vector) and the vector from the air vehicle to the target (short vector). A precision navigation system, composed of multiple sensors and mathematical state models, provides long vector information. The navigation reference point is located at the data link tracking antenna. Short vector information relative to the air vehicle body coordinates is derived from sensor line-of-sight data.

Figure 1 portrays the long and short vectors and their relationship to the true target location. The true target location vector and the target location vector calculated by the Aquila system are also shown. The following definitions apply to the vectors shown in Figure 1:

- $\vec{R}_T \equiv$  **Target ground truth location.** This is the vector from ground truth (or where the ground reference system should be located) to the target. This is the actual target location.
- $\vec{R}_G \equiv$  **Survey error.** This is the vector from ground truth to the survey location of the ground reference (in the case of Aquila this is the ground tracker). This vector contains the position and altitude errors in the survey. This is where the ground tracker really is located.
- $\vec{r}_V \equiv$  **Long Vector.** This is the vector from the ground tracker to the air vehicle. This vector includes survey heading error, ground tracker leveling and tracking errors, air vehicle position estimate errors, and air vehicle altitude measurement errors.
- $\vec{r}_T \equiv$  **Short Vector.** This is the vector from the air vehicle to the target. This vector includes sensor pointing and ranging errors.
- $\vec{R} \equiv$  **Calculated Target Location.** This is the vector from the ground tracker to the target. This vector is the sum of the short vector and the long vector. This vector is calculated by the Aquila system and displayed to the operators.

Since the target location calculated and displayed by the Aquila system is a combination of the long and short vectors,  $\vec{R} = \vec{r}_V + \vec{r}_T$ , the displayed target location will contain the accumulated errors from all system sources in addition to the error introduced by the survey.

### Target Location Error Sources

It is convenient when attempting to isolate targeting error sources to establish a number of different reference frames. Studying error sources in this manner allows effects of individual errors to be traced. Mathematical modeling can trace the propagation of a single error into the final calculated target location since the various reference frames are related by

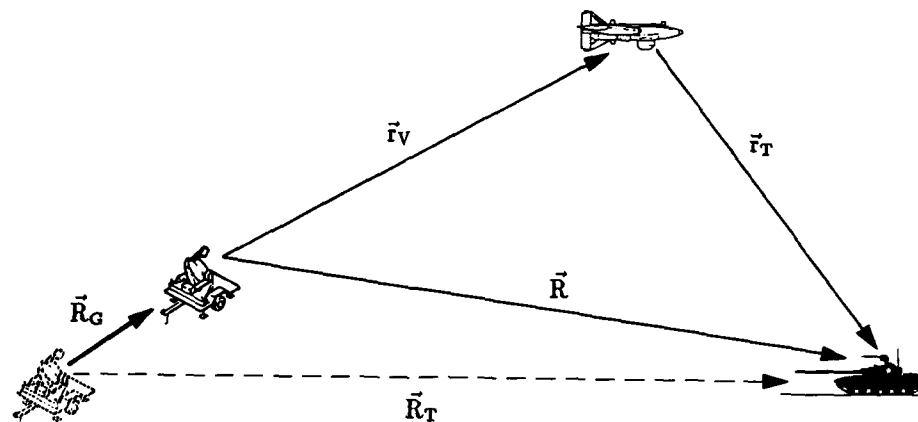


Figure 1: Aquila Targeting Vector Definitions

transformation matrices. The targeting vectors defined in Figure 1 can be described completely by a series of six reference frames as depicted in Figure 2.

The six reference frames in Figure 2 are the ground truth frame, the survey frame, the antenna frame, the ground tracker frame, the vehicle body-axis frame, and the sensor frame. Once error sources have been identified, steps can be taken to reduce the errors. The end product of this process is a more accurate target location.

The overall error in target location is an accumulation of errors from each source. Each reference frame can be thought of as defining a specific number of error sources. Pertinent targeting error sources include: errors in the survey, misalignment of the ground tracker system, tracking errors, orientation errors introduced through the air vehicle instrumentation, errors in range calculation from the air vehicle to the target, and line-of-sight resolution errors in the payload. The following paragraphs describe each error source in detail, and Table 1 is a summary of the error source contributors.

Errors in the survey consist of errors in northing ( $\Delta N_G$ ), easting ( $\Delta E_G$ ), altitude ( $\Delta H_G$ ), and heading reference ( $\Delta \psi_G$ ). These errors are external to the system. Target location accuracy is particularly sensitive to errors in the heading reference ( $\Delta \psi_G$ ). The Aquila system requires a fifth-order survey for emplacement in order to delivery specified targeting accuracies. A fifth-order survey consists of one part error in one thousand parts measured. This translates to 12.5 meters position error and .06° heading error or the same error tolerance as is allowable in emplacing an artillery piece. A standard Precision Azimuth Determination System (PADS) is capable of delivering this level of survey accuracy. Errors accumulated through the survey cannot normally be removed.

Misalignment of the ground tracker system contributes three angular errors. These angular errors correspond to the three standard Euler angles of rotation (roll, pitch, and yaw). An error in yaw ( $\Delta \psi_A$ ) has the same characteristics as a heading reference error. The other two errors, roll ( $\Delta \phi_A$ ) and pitch ( $\Delta \theta_A$ ), are manifested as errors in vertical alignment of the tracker platform. The MICNS ground tracker system has a built-in manual leveling system and a mis-level sensor which warns the operators of alignment errors. Misalignment errors contribute to the overall error in the long vector.

Tracking errors consist of error in the range to air vehicle measurement ( $\Delta r_V$ ) and an azimuth error ( $\Delta \psi_T$ ). Both of these measurements are supplied to the airborne Kalman filter as navigation updates, and any errors are manifested as an erroneous air vehicle location estimate. Errors in elevation (which effectively manifest themselves as ranging errors) can be neglected as a separate source since they are not utilized by the Aquila system for navigation. Tracking errors contribute to the overall error in the long vector.

Instrumentation can introduce errors not only into the air vehicle position estimate (through errors in acceleration measurements), but also into the air vehicle orientation. These errors show up in the standard Euler angles (roll ( $\Delta \phi_V$ ), pitch ( $\Delta \theta_V$ ), and yaw ( $\Delta \psi_V$ )). The altitude sensor can introduce errors into the air vehicle altitude ( $\Delta H_V$ ). These errors are

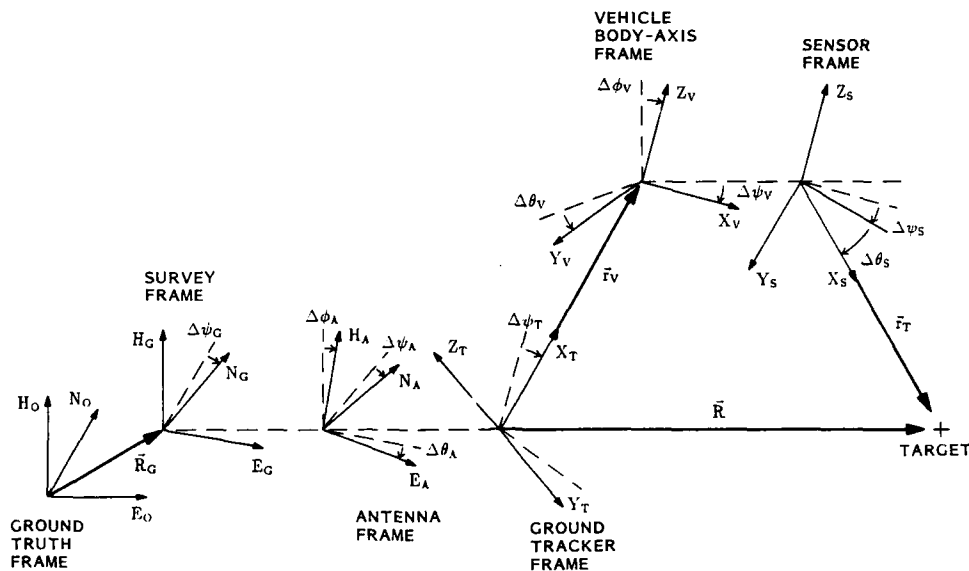


Figure 2: Targeting Error Reference Frames

important since they directly influence the computation of the payload line-of-sight to the target.

Errors introduced through the payload sensor itself include error in the range measurement from the air vehicle to the target ( $\Delta r_T$ ), azimuth error ( $\Delta \psi_S$ ), and elevation error ( $\Delta \theta_S$ ). These sensor errors, in addition to the orientation errors introduced by the air vehicle instrumentation, constitute the total error in the short vector.

Note that the target location computation method employed in the Aquila system does not directly address, nor even take into account, any errors in the surveyed location of the ground tracker. The Aquila system employs a feature, survey update, that is designed to minimize survey errors. Survey update requires targeting two landmarks whose locations are known to at least a fifth-order survey accuracy. The ground computer calculates the landmark locations based on targeting data and compares these to the known landmark locations. Any discrepancy between these two locations is assumed to relate directly to an error in the survey. The ground computer will extract the magnitude of the position and angular error present in the survey. This information can then be utilized by the ground computer to compensate for survey errors. Measured results from flight tests indicate that this method is capable of correcting a map-spotted survey (300-500 meter position error,  $\approx 1^\circ$  heading error) down to fifth-order survey accuracy (12.5 meter position error,  $.06^\circ$  heading error).

#### Computation of Target Location

As stated earlier, the Aquila system calculates target locations from two vectors (the long vector and the short vector). These two vectors are calculated independently and summed in the ground control station to provide the target location. The long vector is derived inside the ground control station computer and is based on downlinked air vehicle position estimates. The short vector is composed of sensor pointing information, air vehicle attitude, and range to target. The short vector is calculated on-board the air vehicle and downlinked to the ground control station.

A precision navigation system composed of multiple sensors and mathematical state models is used to derive the long vector. The Aquila navigation system is broken into two parts: one airborne and one ground-based. The entire navigation system is initialized during prelaunch power-up. The geographical location and heading of the launcher are uplinked from the ground control station to the airborne flight computer. Launcher altitude is uplinked, and the pressure measured by the barometric pressure transducer is correlated with the known altitude.

The airborne navigation system is composed of the attitude reference assembly, the air data sensors (barometric pressure altitude transducer and true airspeed sensors), and an estimator filter. The flight control computer has a 15-state Kalman filter implementation for estimating air vehicle position and velocity. The Kalman filter accepts periodic updates of range and azimuth from the ground tracker. The airborne Kalman filter estimate of air vehicle position (relative to the navigation reference point or ground tracker) is continuously downlinked to the ground control station.

The ground-based navigation system (resident in the ground control station computer) keeps track of both downlinked

Source	Symbol
Survey Errors	$\Delta N_G$
	$\Delta E_G$
	$\Delta H_G$
	$\Delta \psi_G$
Ground Tracker Alignment Errors	$\Delta \psi_A$
	$\Delta \theta_A$
	$\Delta \phi_A$
Tracking Errors	$\Delta r_T$
	$\Delta \psi_T$
Air Vehicle Orientation Errors	$\Delta \psi_V$
	$\Delta \theta_V$
	$\Delta \phi_V$
	$\Delta H_V$
Payload Sensor Errors	$\Delta r_S$
	$\Delta \psi_S$
	$\Delta \theta_S$

Table 1: Target Location Error Source Summary

and measured (by the ground tracker) air vehicle position. The ground navigator determines when navigation updates to the airborne filter are required. The ground navigator also maintains continuous knowledge of the long vector.

The short vector is derived entirely on-board the air vehicle from body attitude information and sensor gimbal measurements. The attitude reference assembly provides highly accurate body attitude measurements. The payload provides gimbal measurements in the form of a direction cosine matrix for the sensor line-of-sight. Both of these measurements are processed by the flight control computer.

The direction of sensor line-of-sight relative to air vehicle body axis orientation is measured directly from the payload gimbals. Two separate methods are provided for determining range to target: passive ranging and active laser ranging. The default ranging method is passive ranging, which is accomplished by mathematically averaging (in a least-squares sense) the intersection points of successive sensor lines-of-sight. This provides a convergent target location solution. Active laser rangefinding provides a nearly-instantaneous range measurement between the sensor and the target. The direction of the sensor line-of-sight in combination with the range from the sensor to the target completely defines the short vector. Short vector information is downlinked to the ground control station.

The downlinked short vector is added to the long vector in the ground control station computer to produce the total vector from the navigation reference point to the target. This resultant target vector is added to the location of the navigation reference point to produce the target location. All computations to this point are accomplished in latitude and longitude. Once the target location is computed, this information is transformed through an algorithm resident in the ground control station computer into standard military Universal Transverse Mercator (UTM) coordinates. These coordinates are displayed on both the payload operator's and the mission commander's consoles.

A perfect system would be expected to deliver the absolute target location, or  $\bar{R}_T$ . Real systems are only able to produce target locations which contain implicit errors (in the case of Aquila,  $\bar{R}$ ). The sources of these errors must be identified, and the magnitude of the errors must be minimized in order to deliver accurate target locations to the operator.

### Aquila Targeting Modes

As described earlier, the Aquila system is equipped with two ranging modes: passive and active. These ranging modes are the basis for the two targeting modes: passive targeting and active targeting. Passive targeting is designed for training and other situations where emitted energy is not desirable. Active targeting is designed for use in tactical environments where rapid target locating is necessary.

Passive targeting is based on algorithms designed to extract short vector information from air vehicle attitude and sensor line-of-sight data. Active targeting uses this data and the range from the air vehicle to the target (provided by the laser rangefinder) to produce the short vector.

#### Passive Targeting

The passive targeting mode is invoked when the operator commands the payload to track a target automatically. When autotracking commences, the airborne flight computer automatically begins accumulating data necessary to generate the short vector. The short vector is downlinked to the ground control station where the target location is computed.

Payload line-of-sight information measured from the payload gimbals along with air vehicle position and attitude es-

Five seconds of data accumulation are required before the initial target location is displayed to the operators. After the initial location is displayed, the target location will be updated once a second as new line-of-sight data is received by the flight control computer and downlinked to the ground control station. Passive targeting mode continues until autotrack of the target is broken.

Active targeting is similar to passive targeting in the sequence of processing to produce short vector information. The primary difference between the two modes is that active targeting uses the laser rangefinder capability of the payload to determine the range from the air vehicle to the target.

Regardless of which active rangefinding mode (single shot or pulsed) is used, the ground control software visually cues the operator that the laser is being fired. The operator is also provided with a cue that the system is calculating a target location based on laser rangefinding data. The resulting target location display remains frozen at the calculated value until the payload operator breaks autotrack of the target or refires the laser.

Various tests have been conducted over the years to determine or demonstrate the capability of the Aquila system to produce accurate target locations. Figure 3 is a summary of tests conducted in relation to the specified target location accuracy.



**Figure 3: Aquila Target Location Accuracy**

Prototype Qualification Testing (PQT) was conducted by Lockheed under the supervision of the U. S. Army Remotely Piloted Vehicle Program Office at Ft. Huachuca, Arizona during the spring of 1985. Test objectives were to demonstrate compliance with specifications. Target boards at surveyed locations were emplaced to provide ground truth reference. A series of tests were conducted for both passive and active targeting at different air vehicle ranges from the ground tracker. As seen in Figure 3, the results from both passive and active targeting are well within the specified limits, with active targeting more accurate than passive.

Development Testing (DT-IIA) was conducted by Lockheed under the supervision of the U. S. Army Test and Evaluation Command at Ft. Huachuca, Arizona during the spring of 1986. Test objectives were to demonstrate that the system was sufficiently developed to enter operational testing. Target boards at surveyed locations were again used for ground truth reference. Since passive targeting is not a specified requirement for the Aquila system, only active targeting accuracy was measured. The results were similar to those demonstrated during Prototype Qualification Testing as seen in Figure 3.

A retest of targeting accuracy to verify proper implementation of software modifications was conducted by Lockheed at Ft. Sill, Oklahoma during the last system software upgrade prior to the start of Army crew training for Operational Testing. Both active and passive targeting were compared to a surveyed ground truth reference. Results on Figure 3 are well within targeting requirements, with active targeting more accurate than passive.

A final demonstration of targeting accuracy was conducted by the U. S. Army Field Artillery School at Ft. Sill, Oklahoma during training for the Force Development Test & Experimentation (FDT&E). The FDT&E was conducted to demonstrate that target detection shortcomings during Operational Testing were corrected with new automated search algorithms. Training for the FDT&E was conducted in September and October of 1987. The objective of this demonstration was to determine whether passive targeting would produce results accurate enough to allow the FDT&E to be conducted without use of the laser. Individual targets (tanks, 5-ton trucks, APCs, etc.) were emplaced, and their locations were surveyed with a Precision Azimuth Determination System. The targets were located first using active targeting and then passive targeting on the same flight. Great care was taken to ensure that the passive targeting algorithm was allowed to converge fully. This demonstration resulted in passive targeting locations that were essentially the same as those obtained in active targeting. Overall targeting results, as seen in Figure 3, were well within the specified accuracy, and the FDT&E was successfully concluded using only passive targeting.

Results from the demonstration conducted during FDT&E training are very interesting. They indicate that the passive targeting algorithm is capable of delivering target locations as accurate as those obtained with active targeting. Analysis of the passive targeting technique reveals that the method employed (least-squares fit) will remove random errors introduced into the range estimate given sufficient time. The remaining errors (assuming small ranging errors using the laser) are the same errors as those present for active targeting. Thus, the two targeting methods should produce the same results.

The limiting factor to the use of passive targeting as the exclusive targeting mode is time or, rather, how much time the operator can afford to spend for a given target accuracy level. Convergence of the algorithm can take upwards of a minute or more depending upon the relative geometry between the air vehicle and the target. This amount of time is unacceptable for many missions since the total number of targets which could be located would be drastically reduced.

An unexpected benefit of the automatic search algorithms implemented for the FDT&E is the automatic guidance of the air vehicle during autosearch. The air vehicle is under automatic guidance during autosearch and maintains an air-vehicle-to-target geometry that is optimal for target detection. This same geometry produces rapid convergence of the passive targeting algorithms, with measured convergence times on the order of 10-15 seconds. Single-shot mode active targeting is still faster, but this convergence time is nearing that of pulsed mode active targeting.

## Conclusions

The Aquila system was originally designed to meet the exacting requirements of the U. S. Army artillery as a locator/designator. The Army wanted a system which would provide real-time video imagery of the battlefield and allow accurate targeting for artillery. The system would have to be able to operate and survive in the environment near the forward line of troops. To accommodate these stringent requirements, the Aquila system was carefully designed from the ground support equipment to the air vehicle. Reliability and survivability were blended into a system designed to provide the most accurate unmanned targeting system in the world.

From Prototype Qualification Testing through Developmental and Operational Testing, Aquila has undergone an extensive full-scale engineering development program. Aquila has proven itself to be a reliable and mature system and has repeatedly demonstrated its capability to deliver accurate target locations under all conditions.

**SYNTHESIS OF CONTROL LAW,  
ON A RPV,  
IN ORDER TO MINIMIZE THE NUMBER OF SENSORS.**

by

Jean-Luc BOIFFIER

ECOLE NATIONALE DE L'AERONAUTIQUE ET DE L'ESPACE  
BP 4032 - 31055 TOULOUSE CEDEX - FRANCE

**ABSTRACT**

Sup'Aéro is a French Aeronautics Engineering Institute, which has been interested in RPV since 1984. The school has built two 25 kg RPV, and has been demonstrating its capabilities in flight. This RPV is equipped with a digital computer which enables the plane to be under automatic control for a sea skimmer flight. Sup'Aéro is now involved in a 50 kg RPV project, with a 20 kg payload under 300 W, for a flight of 2500m high and 6 hour flying time. The first flight is planned for 1990. This specifications need to pay special attention to the weights. One kilo represents 15 % of the performance.

The airplane configuration has been optimised to minimise the weights of the airframe and fuel. Optimal wing area, aspect ratio, area ratio between front and rear lifting surfaces, etc ... have been found. The avionic systems have been treated with the same effort. In particular, control laws have been studied in order to reduce the number of sensors needed to control and guide the plane. In particular this paper describes a method of avoiding the installation of a vertical gyroscope, which is a heavy sensor, for this kind of RPV. The lighter the plane is, the more this proposition is interesting.

In the first part of this paper the plane and turbulence are described, and in the second part, the automatic lateral control is presented. The following topics are approached: Adjustment of the natural mode of the plane in order to reduce the sensivity of the plane under the effect of turbulence, basic control law by LQ method, installation of wash-out filters on the measurement to avoid drift sensors effect, optimisation of the wash-out frequency and general performances with and without bank and heading angle measurement.

**NOMENCLATURE**

$\sigma$	standard deviation (rms)		
p	probability of exceeding a given $\sigma$ on turbulence		
L	scale of turbulence (m)	$\psi$	heading angle (rad)
$\tau$	time constant (s)	$\phi$	bank angle (rad)
$\xi$	damping ratio	$\beta$	slideslip angle (rad)
b	wing span (m)	p	roll rate (rad/s)
f <sub>wo</sub>	wash out frequency (Hz)	r	yaw rate (rad/s)
s	Laplace operator	n	lateral load factor (g)
$\delta$	aileron control (rad)	$\delta_n$	rudder control (rad)
H	altitude (m)		

**ABBREVIATIONS**

AP autopilot      LF low frequency      HF high frequency

**1 - DESCRIPTION OF THE PLANE AND TURBULENCE**

**11 - THE PLANE**

The plane now being developed is a light one, 50 kg maximum take off weight. The interest of such a light weight is easier handling, and also a reduced price, if it can be assumed that the price is proportionnal to the total weight. A light RPV, means a light payload, it is hoped that this plane will obtain a 20 kg operationnal payload, dedicated for one mission. It is an ambitious assumption today, but with the normal rate of decreasing mass and volume of the avionics system, this goal could be reached in few years. An operationnal mission could be achieved with a 20 kg payload. On the other hand, it is not sure that a multipurpose RPV is the best answer from an economical point of view. In that case, a light RPV will present a greater interest.

Weights of some equipment, specially the sensors, are independent of the maximum take-off weight. The lighter the plane, the more it is suitable to fly with the minimum of sensors. For example, on the 50 kg RPV, one kg represent 15 % of the performance in term of fuel. A current vertical gyroscope weighs more than one kg, therefore there is a specific interest to avoid the installation of this sensor. In addition, it is an expensive and fragile instrument.

Optimisation also affects the plane configuration. The optimum is researched in order to minimize the airframe, engine, and fuel weight. For a six hour mission, an optimum for the wing surface is 1.2 m<sup>2</sup>; for the aspect ratio it is around 14, and for the ratio between the front and rear aerodynamic surface there is an advantage for the conventional airplane. The canard airplane is not the best configuration: the analysis shows that the major effect is the increasing

drag of the rear wing due to the down-wash. And the worst configuration is a canard of half the surface of the rear wing. But with a constraint on the wing span, under a given value, the optimum is a twin wing airplane (see figure 1). This value is around 2.5 m for this RPV plane, 3.0 m for a 12 hour mission airplane. Even though for the airframe the twin wing is always an optimum, in the case of wing span constraint, the major effect is an increasing of the aspect ratio of each wing, in regard to a single wing, which improves the aerodynamics performances.

The twin wing has the advantage of a good damping ratio on the short period longitudinal oscillation ( $Cmq$ ), which could avoid the installation of pitch rate gyrometer. It also has the advantage of allowing the control of the plane by the front wing as well as the rear wing. In case of actuator failure, a reconfiguration is possible to save the plane. The RPV studied is the twin wing plane whose drawing is shown figure 1bis.

The chosen, landing configuration, flight point is 10m altitude and 33 m/s speed. Low altitude and low speed are the most severe flight conditions because of turbulence and the natural behavior of the plane.

## 12 - DESCRIPTION OF TURBULENCE

Turbulence is taken as the test perturbation for the adjustment of autopilot of the RPV. It has three components  $uw$ ,  $vw$ ,  $w$ , longitudinal, lateral and vertical wind speeds. For the lateral motion, the longitudinal wind variation along the wing span  $y$  is equivalent to yaw rate speed  $rw2$ . The lateral wind  $vw$  is equivalent to sideslip angle  $\beta w = -vw/V$ , and by its derived value to yaw rate  $rw1 = -\dot{\beta} w / V = -\dot{\beta} w$ . The lateral wind variation along wing span is equivalent to a roll rate  $pw$ . Two yaw rate perturbation exist,  $rw1$  is the influence on the vertical tail plane, and  $rw2$  is the influence on the wing. It is estimated that the relative influence of the two yaw rate on the plane is  $2/3$  and  $1/3$ , the resulting yaw rate is  $rw = 2/3 rw1 + 1/3 rw2$ . The wind model output is  $\beta w$ ,  $rw$ ,  $pw$  and the perturbation matrix of the plane is composed of aerodynamics forces sensitive to sideslip, yaw and roll.

The general hypothesis on turbulence are described in ref. [1]. Turbulence models are characterized by their level, defined by the standard deviation  $\sigma$ , and by their bandwidth, defined by the scale of turbulence  $L$ . The power spectrum used, is a Dryden model. A summary of various models is described, for two altitudes: 10 m for take-off and landing, and 2500 m for cruise.

MIL - F - 8785 C [2]

Standard deviation  $\sigma_u = \sigma_v = \sigma_w = \sigma$

$\sigma < 1$  m/s light  $\sigma = 1.5$  m/s moderate ( $p=0.1$ )  $\sigma = 2.1$  m/s ( $p = 0.01$ )

$\sigma = 3$  m/s severe ( $p < 10^{-4}$ )  $\sigma_p = 1.9 \sigma_w / (L_w b)^{1/2}$

Bandwith:  $h1 = 1750$  ft  $H > h1$   $L_u = L_v = L_w = h1$

$H < h1$   $L_u = L_v = (h1^2 H)^{1/3}$   $L_w = H$

Time constant:  $\tau_u = L_u / V$   $\tau_v = L_v / 2V$   $\tau_w = L_w / 2V$   $\tau_p = 2.6 V / (L_w b)^{1/2}$

ETKIN [1]

Bandwith:  $h1 = 200$  ft

$H > h1$   $L_v = L_w = 2.1 H^{0.73}$  in ft  $L_u = 2 L_v$

$H < h1$   $L_w = L_v = 20 (H)^{1/2}$  in ft  $L_u = 0.4 H$

Time constant:  $\tau_u = L_u / V$   $\tau_v = L_v / V$   $\tau_w = L_w / V$

AC - 120 41 FAA [3]

Standard deviation:  $H = 0$  m  $\sigma_u = 1.7$  m/s  $\sigma_v = 1.4$  m/s  $\sigma_w = 1.2$  m/s

$H = 2500$  m  $\sigma_u = 2$  m/s  $\sigma_v = 1.6$  m/s  $\sigma_w = 1.6$  m/s

Bandwith:  $H = 0$  m  $L_u = 32$  m  $L_v = 15$  m  $L_w = 3$  m

$H = 2500$  m  $L_u = 60$  m  $L_v = 30$  m  $L_w = 12$  m

Time constant:  $\tau_u = L_u / V$   $\tau_v = L_v / 2V$   $\tau_w = L_w / 2V$

AC - 20 57 A FAA [4]

Standard deviation:  $\sigma_u = 0.15$  longitudinal wind  $\sigma_v = 0.15$  lateral wind  $\sigma_w = 0.7$  m/s

Bandwith:  $L_v = L_u = 180$  m  $L_w = 9$  m

Low altitude turbulence has been chosen in order to create the most severe conditions in level and frequency. It is assumed that  $\sigma_2 = \sigma_p$ , the phenomena being of the same kind. Note that in the Boeing model RD - 74 206 [5]  $pw$  is considered as negligible. As a consequence, the turbulence model chosen, can provoke severe conditions, specially in regard to the LF on  $pw$  which is a hard constraint for the AP, and probably not realistic.

There is a large variation of the bandwidth from one model to another one. The chosen level of turbulence is the moderate wind of MIL, which is the the STOL certification wind. And the chosen bandwidth is the larger one. Then  $\sigma_v = 1.5$  m/s,  $\sigma_2 = 0.6$  rad/s,  $\sigma_p = 0.6$  rad/s and  $\tau_v = 0.1$  s which affects  $\beta$  and  $rw1$ ,  $\tau_2 = 15$  s,  $\tau_p = 10$  s. To generate  $rw1$ , the white noise has to be pseudo derived. For this filter, the time constant  $\tau_f = 0.05$  s is taken.

The time simulation of turbulence, over 60s, can be seen on the figure 2.

## SUMMARY TABLE:

kp so that  $\sigma_p = k_p \cdot \sigma_w$ , and kp from MIL model  
 $H=10m$   $V=33m/s$   $b=2.5m$

$H=2500m$   $V=33m/s$   $b=2.5m$

	MIL	ETKIN	AC120-41	AC20-57A		MIL	ETKIN	AC120-41	AC20-57A
Lu (m)	137	33.3	32.2	182	Lu (m)	2500	918	60	182
Lv	137	3.7	15.1	182	Lv	2500	460	30	182
Lw	10	3.7	3.2	9	Lw	2500	460	12	9
$\tau_u$ (s)	4.2	1	1	5.5	$\tau_u$ (s)	75	28	1.8	5.5
$\tau_v$	2.1	0.11	0.25	5.5	$\tau_v$	37	14	0.45	5.5
$\tau_w$	2.1	0.11	0.05	0.3	$\tau_w$	37	14	0.2	0.3
$\tau_p$ (MIL)	1.1	29	29	18	$\tau_p$ (MIL)	1.1	2.5	15.7	18
kp (MIL)	0.38	0.64	0.64	0.4	kp (MIL)	0.024	0.056	0.35	0.4

## 2 - AUTOMATIC CONTROL

The plane is a stable system, so it can recognize vertical direction. Its stability depends on the center gravity position for the longitudinal motion, and the spiral adjustment for the lateral motion. However the modes which brings it back to the vertical direction are slow.

This slow mode in longitudinal is the altitude convergence mode, and it could be accelerated if the propulsion force could decrease more with speed or altitude. This needs a pressure sensor which is equivalent to the measurement of altitude, the same as a conventional control.

The slow mode in lateral is the spiral mode, and it could be accelerated by the adjustment of the airplane, in particular by the dihedral effect. Therefore a sensor is not needed. The spiral mode can then be used to compensate the lack of vertical gyroscope.

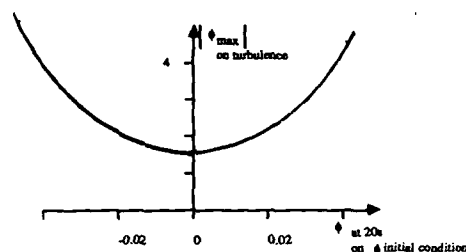
Even if the plane recognizes vertical direction, the heading angle is unknown, due to the plane isotropy of the earth environment. Therefore the heading angle measurement cannot be avoided.

Except for the light altitude pressure sensors, position sensors, that is to say verticals and heading angles, are heavy. Speed and acceleration sensors are lighter, such as gyrometer, pressure transducer, and accelerometer. Then in longitudinal, it could be advantageous to design an autopilot without pitch angle measurement. And in lateral, an autopilot without bank angle measurement will give a precious reduction on weight. An automatic control with only speed measurements, however will give position errors due to the drift of the sensors. For the longitudinal motion, the altimetric sensor will correct the position, though it will lack pitch angle information. For the lateral, owing to the fact that the heading angle of the plane is unknown, this measurement will be necessary for guidance. The control of the bank angle could be achieved at high frequency by integration of roll rate, and at low frequency by the natural plane or the derivative of the heading angle.

The lateral autopilot will be treated in this way. In a first phase the natural plane will be adjusted to minimise its sensitivity to the perturbation. Then an autopilot with LQ method will be defined. The measurement will be filtered by wash out, and the best adjustment of the filter frequency can be found. The observation of bank angle will be discussed and the utility of heading angle measurement in low frequency band will be studied. At the end of this report the robustness of the autopilot to plane model error and to the inboard constraints will be examined.

## 21 - NATURAL PLANE

The plane is described § 11. The natural plane is adjusted in order to obtain a fast return on low frequency. The spiral mode is accelerated inside a reasonable physical boundary, or with regard to the connected behaviour with the Dutch roll mode. For this kind of plane, the obtained optimum adjustment in this situation, is not the faster spiral mode, but the one which has a good connection with the Dutch roll mode, such as the spiral mode cannot be observed on bank angle. Therefore the Dutch roll mode makes the bank angle on initial condition return to zero, with oscillation around zero. This optimum reduces the level on the bank angle, when the plane is perturbed by turbulence, due to less sensitivity of the plane to low frequency. See the diagram below:



With a given fin surface ( $0.05 \text{ m}^2$ ), increasing the dihedral effect ( $Cl\beta$  from  $-1.8$  to  $-2.2$ ), the time constant decreases from  $140\text{s}$  (plane N°3) to  $28\text{s}$ . But the maximum value of bank angle on turbulence change from  $5\text{rad}$  to  $2.3\text{rad}$ , with a minimum at  $1.5\text{rad}$  for a plane with a spiral time constant at  $47\text{s}$ . Another example is a plane with a reduced fin surface ( $0.045 \text{ m}^2$ ) and a  $Cl\beta = -1.8$  (plane N°10) which gives a spiral time constant of  $42\text{s}$ , but a larger level of bank angle. The comparison of the time response of these various plane is given figures 3 to 5.

It is obvious that a value of  $5\text{rad}$ , on bank angle response, has no physical meaning, unless that the plane has no future with such a turbulence. But it could be used for comparison between various solutions. As it is a linear system, with a smaller level of turbulence, it should become realistic.

The basic plane will be the number 1, with following modes:

Dutch roll frequency  $0.26 \text{ Hz}$  damping ratio  $0.12$   
 rolling time constant  $0.076\text{s}$   
 spiral time constant  $47\text{s}$

It is equipped with actuator, modeled by a first order, on roll axis  $0.06\text{s}$ , on yaw axis  $0.1\text{s}$ .

The performance of the natural plane on a  $60\text{s}$  turbulence simulation is:

	$\phi$	$\beta$	$n$	$p$	$r$	$\psi$
maximum:	1.47	0.27	0.14	1.6	0.24	6.3
standard deviation:	0.52	0.12	0.06	0.55	0.13	2.8

The time of  $60\text{s}$  is a compromise between the precision of the standard deviation and an reasonable processing time.

## 22 - BASIC LATERAL AUTOPILOT

This autopilot is designed by the *LQ method* which lies in the minimization of th. criteria

$C = \int (XQX + URU) dt$ , on the linear system  $\dot{X} = AX + BU$ . The result is obtained by the solution of the Riccati equation:  $U = GX$ . Therefore the control is a state feedback.

Three criterias guide the adjustment of the autopilot:

- 1- Adjustment of the modes to obtain not too quick of a response, compared with the actuator rapidity.
- 2- Weigh the control surface order to obtain a reasonable gain on the feedback state, and to limit the maximum level of control surface angle to  $0.35\text{rad}$ , on the basic turbulence.

3- Analysis of the performances on typical perturbation: turbulence, initial condition, constant wind, ...

A compromise is obtained with these weights:  $n_y=100$   $p=1.E-05$   $r=0.1$   $\phi=5$   $\beta=3$   $p=0.01$   $r=7$   $dlc=1$   $dnc=1.5$

The modes of the plane with autopilot are:

Equivalent Dutch roll: frequency  $0.28 \text{ Hz}$  damping ratio  $0.5$   
 Equivalent roll and spiral mode: frequency  $2.22\text{Hz}$  damping ratio  $0.83$   
 Actuator mode: time constant  $0.056\text{s}$  and  $0.1\text{s}$

And the gain on feedback state:

	$\phi$	$\beta$	$p$	$r$	$dl$	$dn$
$dl$	2.1	-1.4	0.16	0.94	-0.67	-0.05
$dn$	-0.73	0.1	0.007	2.9	-0.02	-0.16

The Dutch roll frequency is uncontrollable, and the damping ratio cannot be increased over  $0.5$ . The roll and spiral modes rapidly become a second order mode, which is easily controllable. With a weighing of the heading angle, a first order mode appears around  $3\text{s}$  without any modification. But the gains on slideslip which move on  $dl$  from  $-1.4$  to  $0.6$ , and on  $dn$  from  $0.1$  to  $0.6$ .

The performances (see figure 6) given by the autopilot reduce  $90\%$  of the level on bank angle,  $20\%$  on slideslip,  $10\%$  on lateral load factor,  $75\%$  on roll rate and  $60\%$  on yaw rate. The maximum levels explored by the control surfaces are  $0.31\text{rad}$  on  $dn$ , and  $0.20\text{rad}$  on  $dl$ . The plane time response to an initial condition on bank angle is given in figure 7.

The basic observations on lateral autopilot are first for  $dl$ ,  $dn$ , then slideslip, and bank angle. The  $dl$  and  $dn$  are observed with the control order thanks to the actuator model. The slideslip angle is observed by the lateral load factor because of the relationship:  $n_y = -0.506 \beta + 0.028 dn$ . There almost is a proportionality between  $n_y$  and  $\beta$ . Bank angle is observed by integration of roll rate. The consequence being that the order of autopilot is augmented. Another way to observe the bank angle for the low frequencies will be shown. Without noise and drift on sensors, all these autopilots are strictly equivalent.

In the following text, the autopilot will be name by the input. That is to say  $\phi$ ,  $n$ ,  $p$ ,  $r$  or  $n$ ,  $p$ ,  $r$ .

### 23 - AUTOPILOT WITHOUT BANK ANGLE MEASUREMENT

With an ideal environment, autopilots with and without bank angle are equivalent. The troubles appear with defectiveness of the measurements, specially sensor drift to which the bank angle observation is particularly sensitive. The effects of the drift will be examined on the various autopilots. The method used to eliminate the drift is a filtering of the measurement, with a second order wash out. The problem created, will be analysed. Then, a method will be proposed to optimise the adjustment of the wash out filter.

#### 231 - DRIFT OF THE SENSORS

The employed sensors are a vertical gyroscope ( $\phi$ ), gyrometers ( $p, r$ ), and an accelerometer ( $n_y$ ). The basic sensors taking into account are good aeronautical sensors, but not the best of them. The drift for gyrometer and accelerometer is due in principal to temperature variation, which is estimate at  $0.05^\circ\text{C/s}$  for this plane. The basic value for noise and drift are:

bank angle: noise =  $7 \cdot 10^{-3}\text{rad}$  drift =  $3 \cdot 10^{-4}\text{rad/s}$   
 roll and yaw rate: noise =  $1.2 \cdot 10^{-3}\text{rad/s}$  drift =  $7 \cdot 10^{-5} (\text{rad/s})/\text{s}$   
 load factor: noise =  $0.01g$  drift =  $5 \cdot 10^{-4}g/\text{s}$

The sensivity of the plane with autopilot, to the drifts is evaluated.

#### FOR THE $\phi$ , $N$ , $P$ , $R$ AUTOPILOT:

The response to normed drifts is obtained by a 20s simulation. We examine the response of the plane and the measurement. For exemple on  $\phi$ ;  $md\phi = \phi + d\phi$   $\phi$ =plane response,  $d\phi$ = drift of the sensor (here  $1\text{rad/s}$ ),  $md\phi$ = measurement on  $\phi$ . The analysis of  $md\phi$   $mdn$   $mdp$  and  $mdr$  fonction of time, allows to find this linear relationship:

$$MD = CD \cdot DM + BD$$

$MD^t = (md\phi \quad mdn \quad mdp \quad mdr)$   $DM^t = (d\phi \quad dn \quad dp \quad dr)$ ,  $CD$  and  $BD$  four.four matrix gives the slope and the bias issue from the drift.

$DM$  is in formula:  $DM = DMA \cdot t + DMB$  (here  $DMB = 0$  simultaneous drift)

$MD$  is in formula:  $MD = MDA \cdot t + MDB$

$t^n$ :  $n$   $MDA = CD \cdot DMA$  and  $MDB = BD \cdot DMA + CD \cdot DMB$

$$CD = \begin{bmatrix} 0.14 & -1.1 & -0.07 & -0.5 \\ 0.05 & 1.0 & 0. & -0.15 \\ 0. & 0. & 0.99 & 0. \\ -0.23 & -0.32 & -0.02 & 0.79 \end{bmatrix}$$

$$BD = \begin{bmatrix} 0. & 0.93 & 0. & 0. \\ -0.1 & 0. & 0. & 0. \\ -0.8 & -1.0 & 0. & -0.44 \\ 0. & 0. & 0. & -1.5 \end{bmatrix}$$

It can be noted that  $CD$  is not reversible, therefore no identification of  $DMA$  and  $DMB$  is allowed on the low frequency measurement signal. The ratio between the first and last column is  $0.29$  which is almost  $g/V$ , the ratio between  $r$  and  $\phi$  at equilibrium. The analysis of  $CD$  shows that drift effect is visible on  $n$ ,  $p$ , and  $r$  measurement, when the diagonal is composed with 1. This is not true for  $\phi$ , since only 15% of the  $\phi$  drift appears on the measure of  $\phi$ . This means that the autopilot follows a  $\phi$  order well, and not  $n$ ,  $p$ ,  $r$ , order. Indeed if the plane response is examined, it is observed that:

$$M = MD - I \cdot DM = (CD - I) \cdot DM + BD \cdot DMA \quad CDD = CD - I \quad I = \text{unit matrix}$$

$$CDD = \begin{bmatrix} -0.86 & -1.1 & -0.07 & -0.5 \\ & 0.03 & & \\ & & -0.006 & \\ & & & -0.22 \end{bmatrix}$$

$DM$  is considered as an order, it could be seen that there no response on  $p$ , 3% on  $n$  but inverse, 22% on  $r$ , and 85% on  $\phi$ . This is not a problem for  $n$  and  $p$  because the equilibrium in lateral motion is a stabilize turn, where  $p$  and  $n$  is zero if  $\phi$  is moderate.

The effect of the basic sensor drift on the bank angle, with the basis of a 20s time simulation is now closely examine.  $\phi$  is issue of CDD and BD  $\Delta\phi r20 = -6.9 \cdot 10^{-4} \text{rad}$   $\Delta\phi p20 = 1. \cdot 10^{-4} \text{rad}$   $\Delta\phi n20 = -1.1 \cdot 10^{-2} \text{rad}$   $\Delta\phi\phi20 = -0.5 \cdot 10^{-2} \text{rad}$

For this autopilot, the drift on  $\phi$  and  $n$  are the most effective. These results however are relative because they are sensitive to autopilot performances. For example with the same autopilot, and a weight on the heading angle, this two factor give an major effectiveness of the drift on  $r$ . Therefore there is no longer a response of the drift on the  $r$  measurement, when the drift of  $\phi$  is visible. Later it will be shown that this result is moderated by the wash out filter on measurements.

FOR THE N, P, R, AUTOPILOT :

CD is equal to

$$CD = \begin{bmatrix} 1.1 & 0.73 & -0.08 \\ -0.08 & 0.54 & -0.05 \\ -0.8 & -3.3 & 0.62 \end{bmatrix}$$

Half of the drift of  $p$  and  $r$  is seen on the measurement. The effect of the basic drift on  $\phi$  for 20s time simulation is:  $\Delta\phi n20 = -2 \cdot 10^{-2} \text{rad}$   $\Delta\phi p20 = -1.1 \cdot 10^{-2} \text{rad}$   $\Delta\phi r20 = -0.2 \cdot 10^{-2} \text{rad}$ . The drifts on  $n$  and  $p$  are the most effective, and the effectiveness is double in comparison with the  $\phi$ ,  $n$ ,  $p$ ,  $r$ , autopilot. This obviously shows the increasing sensitivity of the autopilot to the sensor drift, when the number of measurement decreases.

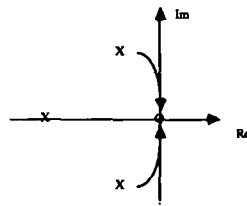
The conclusion is that the effects of sensor drift depend on the adjustment of the autopilot. This could be used to give a special importance to a sensor, depending on its drift performance.

### 232 - WASH OUT FILTER INSTALLATION

In order to eliminate the sensor drift, a second order wash out is installed on the measurement. The input of the autopilot will be, for example on the bank angle, the following formula:

$$\phi_{wo} = \phi \cdot s^2 / (s^2 + 2\xi\omega s + \omega^2)$$

With  $\xi = 0.707$  and  $\omega$  defined by the WO frequency  $f_{wo} = \omega/2\pi$ . The same WO are installed on each measurement to avoid phase shift. The installation of these WO creates a low frequency mode. For example on the  $\phi$ ,  $n$ ,  $p$ ,  $r$  AP, an WO at  $f_{wo} = 0.02 \text{ Hz}$  gives a low frequency mode at  $f = 0.001 \text{ Hz}$  and  $\xi = 0.18$ . For the  $n$ ,  $p$ ,  $r$ , AP  $f = 0.002 \text{ Hz}$  and  $\xi = 0.17$ . The others modes do not move, that is to say the basic mode of the plane with AP, and the WO mode, except for one which becomes a LF mode. On a monovariable system, it can be shown that the poles have a tendency to move toward the zeros, and all the more so, when the value of the control gain is high.



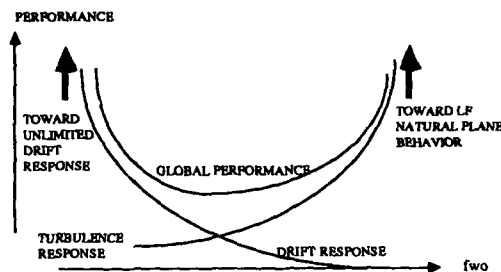
By analogy, on multivariable systems, the created low frequency mode is justified, by the fact that the WO places a lot of zeros on the zero point. This zero becomes a good attractive point, which draw to it the closer mode, that is to say one WO mode. It can be seen that the LF mode is faster for the  $n$ ,  $p$ ,  $r$ , AP because of it has less zero in zero point, due to less WOs. It can be observed, that if the gain decreases (weighing more the control input), the LF mode is accelerate. The more the WO is slow, the more it is close to zero, and therefore the more it is attracted to zero. In this way, a light instability might be reached. A physical explanation could be made, using the response of the plane when input are drifts. It has been stated that the more the AP is efficient the more it follows the drift as an order (it is equivalent to high gain). Therefore the drift is less visible on the measurement. In this case, the WO can eliminate only a reduce part of the drift. This remark is reinforced by the fact that if one measure hides the drift, and if the WO is eliminated on this measure, the LF mode disappears, although the other WO remain. The compromise between AP performances and reduction of the drift will be examined. Furthermore the LF mode could be eliminated by the measurement of the heading angle.

### 233 - ADJUSTMENT OF THE WASH OUT FILTER FREQUENCY

To adjust the frequency of the WOs, a method is proposed in order to optimise the performances of the AP. This method will be applied on the  $\phi$ ,  $n$ ,  $p$ ,  $r$ , AP and on the  $n$ ,  $p$ ,  $r$ , AP (without measurement of  $\phi$ ). Thus the two APs could be compared.

### WO FREQUENCY OPTIMISATION METHOD

For a plane with an AP submitted to a disturbance, such as turbulence, the higher the WO measurement frequency will be, the more the performances will be deteriorated. The natural plane low frequency behavior will progressively appear, and then, little by little, also the high frequencies behavior. For the plane with an AP submitted to a sensor drift, the higher the frequency of the WOs, the more rapidly the drifts will be eliminated. Therefore the drifts will have less effect. The system being linear, the global performance will be considered as the sum of the maximum value of the plane response to turbulence and of the maximum plane response to sensors drift. Then an optimal frequency for the global performance will appear.



The plane will be submitted to a sensor drift of the form  $dc=dt$  proportional to time. The most unfavorable case is when the drift appears simultaneously on each sensor, and this, in the most penalizing sign configuration. It is obvious, for example, that if a constant drift appears and is treated when the plane is on the ground, it will be rapidly eliminated and will not disturb the in-flight performances.

The performance will be observed on  $\phi$  which will condition the plane's safety and performances. Bank angle is a state at a mean level of integration, between heading angle and roll rate, yaw rate.

### FOR THE $\phi$ , N, P, R AUTOPILOT

The results are gathered on the figures 8 and 9. The drift has no effect for  $fwo > 0.15\text{Hz}$ , and the performances with turbulence begin to deteriorate for  $f_c > 0.02\text{Hz}$ . The optimum is reached at  $0.02 < f_c < 0.05\text{Hz}$  and the amplitude explored by  $\phi$  is about twice what was obtained in the ideal case without drift and WOs. The gain with regard to the natural plane remains very important since the attenuation on  $\phi$  is still 78% (compared to 90% in the ideal case), that is to say 12% loss in regard to the ideal AP case. Moving away from the adjustment band gives an important loss of performances.

On the figure 9, the performance on the heading angle can be examined. The degradation of performance is much more perceptible, because of an additional integration with regard to  $\phi$ . This is particularly true for the drift effect and it leads to a larger sensibility to the adjustment of the WOs frequency, the optimum being here at  $0.05\text{Hz}$ . Obviously, the holding of the heading angle requires a heading angle measurement.

The influence of the sensors drift levels is shown by the performance on  $\phi$ . The larger the drift is, the more sensitive is the adjustment of the WO, and the higher its frequency. Inversely, the lower it is, the wider the adjustment band, and the more the optimum moves towards the low frequencies.

There is now available a means to define the classes of the sensors, with regard to airplane performance. This has to be associated with a security bandwidth frequency for the WO adjustment, to take in account the plane model error. This, all the more so, when the sensor drift is high.

On sensor drift input, the time to reach the maximum value of bank angle is:

fwo :	0.1	0.05	0.02	0.01	(Hz)
time:	38	85	234	486	(s)

### FOR THE N, P, R, AUTOPILOT

Figure 10 shows the results. A loss of performance of 15% in regard of the  $\phi$ , n, p, r AP with WO is noted. This leads to a gain of 63%, in regard to the natural plane. The bandwidth for the optimum frequency is narrower, but the optimum frequency stay the same  $0.05\text{Hz}$ . For  $fwo < 0.007\text{Hz}$ , the LF mode becomes instable.

During the plane response on sensor drift, the time to reach the maximum value of bank angle is:

fwo :	0.1	0.05	0.02	0.015	(Hz)
time:	20	50	130	180	(s)

An example of time response to drift input is given in figure 11, for  $fwo=0.05\text{Hz}$ . The sensors drift has twice as much influence on performances, as the AP with bank angle measurement.

The plane's responses to turbulence are given in figure 12, for  $f_{wo}=0.05\text{Hz}$ , and for the two AP. The response to initial condition on bank angle and slideslip are given in figure 13. The initial condition on bank angle is severe, because of the observation of the bank angle by integration of roll rate, without knowing the initial value. So the return is slow, and a means to avoid this disadvantage will be developed in this report.

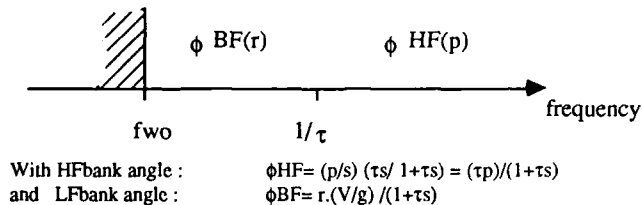
#### 234 - LOW GAIN AUTOPILOT

The LF mode depends on the AP gains. Therefore reducing the gains accelerates the LF mode, then decreases the effects of the sensor drift. On the other hand, the performance of such an AP on turbulence will be worse. The final result does not give an advantage to the low gain AP. The advantage on drift is only sensitive for very low WO frequencies. Then for the optimum frequency the exact share of performance on turbulence is lost on the global performance. A backward on instability frequency is observed. The LF mode is accelerated of 30%, when the control input ponderation are multiplied by three, for  $f_{wo}=0.05\text{Hz}$  :

#### 24 - LOW FREQUENCY OBSERVATION

##### 241 - LOW FREQUENCY OBSERVATION OF BANK ANGLE

The observation of bank angle by integration of roll rate works well for high frequency motion, in return it is not adequate for low frequency motion, where roll rate is equal or closed to zero. Note that, at low frequency equations are almost those of equilibrium, it could be written  $\phi=(V/g).r$ . So the observation of bank angle could be done by yaw rate. If the observation is divided into two fields of frequency, this leads to:



These are two complementary filters. Therefore,  $\tau$  is adjusted in order not to change the fast modes, and with the help of initial condition ( $\phi$  and  $\beta$ ) time simulation,  $\tau=3s$  is found as a good figure. There is no change on the mode but on the first order which corresponds to roll rate integration. This mode moves from 42s to 2.6s. The LF mode is slower due to the LF observation which is equivalent to an increasing gain on yaw rate.

A frank improvement is noticed on the bank angle initial condition simulation (see figure 14 and compare to figure 13), and the same on slideslip. The low frequency behaviour is better, as it could be foreseen by the time constant mode decrease. The performance on turbulence is improved by 33%, due to less sensivity to the sensor drift, but also and especially due to better control of the AP on LF turbulence, which delays the appearance of the LF behaviour of natural plane (see figure 15).

##### 242 - HEADING ANGLE MEASUREMENT

The use of heading angle measurement enables improvement of the very low frequency behaviour of the plane. This is obvious because the vanishing of the LF mode. The heading angle is first used by its derivative, the yaw rate. To avoid overlapping with gyrometer feedback, a complementary filter in regard to the WO filter is installed on the heading angle measurement.

$$r_{wo} = r.s^2 / (s^2 + 2\xi\omega s + \omega^2)$$

Note  $rc$  the derivative of the heading angle, filtered by the complementary filter.

$$\text{and } rc = r - r_{wo} = \xi.(2\xi\omega s + \omega^2) / (s^2 + 2\xi\omega s + \omega^2)$$

Therefore  $rc$  is filtered at the same frequency as the WO. That is to say at a very low frequency, which presents an advantage for this kind of measurement.

At LF, the yaw rate enables a control of the turn by the aileron command. This feedback readily improves the performances on bank angle and specially on heading angle. This efficiency is obtained with a gain of one on  $r$ . For  $f_{wo}=0.02\text{Hz}$ , all the modes of the plane with AP remain, except the LF mode which is accelerated toward the WO mode. This facts lead to the results:  $f=0.03\text{Hz}$  and damping ratio=0.4, the low damping ratio is compensated by the frequency.

The performance on bank angle is then improved and becomes equal to these of the idea: AP without drift nor WO, that is to say a 90% reduction with regard to the natural plane (see figure 16). The bandwidth for  $f_{wo}$  adjustment enlarge and the optimum frequency moves toward LF. The increased rudder activity has to be note because of the high wash out frequencies. To stay under the maximum value of 0.35rad the frequency must be below  $f_{wo}=0.05\text{Hz}$ .

The performance on heading angle are obviously improved. The maximum value reached is 0.15rad, almost the value obtained with the ideal AP equipped with a heading angle feedback (see figure 17). The bandwidth for two adjustment is narrower than for the bank angle, as it has been observed previously. The optimum two is clearly at 0.02Hz. For this frequency, the response to the drift and turbulence are given on figure 18.

To conclude, a heading angle measurement at LF (0.02Hz, equivalent time constant 11s) is sufficient to obtain the performances of an ideal AP. A very good complementary balance between the HF feedback  $n, p, r,$  and the LF feedback  $\psi$  is remarked, because with the optimum wash out frequency there is neither drift effects, nor deterioration of the performance with turbulence.

The installation of the LF observation of bank angle (see §241) improve the performance a little on the heading angle, and the LF mode becomes strictly equal to the WO mode. The previous acceleration of the observation mode of bank angle is kept. This result shows the importance of the yaw rate measurement.

## 25 - INBOARD AUTOPILOT

Here the conditions encountered in flight will be simulated. The effect of this conditions, model errors and discretisation of the AP process, with noise on the sensors will be evaluated.

### 251 - INFLUENCE OF MODEL ERRORS

The influence of model errors on performances of the AP with WO is tested. The effects of model errors are investigated on the dihedral effect (plus or minus 10% on the  $C_{l\beta}$ ), on the fin surface (-10% on  $S_v$ ), and on the velocity (+20% on  $V$ , 40m/s instead of 33m/s).

#### VARIATION OF DIHEDRAL EFFECT 10%

The spiral mode of the natural plane moves from 47s to 28s for  $C_{l\beta} = -2.2$ , and 142s for  $C_{l\beta} = -1.8$ . The other modes are unchanged. The variations of  $C_{l\beta}$  from -1.8 to -2.2 do not generate any modification of the regulated plane modes (<1%).

Performances of the natural plane are seriously deteriorated. Performances' gain of the AP plane with WO at 0.02Hz with regard to the natural plane remains constant, about 75% better than performance of the natural plane. Therefore the AP is robust with respect to  $C_{l\beta}$ .

The drifts at high frequencies are the same. Because of the faster decrease of the performances on the turbulence with the increase of the WO frequency, the optimum frequency is close to 0.02Hz instead of 0.05Hz (see figure 19).

The global performances are better for the plane with a large  $C_{l\beta}$ . The interest of a fast spiral is found again and a faster spiral increases the frequency at which the instability of the slow mode appears.

#### VARIATION OF FIN SURFACE -10%

This variation leads to a change of 20% on  $C_{n\beta}$ , 5% on  $C_{y\beta}$ , and 10% on  $C_{nr}$ . On the natural plane this leads to a slight decrease of the Dutch roll frequency (0.24Hz instead of 0.26Hz), without any modification of the damping ratio. The spiral moves from 47s to 25s.

For the plane with AP, the modes are not modified. The same kind of behavior can be observed with the change of  $C_{l\beta}$ . The drift does not change (the instability zone of the slow mode slightly increases). But since the natural plane has worse performances, the performance of the plane with AP decreases more rapidly, when moving toward the LF natural behavior.

This makes the global performance more sensitive to the adjustment of the WO. But the gain of performance on turbulence, compared with the natural plane, remains constant at a given frequency. For example, a 70% gain is obtained when the WO is adjusted at 0.02Hz. Therefore, the AP is robust in regard to  $S_v$  variation.

#### VARIATION OF VELOCITY 40m/s

For the natural plane the increase of the velocity from 33m/s to 40m/s (+20%) improves the Dutch roll damping ratio (0.17 instead of 0.12); accelerates the rolling mode (0.06s instead of 0.076s) and the spiral (40s instead of 47s).

The modes with AP are perceptibly influenced :

Dutch roll : 0.32Hz instead of 0.28Hz and damping ratio 0.6 instead of 0.5

Equivalent spiral and rolling: 3.2Hz instead of 2.2Hz and damping ratio 0.77 instead of 0.83

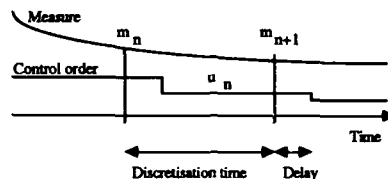
The natural plane performances on turbulence are roughly equal to the basic plane ones :  $\phi = 1.7\text{rad}$  instead of 1.5rad. With the AP a slight deterioration of the performances is noticed. The attenuation reaches 58% with regard to the natural plane, instead of 63% for the basic plane. The adjustment band of the WO also contracts a little and the optimum slightly slides towards the low frequencies (see figure 20).

Consequently, the same behaviors as with the precedent models errors are observed, but with a far weaker amplitude.

To conclude the AP is robust in regard to the model errors and the decrease of the performances is due to the poorer natural LF plane behavior.

### 252 - DISCRETISATION AND NOISE

The sensitivity of  $n$ ,  $p$ ,  $r$ ,  $\Delta P$  is evaluated with the sensors noise, and with the discretisation of  $\Delta P$  process. The standard deviation noise is given § 231, and the measure are filtered at 20Hz. The discretisation time is fixed at 40ms, with control delay of 10ms.



The discretisation method is the bilinear transformation [8], which consists of exchanging the Laplace operator by  $(2/dt)(z-1)/(z+1)$  where  $z$  is the advance operator ( $z x = x^+$ ). This method has the advantage of ensuring the stability even for high discretisation time. After a state exchange in order to have a recurrent process, the discretized  $\Delta P$  becomes the formula:

$$XD^+ = AD XD + BD M \quad \text{and} \quad UR = CD XD + DD M$$

Where  $M$  is the measurement and  $UR$  the control order. The process is done during the discretisation time, and during the time delay only  $DD M$  is calculate, in order to rapidly send the control order after the measurement.

On the  $\Delta P$  without  $WO$ , the noise and discretisation has no effect, except for the roll rate which increases 20% on noise influence, and of 40% on discretisation influence. On the  $\Delta P$  with  $WO$  at  $f_{wo}=0.02\text{Hz}$ , there is no effect on the plane state; the performance still remains the same, except for the roll rate which increases of 100%. The rolling mode is the faster one, which could explain the sensitivity to these perturbations, which especially affect the high frequencies.

### 26 - METHOD FOR LONGITUDINAL AUTOPILOT

The method seen for the lateral autopilot can be applied to the longitudinal motion. The position measurement, meaning the altitude, can give the LF climb angle by its derivative. The gyrometer by integration gives the HF pitch angle. The load factor gives the HF angle of attack. With these two HF angle, the HF climb angle is obtained. Then the plane state is observed.

Previous studies [6][7] show that an longitudinal  $\Delta P$  without vertical measurement works well, and the 25kg ENSAE RPV flies with only a radio altimeter. The good natural damping ratio of the short period mode, really helps to reach this performances, which leads to a variation of plus and minus 0.7m with the same level of turbulence used with the lateral autopilot.

### 3 - SUMMARY

This study shows that a robust lateral autopilot can be design in order to stabilize a RPV, without a vertical gyroscope. The natural plane has been adjusted to minimize its sensitivity to turbulence. And the performances have been evaluated, depending on the measurements: such as the influence of low frequency heading angle measurement, as well as the observation of bank angle by the yaw rate, for medium frequencies. A method has been proposed to optimize the measurement filter frequency. The same method can be applied to the longitudinal control.

### ACKNOWLEDGEMENT

This work has been carried out with the support of the ENSAE and the CERT-DERA of Toulouse. Thanks to Alan and Edith for the friendly help regarding my English.

### REFERENCES

- [1] B. ETKIN Dynamics of atmospheric flight - John Wiley 1972
- [2] AFWAL - TR -82-3081 Proposed MIL standard and handbook- Flying qualities of air vehicles (Vol II) 1982
- [3] AC - 120-41 FAA 1983
- [4] AC - 2057 A FAA 1971
- [5] RD - 74 206 FAA 1974
- [6] J.L. DODELIN, J.M. LEVESQUE, M. PINAUD Pilote automatique pour RPV - PFE 1984 - ENSAE -Toulouse
- [7] E. BSALIS Operational software for numerical RPV autopilot design - Sixth RPVs conference Bristol - 1987
- [8] M. LABARRERE, J.L. BOIFFIER Systeme antiturbulent améliorant le confort des passagers - Rapport Aerospatiale/Dera N° 1/7304 - 1982 - Cert Toulouse.

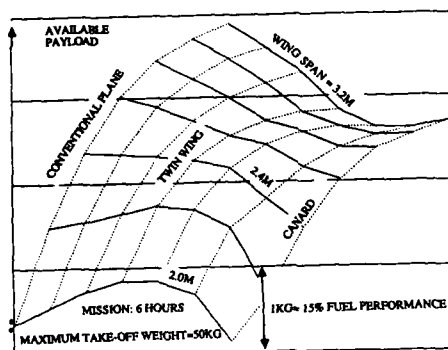


FIGURE 1: PAYLOAD OPTIMISATION DIAGRAM

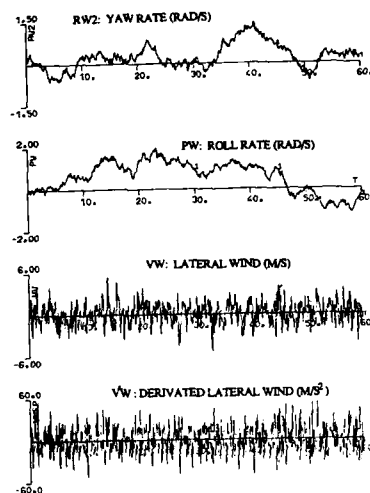


FIGURE 2: 60S TIME SIMULATION OF THE BASIC TURBULENCE

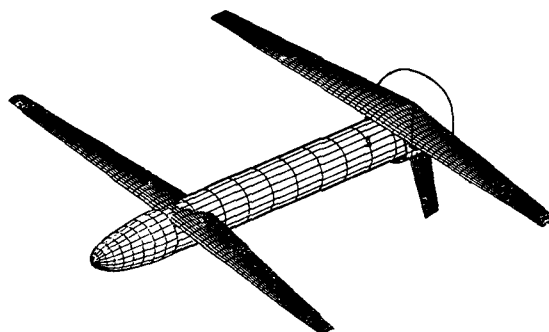


FIGURE 1BIS: TWIN WING 50KG ENSAE RPV

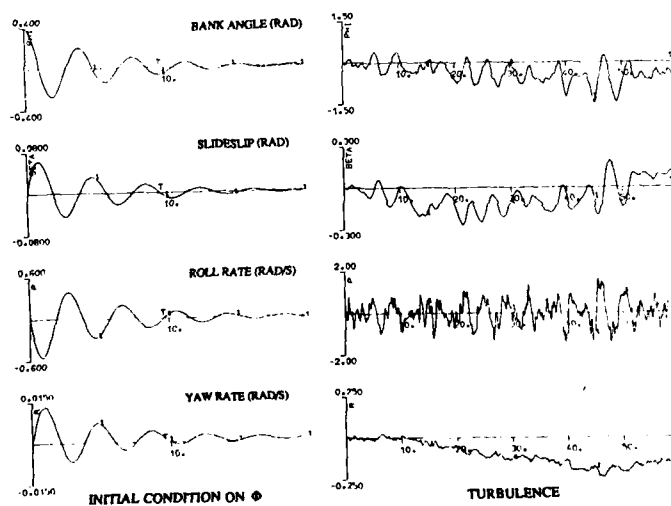


FIGURE 3: TIME RESPONSE OF THE NATURAL BASIC PLANE (N°1)

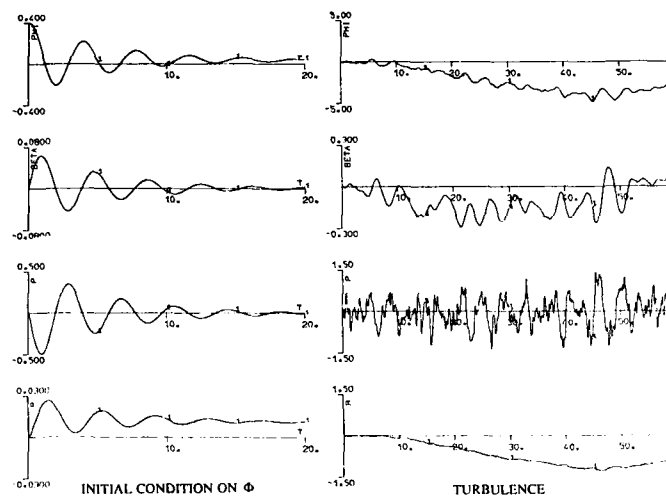


FIGURE 4: TIME RESPONSE OF THE PLANE N°3

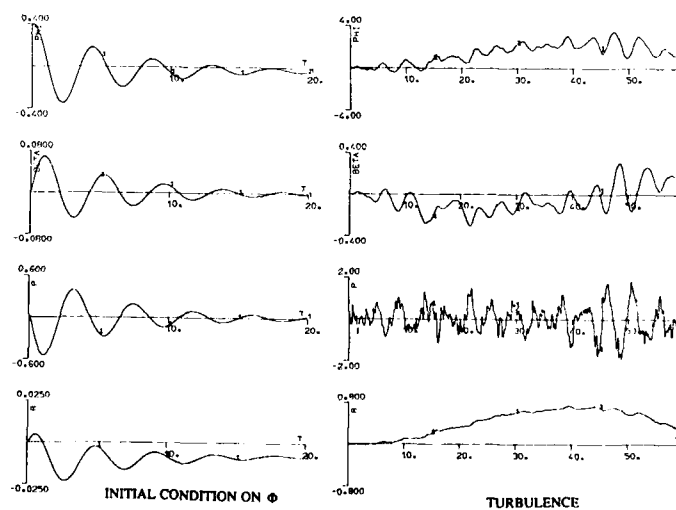


FIGURE 5: TIME RESPONSE OF THE PLANE N°10

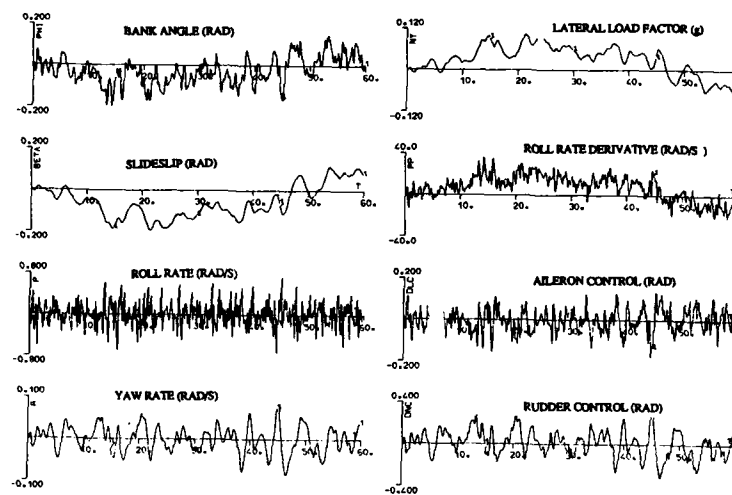


FIGURE 6: TURBULENCE RESPONSE OF THE BASIC AUTOPILOT

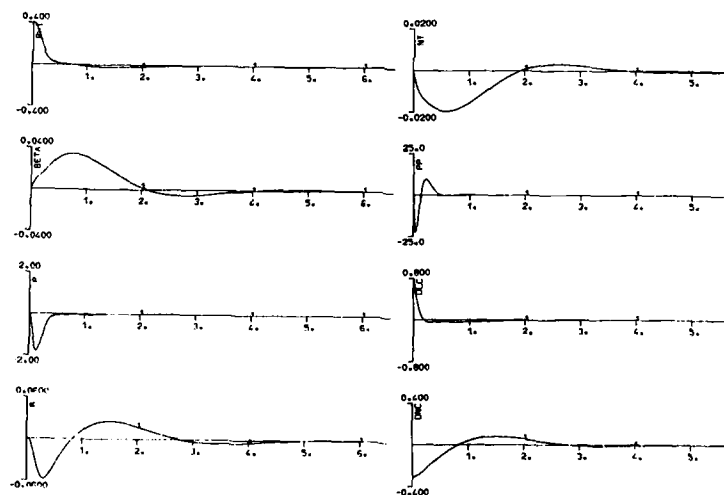


FIGURE 7: INITIAL CONDITION RESPONSE OF THE BASIC AUTOPILOT

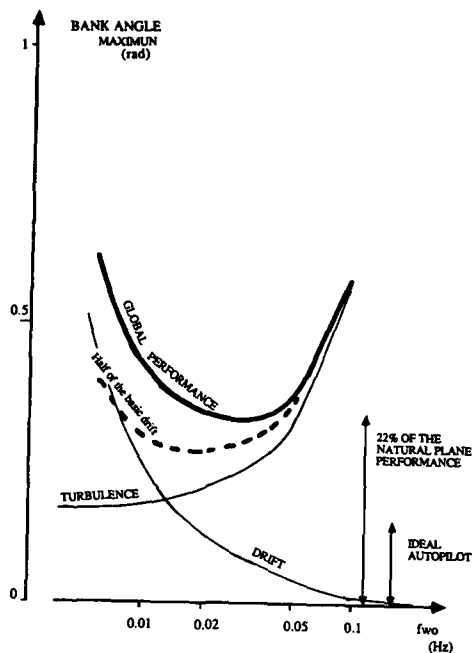
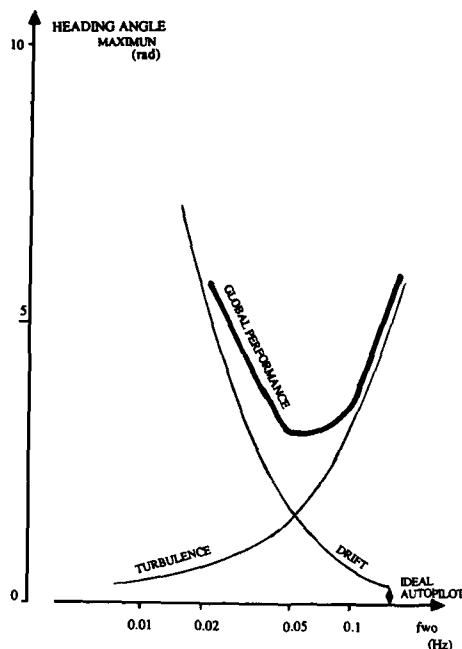
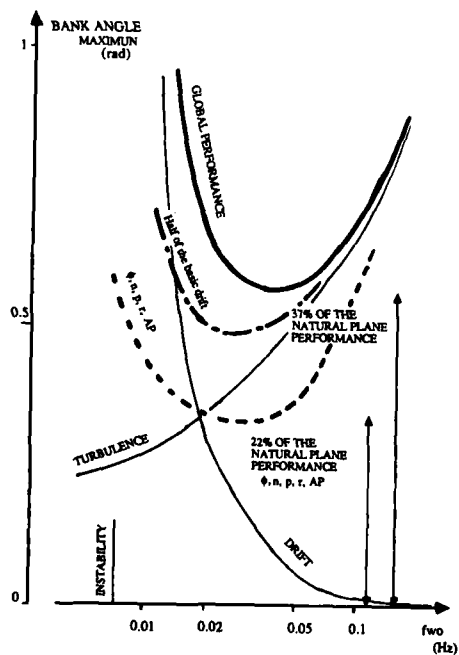
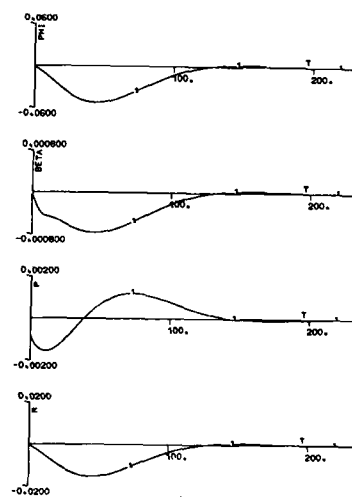
FIGURE 8: PERFORMANCES OF  $\Phi, N, P, R$  AUTOPILOTFIGURE 9: PERFORMANCES OF  $\Phi, N, P, R$  AUTOPILOTFIGURE 10: PERFORMANCES OF  $N, P, R$  AUTOPILOTAUTOPILOT  $N, P, R$  fwo=0.05Hz

FIGURE 11: RESPONSE TO SENSOR DRIFT

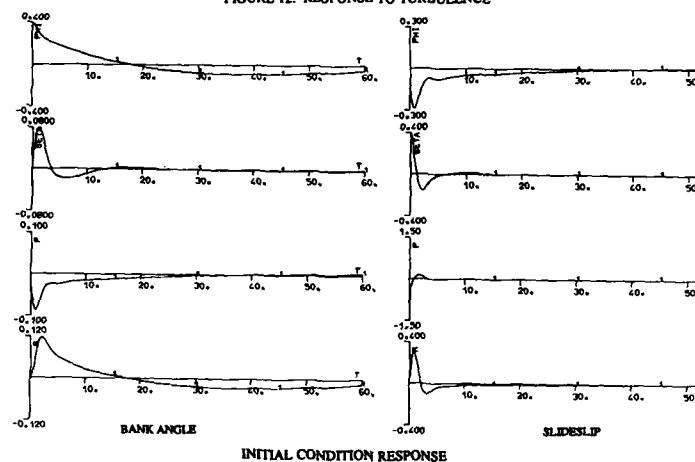
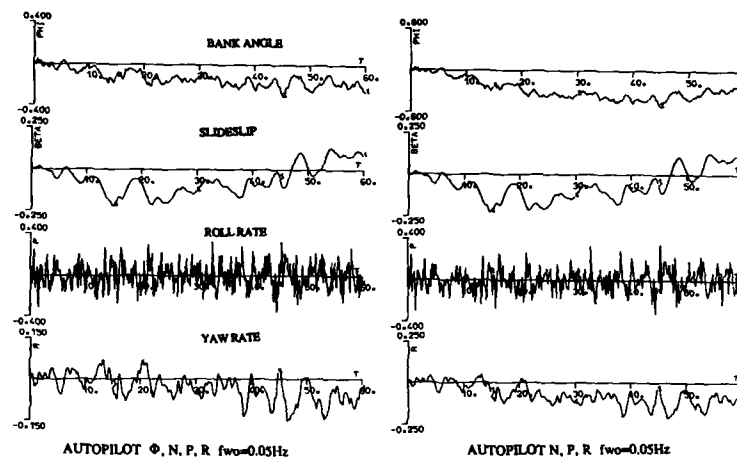
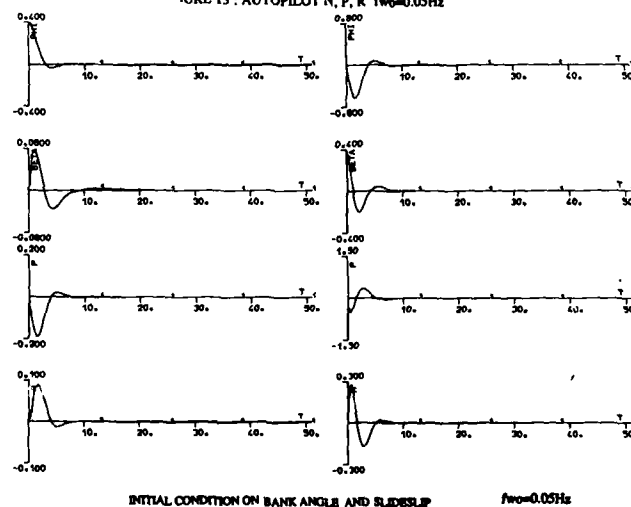
FIGURE 13: AUTOPILOT N, P, R  $f_{wo}=0.05\text{Hz}$ 

FIGURE 14: AUTOPILOT N, P, R WITH LP OBSERVATION OF BANK ANGLE

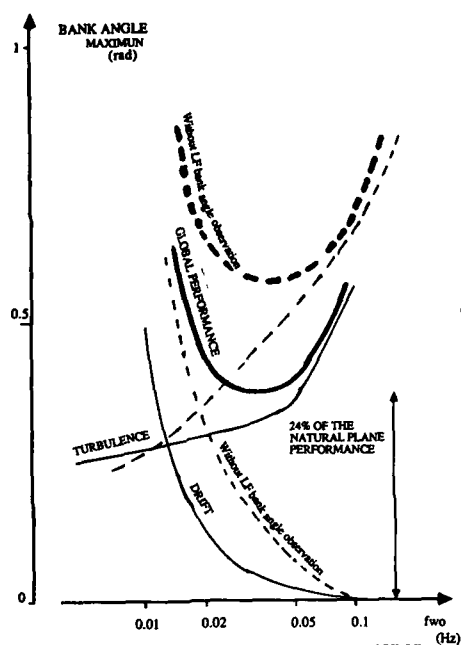


FIGURE 15: PERFORMANCES OF N, P, R AUTOPILOT WITH LF BANK ANGLE OBSERVATION

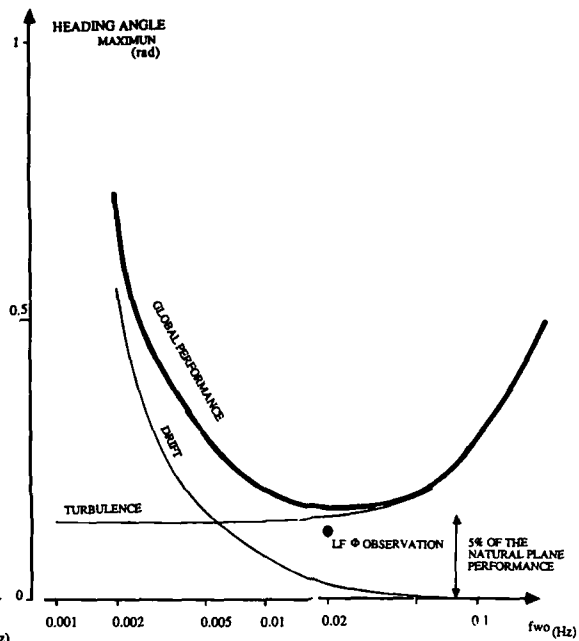


FIGURE 17: PERFORMANCES OF N, P, R AUTOPILOT WITH HEADING ANGLE MEASUREMENT

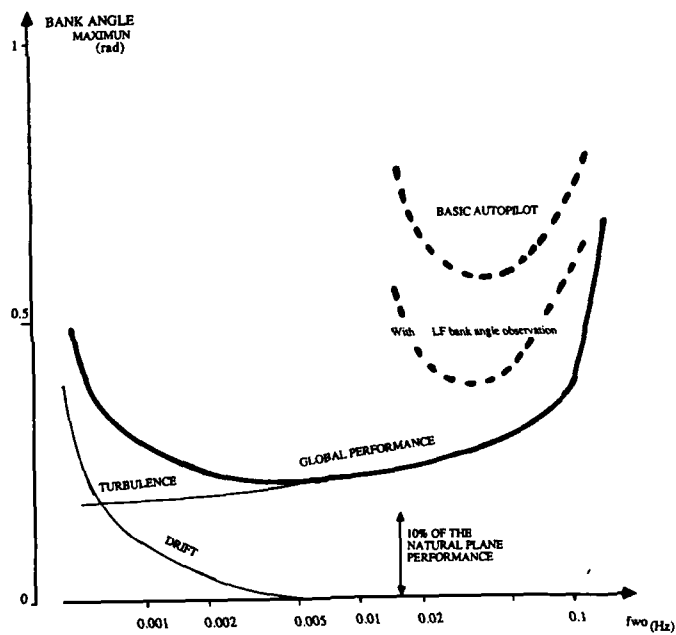
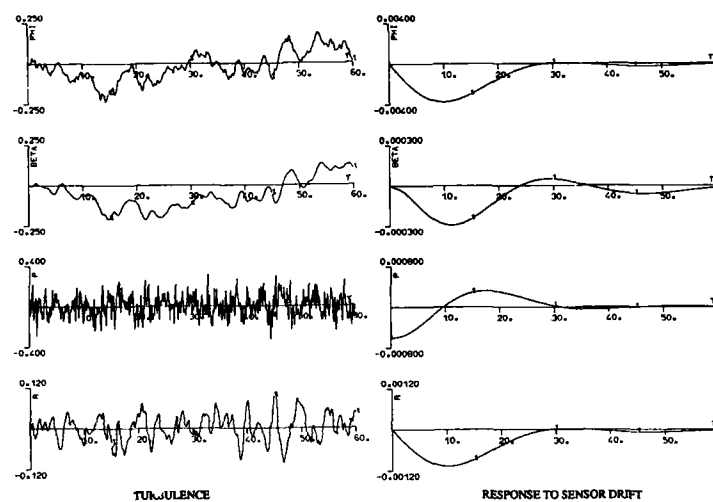
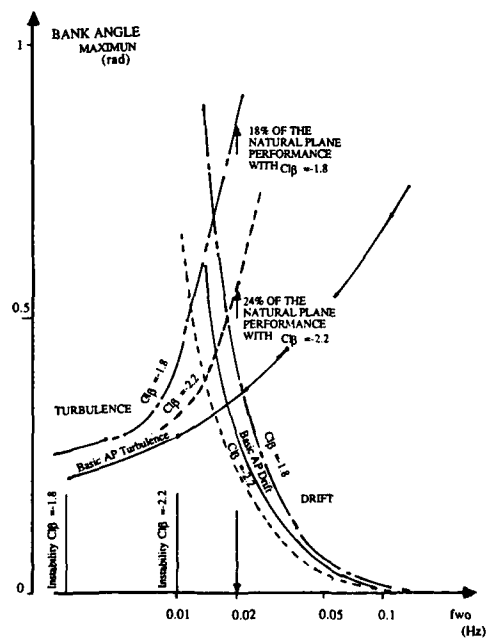
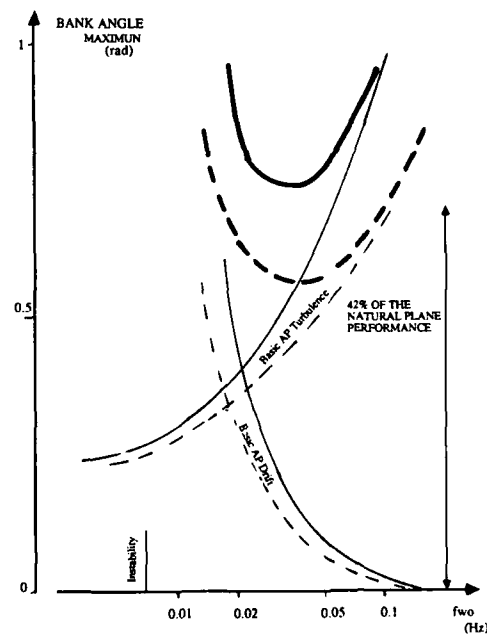


FIGURE 16: PERFORMANCES OF N, P, R AUTOPILOT WITH HEADING ANGLE MEASUREMENT

FIGURE 18: AUTOPILOT N, P, R WITH HEADING ANGLE MEASUREMENT  $f_{wo}=0.02\text{Hz}$ FIGURE 19: PERFORMANCES OF N, P, R AUTOPILOT - MODEL ERROR DIHEDRAL EFFECT  $\pm 10\%$ FIGURE 20: PERFORMANCES OF N, P, R AUTOPILOT - MODEL ERROR VELOCITY  $+20\%$

MIRACH 100 FLIGHT CONTROL SYSTEM

by

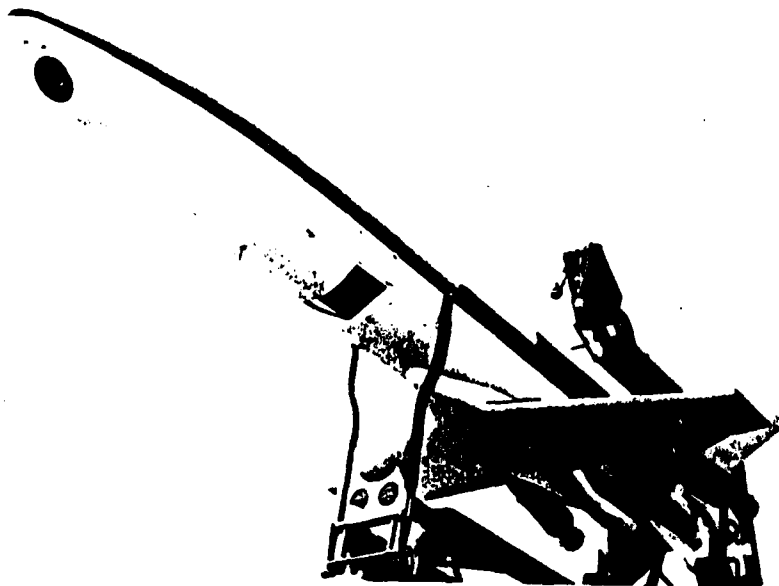
Anes SBUELZ

METEOR - Costruzioni Aeronautiche ed Elettroniche S.p.A.

Via Garibaldi, 2

34077 RONCHI DEI LEGIONARI

I T A L Y



METEOR C.A.E. S.p.A.  
ITALY

MIRACH 100 RECCE U.M.A.

## SUMMARY

The Mirach 100 air-vehicle is a multipurpose RPV-UMA, suited to intelligence missions of target recognition, acquisition and identification up to 150Km.

It is a high-subsonic speed, jet-powered drone having a ceiling altitude of 9000 m and 1 hour endurance.

Different arrangements of the base air-vehicle allow higher altitudes or wider endurances (and consequently larger operational envelopes) according to the mission operational requirements.

The flight control system of the Mirach 100 is mainly a compound of already tested in flight components, that is to say the different control function components of the drone have been adapted and integrated on it.

Autopilot function includes a full control system of stabilization on two axes, simply designed to improve reliability and safety of guidance.

Mechanization is based on a simple analogic control circuit of the actuators that drive the control surfaces of the aircraft, stabilized through the vertical gyroscope feed-back; the gyroscope is installed in the air-vehicle fore structure.

Guidance function includes a complete control system based on altitude, heading and velocity integrated in the flight controller which runs the whole aircraft, payload included.

The mechanization of this function is based on simple computational statements of the autopilot and of the engine control, based on the indication of altitude, speed and heading sensors.

Navigation function is based on a OMEGA/VLF receiver and navigator, suited to memorize a flight plan formed with up to 99 geographical points sequentially navigated, starting from any of it.

The mechanization of this function is based on a position computation interactive process, referred to the on-board sensors and corrected by the position solution, derived from the receiver.

From the computation a "wind" parameter is estimated which includes the on-board sensor errors, giving improved navigation performances even when the omega-receiver operates in marginal conditions (large GDOP, received stations limited number, etc...).

The drone is guided to follow the programmed flight plan.

Each point includes also control commands for the payload driven by the flight controller.

Complete avionics and aircraft itself have been modelled on a computer for dynamic and static stability analysis and performance computations; the results here obtained have been compared with those recorded during the Mirach 100 test flights performed at the experimental range "Salto di Quirra" in Sardinia, supported by Italian Defense Administration.

Test flights gave excellent results about steering, guidance and navigation.

The altitude and speed control were obtained with an accuracy that went far beyond the expectations, reaching the accuracy level of the sensor used in the testing program.

Navigation accuracy was better than 400 m CEP in accordance with the best Omega differential accuracy performances.

These results open new perspectives to the application of improved navigation systems, with enhanced characteristics.

As a consequence the performances here obtained can even improve.

1. MIRACH 100 SYSTEM1.1 AIRVEHICLE

The MIRACH 100 is an high subsonic, automatic or remotely controlled vehicle. It has multirole capability, able to satisfy the following missions:

- Electro-optical reconnaissance, with film camera, or IRLS, and television camera with real time transmission.

- Electronic warfare missions, with dedicated payloads.

The MIRACH 100 is endowed with swept-back low wing, with supercritical airfoil, and with "V" elevators.

It can be launched either from helicopter and fixed wing aircraft or with the aid of two boosters, from a zero-length ramp.

The MIRACH 100 is parachute recovered on ground or in water with the following provisions:

- for ground recovery, it is provided with a shock absorbing bag and expendable fins to absorb the shock energy;

- for water recovery, it is provided with a flotation bag.

In flight, it is controlled in roll by ailerons, in pitch by all-movable "V" elevators. The peculiar characteristics of MIRACH 100 are:

- high subsonic speed;
- high in flight stability;
- high structural strength;
- easy to operate and maintain.

The air-vehicle is arranged to carry the following sensors:

- Pan-Camera or high altitude camera
- IRLS
- TV Camera (day or night, low light level)

IRLS and TV-cameras can use a wide-band data transmitter for real time sensor data transmission.

#### 1.2. TELEMETRY PARAMETERS

The MIRACH 100 can be remotely controlled, in order to allow the GCS operator to properly control the air-vehicle, required information are received through the downlink and displayed on the GCS. These data are listed and described below:

- air-craft attitude
- heading
- altitude
- air-speed
- engine speed

A hardcopy plot of the vehicle flight path is provided to the operator with automatic selection of proper map scale based on initialization. Additional Mirach 100 status information are downlinked to and displayed in the GCS including the flight mode (autonomous or ground controlled). Additional downlinked information are displayed to the operator to denote unusual circumstances as described below:

. The EMERGENCY DEAD-RECKONING status message indicates that the Mirach 100 has experienced a failure in the receiver and in the navigation modules requiring immediate return to the recovery waypoint under dead reckoning navigation using last computed wind information (unless ground control overrides this flight mode)

. The MISSION ABORT status message indicates that one or more of the preprogrammed payload actuations have failed, requiring an immediate return to the recovery waypoint under regular navigation means (unless ground control overrides this flight mode).

. The ENGINE OVERTEMP status message indicates that the engine exceeded preset limits. Usual navigation information are also down-linked.

. The NAVIGATION status message indicates the mode of navigation (autonomous or ground controlled).

. The RECOVERY status message indicates that the Mirach 100 has initiated the recovery sequence.

#### 1.3. COMMAND FUNCTIONS

In order to control the Mirach 100 from the GCS, the herebelow described commands are uplinked to the flight control system:

- . Pitch command in a range of 30 degrees down to 30 degrees up.
- . Roll command in a range of 75 degrees left bank to 75 degrees right bank.
- . Time dependent throttle command increments or decrements (1500 R.P.M. per second)

. Altitude command, (with the pitch command knob), as a time-dependent increment or decrement of the preset altitude, engaged with the altitude mode insertion.

. The heading command (with the roll command knob) as time dependent increment or decrement of the preset heading, engaged with the heading mode insertion.

. The airspeed command (with throttle command push buttons) as time dependent increment or decrement of the preset speed, engaged with the speed mode insertion.

In addition to the above commands used in ground mode, the operator has the option of modifying the programmed flight plan by instructing the Mirach 100 to fly directly to any of the waypoints currently residing in the mission controller memory. The operator can also modify any flight leg by instructing the Mirach 100 to fly parallel to the normal programmed flight path (either left or right) at a distance specified by the operator himself.

#### 1.4. GROUND CONTROL STATION (ALAMAK)

The air vehicle is controlled in flight by two operators in a ground control station (fig. 4) by means of a Rho-Theta tracking system.

The range tone is used to measure the distance between the Airvehicle and the Station. The tracking antenna is constantly oriented toward the incoming telemetry signals. The antenna direction defines the air vehicle azimuth. Azimuth and range data processing, combined with vehicle telemetry altitude, give the air vehicle position which is recorded on a map (fig. 5).

Main functions:

- air vehicle tracking and control;
- air vehicle position recording;
- payloads control;
- real time data display;
- target acquisition;
- communication;
- navigation aids.

#### 1.5. LAUNCH AND RECOVERY

The MIRACH 100 is being launched either from a shipboard launcher system, a ground vehicle launcher system, or from a mother aircraft. The shipboard and ground vehicle launcher systems includes the preflight test equipment to make the MIRACH 100 ready for launch (fig. 6).

The zero length launcher necessary for MIRACH 100 air vehicle positioning and taking-off is of solid, rugged and simple construction. The ramp is installed on a two-wheeled trailer. Its modularity allows quick disassembling which facilitates storage and maintenance. The aerial launch system consists of a pylon adapter that enables in flight GO/NOGO testing, engine start, launch and jettison controlled from the cockpit of the mother-aircraft.

Main functions:

- pre-flight check and initialization;
- MIRACH 100 engine ignition;
- air-vehicle launch attitude;
- engine ignition.

These functions are directly controlled by the launch equipments.

#### 2. FLIGHT CONTROL SYSTEM

The flight control system is a hybrid implementation, analog and digital, that provides a two axes of the air-vehicle control (fig. 7). Air-vehicle attitude is sensed by suited gyroscopic sensors; derived rates are used to maintain simplicity in the aircraft stabilization control circuit. Air data (altitude and airspeed) are sensed from the self-contained air data sensors; heading, from a three axes magnetometer; derived rates are computed in order to steer the aircraft to maintain altitude, speed and route. Steering commands are also shared between the airborne navigation system in autonomous flight and the ground control in manual remotely controlled flight.

**ALAMAK**  
**Ground Section UMA Architecture**  
**ALAMAK Architecture**  
**Aircraft Tracking & Recording - Control & Telemetry**

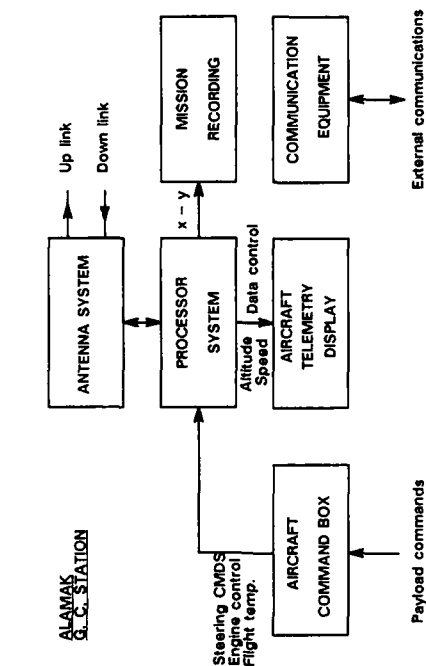


fig. 4

- Antenna steering and link management
- Aircraft tracking and position plotting
- Aircraft telemetry data calibration and display
- Aircraft steering commands and flight termination

**ALAMAK**  
**Ground Section UMA Architecture**  
**ALAMAK Architecture**  
**Payload Control & Display - Data Exploitation**

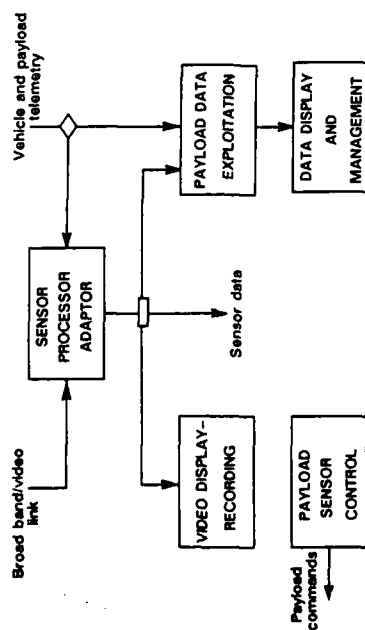


fig. 5

- Sensor data conversion and processing
- Payload data display and sensor control
- Sensor data exploitation and target acquisition processing
- Target display and data management

### Aircraft section architecture - Avionic system

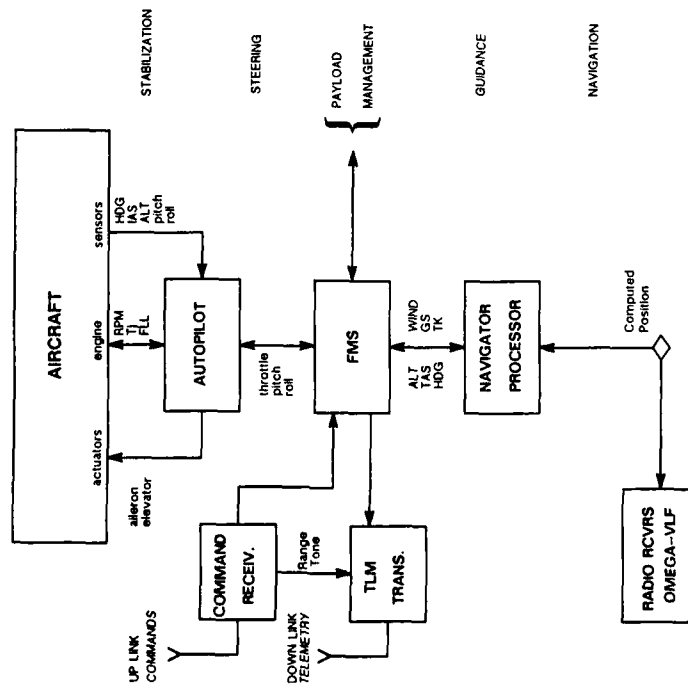
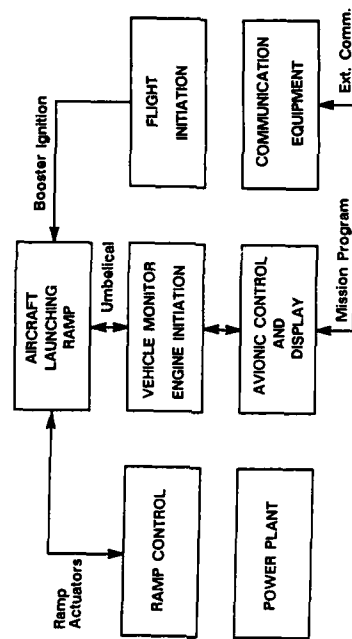


fig. 7

### Ground Section Preflight Checking & Initialization - Launching System



- Preflight checking
- Initialization and sensor calibration
- Mission-plan loading
- Flight Initiation

fig. 6

The flight control system contains two major subsystems: the flight management system (FMS) and the autopilot for aircraft stabilization.

#### 2.1. FLIGHT MANAGEMENT SYSTEM

The FMS is a microprocessor based complex that provides centralized computation and control to the entire air-vehicle.

The following major functions are performed.

- system mode logic interlock
- guidance and autonomous specific flight envelope computation
- centralized command data processing and system I/O.

These functions are controlled by tightly structured software codes.

Air-vehicle steering, payload control and additional subsystem commands, whether autonomously generated from the on board navigation system or received via the command up link, are processed in the FMS.

#### 2.2. AUTOPILOT

The two axes stabilization circuit provides pitch and roll stabilisation and control (fig. 8). Attitude control is taken from a simple integration of the commanded and actual attitude difference, made via gyro response feedback.

Two servoactuators (controlled directly by the autopilot) are installed in the aircraft, one for the elevators, the other for the ailerons.

The engine throttle is controlled via a dedicated engine control box that controls the fuel flow according to the throttle command, controlling engine rpm.

#### 2.3. ENGINE CONTROL

The Motor Control Unit varies the speed of an electrically driven gear pump which supplies fuel to the burners and provides all-speed governing to the engine via a closed loop engine speed control for thrust modulation.

The engine control loop is capable of maintaining engine speed to within  $\pm 0.8\%$  of maximum rated speed over the speed range from idle to maximum at all altitudes and Mach numbers of the flight envelope.

#### 2.4. NAVIGATION COMMAND RECEIVER (NCR)

The NCR is a navigation system package in a militarized airborne chassis which interfaces with the aircraft flight management subsystem (FMS). The NCR determines the air-vehicle position in three dimensions. The system is programmed to compute flight control signals (i.e., track, altitude, and airspeed) for autonomous aircraft control. These commands may be used to fly the Mirach 100 through a sequence of user-defined three-dimensional points stored in the NCR memory. These data represent waypoints in a flight plan. Each flight plan may consist of up to 99 waypoints, and more than one flight plan may be stored within the 99 waypoints. A partial listing of NCR features is as follows:

- . Self contained. Easily adaptable to any subsonic and low supersonic aircraft;
- . Degrees of Navigation Freedom. Four dimensions (X,Y,Z,T);
- . Basic Navigation Mode. Dead reckoning using on-board sensors (speed, altitude, time);
- . Basic Navigation Mode Accuracy. 4% root mean square (RMS) of distance travelled;
- . Primary Navigation Mode. Omega navigation plus auxiliary external aid using differential Omega/VLF;
- . Additional features.
  - Cooperative operation with independent ground control, tracking system;
  - Emergency homing capability;
  - Sensor annotation;
  - Mission reprogramming by uplink commands;

The NCR is composed of two functional groups of subsystems. These are the differential receiver subsystem and the navigation receiver processor subsystem. The differential receiver subsystem receives the differential corrections from the ground

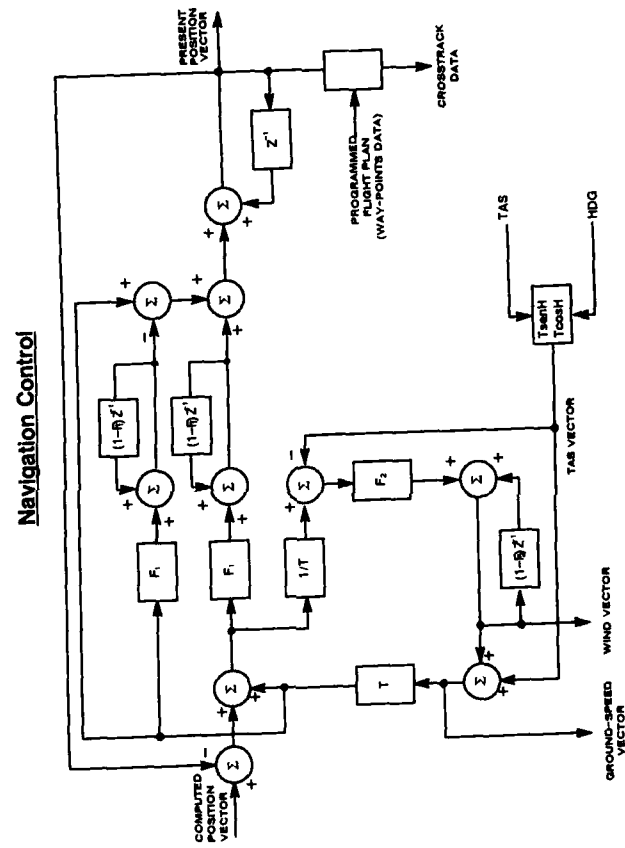


fig. 9

station via a data link, and passes the correction message to the navigation subsystem in order to correct the computed position.

The receiver processor is composed of an E-field antenna, a wide dynamic range constant phase antenna coupler, and RF/IF sections for the Omega common frequencies and the 3 VLF station processing. Four Omega frequencies and any three of up to eight VLF stations are simultaneously processed. The phases of all signals being processed at any given time are sampled and digitalized. The digitalized phase values are directed to the receiver processor where they are balanced and filtered.

The navigation processor develops a position based upon these phase value inputs after the correction for diurnal model variations. Navigation/guidance signals are computed from these inputs and provided to the flight management subsystem (FMS) (fig. 9).

The navigation system is based on an Omega receiver that processes four common Omega frequencies, 3 VLF station signals and defines and develops its position. The position can be corrected by a differential ground-linked correction.

From the computed position the current aircraft position is derived, combining the on-board avionic sensor data, allowing dead-reckoning navigation and smooth switching to and among the Omega fixings. The on-board sensors aids give high dynamic performance to the navigation system, recovering the slow rate of the Omega system. The present position and the stored flight plan define the navigation parameters under which the FMS steers the aircraft.

## 2.5. HEADING-CROSSTRACK CONTROL

Route control will be maintained in either roll mode or heading mode (fig. 10). In autonomous flight control an additional crosstrack mode is engaged under the on-board navigator control.

In the heading mode, the MIRACH 100 is commanded to bank in order to get and maintain the preset heading. In order to have highly straight flight control, aerodynamic asymmetries are computed and added to the loop to minimize turn components at speed variation.

The autonomous flight is based on a pre-programmed flight path: the navigator is able to develop a crosstrack value of the aircraft over the flight leg.

Under this value, a roll parameter is computed with which the roll control loop will operate.

The Roll mode can be activated under ground control only. The command will be a roll attitude command to the autopilot; the autopilot will compare the vehicle attitude received from the vertical gyro to produce an aileron command.

## 2.6. SPEED CONTROL

The Mirach 100 have two modes of speed control: true air (TAS) speed mode and THROTTLE mode (fig. 11). Both modes are available during the ground control. Groundspeed mode will be available during autonomous flight control only.

In autonomous control (groundspeed mode), the flight management processor (FMS) controls a groundspeed to cause the Mirach 100 to arrive at a waypoint. The speed control loop compares this command and adjusts the throttle output control to achieve the commanded speed.

In ground-control speed mode, the speed command is uplinked from the GCS and used as a preprogrammed speed.

In the throttle mode, the pilot operator in the GCS commands the engine throttle directly.

## 2.7. ALTITUDE CONTROL

Altitude control is maintained in either pitch mode or altitude mode. In autonomous flight control, the altitude mode only is available (fig. 12).

In the altitude mode, the Mirach 100 is commanded to climb to the altitude, according to the best rate of climb speed with the engine at full throttle. When the current altitude is close enough to the commanded one, the engine is controlled to maintain the selected speed and the Mirach 100 attitude is controlled to maintain the altitude. The dive command works in the reverse mode with the limitation of the pitch attitude. The engine throttle is controlled to achieve the selected RPV speed (the engine is usually at the idle speed).

The pitch mode can be activated in ground control only. The command will be an attitude command to the autopilot. The autopilot will compare the vehicle attitude received from the vertical gyro to produce an elevator command.

## 2.8. FLIGHT TERMINATION

# Stabilization (autopilot)

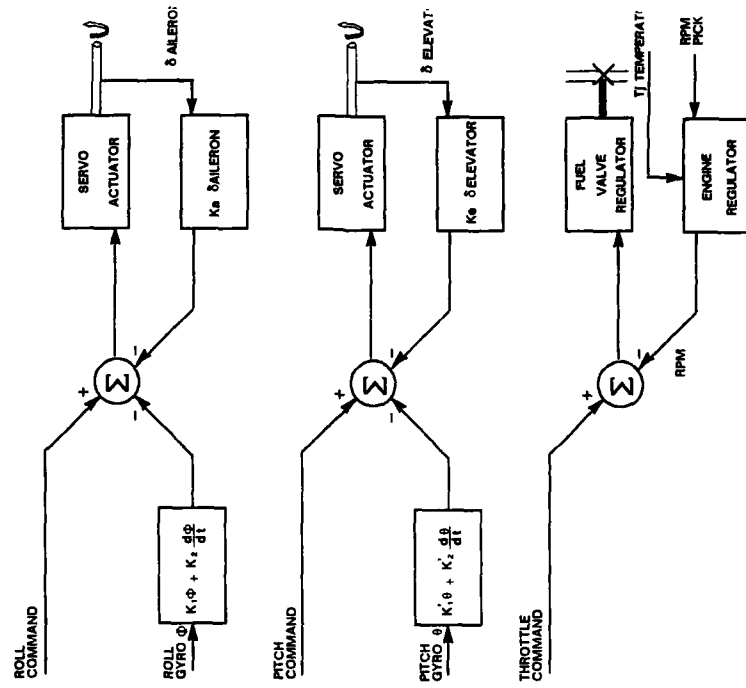


Fig. 8

# Steering (FMS) XTK/HDG control

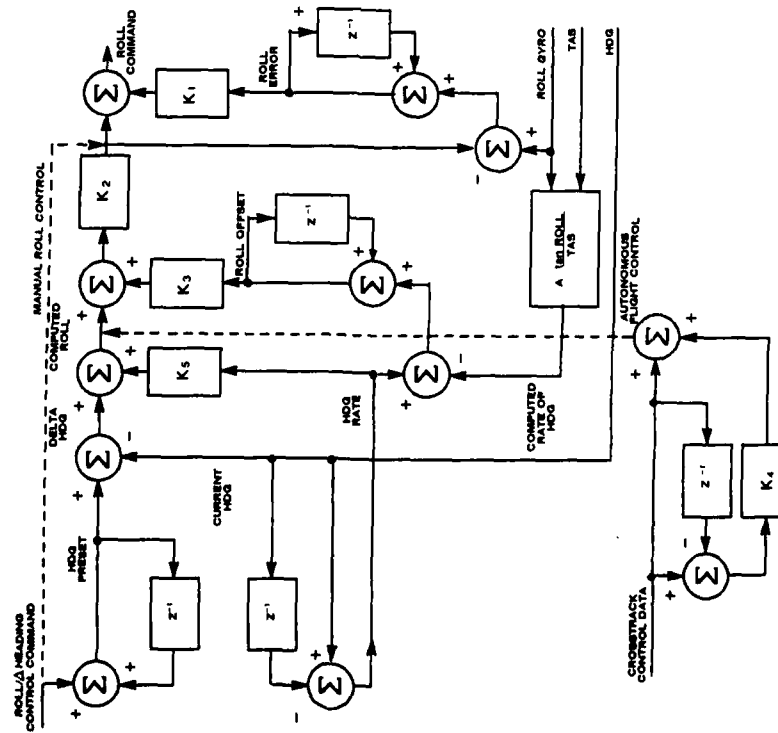
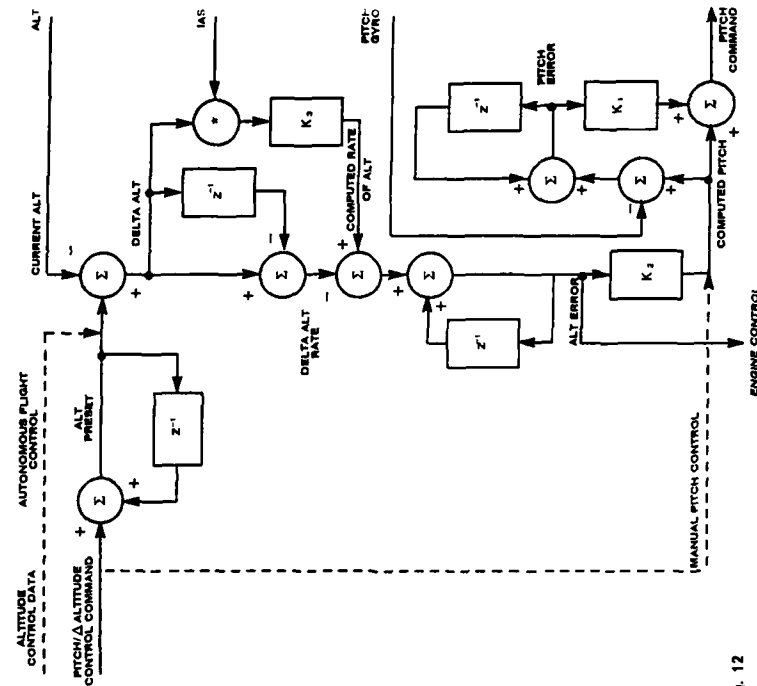


Fig. 10

### Altitude control



**fig. 12**

### Speed control

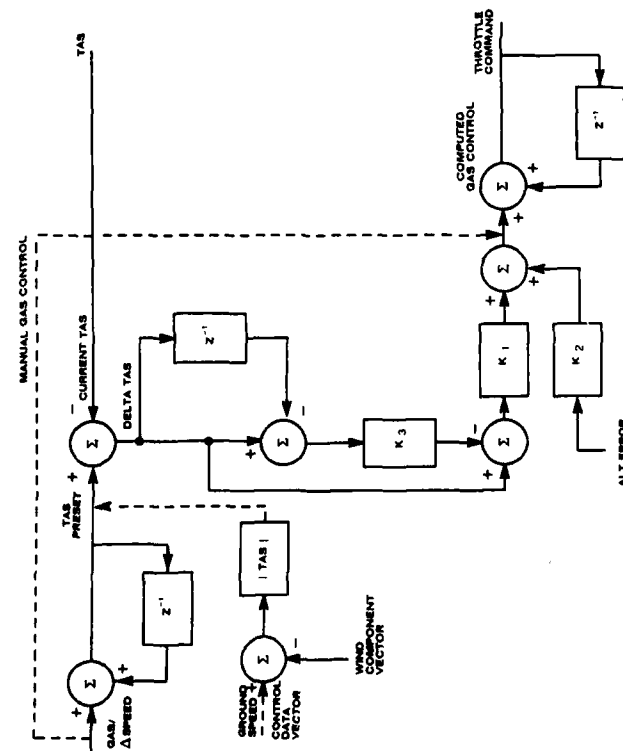


fig. 11

In an operational environment there are two methods of flight termination: recovery by parachute or dive to destruction. Dive to destruction only occurs if a failure prevents the Mirach 100 from returning across the forward edge of the battle area (FEBA). All other flight terminations are accomplished by parachute recovery. Flight termination is activated by the mission program or commanded by the GCS. Both methods use the same hardware. The parachute is deployed when a device unlocks the parachute cover.

On a test range environment, the dive-to-destruction capability is not normally activated, and a duplicated method of deploying the parachute is installed.

### 3. OPERATIONAL FEATURES

The air-vehicle in cooperation with the ground based equipment performs the following operations:

#### -Preflight (fig. 13)

This phase starts with the power-on; each subsystem runs its built-in-test and holds for the initial operations.

The launch operator checks the main aircraft operation via the aircraft umbilical connection; this check is shared with the Alamak Ground Station when present and radio connected with the aircraft.

When the initial check is over, the preflight operation goes on with the flight plan loading and initialization and, at the end, the airvehicle is ready to launch.

#### - Stabilization (fig. 14)

This phase starts with the airvehicle launch and has a fixed time in order to allow the vehicle to stabilize in flight at a preordered flight pattern characterized by:

- engine at maximum revolutions
- roll at zero degrees
- pitch according to a pre-ordered sequence

When the stabilization time expires the aircraft enters autonomous flight or remote controlled flight according to the pre-programmed mission plan.

#### - Transition phase (fig. 15)

This phase is for aircraft remotely controlled flight: the Alamak Ground Station operator will manually control the aircraft through the displayed telemetry data and the recorded vehicle position.

The vehicle has to be in line of sight with the Alamak antenna tracking system; if the radio link breaks off, the airvehicle will go on with the mission along the pre-programmed plan.

#### - Automatic navigation (fig. 16)

In this phase the aircraft mission flies the mission completely autonomous under the preprogrammed flight plan.

The navigation subsystem drives the aircraft over the pre-programmed waypoint sequentially controlling altitude, speed and track of the aircraft and manages the payload.

This mode of operation may have specialized features like radio silence, down link only, or up link enabled to change or reprogramme the mission.

#### - Emergency phases

During the flight some failures may occur. In that case the mission may abort according to the type of failure detected.

For some types of failures the flight will continue or end with the recovery or the vehicle crash.

In the case of navigation receiver failure, the mission will continue in dead reckoning flight on the pre-programmed flight plan at lower accuracy or, if the navigation system is completely out of service, the FMS will fly in dead reckoning mode to the emergency recovery point previously programmed. In this case the Alamak ground control station may take the aircraft control for the recovery operations.

If the failure is on the payload system the mission will abort and the aircraft will fly back to the recovery point.

### 4. MIRACH 100 EXPERIMENTAL RESULTS

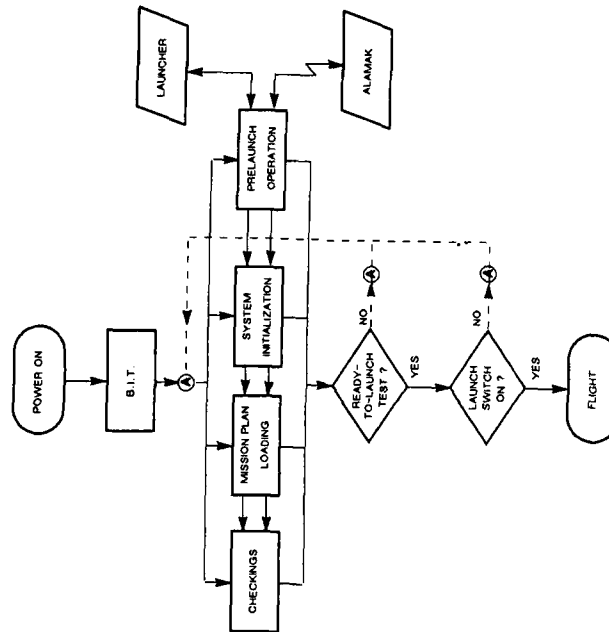
Preflight phase

fig. 13

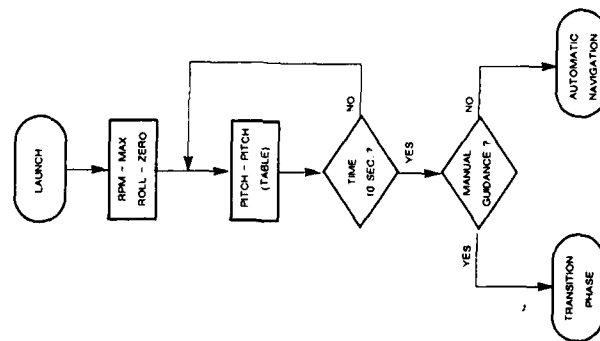
Stabilization phase

fig. 14

# Transition phase

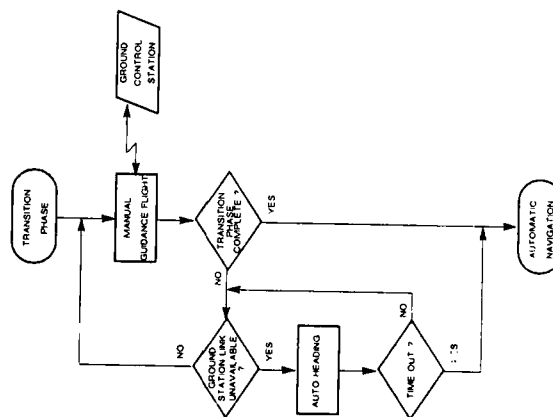


fig. 15

# Automatic flight phase

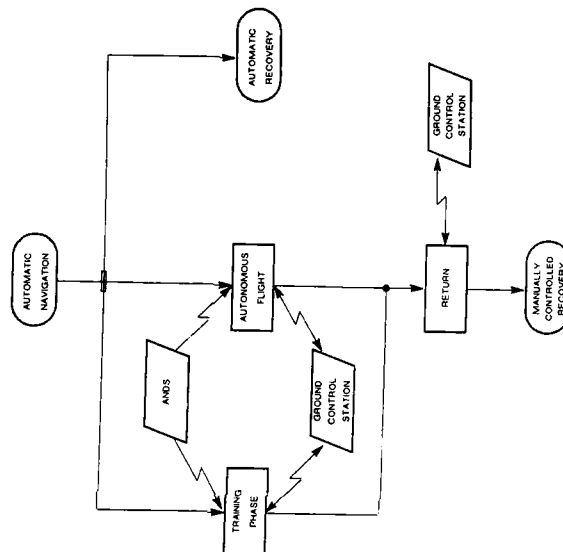


fig. 16

In the flight trials carried out during last year and before the expected flight features were confirmed.

- altitude control : within 50 m. -
- speed control : within 5 m/sec. -
- in route accuracy : better than 400 m
- payload management: any combination over 6 different independent commands.

Here the results of one of those trials are reported and discussed.

The plotter map (fig.1) well shows the horizontal profile of the selected mission; the numbered crosses are the specific way-points of the flight plan, where the aircraft is programmed to fly at different altitudes and speeds.

The Alamak was located at the "0" position, the launcher at the "1" and the Omega differential station close to the Alamak position.

The navigation system was programmed to fly sequentially the numbered way-points.

You can see two independent flight plans, one starting at the way-point "1" and ending at the way-point "9" and the second one starting at the way-point "20" and ending at the way-point "25".

The two coincident way-points, "9" and "25", were the pre-programmed recovery point.

In this particular trial the beginning of the mission was under Alamak remote control, the autonomous navigation was engaged a couple of minutes after Mirach 100 launch.

The Mirach 100 flew over the pre-programmed flight legs, through all the way-points crossing them with high accuracy.

In proximity of the 9th way-point the aircraft was commanded to jump to the 20th way-point, beginning this way the second pre-programmed flight plan.

In this portion of the flight accuracy was reached especially when flying very close to the way points 22-23 and in proximity of the 24th way-point.

During this flight we also had the chance to see the performance of the Omega differential correction. In fact flying the North-South path we detected a cross-track error well shown at the way-point number 5. Once the error was detected, we enabled a differential correction transmission that corrected the navigation error shown near the 6th way-point where the previous cross track error displacement was fully recovered. This mission was terminated manually because of range operation restriction. Before the Mirach 100 arrived at the pre-programmed recovery point it was kept under Alamak control for a radar tracking presentation and then driven to the effective recovery point for the retrieval operations.

This mission was flown with a very high accuracy, the Mirach 100 was constantly kept in a very narrow corridor, post flight analyses show an accuracy better than 400 meters at 50% of the distance flown, even if the Mirach 100 was commanded to different altitudes and speeds at each way-points.

The vertical profile and speed profile are also interesting for flight performance analyses. The fig. 2 - 3 report altitude and speed plot synchronized in time. The combined operation in altitude and speed control is well shown.

When the autonomous navigation was engaged, the Mirach 100 was directed to reach 160 m/sec of speed and 1800 m of altitude, as defined in the flight plan in the first leg of the flight.

When the second way-point was reached a new altitude and speed were programmed, the engine was forced to full thrust and the climb command was controlled for the best speed of climb. When the programmed altitude (3000 m) was touched the engine was controlled to the pre-programmed speed (170 m/sec), then altitude and speed were maintained all the flying leg long.

At the end of the leg we had a combination of climbing and banking of the Mirach 100 with a final speed reduced relating to the previous one.

That transient was promptly recovered just past the 4th way-point and from the pre-programmed point at 3600 m of altitude and 180 m/sec of speed it was maintained with high accuracy and stability.

Diving manoeuvres were also tested during this trial where the Mirach 100 worked in the symmetric way in relation with the climbing manoeuvres, completing shortly any transient and well maintaining the pre-programmed parameters.

As you can see in this trial any combination of manoeuvre was tested, well showing peculiar features of the designed flight control laws that were able to absorb any aircraft flight asymmetry and different attitude, due to different speeds and altitudes of flight and all the occasional perturbances due to weather condition.



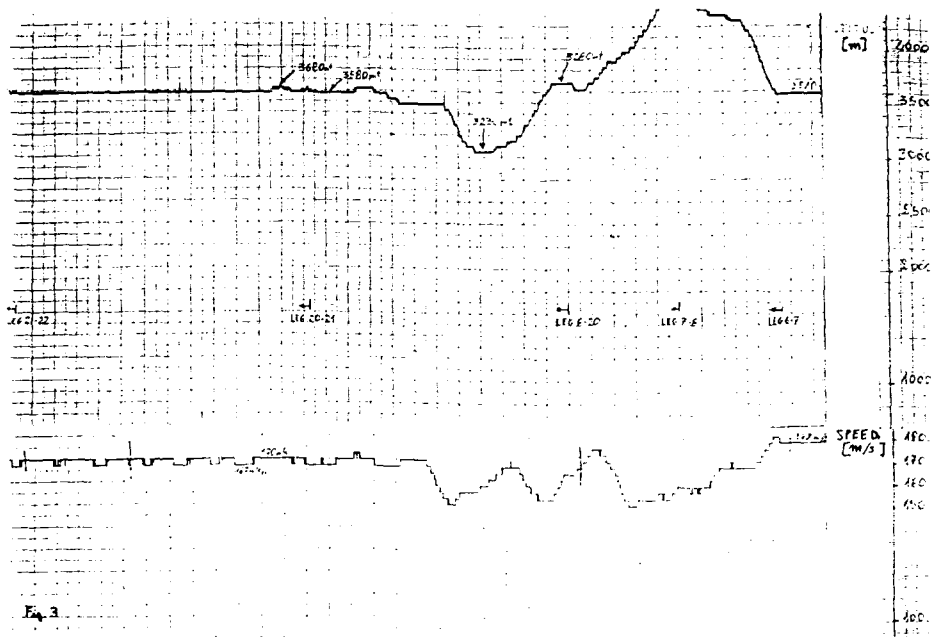


Fig. 3

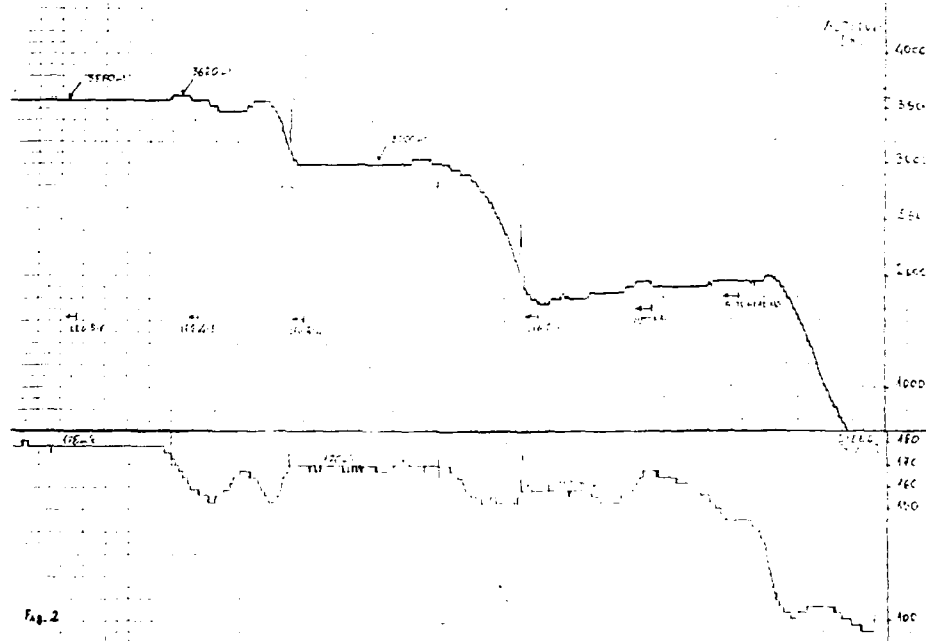


Fig. 2

# NAVIGATION OF AUTONOMOUS AIR VEHICLES BY PASSIVE IMAGING SENSORS

H. Zinner, R. Schmidt, D. Wolf  
MBB GmbH, P.O. Box 801109, 8 München 80, GE

## SUMMARY

Navigation systems of autonomous vehicles must provide 1. information that enables the control of flight and 2. information about the environment that allows for the perception of the 3-d scene. Passive imaging sensors with the appropriate algorithms can supply both types of information. We present a concept that evaluates the optical flow field across the image plane in order to derive the quantities necessary for the guidance and control of the vehicle. The quality of information processing is improved by incorporating knowledge of the environment and the dynamics of the vehicle. In various computer simulations, the performance of an observer is compared with an Extended Kalman Filter. The concept is applied to two kinds of unmanned vehicles: 1. to an autonomous unpropelled submunition, which has to detect, to classify, and to track ground vehicles, and 2. to the fibre-optic guided missile that serves as a testbed towards systems of higher autonomy.

## NOMENCLATURE

$O, X, Y, Z$	Coordinate system, rigidly connected to the imaging system
$X_0, Y_0, Z_0$	coordinates of $O$ in the inertial system
$P$	point in the $X$ - $Y$ -plane of the inertial system
$\mathbf{x} = (X, Y, Z)^T$	coordinates of $P$ in the moving system
$\mathbf{v} = (u, v, w)$	velocity vector of $O$ along the axes of the moving system
$v =   \mathbf{v}  $	absolute value of vector $\mathbf{v}$
$\omega = (p, q, r)^T$	angular velocities about the axes of the moving system
$\phi, \theta, \psi$	Euler angles between inertial and moving system
$A, B, C$	intercepts of $X$ -, $Y$ - and $Z$ -axis of the moving system in the $X$ - $Y$ -plane of the inertial system; $1/A=a, 1/B=b, 1/C=c$
$\mathbf{n} = (a, b, c)^T$	vector, orthogonal to the $X$ - $Y$ -plane of the inertial system
$n =   \mathbf{n}  $	absolute value of $n$
$y, z$	horizontal and vertical image coordinates of $P$
$\mathbf{s} = (\dot{y}, \dot{z})$	vector of optical flow
$I(y, z)$	intensity in the image plane
$I_y, I_x, I_t$	spatial and temporal derivatives of $I$
$f$	focal length of the imaging system

## 1. INTRODUCTION

A system is proposed that enables navigation of an autonomous air vehicle by a passive imaging sensor. Navigation relies on two kinds of information: 1. so-called proprio-specific information that is necessary to control the egomotion of the vehicle and 2. exterospecific information that allows for object detection or avoidance thereof, depth perception, and orientation relative to the environment (fig. 1).

Technical navigation systems are mainly based upon inertial platforms. Because they yield only proprio-specific information, additional sensors such as radar are necessary.

In contrast to technical systems, animals can navigate by visual cues only. Evaluating the optical flow field<sup>1</sup> across the retina provides proprio-specific information as well as exterospecific information. Especially in long-range navigation, inertial systems are of minor importance.

Our system tries to copy these biological examples. By processing the image sequences supplied by the sensor we firstly obtain the following proprio-specific quantities: rate of roll, pitch, yaw, the angle of attack, and the angle of yaw. In addition to this type of information, which is similar to that provided by inertial systems, we derive exterospeci-

fic quantities that enable obstacle avoidance and improve the target acquisition and tracking process.

The first step of the signal processing is the determination of the optical flow. We developed a gradient-based algorithm specially suited for low-contrast infrared images. In a second step, the nonlinear projection equations are solved. It is shown how analytical solutions for the motion parameters can be obtained. The image processing is regularized by global models concerning the structure of the environment. The accuracy of the estimation is improved by a new pixel-recursive method that, in contrast to other algorithms, incorporates global knowledge of the motion.

Dynamic models relate the parameters obtained by image processing to the quantities necessary for the guidance and control of the vehicle. We compare the performance of an Extended Kalman Filter with that of an observer. The Kalman Filter is fed by the quantities obtained by image processing directly, whereas the observer uses the analytical solutions of the projection equations.

Two possible applications are outlined. Firstly, we simulated the flight of an autonomous terminally guided submunition equipped with an infrared focal plane array sensor which is rigidly connected to the missile. The signal processing estimates the motion parameters and the orientation relative to the environment and detects and tracks targets. It is further shown, how the analytically correct description of the background motion improves the tracking process (e.g. the compensation for image explosion).

Furthermore, we applied our method to the guidance and control of the fibre optic guided missile. This is not an autonomous system, but it served as a testbed for different steps towards an unmanned air vehicle. It is shown how our algorithms improve the performance of the missile and assist the man in the loop in various ways: Firstly, the image sequences supplied by the sensor can be stabilized electronically. This is a simple by-product of our method that renders mechanical stabilization unnecessary. Secondly, as in the previous application, the target tracking process can be improved by evaluating the motion of the sensor relative to the environment. Thirdly, because the signal processing provides parameters describing the orientation of the vehicle, it can cruise at constant altitude above ground without further sensors such as radar or laser altimeters.

## 2. OPTICAL FLOW AND MOTION PARAMETERS

### 2.1 Kinematics

The air vehicle moves in a 3-dimensional optically structured environment. Rigidly connected to the vehicle is an imaging system with coordinates  $(O, X, Y, Z)$  (fig.2). Let  $\mathbf{v} = (u, v, w)^T$  be the translational velocity and  $\boldsymbol{\omega} = (p, q, r)^T$  the angular velocity of the vehicle. Then the point  $P$  moves with the velocity

$$\dot{\mathbf{x}} = -\mathbf{v} - \boldsymbol{\omega} \times \mathbf{x} \quad (2.1)$$

Object points are imaged by perspective projection

$$(y, z)^T = f/X (Y, Z)^T \quad (2.2)$$

The optical flow generated by the motion of the vehicle is given by

$$\begin{aligned} \dot{y} &= \frac{1}{X} (-vf + uy) + pz + q \frac{yz}{f} - r \left( f + \frac{y^2}{f} \right) \\ \dot{z} &= \frac{1}{X} (-wf + uz) - py + q \left( f + \frac{z^2}{f} \right) - r \frac{yz}{f} \end{aligned} \quad (2.3)$$

The unknown quantity  $X$  can be eliminated. We obtain (with  $f=1$ ):

$$\frac{z - w/u}{y - v/u} = \frac{\dot{z} + py - q(1 + z^2) + ryz}{\dot{y} - pz - qyz + r(1 + y^2)} \quad (2.4)$$

Instead of eliminating  $X$  one can gain exterospecific information by modelling the environment parametrically, e. g. as a plane:

$$X/A + Y/B + Z/C = 1. \quad (2.5)$$

This assumption is adequate for vehicles flying at a certain altitude above ground. In this case the optical flow is given by

$$\begin{pmatrix} \dot{y} \\ \dot{z} \end{pmatrix} = (a + by + cz) \begin{pmatrix} uy - v \\ uz - w \end{pmatrix} + p \begin{pmatrix} z \\ -y \end{pmatrix} + q \begin{pmatrix} yz \\ 1+z \end{pmatrix} - r \begin{pmatrix} 1+y^2 \\ yz \end{pmatrix} \quad (2.6)$$

with  $a=1/A$ ,  $b=1/B$ ,  $c=1/C$ . Simple rearranging yields

$$\begin{aligned} \dot{y} &= p_1 + p_2 y + p_3 z + p_4 y^2 + p_5 yz \\ \dot{z} &= p_6 + p_7 y + p_8 z + p_4 yz + p_5 z^2 \end{aligned} \quad (2.7)$$

with

$$\begin{aligned}
 p_1 &= -r - av \\
 p_2 &= au - bv \\
 p_3 &= p - cv \\
 p_4 &= -r + bu \\
 p_5 &= q + uc \\
 p_6 &= q - aw \\
 p_7 &= p - bw \\
 p_8 &= au - cw.
 \end{aligned} \tag{2.8}$$

The quantities  $p = (p_1 \dots p_8)^T$  are called "pure" or "essential" parameters (Tsai and Huang<sup>2</sup>); they are nonlinear functions of the motion parameters:

$$p = h(V, \omega, n).$$

We relate these parameters to the change of intensity  $I(y, z, t)$  in the image plane. If the change is only due to motion, then the gradient constraint equation (Thompson and Barnard<sup>3</sup>) is given by

$$I_y \dot{y} + I_z \dot{z} + I_t = 0. \tag{2.9}$$

Combine (2.7) and (2.9) and obtain

$$I^T p + I_t = 0 \tag{2.10}$$

with

$$I = \begin{pmatrix} I_y \\ I_y y \\ I_y z \\ I_y y^2 + I_z yz \\ I_y yz + I_z z^2 \\ I_z \\ I_z y \\ I_z z \end{pmatrix} \tag{2.11}$$

(Zinner<sup>4,5</sup>). Solving (2.8) yields the motion parameters  $p, q, r, w/u, v/u, A/u, B/v, C/w$ . Two points should be emphasized:

1. The exterospecific model (2.6) provides information about the environment and permits navigation and obstacle avoidance because the quantities  $A/u, B/v, C/w$  are related to the so-called time to contact, i. e. the time that passes until the vehicle hits the surface. (Eq. (2.4) also contains some kind of depth information: one can extract the quantity  $X/u$ . Clearly,  $A/u, B/v, C/w$  are more valuable for navigation).
2. The assumption (2.5) regularizes the system and renders the solutions numerically stable. The motion parameters can be obtained analytically, as will be shown.

## 2.2 Analytical derivation of the motion parameters

It will be shown, that the following quantities can be obtained from (2.8):

1. the directions  $e_v = \frac{1}{V} V$  and  $e_n = \frac{1}{n} n$ ,
2. the product of the absolute values  $V \cdot n$  of the vectors  $V$  and  $n$  (but not the values themselves) and
3. the vector  $\omega$ .

In order to solve (2.8), we first eliminate  $p, q, r$  and get the five equations

$$\begin{aligned}
 k_1 &= p_4 - p_1 = ub + va \\
 k_2 &= p_2 = ua - vb \\
 k_3 &= p_5 - p_6 = uc + wa \\
 k_4 &= p_8 = ua - wc \\
 k_5 &= -(p_3 + p_7) = vc + wb,
 \end{aligned} \tag{2.12}$$

which contain only the components of  $V$  and  $n$ . We follow an idea of Longuet-Higgins<sup>6</sup> and introduce the matrices

$$A = V n^T + n V^T = \begin{pmatrix} 2ua & ub + vu & uc + wa \\ ub + va & 2vb & vc + wb \\ uc + wa & vc + wb & 2wc \end{pmatrix}$$

and

$$K = \begin{pmatrix} 0 & k_1 & k_3 \\ k_1 & -2k_2 & k_5 \\ k_3 & k_5 & -2k_4 \end{pmatrix};$$

then (2.12) can be written in the form

$$A = 2ua \cdot I + K. \quad (2.13)$$

$I$  is the  $3 \times 3$  identity matrix.

From now on, our analysis differs from the approach proposed by Longuet-Higgins. It can be shown, that  $A$  has the following eigenvectors:

$$\begin{array}{ll} e_v - e_n & \text{with eigenvalue } V^T n - V \cdot n \\ e_v \times e_n & " \quad " \quad 0 \\ e_v + e_n & " \quad " \quad V^T n + V \cdot n. \end{array}$$

$K$  has the same eigenvectors as  $A$ :

$$\begin{array}{ll} e_v - e_n & \text{with eigenvalue } \lambda_1 = \lambda - V \cdot n \\ e_v \times e_n & " \quad " \quad \lambda_2 = \lambda + V^T n \\ e_v + e_n & " \quad " \quad \lambda_3 = \lambda + V \cdot n \end{array} \quad (2.14)$$

with  $\lambda = -2ua - V^T n$ . Hence it follows that

$$\begin{array}{l} \lambda_1 \leq \lambda_2 \leq \lambda_3; \\ \lambda_1 = \lambda_2 \Leftrightarrow e_v = -e_n; \\ \lambda_2 = \lambda_3 \Leftrightarrow e_v = e_n. \end{array}$$

These results suggest the following procedure for solving (2.12): Firstly, we determine the eigenvalues  $\lambda_1, \lambda_2, \lambda_3$  and the eigenvectors  $E_1, E_2, E_3$  of  $K$  such that the conditions  $\lambda_1 \leq \lambda_2 \leq \lambda_3$  are met. The eigenvectors can be normalized to the absolute value 1 and to nonnegative first component. From (2.14) we get

$$\begin{aligned} V \cdot n &= \frac{\lambda_3 - \lambda_1}{2} \\ V^T n &= \lambda_2 - \frac{\lambda_1 + \lambda_3}{2} \\ e_v^T e_n &= \frac{V^T n}{V \cdot n} = \frac{2\lambda_2 - \lambda_1 - \lambda_3}{\lambda_3 - \lambda_1} \\ \|e_v - e_n\| &= \sqrt{2(1 - e_v^T e_n)} = 2 \sqrt{\frac{\lambda_3 - \lambda_2}{\lambda_3 - \lambda_1}} \\ \|e_v + e_n\| &= 2 \sqrt{\frac{\lambda_2 - \lambda_1}{\lambda_3 - \lambda_1}}. \end{aligned} \quad (2.15)$$

The  $E_i$  are related to  $e_v$  and  $e_n$  according to

$$\begin{aligned} e_v - e_n &= \pm \|e_v - e_n\| E_1 = \pm 2 \sqrt{\frac{\lambda_3 - \lambda_2}{\lambda_3 - \lambda_1}} E_1 \\ e_v + e_n &= \pm \|e_v + e_n\| E_3 = \pm 2 \sqrt{\frac{\lambda_2 - \lambda_1}{\lambda_3 - \lambda_1}} E_3. \end{aligned} \quad (2.16)$$

The solution can be divided into four groups:

	group 1	group 2	group 3	group 4
$e_v$	$\bar{E}_1 + \bar{E}_3$	$\bar{E}_1 - \bar{E}_3$	$\bar{E}_3 - \bar{E}_1$	$-(\bar{E}_1 + \bar{E}_3)$
$e_n$	$\bar{E}_3 - \bar{E}_1$	$-(\bar{E}_1 + \bar{E}_3)$	$\bar{E}_1 + \bar{E}_3$	$\bar{E}_1 - \bar{E}_3$

$$\text{with } \bar{E}_1 = \sqrt{\frac{\lambda_3 - \lambda_2}{\lambda_3 - \lambda_1}} E_1, \bar{E}_3 = \sqrt{\frac{\lambda_2 - \lambda_1}{\lambda_3 - \lambda_1}} E_3.$$

$\bar{E}_1$  and  $\bar{E}_3$  were chosen such that the first component becomes nonnegative. A nonpositive first component of  $e_n$  indicates that the optical axis is directed away from the plane.

Since this makes no sense, group 2 can be discarded. For the same reason another group can be eliminated: If the motion is towards the plane (first component of  $e_v$  positive), group 4 can be excluded, otherwise group 1. Therefore, group 1 and group 3 must be considered in our case.

Both solutions contain the same vectors, but interchanged. We found that in general none of them can be discarded: on the one hand, one obtains the unit vectors of  $V$  and  $n$ ; on the other hand one cannot identify them without further information (ref. 6 suggests a way to discriminate the two solutions; but this method is restricted to special cases and cannot be applied in our case).

We summarize the steps towards an analytical solution for the motion parameters:

1. Determine eigenvalues  $\lambda_i$  and eigenvectors  $E_i$  ( $i=1,2,3$ ) of  $K$  such that  $\lambda_1 \leq \lambda_2 \leq \lambda_3$ ,  $\|E_i\|=1$ , and  $E_1, E_2$  have nonnegative first component.
2. Compute  $V \cdot n = (\lambda_3 - \lambda_1)/2$  and

$$\begin{aligned} M_1 &= \sqrt{\frac{\lambda_3 - \lambda_2}{\lambda_3 - \lambda_1}} E_1 + \sqrt{\frac{\lambda_2 - \lambda_1}{\lambda_3 - \lambda_1}} E_3 \\ M_2 &= \sqrt{\frac{\lambda_2 - \lambda_1}{\lambda_3 - \lambda_1}} E_3 - \sqrt{\frac{\lambda_3 - \lambda_2}{\lambda_3 - \lambda_1}} E_1. \end{aligned}$$

3. Decide (exploiting additional information) whether  $e_v = M_1$ ,  $e_n = M_2$  or  $e_v = M_2$ ,  $e_n = M_1$  is correct.

4. Compute angular velocities

$$\begin{aligned} r &= -p_1 - V \cdot n \cdot e_{v2} \cdot e_{n1} \\ p &= p_3 + V \cdot n \cdot e_{v2} \cdot e_{n3} \\ q &= p_6 + V \cdot n \cdot e_{v3} \cdot e_{n1}. \end{aligned} \quad (2.17)$$

5. If necessary, compute additional quantities such as the time to contact

$$T_a = V^T n = \lambda_2 - \frac{\lambda_1 + \lambda_3}{2}.$$

All relations also hold for  $\lambda_1 = \lambda_2$  and  $\lambda_2 = \lambda_3$ . The case  $\lambda_1 = \lambda_2 = \lambda_3$  corresponds with  $V = 0$  and will not be considered here.

### 3. IMAGE PROCESSING

#### 3.1 General Concepts

The general concept for image processing is described elsewhere<sup>5</sup> and will be only summarized here:

1. Randomly select points in the image, where  $I_y$ ,  $I_z$ , and  $I_t$  should be measured (it is possible, to search for regions, where the spatial derivatives can be measured more accurately than in others; but we found that the computational expense of the search did not pay). The number of points depends on the desired accuracy and on the time available for the computations; we choose from 100 to 400 points.
2. Determine  $I_y$ ,  $I_z$  via  $(\nabla G) \circ I$ , where  $\nabla$  means gradient,  $G$  a Gaussian low-pass filter and  $\circ$  convolution.
3. Determine  $\partial/\partial t G \circ I$  by fitting polynomials through intensity values of successive frames.
4. Compute  $p$  and  $\text{cov}(p)$  from (2.10) by least squares estimation.

#### 3.2 A Pixel-Recursive Iteration

Eq. (2.9) yields reliable results only for small displacements because of limited frame rates. Extensive spatial filtering would prevent aliasing, but is time consuming (if it is not done by simple defocussing) and causes loss of information.

A pixel-recursive algorithm developed by our group<sup>7</sup> alleviates these problems. It exploits local image information and global knowledge of the motion in order to improve the estimation of  $I_t$  and  $p$ . The algorithm is based on an modified Newton procedure that determines the zero-crossings of

$$\Delta I = I(\hat{y}, \hat{z}, t_0) - I(y, z, t_0) = 0. \quad (3.1)$$

Given an estimate  $\hat{s} = (\hat{y}, \hat{z})$  in the  $i$ -th iteration, the procedure is

$$\nabla I(y, z, t_0) \cdot (\hat{s}_{i+1} - \hat{s}_i) = -\Delta I. \quad (3.2)$$

Expressing the optical flow by the pure parameters (2.9, 2.10) yields

$$I^T(\hat{p}_{i+1} - \hat{p}_i) = -\Delta I. \quad (3.3)$$

The gradient method is now applied to small displacements. Our method differs from other pixel-recursive procedures<sup>4,5</sup>, because it evaluates the analytically correct global motion information (3.4) by least-squares estimation. Therefore, the noise sensitivity of the displacement estimation (3.2) is considerably reduced.

#### 4. STATE ESTIMATION

##### 4.1 The Dynamic System

It is shown how an autonomous air vehicle could navigate exploiting the type of measurement described in chapter 2 and 3.

The vehicle is modelled as a controlled dynamic system

$$\dot{x} = f(x, u, y)$$

with  $x(t)$  = state vector,  $u(t)$  = control vector,  $y(t)$  = noise vector (at time  $t$ ). The navigation system has to provide an estimation  $\hat{x}(t)$  of the state  $x(t)$  at discrete time steps  $t = t_0, t_1, \dots$

We based our analysis on the dynamics of an unpropelled submunition with state vector

$$x = (u, v, w, p, q, r, a, b, c, \gamma, X_g, Y_g)^T = (V^T, \omega^T, n^T, \gamma, X_g, Y_g)^T,$$

control vector

$$u = (\eta, \zeta, \xi)^T$$

( $\eta, \zeta, \xi$  = deflections of control surfaces) and noise vector caused by wind

$$y = V_w = (u_w, v_w, w_w)^T.$$

$V_w$  is the air velocity in the moving coordinate system. The force of aerodynamic drag depends on  $\Delta V = V - V_w$  via the angles

$$\alpha = \arctan \frac{w - w_w}{u - u_w} \quad (\text{angle of attack}), \quad \beta = \arcsin \frac{v - v_w}{\Delta V} \quad (\text{angle of yaw})$$

and via  $\Delta V^2$ . The coefficients of aerodynamic drag  $C_T = (C_x, C_y, C_z)^T$  (for translation) and  $C_R = (C_p, C_q, C_r)^T$  for rotation are functions of the arguments  $C_T = C_T(\alpha, \beta, u)$  and  $C_R = C_R(\omega, \alpha, \beta, \Delta V, u)$ . The dynamics of the vehicle is then described by the following equations of motion:

$$\dot{V} = -\omega \times V + g \frac{1}{n} n + \Delta V^2 C_T, \quad (4.1)$$

$$\dot{\omega} = \begin{pmatrix} 0 \\ \frac{I_z - I_x}{I_y} \cdot p \cdot r \\ \frac{I_x - I_y}{I_z} \cdot p \cdot q \end{pmatrix} + \Delta V^2 I^{-1} C_R, \quad (4.2)$$

$$\dot{n} = -\omega \times n + (n^T V) n, \quad (4.3)$$

$$\left. \begin{aligned} \dot{\gamma} &= \dot{\gamma}(\omega, n) \\ \dot{X}_g &= \dot{X}_g(V, n, \gamma) \\ \dot{Y}_g &= \dot{Y}_g(V, n, \gamma) \end{aligned} \right\} \quad (4.4)$$

with

$$I = \begin{pmatrix} I_x & 0 & 0 \\ 0 & I_y & 0 \\ 0 & 0 & I_z \end{pmatrix} = \text{tensor of inertial moments.}$$

Two methods of estimating the state variables of the dynamic system are investigated. If the measurements are exact and if the system is noise-free a Luenberger observer<sup>10</sup> can be

used. If all the observed variables are corrupted by additive noise, the Kalman-Bucy Filter should be selected.

In some cases only a part of the observation variables is corrupted. Then a mixture of both methods is the appropriate approach. In our case, there is no significant difference of noise in the observed variables. Therefore we implemented both methods just to compare their performance.

#### 4.2 Design of an Observer

In this chapter we assume that no noise corrupts the observations nor the system dynamics. Furthermore we assume that the initial state  $x(0)$  is not exactly known, i.e. we start with corrupted variables  $\hat{x}(0)$ . Our goal is to reconstruct  $x(t)$  using the available observations, which means that

$$\lim_{t \rightarrow \infty} \|\hat{x}(t) - x(t)\| = 0.$$

The optical sensor provides the observations

$$\omega, e_v = \frac{1}{V} V, e_n = \frac{1}{n} n, \text{ and } V \cdot n.$$

The state variables  $V, X, Y, \dot{X}, \dot{Y}$  are not observable in the sense specified above with this kind of information. Therefore we consider only  $V, \omega$ , and  $n$ . Since  $V \cdot n$  is known, only  $V$  or  $n$  has to be estimated.

The Luenberger Observer uses the system dynamics and the observations and derives a differential equation of reduced order corresponding to that part of the state variables that is not directly observed, i.e. in our case  $n$  or  $V$ .

##### a) Differential Equation for $n(t)$

With (4.3) we derive a differential equation for  $n(t)$  of the form  $\dot{n} = T_c^{-1} n$ , where  $T_c(t) = (n^T \cdot V)^{-1}$  = time to contact (observed quantity). It came out that the relative errors in  $n(t)$  and  $V(t)$  remain constant. Therefore, the unknown quantities will not be reconstructed in the sense defined above. Nevertheless, it should be mentioned that

$$\hat{z}_g(t) = 0 \text{ iff } z_g(t) = 0,$$

i. e. the estimated time of contact is exact. Furthermore, the above-mentioned equation does not depend on the special dynamics that is used here (this kind of information may be suitable for estimating the general motion towards the plane).

##### b) Differential equation for $V(t)$ :

Using (4.1) instead of (4.3), we obtain

$$\dot{V} = e_v^T \cdot \dot{V} = g \cdot e_v^T \cdot e_n + e_v^T \cdot C_T \cdot V^2 = r(t) + s(t) \cdot V^2$$

with the known functions

$$r(t) = g \cdot e_v^T \cdot e_n = \frac{2\lambda_2 - \lambda_1 - \lambda_3}{\lambda_3 - \lambda_1} \cdot g \text{ and } s(t)$$

Notice that  $\alpha$  and  $\beta$  depend only on  $e_v$ .  $V$  can be estimated by solving the initial value problem

$$\begin{aligned} \hat{V}(0) &= \hat{V}_0 \\ \dot{\hat{V}} &= r + s \cdot \hat{V}^2 \end{aligned}$$

with standard methods. This also provides

$$\hat{n} = \frac{V \cdot n}{V} = \frac{\lambda_3 - \lambda_1}{2 \cdot V} \text{ and } \hat{z}_g = \frac{2 \cdot \hat{V}}{\lambda_3 - \lambda_1}.$$

It can be shown that in case of  $s(t) \leq -\epsilon < 0$  for all  $t \geq 0$  we get

$$\lim_{t \rightarrow \infty} \|\hat{V}(t) - V(t)\| = 0$$

for any corrupted initial value  $\hat{V}_0$ . Hence  $V$  and  $n$  can be reconstructed using the information provided by the optical system.

The assumption  $s(t) \leq -\epsilon < 0$  is natural and nonrestrictive, since  $s(t) \cdot V^2$  is the aerodynamic drag.

#### 4.3 Design of the Kalman-Bucy-Filter

The Kalman-filter exploits the full knowledge of the system dynamics and computes the estimations of the state recursively. In order to design the filter we derive the appropriate system dynamics and measurement equation that relates the observed variables to the state variables.

Firstly we modify the state representation introduced in chapter 4.1. Again we drop the variables  $\dot{Y}$ ,  $X_s$ ,  $V_s$  because they cannot be observed by the optical sensor and because they are not necessary to control the vehicle.

On the other side we introduce additional variables to model the air turbulences within the filter algorithm. We model the wind as additive disturbances of the angle of attack  $\alpha$  and the angle of yaw  $\beta$ . This implies, that the coefficients of aerodynamic drag depend on  $\alpha' = \alpha + \Delta\alpha$ ,  $\beta' = \beta + \Delta\beta$ , where  $\alpha = \arctan w/u$ ,  $\beta = \arcsin v/V$ , and  $\Delta\alpha$ ,  $\Delta\beta$  are due to the wind. Finally, we define the dynamics of  $\Delta\alpha$  and  $\Delta\beta$ . We construct two shaping filters driven by white Gaussian noise to model the wind effect. New variables  $\Delta\alpha_i$ ,  $\Delta\beta_i$  ( $i=1,2,3$ ) are introduced such that

$$\Delta\alpha = \Delta\alpha_1 + \Delta\alpha_3, \quad \Delta\beta = \Delta\beta_1 + \Delta\beta_3,$$

and

$$\left. \begin{aligned} \Delta\dot{\alpha}_1 &= \Delta\alpha_2 \\ \Delta\dot{\alpha}_2 &= -c_1\Delta\alpha_1 - c_2\Delta\alpha_2 + \xi_\alpha \\ \Delta\dot{\alpha}_3 &= 0; \end{aligned} \right\} \quad (4.5)$$

$$\left. \begin{aligned} \Delta\dot{\beta}_1 &= \Delta\beta_2 \\ \Delta\dot{\beta}_2 &= -c_3\Delta\beta_1 - c_4\Delta\beta_2 + \xi_\beta \\ \Delta\dot{\beta}_3 &= 0. \end{aligned} \right\} \quad (4.6)$$

$\xi_\alpha$  and  $\xi_\beta$  are the above-mentioned noise variables and  $c_i$  appropriate constants. This yields the augmented state vector:

$$x^T = (u, v, w, p, q, r, a, b, c, \Delta\alpha_1, \Delta\alpha_2, \Delta\alpha_3, \Delta\beta_1, \Delta\beta_2, \Delta\beta_3).$$

The corresponding differential equations are, according to (4.1) - (4.3):

$$\dot{V} = -\omega \times V + g \cdot e_n + V^2 \cdot C_T(\alpha', \beta', u) + \xi_V \quad (4.7)$$

$$\dot{\omega} = \begin{pmatrix} 0 \\ \frac{I_z - I_x}{I_y} \cdot p \cdot r \\ \frac{I_x - I_y}{I_z} \cdot p \cdot q \end{pmatrix} + V^2 \cdot I^{-1} \cdot C_R(\omega, \alpha', \beta', V, u) + \xi_\omega \quad (4.8)$$

$$\dot{n} = -\omega \times n + (n^T \cdot V) \cdot n, \quad (4.9)$$

where  $\xi_V$  and  $\xi_\omega$  are stationary white Gaussian noise vectors, introduced to compensate for the inadequacies of the mathematical model.

Equations (4.5) - (4.9) form the stochastic differential equation

$$\dot{x} = \hat{f}(x, u) + \xi_x, \quad (4.10)$$

which is one part of the Kalman-Bucy Filter.

The other part consists of the measurement equation. We assume, that the observed variables  $p^T = (p_1, \dots, p_s)$  are corrupted by additive stationary white Gaussian noise  $\xi_p$ , and get

$$p = h(x) + \xi_p, \quad (4.11)$$

with  $h$  defined as in chapter 2. Because (4.10) and (4.11) are nonlinear, the Extended Kalman Filter formalism must be used. Details are omitted; the reader is referred to Maybeck<sup>11</sup>, ch. 5.9.

#### 5. SIMULATIONS

Starting from real images (visible and infrared), synthetic image sequences were generated. The field of view was about  $31^\circ$  in most of the times and was digitized with  $512 \times 512$  pixels, resulting in a spatial resolution of about  $1.2$  mrad. The images were transformed using the simulated state of flight of the vehicle.

As an example, we modelled the dynamics of an unpropelled cross-winged submunition. Two types of experiments were carried out: 1. In order to test the performance of image processing and state estimation independently from the control process, the vehicle had to fly with fixed control surfaces under the influence of wind and turbulence. 2. The complete process of image processing, state estimation, guidance and control was simulated (fig. 3). In this case, the vehicle either tracked a moving or stationary target or it was forced to cruise at constant altitude. Unless specifically stated, the wind velocity was 24 m/s in 500 m altitude, the frame rate 100 Hz, the time delay 10 ms,  $V_0 = u = 200$  m/s.

Fig. 4 shows the rate of pitch during a flight of the submunition, tracking a target. The true values are compared with the estimates of the image processing (analytical solution; these are the values used by the observer) and the estimates of the Kalman filter. It can be seen how the EKF degrades the information produced by image processing. In fig. 5 the values of time to contact, obtained by the different methods, are compared (fixed control surfaces). As predicted in chapter 4, the estimation improves as the vehicle approaches the ground.

In fig. 6 the error of the observer is compared with that one of the Kalman filter. The difference in performance is significant, because the Kalman filter is less sensitive to the disturbance of the initial value ( $\sigma = 5$  m, wind = 12 m/s, fixed control surfaces). Fig. 7 shows the flight of the unpropelled submunition at constant altitude, estimated by the Kalman filter (disturbance of the initial value = 5 m, wind = 12 m/s).

The observer suffers from two drawbacks: 1. Since it uses the analytical solutions (2.15-2.17), it sometimes runs into the wrong solution and cannot be recovered (it should be mentioned, however, that the time to contact is unique). 2. If high angular velocities prevail, the estimation of optical flow is wrong and the state estimation provided by the observer is incorrect.

The Kalman Filter does not face these problems. Since the analytical solutions are not explicitly used, the problem of uniqueness does not arise. Furthermore, it weighs and degrades the quantities produced by image processing according to the variance (cf. fig. 5).

## 6. CONCLUSIONS

We have presented a concept that enables navigation of an autonomous air vehicle by a passive imaging sensor. It has been proved that the optical flow field provides complete and sufficient information to guide and control the vehicle.

The optical flow is not given directly; it must be derived from the intensity changes in the focal plane. The interpretation of optical flow is a complex task; especially the problem of uniqueness has to be carefully addressed.

Why bother with passive imaging sensors? The reason is the following: Vision yields the richest description of the environment. It provides proprio-specific information concerned with the state of flight and exterospecific information related to the depth of the scene, to the orientation of the sensor relative to the environment, and to the position and motion of objects. This kind of information is not provided by a single other sensor.

Many modern weapon systems are equipped with imaging sensors for target acquisition, classification, and tracking. In conventional systems, especially if ground targets are attacked, the sensor motion disturbs these processes. In our concept, the full information provided by the sensor, including motion information, can be exploited to enhance the target acquisition, classification, and tracking process.

Two kinds of applications were envisaged. Firstly, we applied our concept to the flight of an autonomous unpropelled submunition, which was devised to attack ground vehicles ("flight without gyroscopes"). This is a very difficult task because the imaging sensor must acquire, classify and track targets, and must guide and control the air vehicle. This concept cannot be realized in the immediate future, because 1.) the sensors with the necessary physical properties are not yet available (night vision is required!) and 2.) the real-time image processing algorithms are too complex to be implemented in state-of-the-art onboard computers.

There are intermediate steps towards a visually guided autonomous vehicle. In our second application, we simulated parts of our concept with the fibre optic guided missile. It is an advantage of this concept that the image processing can be done on ground, and that the missile is guided by inertial systems. Therefore, the different steps towards a higher autonomy can be tested independently.

A simple by-product of our motion estimation algorithm is the electronic stabilization of image sequences, that renders accurate mechanical stabilization of the sensor unnecessary. Secondly, after target acquisition by the human operator, the tracking process can be improved because our algorithm correctly describes the motion of the background. Features and reference frames can be updated; especially they can be compensated for image explosion. Thirdly, and maybe most important, the vehicle can fly at constant altitude above ground without other sensors such as radars or laser altimeters.

The above-mentioned ideas can be applied to other kinds of unmanned air vehicles, which were not investigated. For example, the navigation of autonomous drones (cf. Noga<sup>12</sup>, 1985) can be improved by our algorithms (flight at constant altitude, transformation of features such as landmarks, registration of images etc.).

Finally, it should be mentioned, that true autonomous navigation in a complex environment requires more visual capabilities than the evaluation of optical flow. But even this limited task is still in its infancy.

#### REFERENCES

1. Gibson, J.J. The Perception of the Visual World. Houghton Mifflin, Boston, 1956.
2. Tsai, R.Y.  
Huang, T.S. Uniqueness and estimation of three-dimensional motion parameters of rigid objects with curved surfaces. IEEE Trans. on Pattern Analys. Machine Intell. **PAMI-6**, 13-27, 1984.
3. Thompson, W.B.  
Barnard, S.T. Lower-level estimation and interpretation of visual motion. IEEE Trans. Comput. **C14**, 20-28, 1981.
4. Zinner, H. Method and Means for Determining the Rate of Roll, Pitch, Yaw, and Heading of an Airborne Vehicle. German Patent DPA P3446009.8, 1984.
5. Zinner, H. Determining the kinematic parameters of a moving imaging system by processing spatial and temporal intensity changes. J. Opt. Soc. Am. **A3**, 1512-1517, 1986.
6. Longuet-Higgins, H.C. The visual ambiguity of a moving plane. Proc. Roy. Soc. Lond. **B223**, 165-175, 1984.
7. Diehl, H.  
Schmidt, R. A pixel-recursive method for determining the motion of imaging sensors. In: Mustererkennung 1986, Baumann, G. (ed.), Springer, Berlin, p. 288, 1986.
8. Robbins, J.D.  
Netravali, A.N. Recursive motion estimation: A review. In: Image Sequence Processing and Dynamic Scene Analysis, Huang, T.S. (ed.), Springer, Berlin, pp. 75-103, 1983.
9. Diehl, N.  
Burkhardt, H. Planar motion estimation with a fast converging algorithm. In: Proc. 8th Int. conf. on Pattern Recogn., Simon, H.C. (ed.), IEEE Comp. Soc. Press, Silver Springs, pp. 1099-1102, 1986.
10. Luenberger, D.G. An introduction to observers. IEEE Trans. on Automatic Control **AC16**, 596-602, 1971.
11. Maybeck, P.S. Stochastic Models, Estimation, and Control, Vol. 2. Academic Press, New York, 1982.
12. Noga, M.T. Image-Based Navigation. Lockheed Missiles & Space Co. Techn. Rep. D060772, 1985.

#### ACKNOWLEDGEMENTS

Part of this research was supported by the German ministry of Defence. The help of Mrs. J. Proske in preparing the manuscript is gratefully acknowledged.

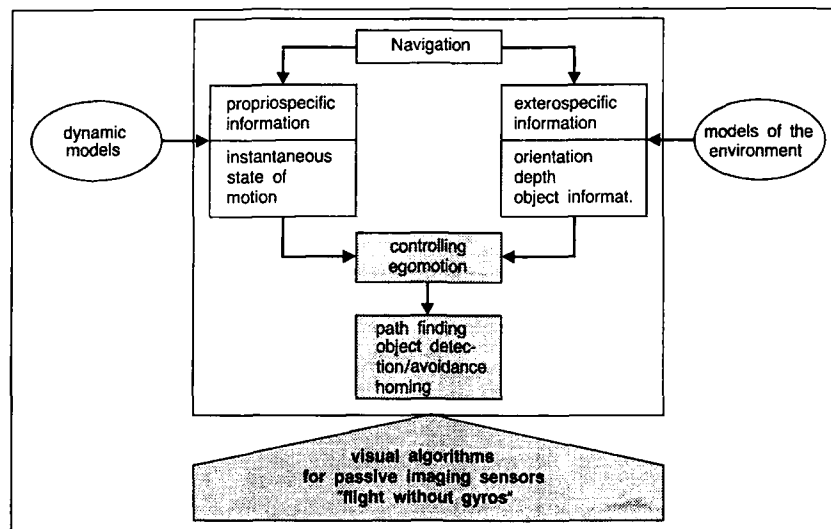


Fig. 1. Kinds of information necessary for navigation

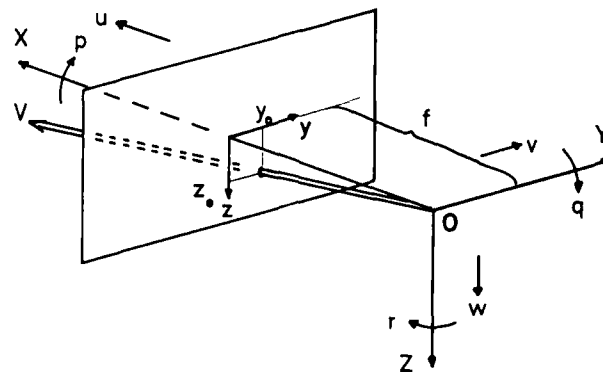


Fig. 2. Coordinate system, connected to the optical sensor

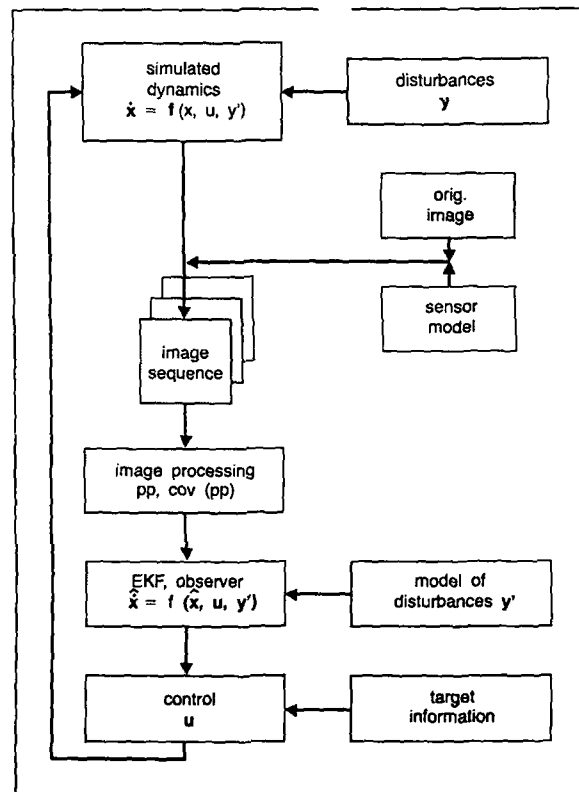


Fig. 3. Concept for the simulation

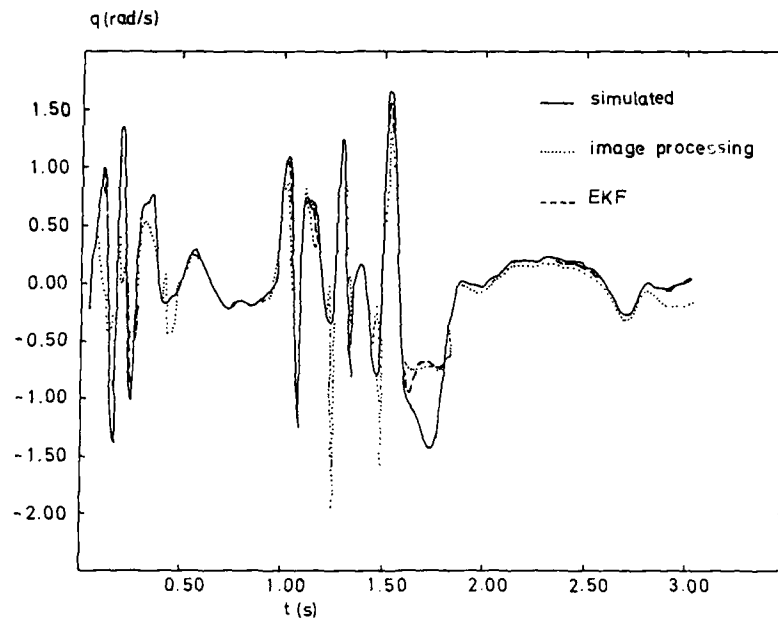


Fig. 4. Rate of pitch of an unpropelled submunition, tracking a target. The observer uses the analytical solutions. It can be seen, how the EKF weighs and degrades the quantities produced by image processing

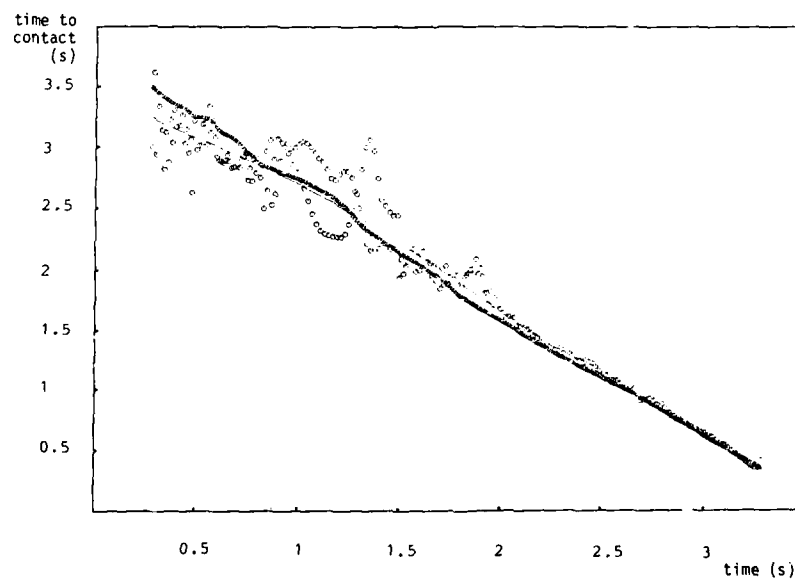


Fig. 5. Time to contact (Flight with fixed control surfaces).  
simulated, oooooo image processing/observer, \*\*\*\*\* EKF

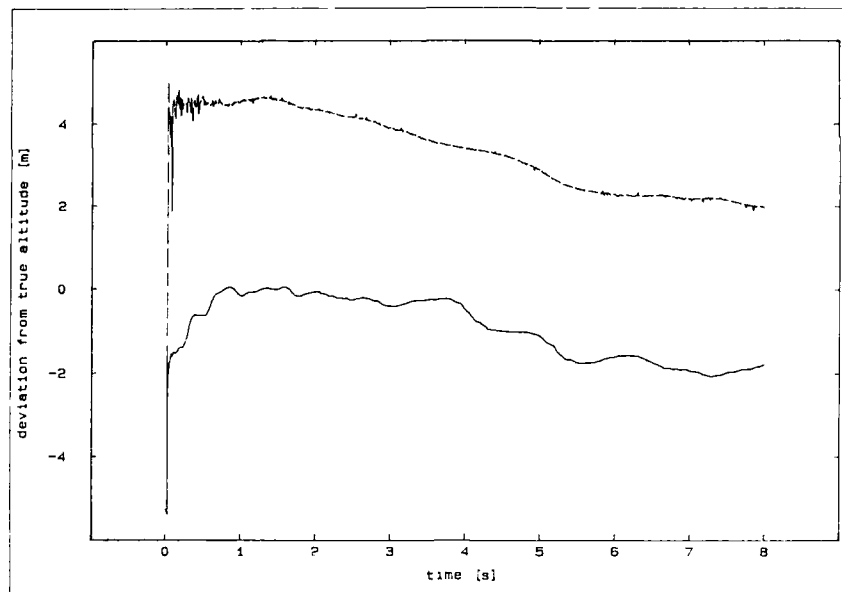


Fig. 6. Error in the estimation of altitude, produced by the observer and the EKF (flight with fixed control surfaces). Error in the initial values  $\sigma = 5$  m; wind = 12 m/s; - - - observer, — EKF

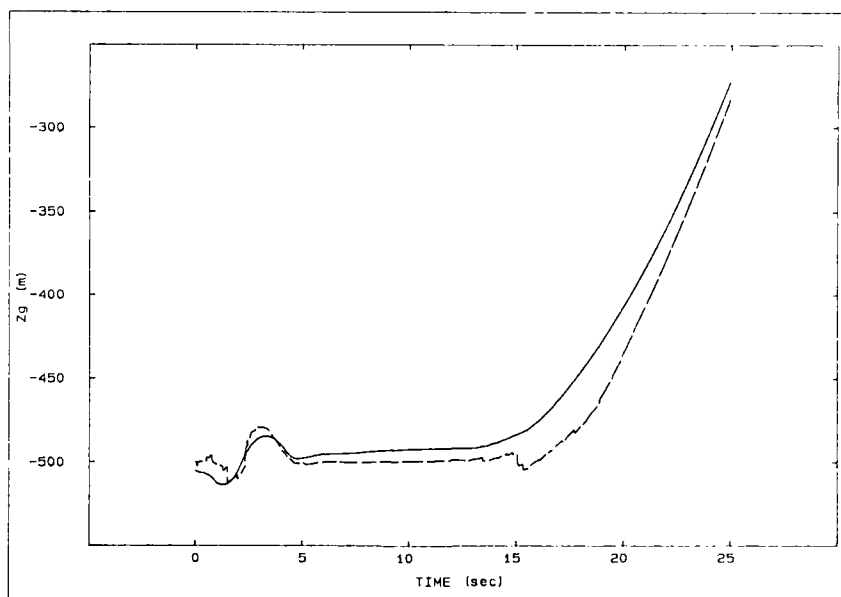


Fig. 7. Flight of the unpropelled submunition at a constant altitude of 500 m. Error in the initial values  $\sigma = 5$  m; wind = 12 m/s. — simulated, - - EKF

# RECALAGE DE NAVIGATION PAR CARTOGRAPHIE RADAR : OPTIMISATION ET VALIDATION PAR OUTIL DE SIMULATION

J.P. GUYVARCH  
AEROSPATIALE - DIVISION ENGINES TACTIQUES -  
Annexe des Gâtines - 91370 Verrières le Buisson - FRANCE -

## RESUME

Pour l'attaque aérienne d'objectifs terrestres de valeur (piste d'aérodrome, pont, concentration de blindés ...), le concept d'un missile air-sol tiré à distance de sécurité (hors de portée des systèmes de défense ennemis) et doté de capacités tous temps paraît être une réponse adaptée. La précision de guidage requise dépassant les possibilités d'un système inertielle seul, l'engin est équipé d'un capteur radar en ondes millimétriques permettant une localisation par cartographie. Ce principe implique au niveau de la préparation de mission le choix de la trajectoire et la réalisation de cartes prévisionnelles introduites en mémoire du missile avant tir. Afin d'estimer les probabilités de réussite d'une mission donnée et aussi d'aider à la réalisation des cartes prévisionnelles, une simulation numérique complète du système a été développée. Cette simulation est validée et enrichie progressivement à partir des données réelles obtenues au cours de l'expérimentation du senseur.

## 1 INTRODUCTION

Dans le cadre de l'étude d'un système d'arme air-sol de moyenne portée, le choix d'une solution repose sur un certain nombre d'éléments déterminants parmi lesquels on peut citer :

- le souhait d'une véritable capacité "fire and forget",
- la possibilité d'emploi tous temps,
- une bonne précision de guidage pour des objectifs désignés par leur coordonnées géographiques,
- une capacité intrinsèque de reconnaissance de certains types de cibles.

Une des solutions qui semble le mieux répondre à ce problème est le concept d'un engin autonome comportant principalement une centrale inertielle, un altimètre et un capteur radar en ondes millimétriques (35 ou 94 GHz).

Le capteur radar millimétrique permet d'une part, l'élaboration en cours de vol de cartes des zones survolées afin de les comparer à des cartes de références introduites avant tir pour permettre un recalage de navigation très précis et d'autre part (et si besoin suivant le type de mission), de détecter et de choisir une cible particulière.

Outre les problèmes de traitement d'images en temps réel inhérents au système, ce concept de senseur cartographique impose la réalisation de cartes de référence radar avant chaque mission.

Afin de permettre un temps de réaction rapide, il est nécessaire de pouvoir élaborer ces cartes aussi simplement que possible à partir des données générales disponibles (photos aériennes ou satellite numérisées, fichiers DLMS...).

De plus, les cartes prévisionnelles doivent, bien entendu, présenter un bon degré de corrélation avec les cartes radar réalisées en cours de vol.

Afin d'optimiser le processus lié à la préparation de mission et en particulier l'élaboration des cartes prévisionnelles, la solution développée s'inscrit dans le cadre d'une simulation numérique complète du système comportant notamment :

- la modélisation du capteur radar,
- la simulation des traitements embarqués,
- la modélisation des zones servant de référence, à partir des données d'altimétrie, de planimétrie,
- la conception des cartes prévisionnelles.

La démarche générale consiste, à partir de trajectoires imposées par des considérations tactiques, à choisir a priori en fonction de critères simples, les zones de recalage, à générer les cartes de référence correspondantes, et enfin à simuler la mission complète en vérifiant ainsi la précision des informations de recalage fournies par le système.

## 2 PRINCIPES GENERAUX DU SYSTEME

### 2.1 Spécifications principales

Les spécifications opérationnelles du système reposent sur un certain nombre de principes et de besoins ; en premier lieu, il convient de définir le type de cibles visées ; la liste potentielle est la suivante :

- piste d'aérodrome,
- blindés (fixes ou mobiles en formation),
- site missiles (sol-sol ou sol-air),
- unités de commandement,
- ponts, routes, chemin de fer, infrastructures...

La précision requise est généralement de l'ordre de quelques dizaines de mètres mais elle peut descendre à quelques mètres pour des objectifs très localisés (arches de pont par exemple).

Parmi les autres spécifications du missile, on peut citer :

- tir à distance de sécurité et suivi d'une trajectoire préétablie :
  - \* tiré hors de portée des systèmes de défense ennemis, le missile peut déjouer les systèmes de détection adverses, d'une part en suivant une trajectoire à très basse altitude pré-programmée, et d'autre part grâce à des efforts importants au niveau de la discrétion radar (réduction de SER) ;
- capacité "tous temps"
  - \* cette capacité correspond à la possibilité de tir de jour ou de nuit, avec des conditions météorologiques éventuellement perturbées (pluie, neige, brouillard...) ;
- détection terminale et possibilité d'identification de certains types de cibles :
  - \* cette possibilité est présentée ici comme une option permettant une orientation du choix d'un type de solution, étant entendu qu'il est avantageux qu'un équipement unique réalise les fonctions de localisation et de détection terminale.

## 2.2 Solutions potentielles

Parmi les équipements répondant à tout ou partie du problème posé, on peut citer :

- les centrales inertielles,
- le système de localisation GPS/NAVSTAR,
- les systèmes dits "terrestres"
  - . Altimètre.
  - . Senseur cartographique (radar ou optique).

## 2.3 Solution présentée

La solution présentée associe 3 des équipements cités précédemment :

- une centrale inertielle,
- un altimètre,
- un radar millimétrique.

La centrale inertielle complétée par l'altimètre permet de suivre une trajectoire dans un repère (OXYZ) lié au terrain avec une précision moyenne. Afin d'assurer la précision requise, on utilise un capteur cartographique radar actif qui compare les cartes obtenues en temps réel avec les données des zones survolées mémorisées dans le missile avant tir.

Ce capteur radar actif permet, en outre et si besoin, la détection et l'identification d'objectifs (chars par exemple).

Le choix de la bande millimétrique (35 GHz ou 94 GHz) résulte d'un compromis entre précision (largeur du faisceau de l'antenne) et capacité tous temps. Les limitations en résolution angulaire dues à la diffraction en fonction de la bande de fréquence ainsi que les conditions d'utilisation correspondantes sont résumées dans le tableau 1.

## 2.4 Localisation par cartographie radar

### 2.4.1 - Principe

La localisation par cartographie radar consiste à comparer une image relevée en vol par un senseur radar de pointe avant à une image dite prévisionnelle, mise en mémoire et représentative de la "vision" du terrain du capteur embarqué.

La carte prévisionnelle est établie avant tir en tenant compte de la planimétrie (structures) et de l'altimétrie, ses dimensions étant homogènes avec les erreurs de navigation escomptées au moment du survol de la zone considérée. Cette carte est élaborée à partir d'une ou plusieurs bases de données (DLMS, photos satellite, photographies aériennes, SLAR...). Avant mise en mémoire, cette image est traitée afin de ne faire apparaître que les détails les plus caractéristiques et les plus significatifs pour le capteur radar.

La carte radar est quant à elle relevée lorsque le missile se trouve au point théorique de la trajectoire correspondant à la zone mémorisée, (fig.1). Suivant la taille de la tache d'illumination au sol, un ou plusieurs balayages d'antenne peuvent être nécessaires pour établir une carte radar. La cellule élémentaire de résolution au sol (pixel) n'a en général pas les mêmes dimensions en radial et en latéral, et sa taille dépend des caractéristiques de l'émetteur, de la largeur du faisceau et de la distance (fig.2).

La carte radar relevée par le missile est traitée par le calculateur embarqué (mise en conformité, filtrages...) pour finalement ne conserver que les structures significatives et être ensuite corrélée avec l'image prévisionnelle. Le résultat de la comparaison des 2 images fournit l'écart dans le plan horizontal entre les points théoriques et réels de prise de carte ( $\Delta X \Delta Y$ ) et optionnellement l'erreur de direction (rotation) ; ces informations permettent de corriger l'erreur de navigation.

#### 2.4.2 - Cartes radar obtenues lors d'essais réels

Les équipementiers français Electronique Serge Dassault et Thomson/CSF ont étudié chacun un capteur radar répondant aux besoins précédemment évoqués, les particularités de chacun de ces projets résidant dans le choix de la bande de fréquence (35 et 94 GHz) et les traitements des différentes images.

##### a) Mesures à 35 GHz (capteur E.S.D.)

La carte prévisionnelle (fig. 3a) a été réalisée à partir d'une carte géographique. La zone délimitée par des tirets correspond à la zone de la carte relevée par le radar (fig. 3b). Cette dernière est représentée après transformation des coordonnées polaires en coordonnées cartésiennes (X,Y) et après seuillage. Le résultat de la comparaison est présenté figure 3c.

##### b) Mesures à 94 GHz (capteur Th/CSF)

La carte géographique (fig. 4a) permet de mettre en évidence des éléments caractéristiques à conserver pour la carte prévisionnelle : routes, bâtiment, bois, étang. On peut distinguer assez facilement ces éléments (ou leurs ombres portées) sur la carte radar (fig. 4b).

### 3 SIMULATION NUMERIQUE

#### 3.1 Intérêt d'une simulation numérique

Comme il a été vu précédemment, la localisation par cartographie radar repose sur la comparaison entre cartes prévisionnelles et cartes "vues" par le radar en vol. Il est donc nécessaire d'obtenir la meilleure adéquation possible entre ces deux types de cartes, obtenues à partir de données de nature généralement différentes (carte prévisionnelle établie par exemple à partir de photos satellite).

Les premiers essais sur maquette ont permis de valider le principe et de collecter des données. Toutefois, les essais en vol sont coûteux et demandent un temps important ; il est de plus difficile de réunir des conditions très variées. Il est alors avantageux de compléter ces essais par une simulation numérique comprenant la modélisation du capteur et des terrains.

Pendant la phase étude du système, l'outil de simulation permet l'évaluation du capteur dans des conditions très diverses par modification des paramètres introduits (nature des terrains, conditions météorologiques, altitude de vol, etc...), et l'optimisation des traitements embarqués. En parallèle, cet outil permet aussi de définir des règles pour l'élaboration des cartes prévisionnelles afin de concilier simplification (ne garder en mémoire que les éléments réellement "utiles" et a priori invariants pour les différentes saisons et pour des conditions météorologiques diverses...) et efficacité (précision de localisation et robustesse).

En phase opérationnelle, cette simulation pourrait devenir un outil permettant d'une part de générer les cartes prévisionnelles, et d'autre part d'évaluer les chances de réussite de la mission compte-tenu des zones de corrélation choisies. Le processus général correspondant est décrit par la figure 5.

#### 3.2 Principe de simulation

Connaissant à un instant donné la position du missile dans un repère (XYZ) lié au terrain, il est possible de calculer la zone au sol éclairée par le faisceau de l'antenne (fig. 6) en tenant compte pour chaque cellule de résolution (fraction radiale  $\Delta r$  de la zone éclairée) des caractéristiques du terrain (incidence moyenne par rapport au faisceau et réflectivité), il est alors possible de calculer le signal en retour au niveau du récepteur du radar.

Les traitements internes au calculateur du missile sont également simulés (fig. 7) :

- transformation de la carte radar (coordonnées polaires  $r, \varphi$ ) en coordonnées cartésiennes (X,Y),
- traitement d'image,
- comparaison.

Aux données d'entrée sont ajoutés des termes aléatoires caractérisant tous les éléments imprévisibles (erreurs de trajectoire, conditions météorologiques, nature des terrains cultivés, imprécisions dans les données planimétriques...).

En parallèle, le programme de simulation génère les cartes prévisionnelles à partir des informations d'altimétrie et de planimétrie, en ne gardant que les éléments a priori invariants.

Pour un scénario donné, l'évaluation des résultats consiste à analyser les écarts  $\Delta X, \Delta Y$  (et optionnellement de rotation) obtenus pour plusieurs passages en jouant sur les paramètres aléatoires d'entrée.

Avant son utilisation opérationnelle, il est nécessaire de valider cet outil de simulation. Cela se fait en comparant les cartes radar simulées avec les cartes obtenues lors d'essais réels ; la comparaison peut porter directement sur les cartes obtenues, mais aussi sur les histogrammes calculés à partir de cartes.

### 3.3 Modèles utilisés

#### 3.3.1 - Modèle du senseur

Le senseur est principalement représenté par :

- le diagramme d'antenne (site et gisement),
- les caractéristiques du balayage,
- une modélisation de l'ensemble émetteur-récepteur faisant intervenir le bilan de puissance (puissance d'émission, sensibilité du récepteur, pertes ...) et la fonction d'ambiguïté,
- les traitements des signaux (intégration, changement de coordonnées, traitement d'images etc...).

#### 3.3.2 - Modèle terrain

Le terrain est représenté par ses caractéristiques d'altimétrie et de planimétrie d'une part, et par les données de réflectivité associées d'autre part. Parmi les sources d'informations possibles, on peut citer :

- les fichiers D.L.M.S. (Digital Land Mass Storage),
- les cartes géographiques,
- les photos satellite,
- les photos aériennes,
- les cartes radar.

D'autre part il est aussi possible de générer des terrains de type particulier (montagnes, falaises, plateaux...) par des processus entièrement aléatoires (méthodes dérivées de la génération de fractales).

Pour la représentation de la réflectivité moyenne et des lois de répartition spatiales, on a utilisé le modèle développé par Currie, Zehner et Dyer (1).<sup>B</sup>

La réflectivité moyenne  $\bar{\sigma}$  est représentée par  $\bar{\sigma} = A (1 + C)$  avec  $I$  : angle d'incidence

$A$ ,  $B$  et  $C$  : paramètres qui dépendent du terrain (forêt, cultures ...), de la fréquence radar, de la polarisation et des conditions météorologiques.

La diversité de cas possibles nécessite la création d'une bibliothèque enrichie au fur et à mesure du déroulement des essais.

Les lois statistiques spatiales caractérisant les variations autour de la valeur moyenne sont modélisées par :

$$\sigma = \bar{\sigma} \frac{1}{\Gamma(1+a)} (-\ln u(0,1))^a$$

avec  $u(0,1)$  : loi équiprobable entre 0 et 1 (0 exclu)

$a$  : paramètre dépendant de  $A$ ,  $B$  et  $C$  et de la taille des cellules de résolution

$$\Gamma(1+a) = a \int_0^{\infty} x^{a-1} e^{-x} dx \quad (\text{fonction Gamma}).$$

#### 3.4 Exemple de carte simulée

La figure 8 donne un exemple de carte obtenue par simulation.

Le terrain a été modélisé à partir d'une carte géographique ; le capteur modélisé a une fréquence de fonctionnement de 94 GHz.

Le résultat obtenu à partir d'une carte géographique (fig. 8) peut être directement comparé à la carte obtenue lors d'essais réels (fig. 4b).

Les principales différences avec la carte radar réelle proviennent de facteurs non prévisibles à partir de la carte géographique (par exemple l'étang est à moitié asséché dans la réalité).

### 4 CONCLUSION

Le concept de recalage de navigation par cartographie radar est prometteur car il permet de concilier d'importants problèmes opérationnels (précision, capacité tous temps, tirs à distance de sécurité...). Toutefois, il nécessite aussi un soin particulier à apporter au niveau de la préparation de mission :

- stockage préalable de "données terrain" pour les différents théâtres d'opération possible (fichiers à renseigner en permanence),
- choix d'une trajectoire optimale, choix des zones de recalage et génération des cartes prévisionnelles correspondantes (avant chaque mission).

Sur le premier point, il semble dès à présent que les données extraites de photos satellite puissent apporter une réponse satisfaisante.

En ce qui concerne la phase préparatoire d'une mission donnée, il paraît important de favoriser les facteurs de rapidité et d'automatisation.

L'outil de simulation numérique constitue une première étape allant dans ce sens, en particulier pour la génération des cartes prévisionnelles.

L'étape suivante consiste à inclure cette simulation dans un outil plus général (du type système expert par exemple) permettant de prendre en compte en entrée des considérations tactiques, afin de choisir de façon entièrement automatique la trajectoire et les zones de recalage.

REFERENCE : NC Currie, SP Zehner, FB Dyer  
"MMW Land Clutter model update"  
(1) IEE RADAR - 87 Record, London (England)  
October 1987

BANDES DANS LE SPECTRE	$\lambda$ ou F	D - $\lambda$ OPTIQUE OU ANTENNE = 24 CM		LIMITATIONS
		DIFFRACTION ANGULAIRE $1.22 \lambda \frac{\Delta}{D}$	$\Delta$ DU "PIXEL" A 1 KM	
VISIBLE	0.5 $\mu$	2.5 $\mu$ RAD	2.5 MM	JOUR TEMPS CLAIR
PROCHE IR	1 $\mu$	5 $\mu$ RAD	5 MM	
IR THERMIQUE	10 $\mu$	50 $\mu$ RAD	5 CM	(JOUR/HUIT TEMPS CLAIR)
MILLIMÉTRIQUE	3 MM	15 MRAD	15 M	TOUT TEMPS À COURTE PORTÉE
	100 GHZ			
	1 CM	45 MRAD	45 M	TOUT TEMPS
	35 GHZ			
BANDE X	3 CM	150 MRAD 8°	150 M°	
	10 GHZ			

EN MODE RADAR COHERENT À ANTENNE SYNTHÉTIQUE UTILISANT LE DÉPLACEMENT-DE-PORTÈRE.  
ON PEUT, AU PRIX D'UN TRAITEMENT COMPLEXE ( $> 10^8$  OPÉRATIONS/S) OBTENIR UNE RÉOLUTION  
100 À 1000 FOIS MEILLEURE.

TABLEAU 1 : Résolution angulaire et conditions d'utilisation  
en fonction de la bande de fréquence.

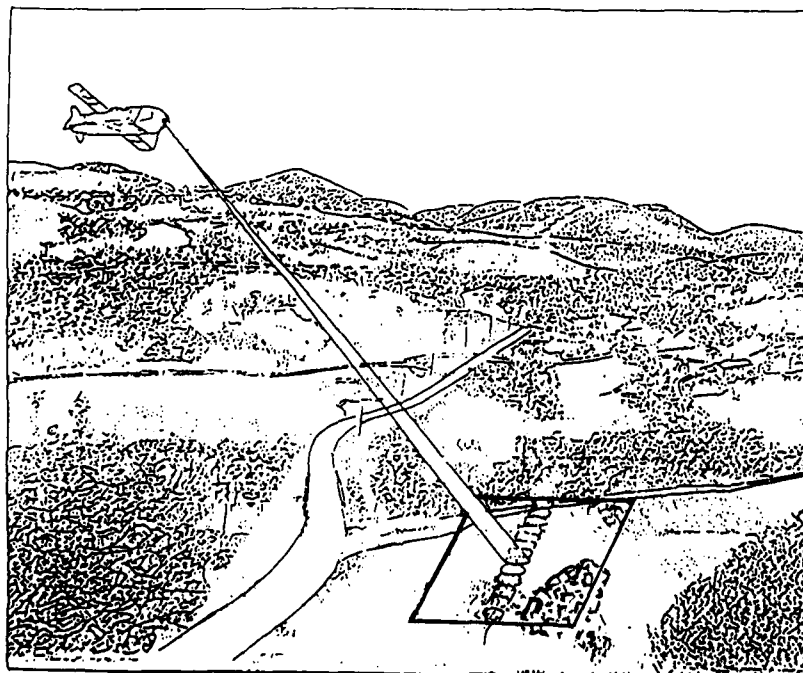
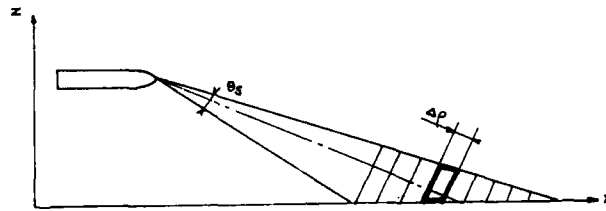
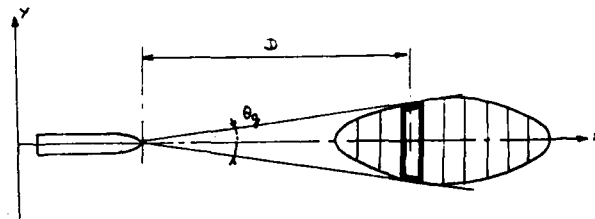


FIGURE 1 : Relevé de carte radar.



RÉSOLUTION RADIALE :  $\Delta \rho$

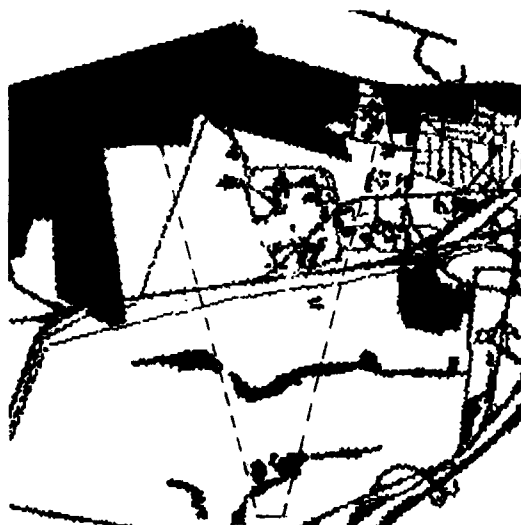
LIÉE À LA MODULATION



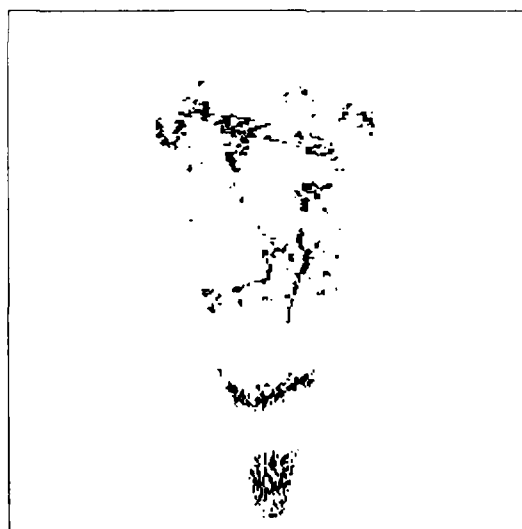
RÉSOLUTION LATÉRALE :  $D \theta_s$

AVEC  $\theta_s = k \cdot \frac{\text{LONGUEUR D'ONDE}}{\text{DIAMÈTRE D'ANTENNE}}$

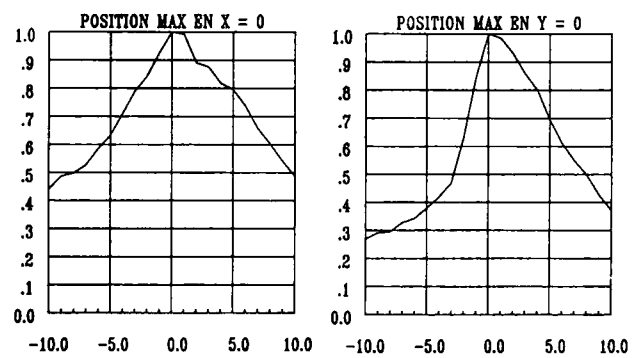
Figure\_2 : Définition d'une cellule élémentaire de résolution.



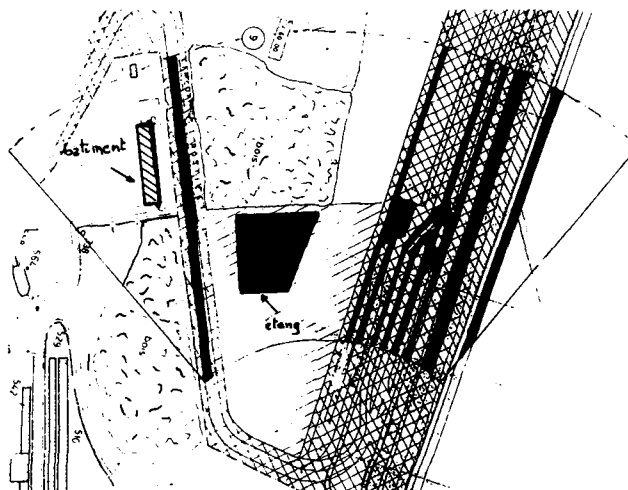
FIGURE\_3a : Carte prévisionnelle.



Figure\_3b : Carte radar après seuillage.



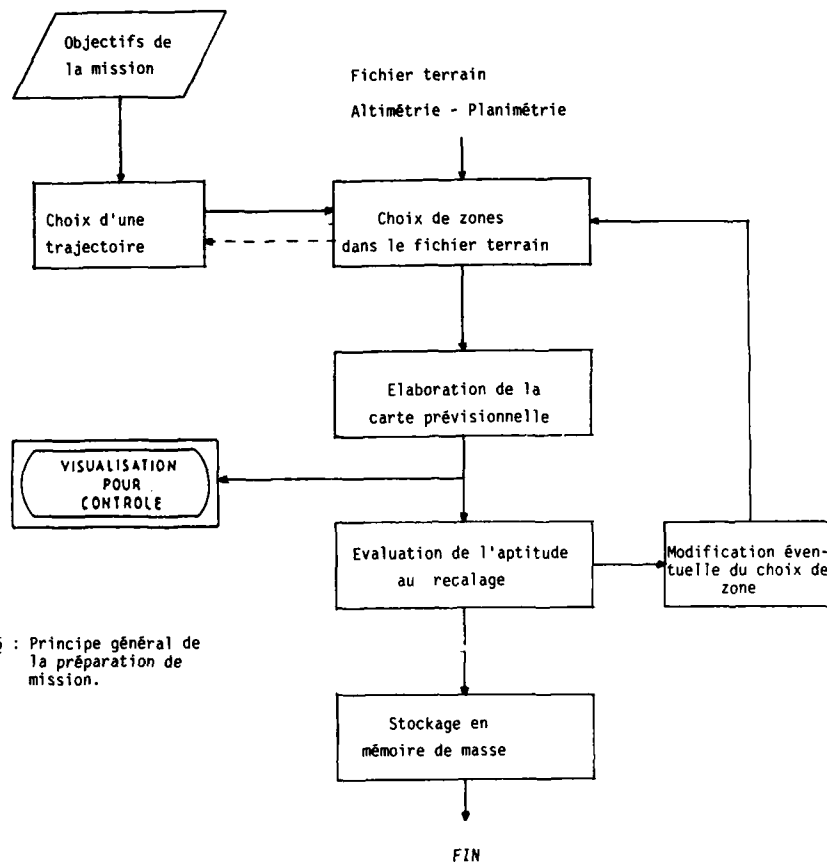
Figure\_3c : Résultat de corrélation.



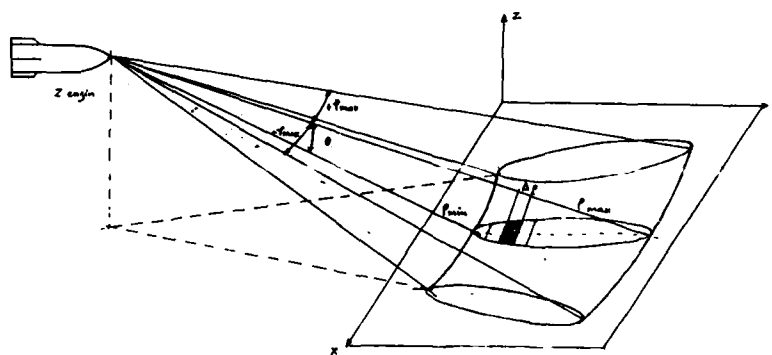
Figure\_4a : Carte géographique.



Figure\_4b : Carte radar.



Figure\_5 : Principe général de la préparation de mission.



Figure\_6 : Zone sol éclairée par le faisceau au cours d'un balayage.

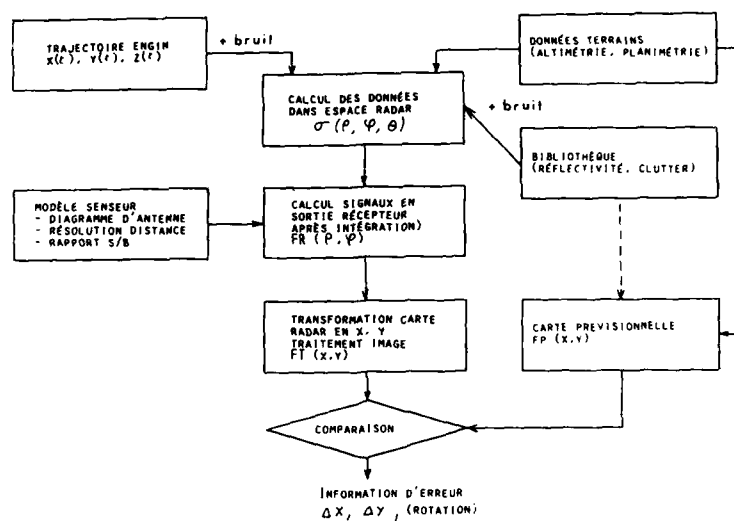


Figure 7 : Principe de la simulation.



Figure 8 : Carte radar simulée.

**Electro-Optic Sensors for Surveillance  
and Target Acquisition**

by  
**Dr. J.W. Jack and Mr. A. Houston**  
**Electro-Optics Department**  
**Ferranti Defence Systems Limited**  
**St. Andrews Works**  
**Robertson Avenue**  
**Edinburgh**  
**U.K.**

1. **Summary**

The synthesis of a compact electro-optical payload suitable for tactical reconnaissance, target spotting and fire control is described. The selection criteria for the electro-optical sensors comprising an imaging sensor, lens and laser are discussed and the performance of an actual system is predicted. The predicted performance is compared with the results of flight trials in which an equipment was used to acquire, range and designate ground targets. Finally the experience of using the equipment against ground targets in collaboration with fixed wing aircraft is discussed.

2. **Introduction**

Payloads for UMAs must meet very demanding constraints on size, weight and cost. It is essential therefore to trade-off the performance requirements to obtain the optimum configuration. As an integral part of a weapon system the UMA offers considerable advantages particularly if the weapon is remotely launched. In this paper the development of a UMA payload is presented in which an acquisition sensor is fused with a laser which provides improved target position accuracy and closed loop designation. Such a payload has immediate application as part of a weapon system but is also sufficiently flexible not to constrain the weapon system with which it may be integrated. The key operational requirement which we believe can be satisfied is that of target acquisition and hand off for attack by a weapon system. The rangefinding designator allows hand off through both accurate target position information and also direct target designation for weapons fitted with a laser seeker.

The task of target acquisition by means of an imaging sensor has been debated extensively and is not repeated in detail. It is necessary to carry a sensor which will allow target search, detection and recognition. Once this part of the task has been successfully completed target information must be passed on for further action. In the simple surveillance role, information in the form of a video image or a verbal description may be sufficient. When the surveillance sensor is to be integrated with a weapon system additional information will be required. The next stage in performance enhancement is to provide target position information. To achieve a satisfactory accuracy the performance of the UMA system must be optimised and our trade off studies suggest that the addition of a rangefinder provides the optimum solution.

Further enhancements are required if the weapon system requires target designation for the closed loop guidance of a precision weapon. The addition of a laser designator provides accurate real time targeting for the guidance of hittile type weapons. The laser designator could also permit cooperative weapon attack with other weapon platforms carrying laser seekers. An example of such a platform is the

manned aircraft carrying a laser seeker and delivering dumb weapons. The availability of precision target location through the seeker system considerably reduces pilot workload and also reduces miss distance substantially.

In the following paragraphs we present a discussion of the performance of the various component parts of a UMA payload and describe the trade offs leading to the solution of the optimised design. A particular configuration is described of a television and laser designator combination mounted on a stabilised gimballed platform. This represents a stage in the development of a full infra-red laser designator payload. The payload has been flown on a helicopter platform and trials are described in which the rangefinding and designation performance were successfully demonstrated. Cooperative attacks with Jaguar aircraft were also carried out and the resultant weapon system lock-on ranges compared with predicted performance.

### 3. Requirements

Three aspects of the requirement are addressed. The task of target acquisition is obviously of first importance and the various choices of sensor and their suitability for the UMA payload are discussed. When a target has been acquired and classified, the second most important task is normally that of locating its position. There are certain trade offs that can be investigated to arrive at a suitable solution. The impact of adding a target rangefinding capability is explored and its effect on system performance put forward. In the target attack task, the UMA payload becomes part of a closely integrated weapon system where closed loop guidance has a number of distinct advantages. The addition of a target designator immediately offers the capability for integration with such a weapon system.

#### 3.1 Target Acquisition

The chosen sensor must allow a target search to be carried out, targets to be acquired and classified and in a defensive situation it may be necessary to launch an attack against selected targets.

There are a number of wavelength windows for which imaging sensors have been developed. These are determined in the main by the atmospheric attenuation which varies widely with wavelength due to molecular and atomic absorption. For a passive surveillance system one is restricted to those sensors utilising reflected radiation incident from some naturally occurring source or to those sensors utilising the inherent radiation emitted by bodies as a consequence of their temperature.

Television cameras operating in the visible spectrum have been under development for the last 50 years and their performance is continually being extended and improved. Cameras suitable for a UMA must be small, reasonably rugged and offer a good resolution. The 2/3 inch format tube can be packaged to provide a small compact unit and yet provide a resolution in the order of 600 lines. There are also a multitude of compact high performance lenses available suited to this tube size. Recent developments with solid state imagers have increased the resolution available from these devices. However the tube camera can still provide approximately 50% more resolution.

A television payload equipment will only provide good performance when the light level is adequate. A plot of the light level due only to the sun and the sky for the latitude of Edinburgh at the autumn equinox is shown in Figure 3.1. As the light level is decreased the system resolution degrades. The performance falls off very steeply with decreasing light level and the lower limit of useful performance for a television payload based on the newvicon tube corresponds to approximately 10 lux.

By reference to Figure 3.1, it can be seen that such an equipment can only be used between the times of 5.30 a.m. and 6.30 p.m., a total of 13 hours or 54% of the day. The presence of heavy cloud will produce a further attenuation of the light level but this would not be expected to significantly reduce the utilisation factor.

The provision of a device operating at lower light levels could provide a significant increase in the utilisation. A common approach to increasing the low light level capability of television cameras is to provide an image intensifier stage.

For a compact camera unit with a reasonable performance at a modest cost and capable of flexible configuration, the Generation Two microchannel plate Image Intensifier has been found to be a suitable choice. With a Generation Two image intensifier, performance can be provided down to scene illumination levels of approximately  $5 \times 10^{-2}$  lux. With the more sensitive Generation Three devices the performance can be extended to slightly lower levels. By reference to the curve of the scene illumination level, Figure 3.1, it can be seen that intensification will allow the utilisation to be increased. The improved utilisation figure will depend on the light level during the night. During a clear night with full moon the utilisation can be increased to 100%. However on a heavily overcast night with no moon, the utilisation will not be increased by a significant amount. The cost effectiveness of the intensified television payload depends therefore on a very careful estimate of the system utilisation.

To avoid the dependence on an external source of illumination it is possible to utilise the black body radiation emitted by all objects as a consequence of their temperature. A consideration of the black body spectral radiance at 300°K and the atmospheric transmission shows there are two wavelength windows which may be considered 3 - 5 $\mu$ m and 8 - 14 $\mu$ m. The radiated energy in the near infra-red window is much less than that in the far infra-red window and detectors must be more sensitive by a factor of approximately six to achieve the same signal to noise ratio. Despite the advantage of the shorter wavelength which would give a greatly increased resolution for the same aperture, detectors for the 3 - 5 $\mu$ m window are not so advanced in sensitivity and few suitable surveillance cameras exist for this wavelength band. The following discussion will therefore concentrate on the 8 - 14 $\mu$ m window.

One of the simplest imaging sensors operating in the 8-14 $\mu$ m waveband is the pyroelectric camera. The camera operates at normal temperature as an uncooled infra-red television system and a temperature sensitivity of better than 0.5°C at 200 lines is readily available. Sensor payloads utilising a pyroelectric device have the two advantages of not requiring to be cryogenically cooled and being relatively low cost. However the sensitivity of the device is moderate and existing lenses normally constrain the design through a limitation of the modulation transfer function(MTF). Calculations show that detection and recognition ranges are approximately 1.2km and 0.4km respectively. This limited range performance seriously constrains the effectiveness of this type of payload.

A higher performance device is the framing thermal imager with cryogenically cooled detector. The major improvements in performance which have occurred over recent years have been the result of progress made in signal processing. Further improvements are likely to come from the use of alternative detector materials and different sensor arrays. The thermal imager has a number of advantages. It does not depend on the presence of external illumination, it is not susceptible to bright lights and it is good in light precipitation and haze. Since the thermal imager responds to received radiation, the imagery which is displayed depends on both the scene temperature and the emissivity of the objects in the scene. Small changes in emissivity can provide good contrast between objects which have similar temperatures.

A number of thermal imagers are available and a variety of suitable telescopes including zoom and switched field of view types can be obtained. Many use the Sprite detector and therefore the main difference between these devices is due to the scanning mechanism and the subsequent signal processing. Fields of view are chosen to match approximately detection in wide field of view with recognition in narrow field of view and ranges in excess of 2km against tank targets are easily obtained from imagers that can be configured into payloads suitable for UMAs.

### 3.2 Target Position Measurement

Following target acquisition it is normally a requirement to determine target position accurately. Target position measurement to an accuracy of 50 metres circle of equal probability (CEP) is considered to be a reasonable and achievable objective for a UMA System. This requirement imposes many constraints on the System and its operation. In particular, Electro-optical (E.O.) sensor pointing and the UMA navigation systems are influenced greatly by this requirement.

Our approach to defining sub-system performance requirements and the techniques needed for position measurement was to consider three areas

- (i) Given a UMA in the neighbourhood of a target, assume a nominal value for its position uncertainty. Then determine the pointing accuracy and UMA heading accuracy required as a function of UMA height and range from the target.
- (ii) Introduce the effects of UMA position uncertainty and determine the positional accuracy required to give a reasonable stand-off from the target.
- (iii) Given the requirements for pointing accuracy, UMA heading and attitude and UMA positional accuracy, answer the question - What has to be done by the system before the target area is reached to allow these requirements to be met? e.g. Several waypoint updates may be required or the flight path approach options to the target might be constrained.

Several options were considered for measuring target position relative to the UMA, each involving pointing the E.O. sensors at the target.

- (i) measure UMA height above the target area and the sensor pointing angles in azimuth and elevation relative to inertial axes.
- (ii) measure range to the target directly and combine with sightline pointing angles and UMA attitude and heading.
- (iii) measure range to target and combine with measured height.

It is highly desirable to be able to measure target position without overflying the target. Indeed the greater the zone of height and distance from the target over which the UMA can operate to the accuracy required, the faster will be the response and flexibility and the lower the vulnerability; flight paths can be chosen to avoid defences, stand off range can be greater, and exposure time can be reduced.

The objective is, therefore, to be able to determine target position (i.e. "targeting") accurately over as large a zone of height/distance from the target as possible with the minimum accuracy (and cost) of sensors of all types. Experience indicated that the practical useful range of an E-O sensor would be about 3 to 4km and the UMA operating height limits above target would be about 300m to 2km.

The assumed geometric relationship between UMA and target, together with a definition of the relevant parameters are shown in Figure 3.2. A required target

location accuracy of 50m CEP was assumed and the effects of inaccuracies in UMA height measurement, target range, platform pointing accuracy and operator aiming accuracy on the available operating region of range and height were plotted. Realistic values for the magnitude of component errors were taken to be

- |                                 |             |
|---------------------------------|-------------|
| (i) operator aiming accuracy    | = 2.5mRad   |
| (ii) platform pointing accuracy | = 15mRad    |
| (iii) height error              | 30m         |
| (iv) range errors               | < 10 metres |

The resulting operating regions are shown in Figures 3.3, 3.4 and 3.5. Even when the required platform accuracy is increased to 10mRad or even 5mRad the very restrictive operational region of height and range when a rangefinder is not present is clearly shown in Figure 3.3. By contrast Figures 3.4 and 3.5 show how a rangefinder significantly expands the operational region, with the combination of range and platform pointing accuracy measurement shown in Figure 3.4 being particularly attractive.

The principal conclusions from the assessment of the target positioning techniques are as follows:-

- (i) Overflying the target is technically the simplest solution. However, the costs for this simplicity are severe constraints on how the UMA is flown in the target area, particularly if several targets are present, and the risk of attrition as a result of these constraints.
- (ii) Stand-off position determination, using UMA height and sensor pointing angles is a feasible method of determining target position to <50m CEP. We believe that a baro-altimeter should give sufficiently accurate height measurements although the constraints on sensor pointing are relatively severe. Furthermore the operator must determine from sightline direction, UMA height and map contour data, where the sightline cuts the terrain.
- (iii) The introduction of a target rangefinder reduces errors significantly. For typical stand-off ranges, say around 2Km, the use of accurate target range combined with sensor pointing angles is preferred. Accurate range data eliminates the need for height measurement and, for a given CEP, permits greater pointing errors than the previous technique. In addition, the operator involvement is reduced to centring the rangefinder boresight on the target and pressing a button to demand range.

The target range measurement requirements described above can be satisfied by using a laser. Suitable laser rangefinders are available and give accurate range measurements over target distances which are normally in excess of sensor detection ranges.

### 3.3 Target Attack

When a target has been acquired and its position determined it can be a requirement to attack the target. The UMA payload can therefore become part of an integrated weapon system.

In a static situation, accurate target information can be passed to a suitable weapon system and a reasonable attack success can be expected from a relatively simple weapon. However in a dynamic situation, target positions will be

continuously changing and the positional information available from the UMA platform will degrade rapidly with time. Any delay in the propagation of the positional information will almost certainly reduce attack success, probably to an unacceptable level. It becomes highly desirable, therefore, to provide real time position information or to provide direct closed loop terminal guidance. Weapon systems are available which implement closed loop terminal guidance by the provision of a laser designator and when a laser designator is added to the UMA payload, the UMA then becomes capable of being integrated into a weapon system. With a suitable choice of performance parameters, flexibility in the types of attack that can be supported can be maximised.

In the consideration of the effectiveness of a laser designator payload, we have examined the accuracy of a number of weapon systems. The use of unguided weapons dropped from an airborne platform can be significantly aided if the aircraft is fitted with a laser seeker and can detect the location of the designated target. Operator workload is considerably reduced and weapon miss distance is improved. The use of terminally guided weapons fitted with a laser seeker head is permitted in areas which may only be available to the UMA. Such hittles have a high probability of success provided the designation accuracy is sufficient.

The selection of a suitable laser was dictated by the following major requirements

- a) size, weight and power consumption must be consistent with integration in a stabilised payload suitable for installation on a UMA.
- b) the laser must be compatible with existing in-service laser equipments and laser guided munitions.

These requirements effectively limit the choice of lasers to the Neodymium doped Yttrium Aluminium Garnet family operating at  $1.065\mu\text{m}$ . This type of laser offers the essential performance features of short pulse length, high output energy, low beam divergence and good harmonisation.

A short pulse length is required to achieve good range resolution. A pulse length of 20nsec is readily achievable and results in a resolution of approximately 3.5 metres. To achieve a high missile hit probability, the pulse repetition rate should be as high as possible. The trade off between pulse repetition frequency (PRF) and hit probability is not expected to show a significant increase in performance beyond 30 pulses per second. A high repetition rate creates severe cooling requirements which, from experience, limits the feasible PRF to between 10 and 20 pulses per second. It was estimated that this repetition rate would provide adequate performance for attacks using existing laser seekers as fitted to Copperhead and the Laser Ranger and Marked Target Seeker equipment in the Jaguar and Harrier aircraft. To enable more than one designator to be employed in the same area, pulse coding is essential. Pulse coding compatible with NATO standard was regarded as essential. In particular the PRF should be compatible with Stanag 3733 bands I and II.

The required laser output energy is dictated by the designation requirement and not the rangefinder requirement. Target characteristics, atmospheric conditions and receiver sensitivity of the laser seeker all have a significant effect on seeker lock-on range for a given laser output energy. Operational experience with existing seekers suggested that in atmospheric conditions equivalent to  $R_{\text{met}}$  of 10Km, lock-on ranges of greater than 5km should be achieved against tank type targets. Analysis of T.V. systems indicated that recognition slant ranges of between 2km and 3km could be expected and for this magnitude of stand-off range between designator and target a laser output energy of at least 60mJoules is required.

Laser pointing errors are a function of errors from the gimbal, mechanical misalignment between the laser and imaging sensor and errors due to stability and

divergence of the laser beam. An overall pointing accuracy of 1.0mrad was considered to be readily achievable. Experience with previous equipments indicated that pointing errors, beam stability and boresight alignment errors would account for half of this overall budget leaving a residual 0.5mrad for laser beam divergence. This magnitude of beam divergence can be achieved by mounting a X6 transmit telescope on the output from a laser with a raw beam divergence of 3mrad. A 3mrad raw beam divergence is both practical and relatively easily achieved.

To achieve valid target range information the boresight of the laser must be harmonised to the sightline of the imaging sensor. From the overall pointing error budget, 0.1mrad was allocated to sightline harmonisation errors. The sightline reference direction was taken to be defined by cross hairs superimposed on the display. Laser telescope magnification allows the laser body misalignment to be increased by the telescope magnification factor. From previous consideration of beam divergence requirements a X6 telescope was considered to be adequate and therefore the laser body misalignment could be increased to 0.6mrad.

#### 4. Sensors and Sensor Fusion

As part of ongoing development a daylight designator payload has been produced comprising a daylight T.V. with suitable lens and Nd YAG laser. The requirements and considerations which resulted in the selection of an actual lens, T.V. and laser combination which could be packaged in a suitable Sensor Payload for evaluation trials are discussed below.

##### 4.1 Lens

The operator requires a reasonably large field of view to aid the target acquisition task and a narrow field of view to allow objects of interest to be magnified for examination and classification. An upper limit to the magnification is set by atmospheric effects and the stability of the sensor sightline against angular jitter. The lower limit is driven by the ability of the operator to search the displayed scene.

To be able to operate efficiently over a wide range of conditions, a variable field of view has considerable advantages and a zoom lens giving a continuously variable field of view between wide and narrow limits was considered to offer attractive operational benefits.

In our experience the wide field of view must be sufficient to maximise the ability of the operator to carry out an efficient search task and also be aware of the topographical features of the search area. This requires a field of view of approximately 15 degrees to 20 degrees. If a smaller value is provided the operator cannot relate his scene to the surrounding geography although the target detection range would increase.

Lenses are normally specified by their focal length and the relationship between focal length and field of view is

$$\text{Field of View} = 2 \tan^{-1} (a/2f)$$

where a:- sensor dimension (T.V. camera format)

f:- focal length.

A range of T.V. cameras are available in both 1/2 inch and 2/3 inch format however, as can be seen from Figure 4.1, the 2/3 inch format requires a greater focal length to achieve the same field of view. This results in a lens which is larger and heavier and for this reason the decision was taken to use a 1/2 inch format camera.

Lenses are readily available with zoom ranges of 10:1 and are of such a size as to be compatible with a compact airborne payload. Typically focal length ranges of 11mm to 110mm, 16mm to 160mm and 22mm to 220mm can be obtained. Of these we felt that a 22mm to 220mm focal length lens offers a good all round performance well matched to laser performance and the primary tasks of target detection and recognition. The actual lens which was selected was an auto iris variable focal length device with the following key characteristics.

10:1 zoom  
22mm to 220mm focal length  
1° 40' x 1° 15' narrow field of view  
16° 33' x 12° 27' wide field of view  
motorised zoom and focus  
length 154mm  
diameter 80mm (with protrusions for focus control)  
weight 1.5kg

#### 4.2 T.V. Camera

The solid state cameras which are available cover the range of technologies from MOS to CCD. It is our belief that the CCD frame transfer chip offers the best all round performance in that it has the highest sensitivity, greatest resolution and suffers least from high level bright spots in the scene. The advantages of a CCD camera in terms of size, weight and ruggedness made this type of sensor a natural choice for our particular application. However before a final selection was made a comparative trial of 6 small cameras was carried out. The trial was carried out on a bright clear day on a range with targets available at distances up to 8km. Each camera was fitted with the same lens and the same monitor was used. Operators were asked to judge each camera performance in terms of their ability to recognise a variety of targets including vehicles, groups of animals and men.

The trial was an empirical and somewhat subjective approach to the final camera selection therefore, as a parallel exercise, a mathematical model of the lens and camera performance was used to predict detection and recognition ranges. The target was assumed to be a small vehicle 2 metres square with a 10% contrast with its background. The model was run for three different weather conditions corresponding to 3km, 12km and 20km visible range. The results are plotted against lens focal length for the 22mm to 220mm zoom lens and show how the detection and recognition ranges vary through the range of this zoom lens. The results are shown in Figure 4.2.

#### 4.3 Laser

The primary constraints on the choice of laser were that it should offer rangefinder and designator capabilities, operate at 1.06µm, be small and lightweight and be available. The laser which was ultimately selected is a variant of an existing Ferranti high energy designator. This unit has a common laser transmit and receive path which makes it particularly suitable for integration with imaging sensors within compact airborne payloads. Additional key features which confirmed the units suitability for the target position and designation task are as follows:-

Output energy	> 60mJoules
Pulse Repetition Rate	10 pulses/second
Beam divergence	2mRad max
Receiver Range	300m to 10km
Accuracy	2.5m
Weight	6kg
Dimensions	200mm x 180mm x 130mm

The rangefinder performance of the laser should exceed that of the T.V. sub-system so that the range to any target which is acquired by the T.V. can be measured. Range performance is a function not only of the laser characteristics but also target reflectivity, target area and the prevailing atmospheric conditions. Anticipated range performance against targets such as buildings and camouflaged vehicles is plotted against visual range in Figure 4.3. Comparison of Figure 4.3 with the T.V. model results plotted in Figure 4.2 clearly shows that the rangefinder performance always exceeds the T.V. recognition range thereby confirming a matched combination.

The performance of the laser as a designator is determined by the transmitter characteristics, atmospheric conditions, target characteristics and laser seeker sensitivity. The primary objective is to enable the designator to stand off from the target as far as possible and for the weapon seeker to achieve lock-on at long range. Once again the constraint that the designator stand off range should exceed the T.V. sub-system target recognition ranges applies.

It was anticipated that the designator would be used in conjunction with the Laser Ranger and Marked Target Seeker (LRMTS) equipment as currently fitted to the Harrier, Jaguar and Tornado aircraft. In addition to a laser rangefinder and designator the LRMTS incorporates a stabilised laser seeker. The predicted lock-on range for the LRMTS equipment was computed for different conditions of visual range and different designator to target ranges. The results are shown in Figure 4.4. In conditions of reasonable visual range of 10km with a designator stand off range of 4km the predicted lock on range is 5km. However from Figure 4.2 it can be seen that in conditions of 10km visual range the T.V. recognition range only extends to 2.9km and for this stand off range a seeker lock-on range of 5.2km is predicted.

These anticipated stand-off ranges and lock-on ranges were considered operationally attractive and worthy of confirmation by a short trials programme.

#### 4.4 Stabilisation Platform

Once the physical characteristics of the actual laser, T.V. and lens had been established, the task of configuring these items in a compact stabilisation and pointing platform could be addressed. This section is not intended to be a rigorous and detailed explanation of the design and evolution of a stabilised platform, a subject which would easily justify a paper in its own right, but is rather a description of how the sensors were packaged within a suitable platform.

The basic functions which a good stabilisation platform must achieve can be summarised as follows

- (i) stabilise the sensor sightlines against angular perturbations induced by host vehicle vibrations, aerodynamic forces etc.
- (ii) steer the sensor sightlines over a wide field of regard - ideally complete lower hemisphere coverage for airborne surveillance of ground targets
- (iii) support and sustain the sensors against adverse environmental effects such as moisture, dust and sand, temperature extremes etc.

The two fundamental approaches to sensor stabilisation and steering are either to stabilise the sightlines only, via a gyro stabilised mirror or to stabilise and steer the complete sensor by mounting it directly onto a stabilised gimbal. We adopted the latter approach since in general this technique results in a lighter more compact payload which is better suited to installation in UMAs.

A photograph of the sensor head configuration is shown in Figure 4.5. A horizontal interface plate at the bottom of the upper cylindrical section allows the

sensor head to be suspended in the airstream beneath the UMA. Two outer servo drives operating about the pitch and yaw axes are capable of steering the head and its contents over the entire lower hemisphere. The pointing accuracy requirements for these outer servo drives are low since their basic performance requirement is that they need only follow the sensor sightline well enough to position the window over the sensor field of view, a task requiring a following accuracy no more precise than two to three degrees. The most important function which these outer servo drives fulfill is to isolate the inner stabilisation axes incorporating the sensors, from disturbance by aerodynamic torques. The two inner gimbals are also disposed about the pitch and yaw axes with the innermost yaw gimbal incorporating not only the laser, T.V. and lens but also two rate gyros which provide the sightline inertial reference. The inner gimbals remain at all times perpendicular to the sensor sightline and perpendicular to each other.

If blurring of the picture is to be avoided when the T.V. is operating in the narrow field of view then the sightline must be stabilised to within 50 $\mu$ Rad to 100 $\mu$ Rad (rms) jitter. The arrangement shown in Figure 4.5 offers the best possible opportunity of achieving this requirement through isolation of aerodynamic disturbances via the outer gimbal axes and close coupling of the laser and T.V. to maintain good sightline harmonisation and give a centre of gravity for the moving mass which is located as close as possible to the intersection point of the stabilisation axes. Precision duplex bearing pairs and brushless d.c. torquers were used to minimise disturbance torque transfer across the stabilisation gimbals and high quality potentiometers ensured that the error in the output signal and the angular position of the sightline in each axis is less than 10mRad.

The gimbals, gimbal drives and sensors are protected from the external environment by the sealed spherical outer skin which incorporates a glass windows for the T.V. and laser. The air inside the ball is dried by a breathing desiccator. Forced air cooling of the laser was not provided and in operating ambient air temperatures up to 40°C overheating problems were not experienced.

Key features of the stabilisation platform are as follows

Sensor Head diameter	381mm
Overall height	568mm
Angular Freedom	+ 50 deg to -120 deg pitch + 180 deg yaw
Pointing Accuracy	10mRad allowable error from true sightline position
Sightline Slew Rate	1 rad/sec pitch and yaw
Sightline Acceleration	1 rad/sec <sup>2</sup>
Sightline Jitter	70 $\mu$ Rad RMS

## 5. Trials

Trials have been carried out using the combination of a vision sensor and a laser. As has been mentioned earlier in this paper the payloads we have described are at a stage in an on-going development programme which is directed towards achieving the capability of all weather target acquisition and weapon attack. This will be satisfied, we believe, by the fusion of a television and infrared imaging system with a laser rangefinder designator. The fusion will be contained within boundaries that are compatible with installation on a UMA.

In the trials carried out to date a television sensor and laser rangefinder designator have been fused, integrated and mounted on a stabilised gimballed platform as described above. Trials have been conducted using a helicopter which has a similar performance to that of the majority of UMAs and which has the great

advantage of high reliability. This was considered acceptable since no attempt was made to simulate full system operation. The operator sat in the rear of the helicopter cockpit and viewed the scene on a monitor. Thus a more demanding situation was created than perhaps would exist for a UMA system.

Trials have been carried out in two stages. In the first, target acquisition and ranging was demonstrated. In the second, integrated weapon attack was added.

First Stage: flying was carried out at a controlled range in the UK against a variety of targets including artificial square targets and a Land Rover vehicle. The site contained a shallow valley and approaches were made against the targets from well out in the main valley and also over a ridge from the adjoining valleys. In all cases the helicopter was flown on a pre-arranged track and the operator therefore had reasonable expectation of what would be displayed on his screen. The angular position of the sightline relative to helicopter datum was displayed on the video. The site was instrumented by locating an IR sensitive television camera approximately 15 metres in front of the targets. It was thus possible to view and record the laser spot on the target. No instrumentation was provided for helicopter position determination since the most accurate rangefinder available was the laser installed in the equipment.

On each run the operator was required to detect the target in wide field, zoom in to narrow field, refine his aim to place the graticule over the target and then fire the laser. The laser was boresighted to the graticule. Range was immediately displayed above the monitor on an LED four digit display to the nearest  $\pm 5$  metres. The operator was a Ferranti trials engineer who had several hundred hours of flying experience with similar equipment.

The range at which target tracking was achieved was noted and varied from 2.5km to 4.5km. The helicopter approached at an altitude of approximately 150 metres above ground level at the valley entrance which was approximately at target height. It approached the target area at a constant altitude. The approach speed was in the range 25 metres/second to 36 metres/second. Our results showed that with increased operator experience, the lock on range could be increased until fatigue became important. The time required from target detection to lock on was determined by the control panel layout and the speed of the zoom mechanism. A very slow gimbal rate was found to be preferred and the hand control rate law was switched between a high rate and a low rate. It was also noted that the operator required to look away from the monitor in order to read target range and when this happened the sightline invariably drifted away from the target. A facility to superimpose the range on the display monitor has since been incorporated and is confidently expected to eliminate this difficulty. The ground based camera was able to detect the laser spot on the target and thereby confirm that laser energy was incident on the target.

Second Stage: flying was carried out at a controlled range against small vehicle targets. The site was relatively flat. The designation was again carried out from a helicopter and attack passes were carried out by Jaguar aircraft fitted with LRMTS. The LRMTS equipment consists of a laser seeker carried on a gimballed head. In the acquisition mode the head scans in azimuth at a defined depression angle. When laser radiation at the correct repetition frequency is detected, target lock occurs and this information together with the target position is displayed on the Head-Up Display (HUD). The pilot then flies the aircraft on the correct flight path and releases his weapon at the indicated point. Both of these can be displayed on the HUD and weapon release can be automatic. Target acquisition was not tested and the operator was allowed an unrestricted amount of time to acquire the target, zoom in and refine the aim point. The rangefinding facility was used to measure the target range. The helicopter carried out hover while the attacks were completed and stand off ranges of 1, 2 and 3km were set up. Aircraft lock on ranges were noted by radio

communication and the results of each attack discussed as the aircraft circled for a return pass. Aircraft lock on ranges were obtained of up to 7.3Km. The measured lock-on ranges are shown on Figure 4.4.

The weather conditions during which the trial was carried out corresponded to very good visibility. The results should therefore follow the curve for R met equal to 20 km. It can be seen however that the seeker lock-on range does not decrease as the designator range is increased, at the expected rate. The curves plotted in Fig. 4.4 assumed that the full beam is incident on the target and that no overspill occurs. The beam divergence provided by the equipment in conjunction with the small size of the target, a three ton truck, resulted in the beam completely covering the target at 1 km range. At increased designator ranges, significant overspill occurred and the fraction of incident energy which may be reflected is reduced. Operator aiming errors which will tend to have fixed angular values will also increase the beam overspill as the designator range increases.

However, it is apparent that at the stand-off range of 3 km a seeker lock-on range in excess of 4 km was achieved. This useful lock-on range would be further extended by increasing the laser telescope magnification and thereby reducing the laser beam divergence.

Attacks were also carried out for groups of four Harrier aircraft flying at 20 second intervals against a variety of targets including a building and a row of vehicles, however the collection of reliable data has so far proved to be very difficult since it was not possible to place instrumentation at the target as the aircraft were dropping practice bombs.

## 6. Conclusion

We have discussed the requirement, described an engineering solution suitable for a UMA and discussed trials work. The aspect of operational deployment has also been addressed.

It has been shown that sensors can be provided that allow target acquisition at reasonable ranges and can therefore give the system a stand off range that should prove safe. The addition of a rangefinder allows target position to be determined with an accuracy that can give a suitably small CEP. A rangefinder which also can be used as a designator offers the added advantage of being suitable for use with precision guided weapons. When used with aircraft in cooperative attacks, lock-on ranges were obtained which would allow target attack to be carried out with high accuracy. Even for attack with free fall bombs the miss distance calculations would show a considerable reduction in error. With hittile type weapons having a similar receiver sensitivity the lock-on range, together with the target position accuracy which is available, would allow high success probability.

In a multiple attack scenario we have identified some difficulties which we believe require to be solved before the full potential of the system can be realised. In any weapon attack when weapons are being launched at a reasonable rate, it is essential to have a planned course of action and not to rely on communication during the attack. The reason for this is twofold, the operator requires a high degree of concentration to carry out the acquisition and targeting role and therefore does not have much time for accepting new commands or plans, the scene will rapidly become confused with smoke and battle debris and the ability to adhere to the original plan will be severely tested.

The operational control of such an attack is going to provide some challenges as the UMA operator will be seated at a console some distance from the attack site and will require detailed information on weapon platform location, attack timing and

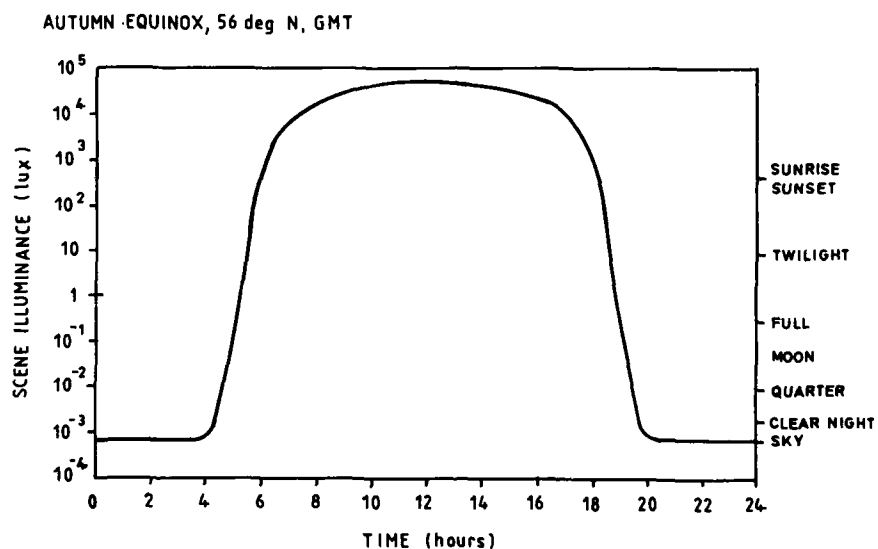
attack details. He must also be able to accommodate changes to the plan and rapidly respond to a requirement to find and designate an alternative target.

Our development programme will now concentrate on extending the performance of the television laser system by increasing the telescope magnification and decreasing the laser beam divergence. The final stage in the development programme will be the integration of the laser with a thermal imaging system.

### Acknowledgments

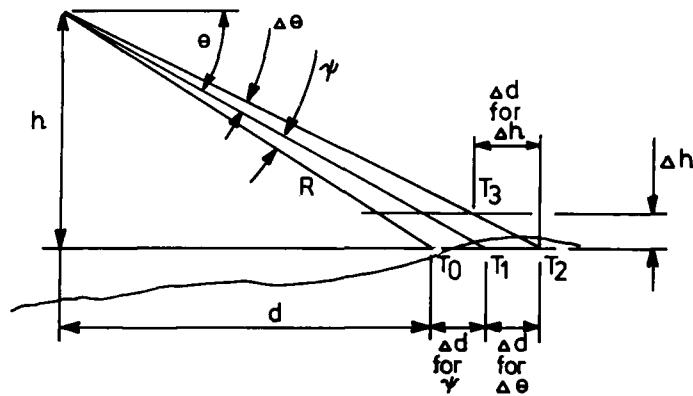
We acknowledge the assistance provided by all our colleagues at Ferranti Electro-optics Department, Edinburgh. The helicopter flying was undertaken by Captain Jerry Hermer of Dollar Helicopters UK and also by Captain A. McFarlane of Gleneagles Helicopters.

Particular reference should be made to Dr. W.H. McKendrick for contributions to the system performance trade off and to Mr. I.F. Bennett who carried out all the trials work. We are also grateful to No. 3 Squadron RAF for an opportunity to carry out joint trials with their Harrier aircraft fitted with LRMTS.



SCENE ILLUMINATION LEVEL DURING 24 HOUR PERIOD

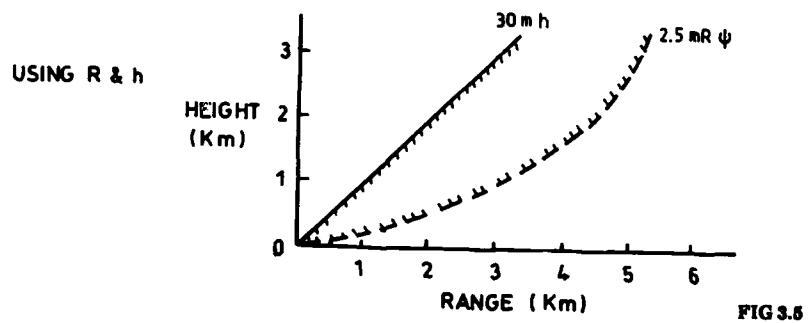
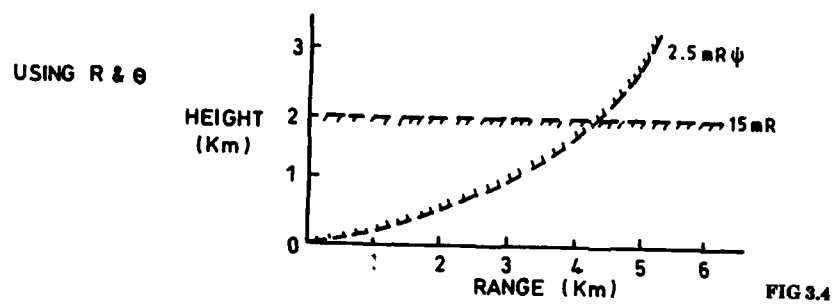
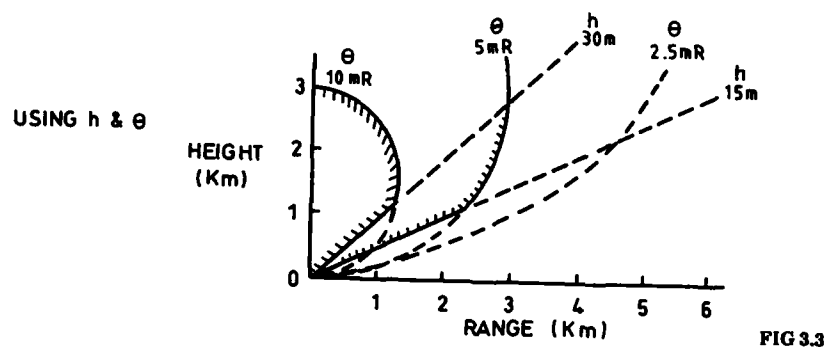
FIG 3.1



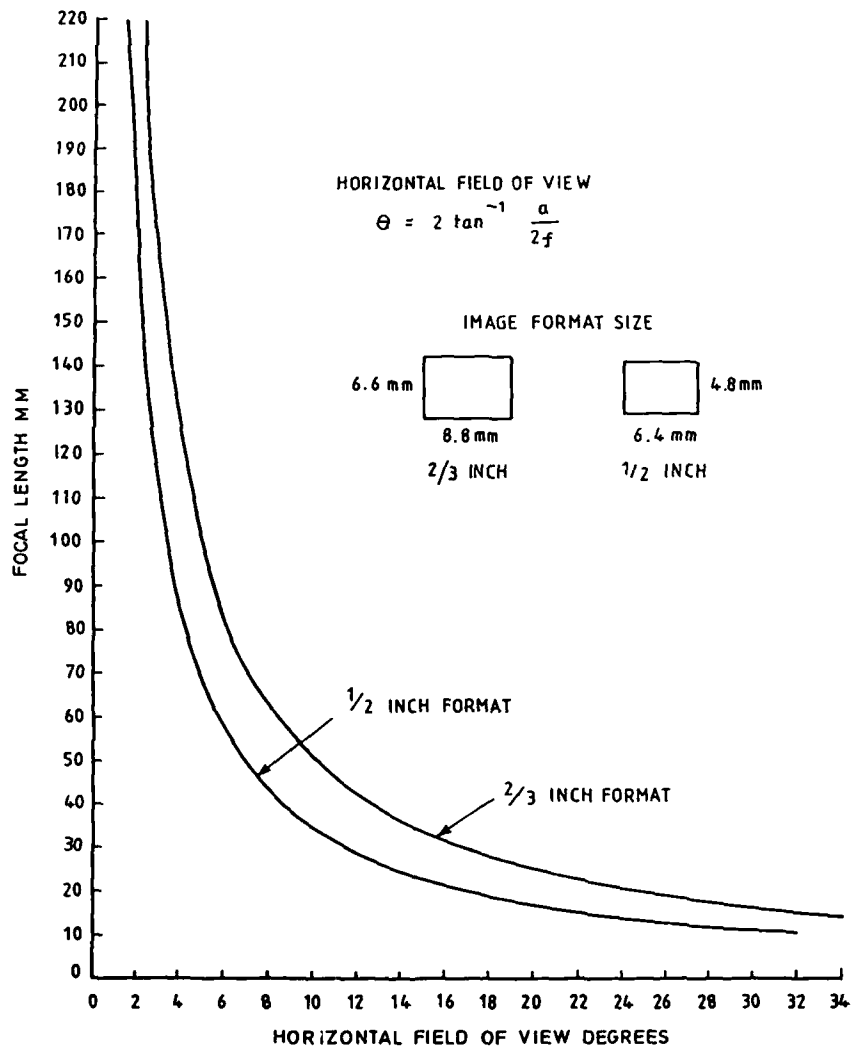
$\theta$	SENSOR GRATICULE LINE ELEVATION ANGLE
$\Delta\theta$	ERROR IN $\theta$ DUE TO VEHICLE PITCH AND ROLL ERRORS AND EO SENSOR PICK OFF AND OTHER ERRORS
$\psi$	ERROR BETWEEN GRATICULE LINE AND TARGET LINE DUE TO OPERATOR ERROR
$h$	HEIGHT VEHICLE ABOVE TARGET
$\Delta h$	ERROR IN HEIGHT VEHICLE ABOVE TARGET
$d$	HORIZONTAL DISTANCE VEHICLE TO TARGET
$\Delta d$	ERROR IN HORIZONTAL DISTANCE VEHICLE TO TARGET
$R$	RANGE TO TARGET
$\Delta R$	ERROR IN RANGE TO TARGET

AIR VEHICLE/TARGET GEOMETRY

FIG 3.2

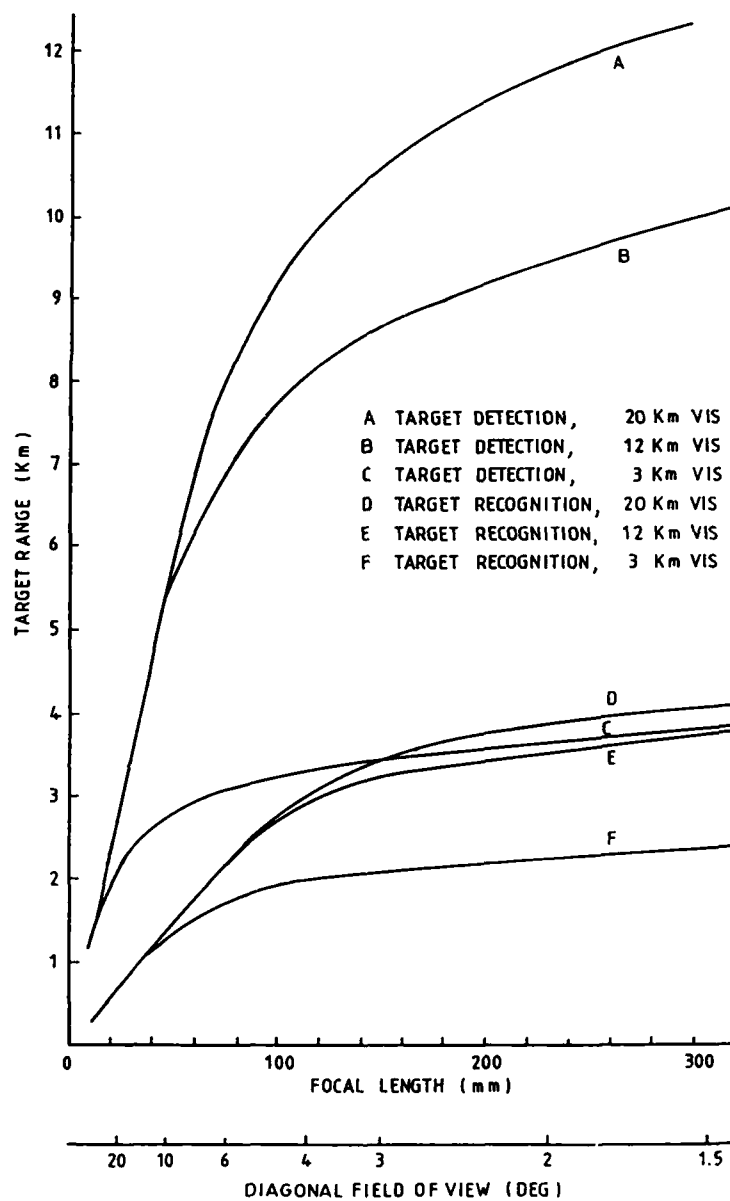


COMPARISON OF TARGET LOCATION METHODS



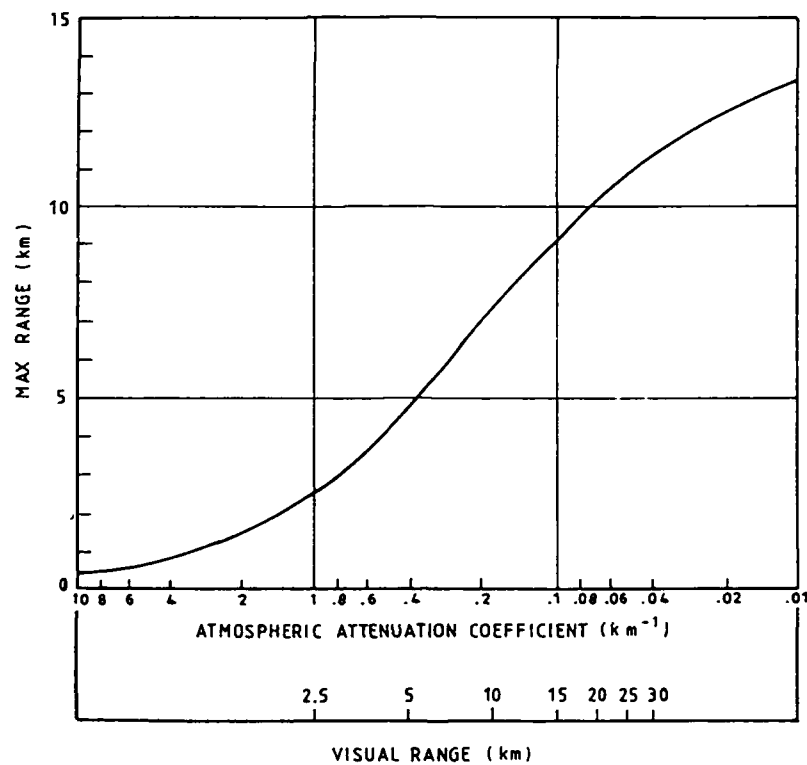
FIELD OF VIEW VERSUS FOCAL LENGTH

FIG 4.1



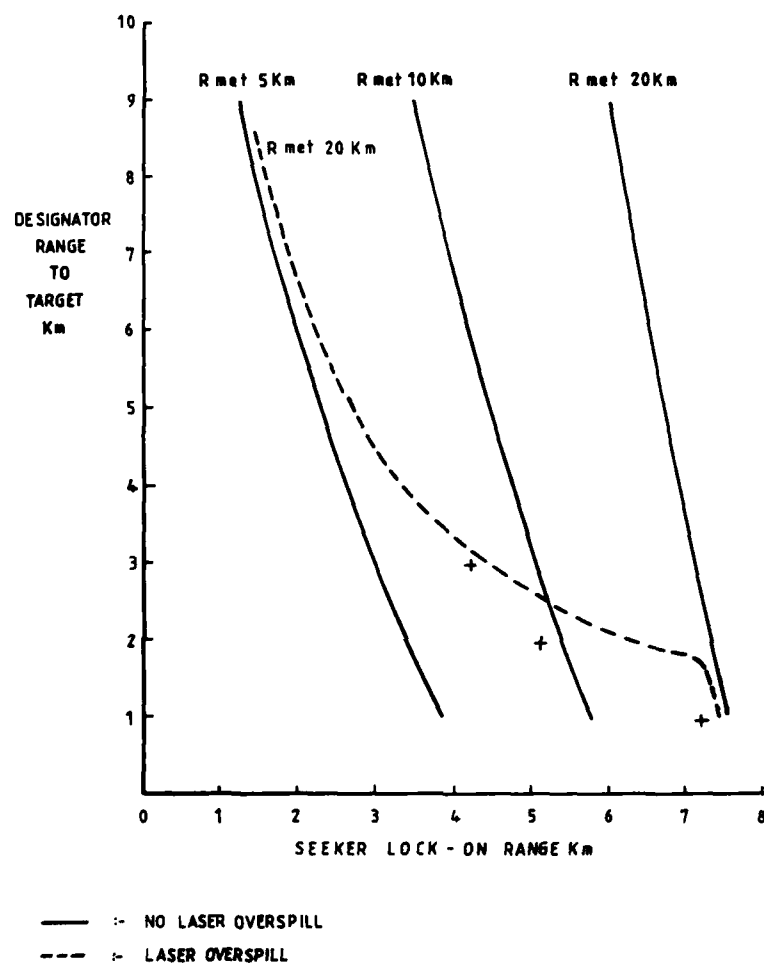
TELEVISION DETECTION AND RECOGNITION RANGES

FIG 4.2



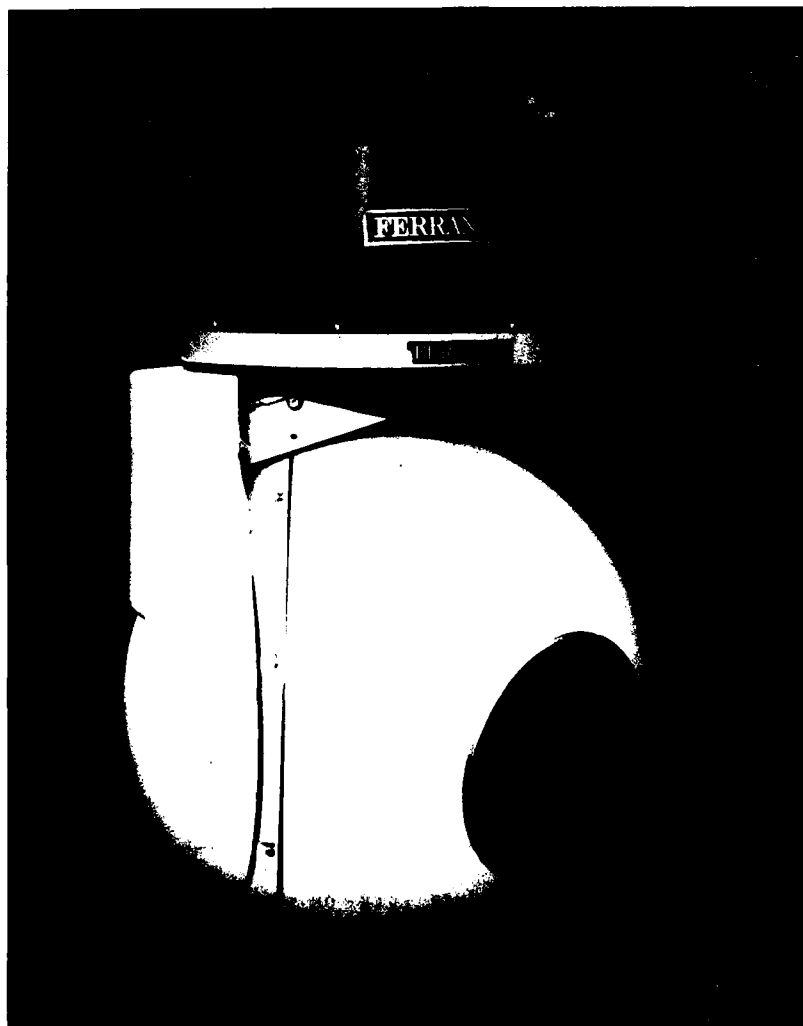
PERFORMANCE OF RANGEFINDER

FIG 4.3



DESIGNATOR RANGE VERSUS SEEKER LOCK-ON RANGE

FIG 4.4



SENSOR HEAD CONFIGURATION

FIG 4.5

## UNMANNED AIR VEHICLES PAYLOADS AND SENSORS

Grover S. Amick  
Program Engineer  
Lockheed Missiles & Space Company, Inc.  
O/T7-40, B/312  
6800 Burleson Rd.  
Austin, Texas 78744-1016

*Summary. The Lockheed Corporation developed a family of payload sensors for use in unmanned air vehicle applications. The program was initially conceived as an extension of the U. S. Army Aquila Remotely Piloted Vehicle (RPV) Program and is applicable to a much wider variety of uses and applications. The design concept utilized a universal gimbal platform with interchangeable sensor spheres. The concept and implementation process was directed to develop a low-cost sensor system which could easily accommodate new sensors as they became available. The system has been developed and demonstrated using the Lockheed Altair UAV system and is available for use. A family of seven sensor types have been successfully demonstrated, and others are in development. The system is known as the Lockheed Adaptive Modular Payload System (LAMPS).*

### Introduction

(Figure 1) Lockheed Missiles and Space Company is sponsoring the development and demonstration of advanced technologies in Unmanned Air Vehicle (UAV) Systems. This fly before sell concept has been applied to every component of a UAV system. Prototypes of launch, recovery, ground control, data link, air vehicle, and payload equipment have been developed, fabricated, integrated, and are in active test at the Lockheed Austin Division. This paper deals with one aspect of our UAV system—the UAV payload. The Lockheed Palo Alto Research Laboratory spearheaded the concept of using a standardized two-axis gimbal platform and associated electronics which promotes the use of many different imaging sensors. This unique concept is called LAMPS, for Lockheed Adaptive Modular Payload System, and has successfully integrated daylight television (TV), nighttime forward looking infrared (FLIR), photographic camera and a daylight TV with integrated laser rangefinder—all utilizing the same payload platform. Interchangeability from one sensor sphere type to a different type can be accomplished on the air vehicle in less than ten minutes. In addition to the UAV technology advancements developed by Lockheed, we have acquired a full spectrum of test facilities which include manned aircraft for UAV testing and a fully operational UAV free flight test range.

Of specific interest in this paper is the manner in which these multiple sensors interact with the host air vehicle to provide operational capabilities beyond that of simple reconnaissance sensors. The host air vehicle, Altair, employs an inertial navigation system which is periodically updated from the ground tracking data link. The use of satellite or ground station positioning systems such as global positioning system (GPS) or Omega can easily be accommodated to interface with the existing navigation update capabilities. Our on-board computer subsystem combines navigation and flight dynamics functions to give the air vehicle the capability to accurately navigate to any specific location, and, while on station, direct the payload sensor line-of-sight to any pre-selected target coordinates. Conversely, if a target is located in the sensor imagery, crosshair alignment on the target will permit the computation of the actual target coordinates (in any selected coordinate system) for accurate target spotting for tactical intelligence purposes or for artillery targeting. In this latter case, offset adjustments of the burst impacts may be accomplished in the same manner to permit precise artillery adjustments. For those cases where inconsistent terrain altitudes affect the coordinate accuracy, the use of an eye-safe laser ranger capability provides the actual slant range to target values to permit precise target coordinate location.

These imaging sensors, operating with our capable and proven UAV system, provide an operational capability in tactical reconnaissance, target spotting and fire control.

### Payloads and Sensors

We at the Lockheed Austin Division of the Lockheed Missiles and Space Company are deeply involved with the development and testing of tactical unmanned air vehicles. Although a wide variety of unmanned air vehicles have been prototyped by us and others over the past ten years or so, one air vehicle in particular has progressed to a high degree of maturity. (Figure 2) The air vehicle pictured here was developed for the U.S. Army under a full scale development contract and is known as the Aquila.

The Aquila was specifically designed to survive in a hostile battlefield environment. The U.S. Army full scale development program culminated in the Army's full scale operational testing conducted during 1986 and 1987. During this operational testing a total of 143 flights were conducted with 134 automatic recoveries and 9 parachute recoveries. But this paper is not

about Aquila, but rather a derivative of this mature air vehicle.

Under Lockheed in-house funds the basic Aquila air vehicle was modified with added fuel tanks to provide extended range and endurance capabilities and a new sensor payload concept was implemented for expanded operational applications. Other modifications were also included to expand the various types of mission and roles which could be satisfied with this derivative of Aquila which we call Altair. The Altair air vehicle exists and is in active use today after having its first successful free flight on September 19, 1987.

(Figure 3) Before I go on with Altair, I suspect not all of you are familiar with Aquila so I'll do a thumbnail sketch of the Aquila. This vu-graph shows the major components of the air vehicle. Note that it has a full set of avionics—navigation system, autopilot, data link, and of course the sensor payload. The vehicle is some 7 feet long with a 13 foot wingspan and weighs some 285 pounds fully loaded. (Figure 4) The rest of the Aquila system is shown here. The air vehicle is catapulted to flight speed by the launcher and automatic recovery is accomplished using vertical and horizontal position sensors located on the arms of the recovery system to provide for a hands-off recovery into the centerpoint of the net. The Ground Control Station, through the data link, receives flight status data and provides payload control and monitoring. The air vehicle flies a pre-programmed mission scenario unless commanded otherwise by the ground controller.

(Figure 5) In developing our in-house UAV system, several requirements were re-examined in order to optimize the system developed. The first requirement addressed dealt with the potential user requirements. Did they need a combat hardened system or could these requirements be relaxed, in order to achieve a lower cost, highly mobile system. Another key issue dealt with mission requirements. Was target designation a critical mission requirement? If the designation requirement was relaxed, a much simplified payload could be developed.

With these key requirements relaxed, we proceeded with an internally funded full scale development effort which resulted in the first Altair free flight during September 1987.

(Figure 6) The Altair air vehicle is as shown. The changes introduced into the basic Aquila airframe are highlighted. Briefly, these changes incorporated additional fuel bladders in both wings, a different data link, a new payload package (physically interchangeable with the Aquila mission payload system) and an optional center fuel tank which could be removed and the compartment used for additional functional elements such as GPS, OMEGA, remote video recording, FAA transponders, electronic intelligence (ELINT) or other electronic warfare (EW) payloads. But in all other areas the Altair is essentially an Aquila.

(Figure 7) The rest of the Altair System is shown here. Note that all the same type of functional units are shown, but that they all ride on 5/4 ton vehicles, presumably CUCV or HMMWV in military parlance. These are highly mobile, non-hardened vehicles, but are fully C-130 transportable. The cost of these lightweight components directly results in a significantly lower cost operational Altair system as compared with the fully hardened Aquila.

In developing the payload requirements for the Altair, several constraints were imposed on us. (Figure 8) It was mandatory that our payload be physically interchangeable with the Aquila Mission Payload System. This strict form and fit was adhered to. However, we also had a requirement to support an unspecified number of different sensors. Unspecified was the operative word to ensure that whatever concept or architecture we used, it would retain the inherent capability to incorporate newer type sensors whenever they became available. It had to be modular in architecture to ensure the flexibility to be utilized on a wider variety of host vehicles than just Altair. Minimal cost was also stressed as a highly desirable goal. The cost reduction goal is well emphasized in this vu-graph (Figure 9) which shows that sensor payloads can comprise from forty-five to forty-eight percent of the Aquila air vehicle cost. The variation being due to the cost differentials which exist—for example, a TV camera vs. a Forward Looking Infrared sensor.

Not to get ahead of myself, but we are achieving a ten to twenty percent UAV cost ratio with our new payloads.

(Figure 10) Looking at the generic payload development process we found that to a large extent the sensor manufacturers, themselves, developed and produced their own payload systems. The design was unique to his sensor and the resultant platform design was included in the design package and sold as a unit. The controls and displays were similarly single-unit designs—again centered around the sensor manufacturers requirements. Likewise for documentation, spares, ground support equipment, maintenance, and so on.

The impact of all this is that a proliferation of gimballed platforms exist to provide the pointing control to the multiplicity of sensors which exist. More discouraging is the untold design hours spent redesigning the same basic mechanical chassis which support the various sensors. Ever try to replace a small TV sensor with a FLIR? Generally it won't even fit, even if you are willing to buy the whole gimbal system that comes with it. Need another full set of documentation?

(Figure 11) The concept which our Palo Alto Research Laboratory came up with was pure simplicity. Why not develop a Common Platform for all sensors? Define the Form, Fit and Function of the sensor as an interchangeable unit. Pick a sphere size which is compatible with the UAV aerodynamics.

For some sensors it is an easy fit, for others you need a shoehorn. In extreme cases off-platform boxes may be required. But the platform itself is used and re-used over and over again. Thus a mature platform with its mechanical complexity of gimbals, bearings, resolvers and gyros emerges as a standardized item. Standardized spares and documentation greatly

reduces implementation costs.

Need a new sensor? No problem, stuff it into the ball and "plug her in". Minimal cost, minimal sparring, minimal documentation costs—like an appendix to existing manuals.

The concept is carried even further. Our operator control panel and test equipment utilize software programmable plasma panels. These easily changeable panels permit re-programming to accommodate the different control requirements which seem to come along with any new sensor being integrated.

This concept became the baseline architecture for the development of Lockheed Adaptive Modular Payload System or, as we call it, LAMPS. Let's look at this again. (Figure 12).

(Figure 13) Now we'll look at the individual components that make up LAMPS. I'll first cover the platform description and follow with the various sensors and will eventually end up with a few words on operational uses and non-UAV applications.

(Figure 14) The platform physical parameters are shown on this vu-graph. Pay particular attention to the stability cited. The only way that a stability value may be quoted is when it is in the context of the input vibration levels—either explicitly in terms of a host vehicle power spectral density or as implicitly in terms of the specific host vehicle. The Altair, typical of all mini-RPV's is a small, vibrating airframe subject to environmental induced motions and maneuvers. For other applications on larger airframes, the vibration environment would be expected to be much more benign than the Altair, and as a result, the resultant stability will be much better. The best we'll be able to do will be quiescent conditions (without any mechanical motion inputs at all). Our value of stability under this optimal condition is some 10 microradians. If we postulate a large aircraft with some 20 dB less vibration than our UAV, we would achieve a stability close to the quiescent value. We're still in the process of further defining and refining this value.

(Figure 15) The LAMPS physical assembly and component boards are shown here. The placement of the electronic components into modules at each end suggest that repackaging of these modules off-platform could be accomplished if a smaller turret footprint was required. The printed circuit cards shown were specifically developed along functional lines to accommodate changes which may be dictated by user, application or sensor requirements. As a specific example, the Input/Output board was recently modified to provide control functions for a on-board video recorder which would automatically begin recording whenever the aircraft lost link with the ground station—for example, a mission which extends beyond the range of the data link and the aircraft is flying a purely autonomous mission. Playback could be commanded when the vehicle's link was re-established. The Altair uses an RS-422 buss but conversion to 1553 or 232 buss could also be accommodated with a modified I/O board.

(Figure 16) With our standard platform described, we'll now tackle the sensors. As is shown a variety of sensor spheres may be interfaced to the platform. The sensor sphere actually consists of a truncated sphere 13.5 inches (34.3 centimeters) in diameter and 9.5 inches (24.1 centimeters) wide (about 900 cubic inches of sensor volume), which is sufficient to house the range of sensors shown. The sphere attaches to the azimuth gimbal yoke with half shell bearing retainers which can be easily removed, thereby allowing sensor changeout in less than ten minutes in the field, and with no need to disturb the UAV panels. All access is external to the aircraft. Command signals and video enter/exit the sphere through a centerline connector while a similar connector on the other side is used for 28 VDC power. Each sensor sphere has a unique identification module in it which is used to automatically activate the proper software for system operation, plasma panel configuration as well as to confirm to the operator as to the type of sensor in operation on the air vehicle.

The sensors shown will be covered in more detail in the forthcoming vu-graphs. Recognize that no inherent limit is to the types of sensors which may be integrated, save that of physical size—and we can generally overcome this problem when necessary.

(Figure 17) This table presents the relevant parameters associated with the daytime TV imagers which have been built up and successfully tested in LAMPS on-board the Altair air vehicle. The Charge Coupled Devices (CCDs) available on the market today are surprisingly compact units and integrate quite easily into the sphere. As mentioned previously, any manufacturer's cameras can be used with our LAMPS, given that they fit our space/weight/ power limitations. The first unit shown is an inexpensive, commercial Sony TV camera and has performed extremely well during our testing program. This demonstrated use of a very low cost commercial unit in the rather severe UAV environment should be seriously considered by any customer. Ease of replacement and low cost can be a most effective tradeoff and is made more attractive with our total independence between the high-performance platform and the replaceable sensor sphere.

(Figure 18) The FLIR development world is quite fast moving these days. Several FLIRs have been integrated and used with our LAMP. In some cases, older units drift into obsolescence as the manufacturer improves the product. Fortunately, in most cases the newer model is smaller than the predecessor and thus incorporation of product improvements is accomplished quite easily. Our newest FLIR model is the Kollmorgen micro-flir, most significant in that it utilizes the Mullard 8-bar SPRITE detector (SPRITE stands for signal processing in the element) and results in significant performance gains. I would expect to see us eventually incorporating focal plane arrays and multi-spectral sensors in the not too-distant future. How refreshing it is to have a product line which readily accepts the technological advantages achieved by all vendors.

(Figure 19) Some of the other sensor spheres which we've developed are shown here. During 1987 we introduced a Raman-shifted Nd:YAG eye safe laser rangefinder coupled with a CCD imager. Our plans call for a similar integration with

a FLIR imager—but we're still looking for a bit more of a size reduction in the FLIR. A couple of vendors are working the problem and a FLIR-laser ranger capability is not too far away. It might be worth noting before we leave our laser ranger that the eye safe term incorporates both the peak pulse power as well as the pulse repetition rate. In the multiple pulse repetition frequency (PRF) mode (5 pps) the laser is rated a Class III (i.e., not eye safe) at ranges within the sphere. Beyond the sphere, in the outside world, it is eye safe.

The photo-recon sphere illustrates a use of some of the fully automatic compact 35mm cameras on the market today. Quite a large variation in performance can be obtained through selection of appropriate lenses—both for the camera as well as the TV imager. Of course, other cameras can be used, but the 35mm capabilities available today offers a lot of performance for the dollar.

In the development arena we have prototyped a chemical sensor and brass boarded an active laser illuminator coupled with a gated, intensified, GEN III camera. The chemical sensor is essentially an area search device to detect the presence of a chemical agent cloud while the active gated TV sensor is developed to provide visual scene imagery during nighttime operations where the desired targets do not exhibit sufficient thermal contrast to permit use of a FLIR. These are development programs so actual data is not firm and in some cases proprietary data is involved, so specific details will not be provided in this paper.

(Figure 20) As has been abundantly demonstrated, the LAMP is a Lockheed payload—however, we serve only as system integrator when it comes to the sensors used. This rather dual role separating the platform from the sensor provides for several unique advantages. We can focus on the customers mission requirements, evaluating the full spectrum of applicable sensors available from all vendors and can select the best one consistent with the program requirements. We accomplish the acquisition, integration and test of the unit and marry it to our standardized platform.

Our extensive test capabilities include a fully functional UAV system, as well as laboratory and simulation capabilities. The manned aircraft for testing sensors is a modified Piper Cherokee with a centerline canoe for electro-optical (EO) installations while a twin Otter, designated the MAC III, is available for full UAV captive flight testing with the Altair suspended on a belly mounted trapeze. In this case, the full Altair system, from AV to engine to data link to ground control station is fully functional. We also have an image exploitation system which is capable of performing both on-line and off-line image processing and analysis. This capability is priceless during competitive evaluations of different imaging systems, as well as performing quantitative assessment of sensor performance. The ultimate test resource, as mentioned before, is the full free flight UAV system known as our Demonstration and Research Test System, or DARTS operating in restricted air space at our South Texas Test Facility.

In addition to the physical resources, we also maintain an active group responsible for system modeling whose major tools consist of the Rosel model for visual imagers and the Ratches model for infrared imagers.

(Figure 21) A specific example of our modeling capability is shown here for an effort conducted in 1987. A need emerged for a high resolution FLIR with a rather specific and ambitious schedule requirement. We looked at our current FLIR sensors as well as other available sensors, collecting all the required data needed for technical, cost and schedule comparisons. Technical performance was of paramount importance and successive Ratches model runs were made with the vendor performance parameters as well as the Altair performance parameters (for example, the modulation transfer function (MTF) characteristics of the video data link) to perform a system level comparison of all candidate sensors. Those sensors which satisfactorily met the performance criteria were then further evaluated with respect to schedule, risk and cost. From this competition the successful candidate was awarded a contract to provide us with our high-resolution FLIR sensor.

It is entirely possible that if another evaluation were conducted today, a newer FLIR from a different vendor might well win the competition. The main point to remember is that at any instant of time we can respond with the best available system.

(Figure 22) This graph shows the comparative evaluation of all candidate FLIR systems considered. Note that in some cases, the differences were insignificant. Subsequent cost/schedule/risk assessments provided the added criteria needed for winner selection. I must caution you regarding the performance values estimated. These are Ratches runs using our Altair system with the Altair parameters being projected values. The validation of these estimates under actual flight conditions is not yet completed. The relative comparison between the various FLIR sensors should, however, be correct.

(Figure 23) Let us leave the sensors for a description of the other components which make up a LAMP system. The Altair Payload Operator is responsible for the sensor performance during the conduction of a mission. His suite of equipment consists of a image display unit, typically a TV monitor, a joystick for sensor pointing and a control panel to control the payload functions as well as readouts for status.

The control panel provided to the payload operator is shown in this vu-graph. It is a software driven plasma display with a touch sensitive panel and interacts directly with the operator. Being software programmable, the system provides for maximum flexibility. Each sensor typically has its own set of unique controls requirements. For example the CCD/laser rangefinder needs a LASER ENABLE switch as well as a LASER FIRE button which obviously would not be needed for a FLIR which has such controls as BLACK HOT/WHITE HOT. A programmable plasma panel provides an excellent means to engineer the optimum panel layout, labeling and functions to provide unambiguous sensor commands and status to the operator. Each sensor sphere has its own unique identification module which automatically invokes the appropriate panel

layout for the payload operator. Any assortment of switches, guarded switches, alphanumeric displays, calls for help, menus and so on is available for use by the designer. A new sensor type never before integrated? no problem—re-program the panel. By the way, what language do you want it in? several?? OK! The panels we use are available both mil-spec as well as commercial.

The TV displays are really a customer preference. An number of quality displays are available. We, on Altair, use black and white imagery with color annotations on the screen. The Ground Control Station receives the sensor imagery in RS-170 black and white format and converts it to RGB format and use the color as input ports for annotation. As I mentioned, other types of displays are easily accommodated. The joystick can be either analog or digital, with a stick or a pilot-type pistol grip. The functions are so similar that conversion from for one type to another can easily be made.

The two axis LAMPS gimbal system does not correct for image rotation. However, the Ground Control Station has implemented an off-platform derotation capability which uses the air vehicle and sensor geometry to compute the appropriate derotation angle which must be applied to restore a vertical image. The choice for derotation is left as a customer option. The image de-rotation unit we use is a DATACUBE unit and there are other similar units available for image processing in the industry.

(Figure 24) Let me take a few minutes to describe how LAMPS operates in conjunction with the Altair air vehicle. Recall that the Altair has a strapdown inertial system which is constantly updated from external references such that UAV position and altitude is known quite accurately. This present position can be related to any desired coordinate system. We usually use Universal Transverse Mercator (UTM) coordinates. The target coordinates can be input to the system and the payload will automatically slew to the required azimuth and elevation angles to point the optical axis of the sensor at the target. As the aircraft moves through velocity, roll, pitch, yaw or altitude effects, the sensor pointing is modified appropriately. A slight outgrowth of this permits the operator to slew his crosshairs to a different geographical position. The Altair will compute the offset you've presented (if this is needed for burst offset for artillery correction) or will compute the new coordinates (if you were looking for more accurate target location coordinates). This offset feature it can be used to calibrate your navigation system should that ever be needed. The target tracking method I've just described works well on static targets. We are currently developing a scene correlation/target tracking processing system which will provide for moving target tracking. The next paper will deal with the optimized and automatic area search technique we've developed. Paper #25 dealt with the target location accuracies we're able to obtain for Aquila.

(Figure 25) However, Altair isn't the only host vehicle to use LAMPS. Several applications, both ground and air have developed and either have been, or soon will be, demonstrated and made available. In early 1987 a LAMP unit was integrated into a Lightweight Target Acquisition/Surveillance System (LTASS). The LAMPS was mounted on top of an extendable 27 foot (8.2 meter) folding mast on top of a military ground vehicle. The vehicle co-pilot station had an operator control unit (panel, display and joystick). The vehicle also contained a land navigation unit. The LAMP provided was supplied with two interchangeable sensors: daytime TV (CCD) and a FLIR. The unit is designed for monitoring the immediate forward area from a reasonably obscured location—behind a hill, in the woods or dense vegetation where the sensor head could be unobtrusively located such that covert surveillance of an area could be conducted. This LTASS unit was developed and produced by Lockheed Aeronautical Services Co., Georgia and was subsequently tested by the Army at the Yakima, Washington test range. Excellent results were reported by the Advanced Development Evaluation Agency (ADEA) as a result of the two week evaluation program.

A LAMPS installation in the nose of a C-130 aircraft is underway to provide a Pilots Vision Aid to Navigation (PVANS). This installation of a LAMPS with the laser ranger and imaging sensor will provide the pilot with accurate "range to touchdown" data to permit landing on unimproved runways. A FLIR/ Laser Ranger, still in development, will extend this landing capability to nighttime operation.

What these applications are meant to illustrate is that LAMPS is a versatile system with applications to a wide variety of other host vehicles. We'd enjoy discussing your needs with you.



# **UNMANNED AIR VEHICLE PAYLOADS AND SENSORS**

**PRESENTED BY**

**GROVER S. AMICK  
LOCKHEED MISSILES & SPACE COMPANY, INC.  
LOCKHEED AUSTIN DIVISION  
AUSTIN, TEXAS**

**6 OCTOBER 1988**

Figure 1: Title Page



**AQUILA — U.S. ARMY FULL SCALE  
DEVELOPMENT PROGRAM  
THROUGH ARMY  
OPERATIONAL TESTING—  
COMPLETED SPRING 1987**

**ALTAIR — DERIVATIVE OF AQUILA  
MODIFIED FOR EXTENDED  
RANGES AND ADDITIONAL  
MISSION ROLES THROUGH  
EXPANDED PAYLOAD  
OPTIONS--DEMONSTRATED  
SUMMER 1988**

Figure 2: Lockheed Air Vehicles

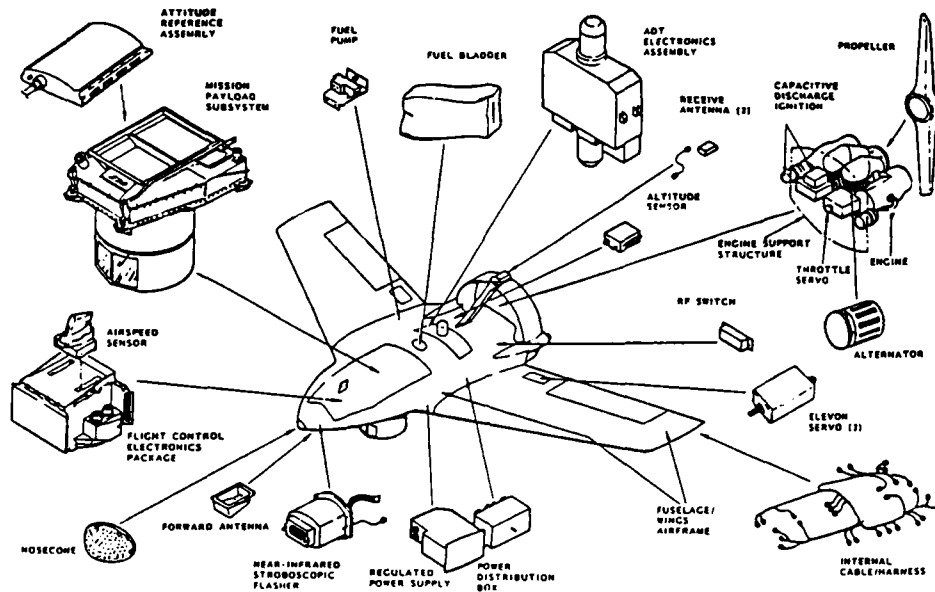


Figure 3: Aquila Air Vehicle Subsystem

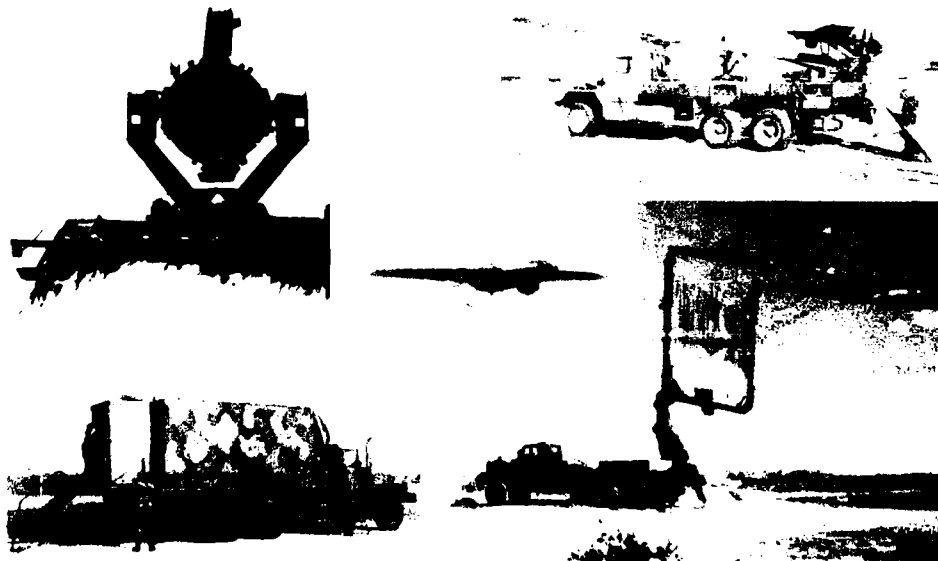


Figure 4: U. S. Army Aquila

- NOT ALL USERS REQUIRE FULLY-HARDENED SYSTEM
- COST, MOBILITY, ENDURANCE, AND EXPANDED MISSION ROLES WERE IDENTIFIED AS KEY ISSUES
- INTERNALLY FUNDED FULL SCALE DEVELOPMENT PROGRAM WAS CONDUCTED
- FIRST FULL SYSTEM FREE FLIGHT IN SEPTEMBER 1987
- REFINEMENTS AND DEMONSTRATIONS CONTINUE
- SYSTEM DESIGNATION IS **ALTAIR**

Figure 5: Lockheed Independent Development UAV

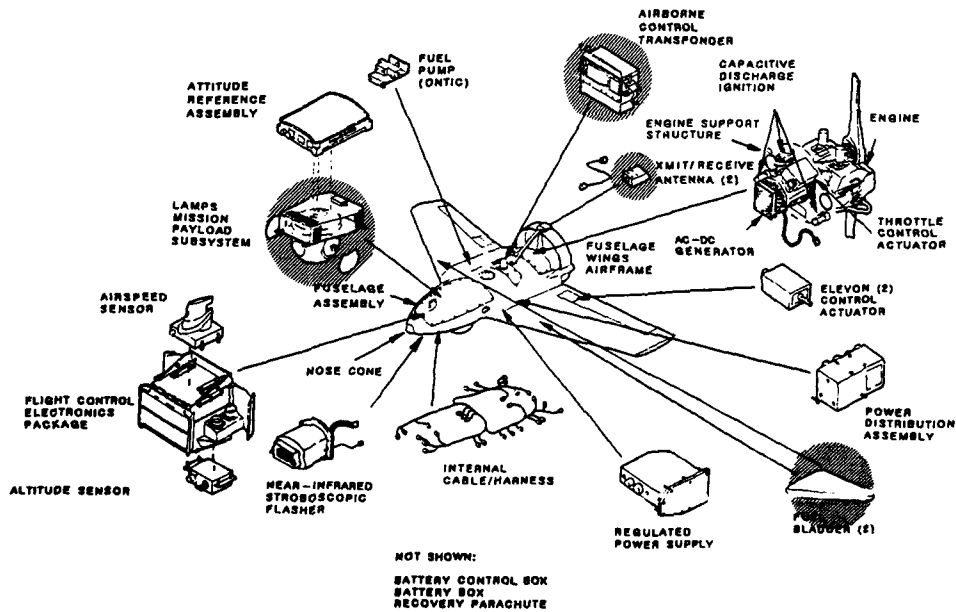


Figure 6: Altair Air Vehicle Subsystem

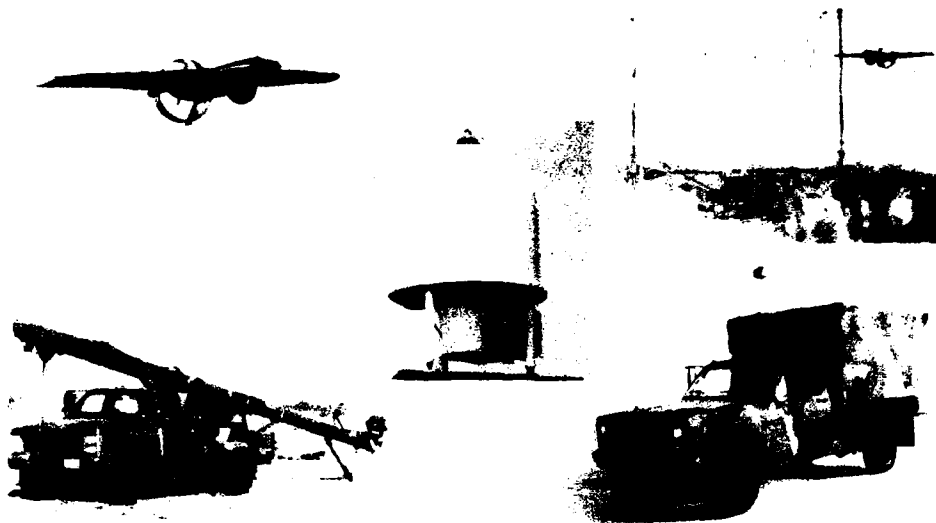
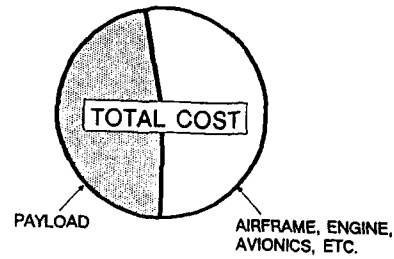
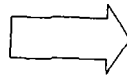


Figure 7: Lockheed Altair System

- INTERCHANGEABLE ON AIR VEHICLE
- PROVIDES FOR MULTIPLE SENSOR TYPES
- MINIMAL COST
- MODULAR AND FLEXIBLE
- GROWTH CAPABILITY

Figure 8: Lockheed UAV Payload Development Requirements

**PAYLOAD COST RANGES  
FROM 45% TO 48%  
OF TOTAL AQUILA COST**



**LAMPS GOAL IS TO  
ACHIEVE 11% TO 20%  
OF TOTAL ALTAIR COST**

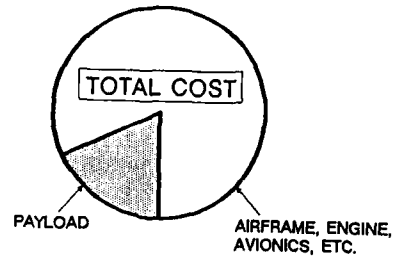
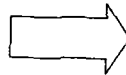


Figure 9: Payload is a Major UAV Cost Driver

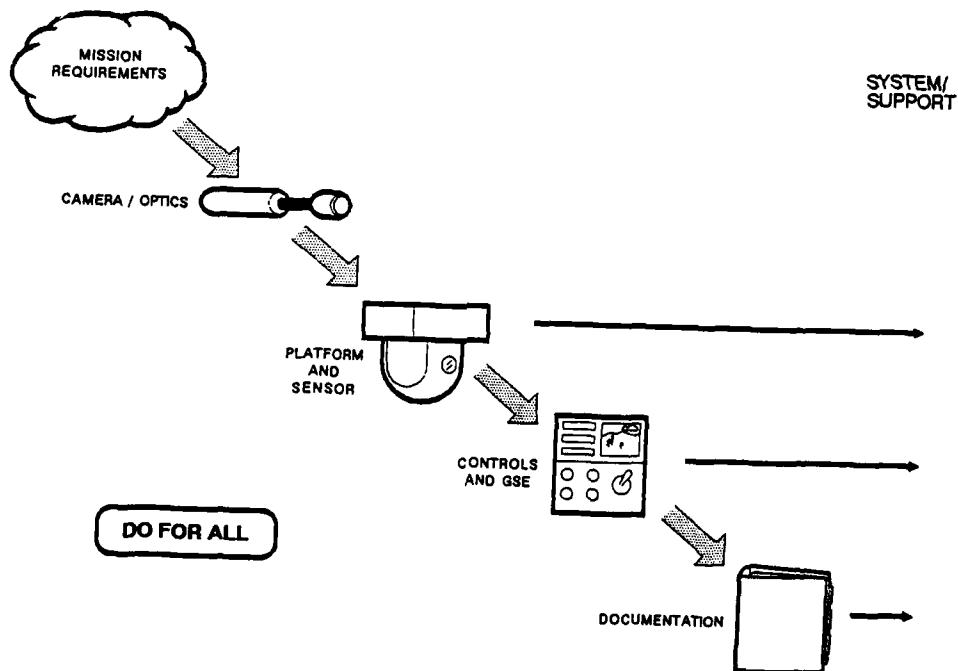


Figure 10: Typical Sensor System Development

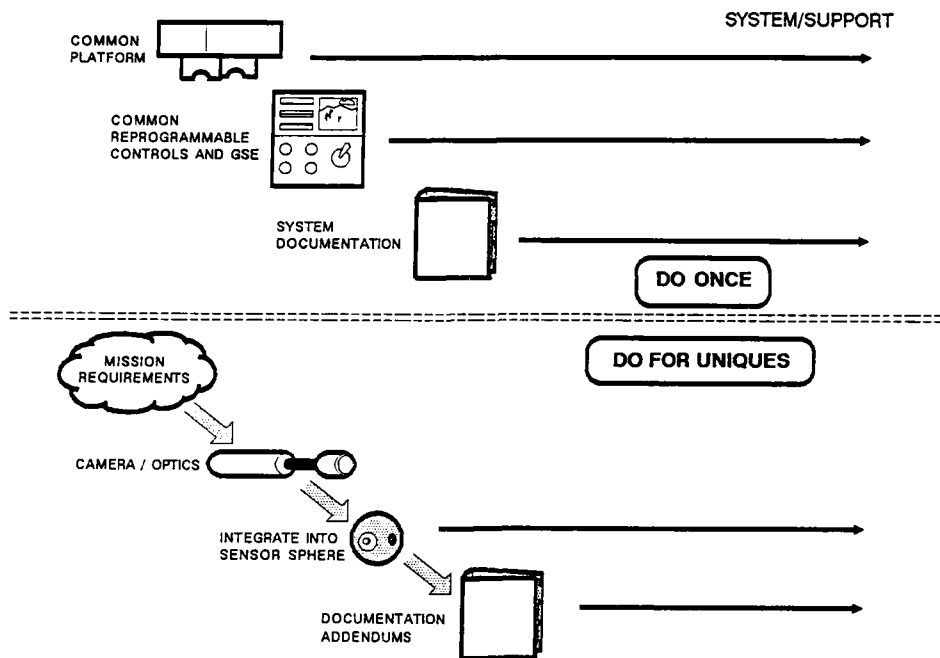


Figure 11: LAMPS Sensor System Development

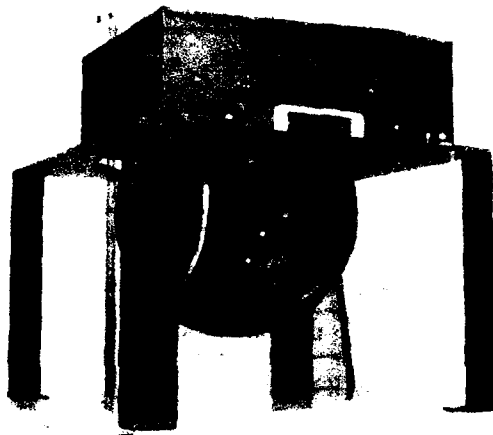
**STANDARDIZED/COMMON PLATFORM**

- SINGLE DEVELOPMENT/IMPLEMENTATION
- DESIGNED FOR GROWTH SENSORS
- MODULARITY/ADAPTABLE TO CHANGES
- COMMON SUPPORT REQUIREMENTS
- SUPPORTS EVOLUTIONARY CHANGES

**INTERCHANGEABLE SENSOR SPHERES**

- VARIETY OF SENSORS TO SUPPORT MULTIPLE MISSIONS
- EASY "IN/OUT" VERSATILITY/MAINTAINABILITY/SUPPORTABILITY
- ACCOMMODATES NEW SENSOR TECHNOLOGIES
- MINIMIZES IMPLEMENTATION COSTS

Figure 12: LAMPS Architecture



- ✓ PLATFORM
- ✓ SENSOR(S)
- ✓ CONTROL STATION
- ✓ TEST EQUIPMENT
- ✓ OPERATION/APPLICATIONS

Figure 13: Lockheed Adaptive Modular Payload (LAMP)

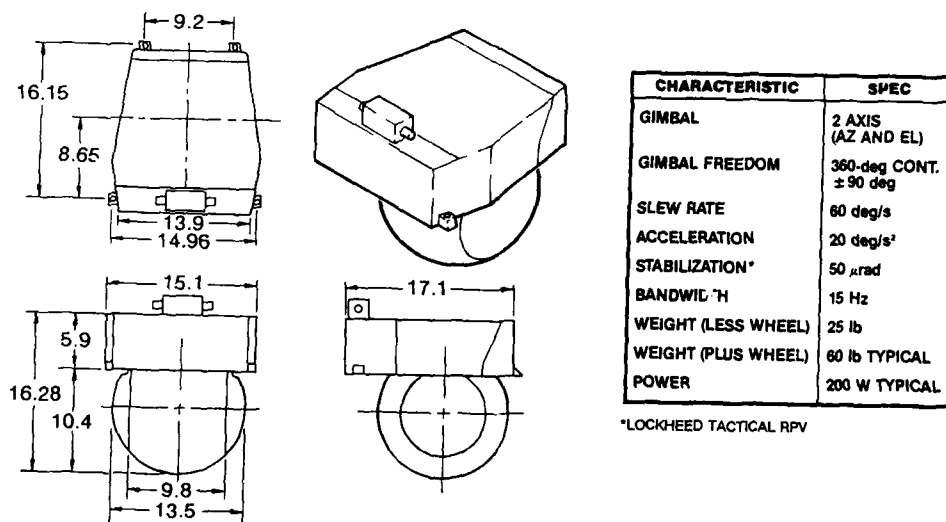
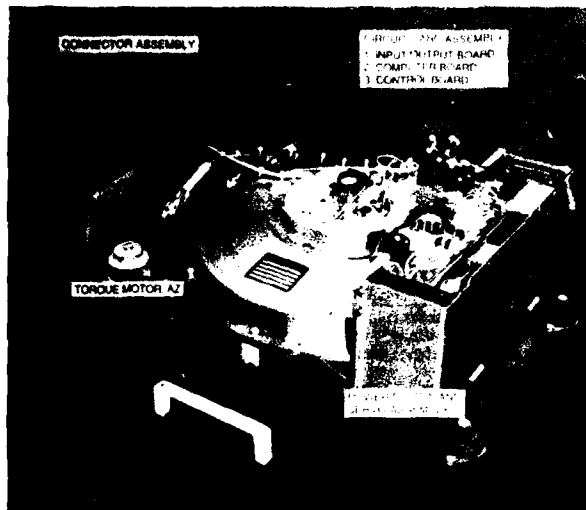


Figure 14: LAMP Platform Specifications



TOP TO BOTTOM:

- CPU BOARD
- CONTROL BOARD
- I/O BOARD
- INTERCONNECT BOARD

Figure 15: LAMPS Platform Assembly

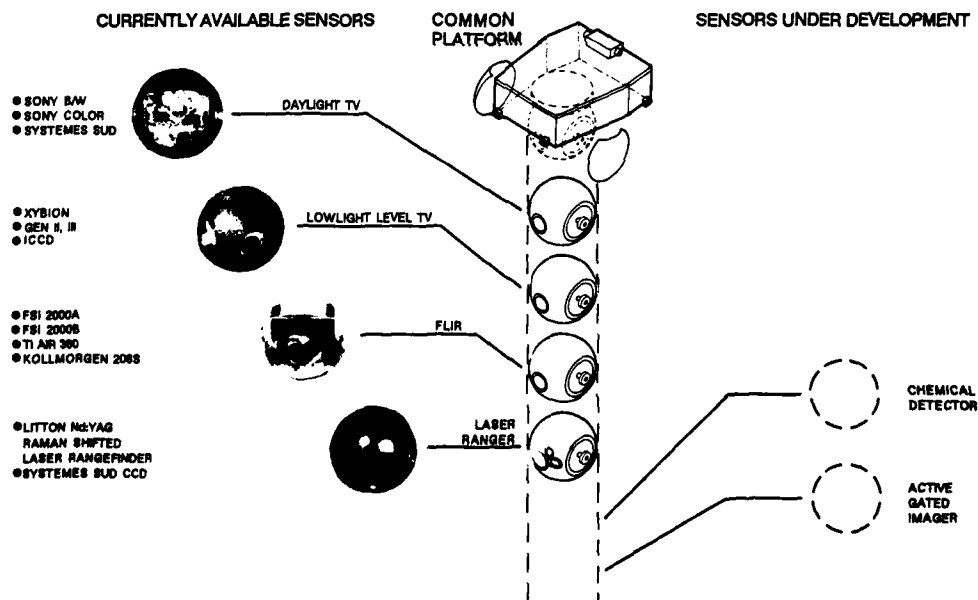


Figure 16: Lockheed Family of Sensors

TYPE NO.	SPHERE TYPE	MAJOR COMPONENTS	VENDOR	SENSOR CHARACTERISTICS	SPHERE CHARACTERISTICS	STATUS
SB-1	DAYTIME CCD (TV)	FE-22 CCD CAMERA  H10 x 11B-SND2C	SONY  FUJION	384 x 491 PIXELS, 525-LINE SCAN; 0.3 LUX (0.3 FT. CANDLES); F1.4 MIN ILLUM; 280(H) x 350(V) LINES RESOLUTION  10:1 ZOOM LENS, AUTO IRIS, MOTORIZED FOCUS AND ZOOM	TOTAL WEIGHT: 19.5 LBS TOTAL PWR REQ'D: 3 WATTS	AVAILABLE
SB-3	COLOR CCD	XC-117 COLOR CCD  H10 x 11B-SND2C	SONY  FUJION	570 x 492 PIXELS, 525-LINE SCAN; 30 LUX (3.0 FT. CANDLES); F1.4 MIN ILLUM; 320(H) x 350(V) LINES RESOLUTION  10:1 ZOOM LENS, AUTO IRIS, MOTORIZED FOCUS AND ZOOM	TOTAL WEIGHT: 19.5 LBS TOTAL PWR REQ'D: 3 WATTS	AVAILABLE
SB-4	HI RESOLUTION CCD	MICAM-HRS  H10 x 11B-SND2C	SYSTEMES SUD, INC.  FUJION	510 x 492 PIXELS, 525-LINE SCAN; 30 LUX (0.1 FT. CANDLES); F1.4 MIN ILLUM; 370(H) x 350(V) LINES RESOLUTION  10:1 ZOOM LENS W/1 = 1.5 LENS, AUTO IRIS, MOTORIZED FOCUS AND ZOOM	TOTAL WEIGHT: 19.5 LBS TOTAL PWR REQ'D: 3 WATTS	AVAILABLE

Figure 17: Daytime TV Sensors

TYPE NO.	SPHERE TYPE	MAJOR COMPONENTS	VENDOR	SENSOR CHARACTERISTICS	SPHERE CHARACTERISTICS	STATUS
SB-2	TI FLIR	AIR 360/3 FLIR	TEXAS INSTR.	8-12 MICROMETERS IR REGION. HgCdTe DETECTORS GaAsP LED FOR CCD PICKUP (VIDEO)  MIN TEMP DIFF = 0.2°C NET = 0.5°C FOV: 30° x 15°, 10° x 5°, 3.4° x 1.7°	TOTAL WEIGHT: 36.0 LBS TOTAL PWR REQ'D: 300 WATTS  CLOSED CYCLE COOLER	AVAILABLE
SB-6	FSI FLIR "A"	FSI 2000A	FLIR SYS.	8-12 MICROMETERS IR REGION. HgCdTe DETECTORS (2), SERIAL SCAN FOR VIDEO OUTPUT  MIN TEMP DIFF = 0.2°C NET = 0.15°C FOV = 28° x 15°, 7° x 3.3°	TOTAL WEIGHT: 40 LBS TOTAL PWR REQ'D: 320 WATTS OPEN CYCLE COOLER	PROTOTYPE
SB-7	FSI FLIR "B"	FSI 2000B	FLIR SYS.	SAME AS SB-6 EXCEPT: DETECTORS (2 x 4) NET = 0.1°C FOV = 28° x 15°, 5° x 2.4°	SAME AS SB-6 OPEN CYCLE COOLER	AVAILABLE
SB-8	ISG FLIR	206S MICRO-FLIR	KOLLMORGEN	8-12 MICROMETERS IR REGION, 8-BAR SPRITE DETECTOR ARRAY, SERIAL/ PARALLEL SCANNING, HgCdTe DETECTORS. 8X OR 10X TELESCOPES AVAILABLE. WITH 8X TELESCOPE: MIN TEMP DIFF = 0. °C NET = 0.19°C FOV = 4.7° DIAG/16.2° DIAG	TOTAL WEIGHT: 36.5 LBS TOTAL PWR REQ'D: CLOSED CYCLE COOLER	AVAILABLE

Figure 18: FLIR Sensors

TYPE NO.	SPHERE TYPE	MAJOR COMPONENTS	VENDOR	SENSOR CHARACTERISTICS	SPHERE CHARACTERISTICS	STATUS
SB-5	CCD/LASER RANGER	LASER  MICAM-HRS  H10 x 11B-SND2C	LITTON  SYSTEMS SUD, INC.  FUJI	ND:YAG RAMAN SHIFTED (1.54 MICROMETERS) MODES: SINGLE SHOT (CLASS 1 LASER); 5PPS (CLASS IIIA LASER); LASER BEAM: 3 MILLIRADIAN  SAME AS SB-4 ABOVE  SAME AS SB-4 ABOVE	TOTAL WEIGHT: 40 LBS TOTAL PWR REQ'D: 200 WATTS EYE-SAFE LASER WHEN INSTALLED IN UAV	AVAILABLE
X-1	PHOTO-RECON W/CCD	35MM CAMERA  FE-22 CCD CAMERA  H10 x 11B-SND2C	CANNON  SONY  FUJION	35MM REMOTE CONTROL SELF FOCUSING, AUTO WIND, 36 EXPOSURE FIXED FOV (SELECTED)  SAME AS SB-1  SAME AS SB-1	TOTAL WEIGHT: TOTAL POWER REQ'D:	PROTOTYPED

#### WITH OTHER SENSORS IN DEVELOPMENT

- CHEMICAL SENSOR
- ACTIVE GATED TV IMAGER
- MULTI-SPECTRAL SENSOR
- FLIR LASER RANGER

Figure 19: Other Sensors

- **LOCKHEED SERVES AS SENSOR INTEGRATOR**
  - FOCUSES ON MISSION REQUIREMENTS
  - ASSESSES INDUSTRY FOR CANDIDATES
  - SELECTS MOST APPROPRIATE VENDOR
  - PARTICIPATES IN INTEGRATION
  - PROVIDES TEST BED FOR TESTING
  - UNBIASED CHARACTERIZATION
  - SERVES AS PRIME FOR SUBSEQUENT SALES
  - OPERATOR CONTROL/PLATFORM MODS
  - MAINTAINS SYSTEM CONFIGURATION/DOCUMENTATION
  - CONDUCTS SYSTEM INTEGRATION, TEST, AND DEMONSTRATION
- **MAINTAINS SUPPORTING ELEMENTS**
  - ACTIVE UAVs AND SIMULATION/TEST CAPABILITIES
  - MONITORS STATE-OF-ART STATUS
  - MAINTAINS COMPUTATIONAL MODELS
  - CURRENT ASSESSMENT OF AVAILABILITY, COST, SCHEDULE REQUIREMENTS, AND CONSTRAINTS
  - COORDINATES WITH LOCKHEED R&D PROGRAMS
  - COORDINATES WITH OTHER LOCKHEED COMPANIES
  - ACTIVELY PURSUES OTHER LAMPS APPLICATIONS

Figure 20: Sensor Development

- NEED EXISTED FOR A VERY HIGH RESOLUTION FLIR SENSOR FOR TACTICAL TARGET DETECTION, RECOGNITION, AND IDENTIFICATION
- INDUSTRY-WIDE ASSESSMENT CONDUCTED FOR COMPARATIVE ASSESSMENT—INCLUDING COST AND SCHEDULE
- RATCHES (U.S. ARMY NIGHT VISION LAB FLIR MODEL) USED WITH CANDIDATE PARAMETERS INPUTTED
- OPERATIONAL D, R & I PREDICTIONS OBTAINED
- COMPETITIVE COST/SCHEDULE/RISK SELECTION PERFORMED
- CONTRACT AWARDED TO SUCCESSFUL CANDIDATE

Figure 21: Case Example—FLIR System Upgrade

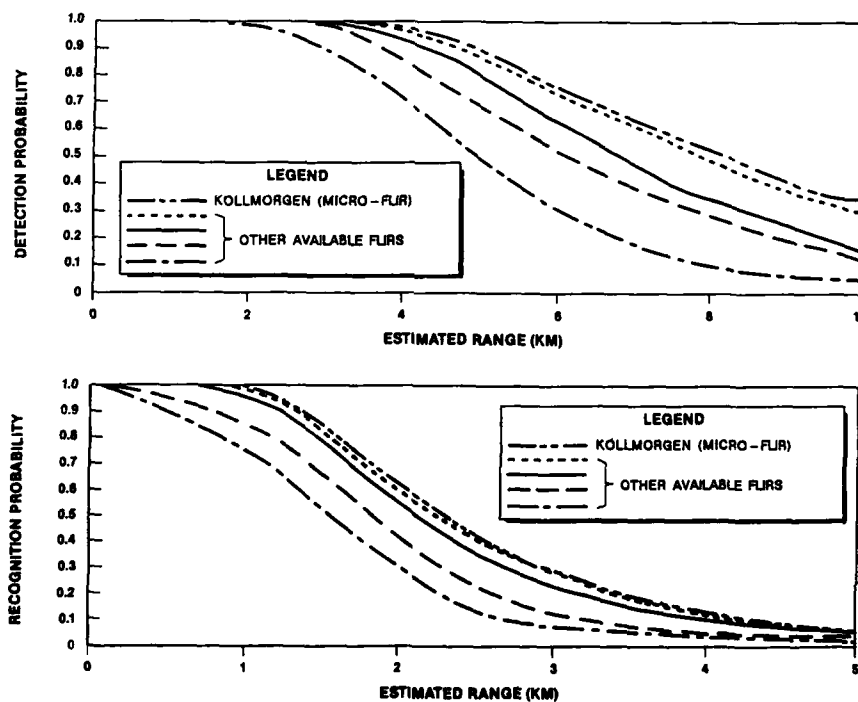


Figure 22: Ratches Assessment of FLIR Capabilities

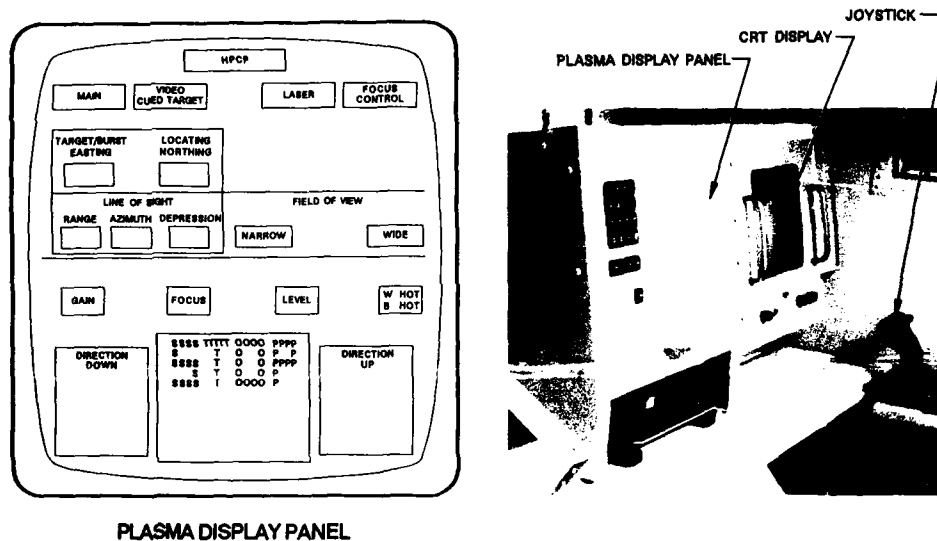


Figure 23: Payload Operator Control Station

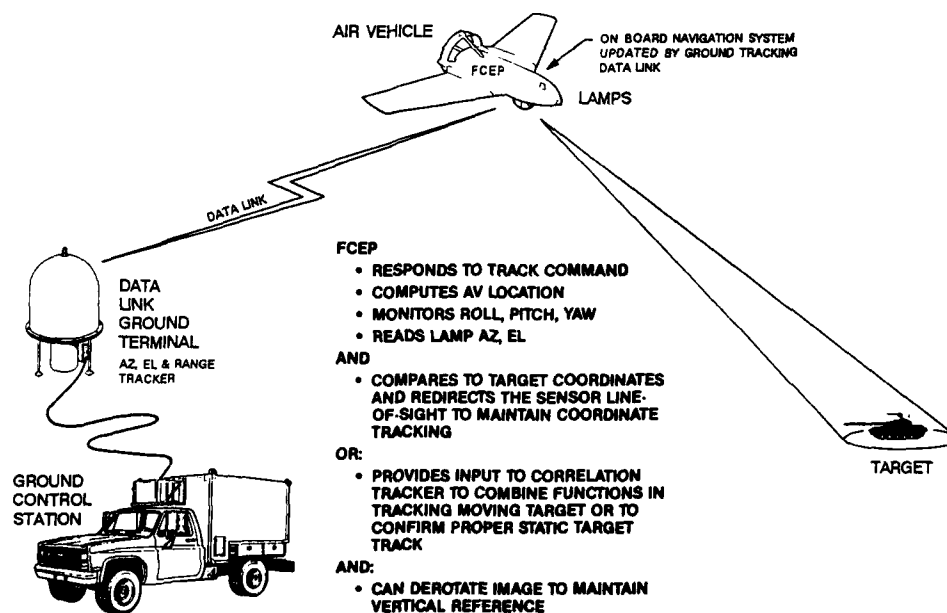


Figure 24: Operational Overview



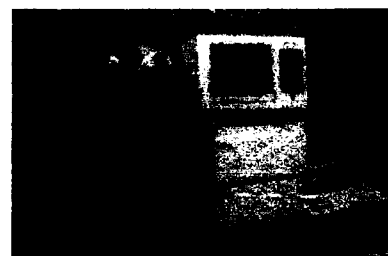
LOCKHEED TACTICAL RPV



MILITARY GROUND SURVEILLANCE



C-130 AIRBORNE RECONNAISSANCE



PASSIVE IR CHEMICAL SENSING

Figure 25: Some Current LAMPS Applications

## AUTOMATED SEARCH TECHNIQUES APPLIED TO OPTICAL PAYLOADS IN UNMANNED AIR VEHICLES

Robert L. Moody     James L. Thompson  
Associate Engineer, Sr.     Research Specialist  
Lockheed Missiles & Space Company, Inc.  
O/T7-40, B/312  
6800 Burleson Rd.  
Austin, Texas 78744-1016

*Summary.* The missions of the U. S. Army Aquila Remotely Piloted Vehicle (RPV) system include reconnaissance and target acquisition. To aid the operator in the accomplishment of these missions, Lockheed has developed automated target search software which ensures a thorough, systematic search of a designated area and reduces the operator workload while the search is being conducted. Various factors, internal and external to the unmanned air vehicle (UAV) system, are discussed which affect the probability of detecting a target of military interest. Search parameters have been implemented within the software to optimize the capabilities of the Aquila System to detect targets under varying environmental conditions. The automated search algorithm (autosearch) has been successfully demonstrated in flights conducted by the Army in a Force Development Test & Experimentation (FDT&E) conducted at Ft. Hood, Texas.

### Introduction

Lockheed has developed an unmanned air vehicle system for use in performing reconnaissance, surveillance, target acquisition, active and passive target location, target designation, and artillery forward observer roles--The U. S. Army Aquila Remotely Piloted Vehicle System. The Lockheed/Army Aquila has successfully demonstrated this multi-mission capability in 525+ free flights (940+ hours). The target acquisition function has been further enhanced by the addition of an automated search capability.

### Background

The Aquila system is a fully-militarized, tactical system incorporating rigid reliability and maintainability standards. The system consists of a miniature unmanned air vehicle (mini-UAV), ground control station (GCS), remote ground terminal (RGT), launcher subsystem (LS), recovery subsystem (RS), and support equipment. The mini-UAV contains an electro-optical mission payload subsystem (MPS) consisting of a daylight television sensor with a laser rangefinder/designator that is inertially stabilized in three axes.

The Aquila system is the final product of a full-scale engineering development program. The program required the air vehicle to be able to operate for 20 minutes in a dead-reckoning mode during which no navigation data are transmitted to the air vehicle. This requirement resulted in the incorporation of an on-board inertial guidance system. This on-board system, in combination with highly accurate data link location information and a stabilized mission payload subsystem, allows precise target location and payload pointing.

These capabilities permit the incorporation of software which automates the target search process and enhances the remotely piloted vehicle's target acquisition capabilities. This software significantly reduces operator workload and allows the operator to plan missions and search for targets in defined areas in a thorough, systematic manner.

### Target Acquisition

The target acquisition mission is fundamentally concerned with detecting, recognizing, identifying, and locating targets of military significance in sufficient detail to permit the effective employment of a weapon system. The problem of searching for targets with an electro-optical imaging system is often complicated by the fact that targets are presented in less than ideal conditions against confusing and often unfamiliar backgrounds. Mission success depends on the high probability of accomplishing four separate tasks: (1) bringing the target into the imaging system's field-of-view (FOV), (2) detecting a target when it is in the field-of-view, (3) recognizing and identifying the target after detecting it, and (4) locating the target with sufficient accuracy to employ munitions against it. All four of these tasks must be accomplished before a target can be engaged.

The primary purposes of autosearch are to increase the probability of accomplishing Task 1 by ensuring that the target enters the field-of-view and accomplishing Task 2 by optimizing the manner in which the target is presented at the operator's console. Task 2 is also dependent upon overall system resolution. The probability of accomplishing Task 3 is dependent

on system resolution as well as operator experience, training, and skill level. Accomplishment of Task 4 depends upon the targeting accuracy of the entire system.

By performing a thorough, methodical search, autosearch increases the probability that the target will enter the field-of-view (Task 1). Three types of automated search routines have been developed to satisfy differing search requirements. The most general of these is the area search, which is designed to search an area one kilometer square or larger. The second type of search is the point search, which is designed to initiate a search at a predetermined grid coordinate and then spiral outward. The third type of search is the linear search, which is designed to cover a line-of-communication (LOC) or other long, narrow target area.

By controlling the presentation conditions at the operator's console, autosearch increases the probability the target will be detected once it enters the field-of-view (Task 2). These conditions include target contrast, displayed image size, and operator display stare time. The autosearch algorithm governs these conditions by controlling air vehicle position, sensor field-of-view, sensor pointing, and sensor step rate.

### Search Methods

The operator can select from three different types of searches depending on the specific objectives of the mission. The different search types may be intermixed on a single mission, and searches may be conducted in any order, regardless of the order of input during mission planning. For all three search types, the mission planner needs only to define the individual search areas by entering the required number of Universal Transverse Mercator (UTM) grid coordinates into the ground control station computer. With this information provided, the autosearch software generates the necessary payload pointing commands and air vehicle loiter waypoints, subdivides the target area into sectors as necessary, generates cued targets corresponding to each search sector, and draws the area on the hardcopy map mounted in the ground control station navigation display unit (NDU). Once the air vehicle is airborne, the operator needs only to insert the appropriate cued target number for the desired search sector, enter the number of the desired loiter position, and depress the autosearch button to initiate the search.

#### Area Search

The area search is the most general type of search and is based upon an  $m \times n$  kilometer, rectangular search area. The rectangle does not have to be aligned with the northing/easting UTM map grid, but rather is aligned by the mission planner to cover the intended search area best. Once the area is defined by the mission planner, the intended search area is input to the ground control station computer by entering three consecutive corner points of the rectangle in clockwise order. The autosearch software then subdivides the area into one kilometer square sectors and defines the air vehicle loiter waypoints. One of these waypoints is directly over the payload footprint, while the other four are offset and spaced at 90° intervals around the footprint. The search order of these sectors and the orientation of the four offset loiter waypoints are determined by the order of entry of the corner points. A computer simulation of a typical area search is illustrated in Figure 1.

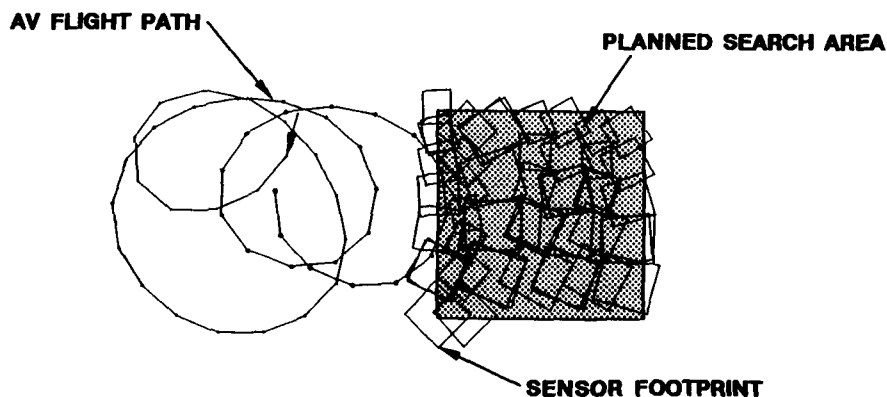


Figure 1: Area Search

#### Point Search

The point search is most effective when mission planners have premission battlefield intelligence regarding a suspected target location. A single grid coordinate is entered in the ground control station computer to define the search center. The point search is initiated at the most probable target position and then progresses in a clockwise spiral outward from the defined center point. Once the maximum radius of 500 meters is reached, the search ceases. Loiter waypoints are defined

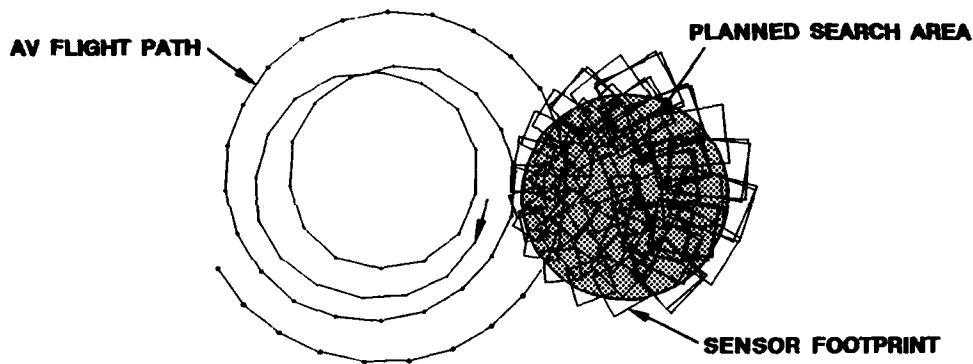


Figure 2: Point Search

north, east, south, west, and directly over the sensor footprint. A computer simulation of a typical point search is illustrated in Figure 2.

#### Linear Search

The linear search is most effective when used to search well-defined terrain features such as highways, rivers, narrow avenues of approach, and tree lines. The search area is 300 meters wide  $\times$   $n$  kilometers in length. A minimum of two grid coordinates must be input to the ground control station computer to define the area, but as many coordinates as are required to completely define the linear strip may be input by the mission planner (e.g., more than two will be required for winding roads). The five loiter waypoint positions are defined by the order of entry of the grid coordinates defining the linear strip and are oriented in a manner similar to an area search. A computer simulation of a typical linear search is illustrated in Figure 3.

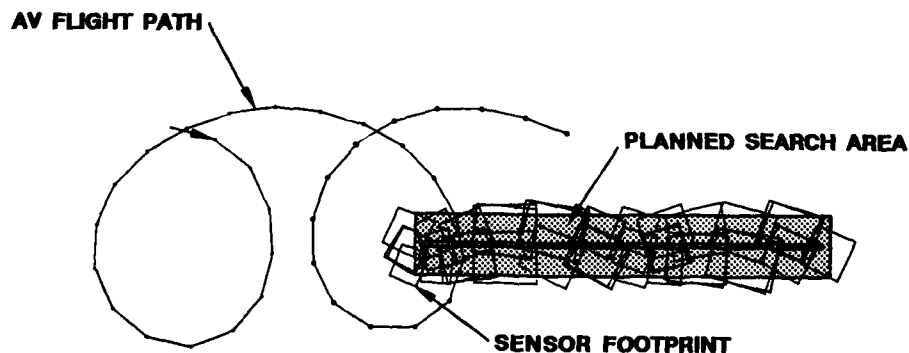


Figure 3: Linear Search

#### Presentation Conditions

For a UAV system using an imaging sensor payload, there are a number of important items to be considered when searching for targets of military significance. Among these are the overall system resolution, target size at the display, operator display stare time, and target contrast/environmental conditions. The autosearch software does not affect system resolution. Rather, the algorithm takes air vehicle altitude and attitude, desired search aspect, and target area environmental conditions as inputs and automatically adjusts:

- sensor field-of-view and air vehicle slant range to the target area—for a given system, these parameters control the target size at the display and
- sensor dwell time—this corresponds directly to operator display stare time.

Additionally, the operator is free to select the air vehicle loiter position and altitude these give the operator some flexibility to adapt the search to different target environments.

#### Displayed Image Size

Sensor field-of-view, determined as a function of air vehicle altitude above ground level, and slant range to the target area are set to maintain a specified number of television lines of resolution on the target area.

The Johnson Criteria (Reference [1]), summarized in Table 1, establish the minimum number of television lines on a target required for target detection, orientation, recognition, and identification. These criteria hold that two television (TV) lines of resolution across a target's minimum dimension are required for a 50 percent probability of detection ( $P_d$ ). These criteria determine a system's maximum theoretical slant range for detection, orientation, recognition, and identification. Since the Johnson Criteria are for low scene congestion situations, actual detection ranges in a cluttered environment will generally be less than those predicted by the model. Bates (Reference [2]) suggests that four lines (two line pairs) are more appropriate for detection in a cluttered environment. To control the displayed image size and the television lines of resolution on the target for a given probability of detection, the sensor field-of-view and slant range from the air vehicle to the target must be controlled during autosearch.

Task	TV Line Pairs
Detection	$1.0 \pm 0.25$
Orientation	$1.4 \pm 0.35$
Recognition	$4.0 \pm 0.80$
Identification	$6.4 \pm 1.50$

Table 1: Spatial Frequencies Required for 50 Percent Probability of Success.

#### Operator Display Search Time

Simon (Reference [3]) has determined that the minimum time to search through one frame of video is related to the eye's circular field of clear vision and the angular size of the video display. With the current Aquila display screen size and observer position, this time is 4.6 seconds as determined by Bates (Reference [2]). This is the minimum theoretical time to completely scan a scene presented on a video monitor of this size.

To compound the problem, a congested (or cluttered) scene places an additional time burden on the operator because it is difficult to distinguish targets in complicated contrast and scene congestion situations. Additionally, the area presented on the screen changes because the air vehicle position relative to the sensor footprint changes. To compensate for these factors, the operator display search time can be varied using a model to select stare time based on scene conditions. The variables which control this time are functionally related to probability of detection by the following functional relationship:

$$P_d = \mathcal{F}(a, A, t, G)$$

Where,

- $a$   $\equiv$  Area of target projected on a plane perpendicular to the sensor line of sight
- $A$   $\equiv$  Ground area to search in a frame of video
- $t$   $\equiv$  Time to search one frame of video
- $G$   $\equiv$  Scene congestion factor
- $P_d$   $\equiv$  Probability of detection

A conservative estimate of target size (e.g., a head-on view of a tank-sized target from a nominal air vehicle search altitude and slant range) can be made. Holding this estimated target area constant and requiring a probability of detection of 0.5 leaves:

$$t = \mathcal{F}(A, G)$$

The time required to search one frame of video is, therefore, related to the ground area and the actual scene congestion. This time is the sensor dwell time. Based on real-time assessment of the target environment, the operator can select low, medium, or high clutter search modes. Dwell time is successively increased for a constant viewing area when the clutter mode is adjusted to a higher level. Conversely, for any one clutter mode, the actual dwell time is varied as a direct function of sensor viewing area between the minimum and maximum viewing times.

During autosearch, the dwell time for a selected clutter level varies dynamically, based on this calculated viewing area. This area is calculated from the projection of the sensor field-of-view onto the ground and is referred to as the sensor footprint. Within the autosearch algorithm, this function is implemented along three curves for high, medium, and low clutter conditions.

Since autosearch is conducted from a dynamic, maneuvering platform, footprint sizes vary between frames. The time to search a frame of video is, however, never shorter than the minimum theoretical scan time of 4.6 seconds plus an additional 2.0 seconds allotted for sensor stabilization. This stabilization time allows the sensor sufficient time to traverse the distance between two consecutive scenes. Additionally, the dwell time is limited at a reasonable upper end to account for operator attention span. This precludes the operator from spending excessive time searching for targets when there is a low probability of finding them.

Sensor footprints are also irregular in shape and cannot be laid exactly side by side for a perfect fixed overlap. In addition, to ensure complete coverage of an area, overlap between rows of footprints is based upon the smallest footprint in a row, not upon a standard size or an average size. The software must account for these deviations if 100 percent coverage is to be obtained. These factors, in addition to the two-second stabilization time already added to each dwell time, produce search times generally longer than theoretical predictions.

#### **Target Environment**

Target contrast is a function only of the target and its environment. These parameters cannot be controlled directly by the system. However, since target illumination (available sunlight) and target reflectivity are important contributors to contrast, the viewing aspect angle is important in the overall detection process. By controlling the air vehicle loiter position and altitude, the operator controls the viewing aspect angle and relative sun angle and, thus, does have some indirect control over the target environment.

As previously noted, scene congestion or clutter complicates the detection process. A clutter object is defined as any object of about the same size as a target that must be momentarily examined to determine whether or not it is actually a target. For a reasonable amount of scene congestion, the Johnson Criteria for detection resolution are low, and theoretical display search times are too short. As a result, the slant range to the target must be reduced from the theoretical maximum to increase the number of television scan lines on target, and the display search time must be lengthened, based on the operator's educated assessment of the congestion conditions.

#### **Operator Indications**

To facilitate the search of a geographic area, several enhancements were made to the basic automated search software to ease operator workload. These include on-screen graphics to indicate relative range information and percent-of-search completed information. In addition to the on-screen graphics, the operator has other bookkeeping aids which automatically keep track of search completion times and areas which have been searched and which automatically position the air vehicle for the next sequential area to be searched when the current area is completed.

#### **Automatic Bookkeeping**

The autosearch software provides the operator with an automated bookkeeping capability. A percent-to-go bar provides a continuous on-screen indication of the percentage of the current search segment or sector remaining to be searched. When a sector is completed, the teletype (TTY) prints out a completion message and the navigation display unit crosses out the completed sector. The operator knows at any time during the mission exactly which sectors have been searched and what percent of the current sector remains to be searched. On completion of a sector, the software automatically steps to the next sector in sequence and awaits the operator's command to begin searching the new sector. The operator has the option of overriding this automatic stepping function and manually selecting the next sector to be searched.

#### **On-Screen Range Indication**

The operator has an on-screen in-range indication to cue him when a pending autosearch area (or point or linear) search is within the theoretical range required to achieve detection of a tank-sized target. While the system is still in the manual search mode, the percent-to-go bar will appear when the air vehicle comes within range of the pending search area. Once the bar appears, the operator only needs to depress an autosearch button on the mission payload operator's console to begin the autosearch. Additionally, when the operator is conducting a manual search, a detection window is presented on the video screen. The video presentation within the window provides a theoretical probability of detection of 0.5 or greater based on sensor field-of-view and slant range.

#### **Automatic Guidance**

##### **Guidance and Control**

Sensor footprint placement on the ground and air vehicle loiter positioning are closely linked through the movable waypoint guidance system. This system maintains a relatively constant slant range to the target which is necessary for the required probability of detection.

When conducting an area search, the sensor footprint is automatically stepped back and forth across the area beginning at the edge closest to the air vehicle. Meanwhile, the air vehicle flies in a circular loiter pattern whose center follows the advancement of the sensor footprints toward the opposite edge. The point search is implemented by positioning the air vehicle in a circular loiter whose center maintains the same position relative to each successive sensor footprint. The sensor footprints spiral outward from a central grid coordinate until the search concludes. The linear search is similar to the area

search in that the sensor footprint steps back and forth across the width of the defined line of communication as the center of the air vehicle loiter moves along the line. Percentage of footprint overlap for all three search types is maintained in real time based on the computed footprint size.

Often, the clutter mode and sensor footprint size allow for high rates of advancement across the search area. This may result in excessive slant range to the target and air vehicle positioning being outpaced by sensor footprint advancement. To correct this situation, the search is momentarily suspended at the current footprint position until the air vehicle is again within range to continue the search.

#### **Selectable Search Waypoints**

The operator is given the capability to conduct an automatic search from any one of five selectable loiter waypoints. Once established in the search, the operator can also change the selected waypoint without interrupting the search. As a result, the operator can adjust for existing terrain features, sun position, vegetation patterns, threat location, etc. By being able to adjust the search pattern in this manner, the operator is also able to optimize the search for existing target contrast levels.

#### **Movable Waypoint Guidance**

The commanded center of the air vehicle loiter circle is always in the same position relative to the sensor footprint. There may be some lag in the actual air vehicle loiter position, however, since the sensor step rate is generally faster than the air vehicle guidance update rate. The guidance algorithms compensate for this and ensure that the number of television lines on the target and the target size at the display remain relatively constant during a search. By maintaining the proper relationship between slant range and air vehicle altitude, the guidance algorithms ensure correct sensor depression angles throughout the search. Additionally, since the operators do not have to continually update the air vehicle loiter position during the search or manually point the payload during the search, they are able to concentrate attention on the search process rather than on the mechanics of the search (i.e., flying the air vehicle and operating the payload).

#### **Maximum Search Range Lockout Provision**

The air vehicle suspends the search at the current footprint when the slant range from the air vehicle to the sensor footprint exceeds a predetermined maximum value. This provision prevents the sensor from stepping through any portion of the area with television lines on target and target size at the display below recommended values for the desired probability of detection. This also ensures that sensor depression angles do not decrease below a minimum value for any portion of the search area. When the slant range again decreases below the lockout range, the search will resume automatically.

### **Operational Control**

#### **Selectable Dwell Times**

The operator can select the relative dwell time based on a real-time estimate of scene congestion (clutter). However, since the slant range from the air vehicle to the sensor footprint (and consequently the footprint size) is constantly changing, the dwell time must also change to accommodate this variation in the size of the sensor footprint so that dwell time per unit area remains constant. The change in dwell time with respect to area is then the dwell time slope.

Theoretically, the dwell time lower limit would be a minimum time for the operator to scan a frame of video the size of the video screen in the ground control station. However, clutter level in the observed scene acts much the same as noise and increases the operator's scan time. The dwell time lower limits were increased for medium and high clutter modes to incorporate the effects of clutter level. As a result, below a predetermined footprint size, the dwell time per unit area increases as the footprint size decreases and the total search time increases.

As a result of testing and operator feedback at Ft. Sill during Force Development Test and Experimentation (FDT&E) training, a two-second sensor stabilization time was added to all dwell times. This added time ensures the operator has sufficient time to scan a scene after the sensor has come to rest in a new position. Its addition to all dwell times is another contributing factor which causes actual search times to be higher than theoretical predictions.

#### **Automatic Return**

At any time during any type of autosearch, the operator can suspend the search, change sensor field-of-view, and manually examine an area of interest. The air vehicle can even be diverted to a higher priority mission elsewhere. Once the diversion is completed, the suspended search can be resumed at the point it was suspended as long as another cued target has not been entered at the mission commander's console in the interim.

## Additional Benefits

### Simplified Mission Planning

The operator is required only to enter three points to define an area search, one point for a point search, and enough points to approximate a road or other line of communication (LOC) for a linear search. Once this is done, the autosearch software divides the area into standard sectors, generates the necessary cued targets, establishes the search waypoints, and plots the individual search sectors on the map mounted in the navigation display unit.

### Simplified Mission Operations

During a mission, the mission commander (MC) has only to enter the cued target associated with a particular area search sector (or point or linear search segment). The air vehicle operator (AVO) then enters the selected autosearch waypoint. When the air vehicle is within range, a graphic cue is presented to the operator on the screen. This operator indication is a part of the automatic bookkeeping function discussed above. At this time, the mission payload operator (MPO) initiates autosearch by pressing either one of the two autosearch buttons. The remainder of the process is automatic until search of the sector is completed. The autosearch automatic guidance maintains the proper air vehicle position relative to the sensor footprint position, and the sensor is stepped automatically through the selected pattern until search of the sector is completed.

## Results

This automated search capability has been demonstrated in actual flight testing during FDT&E training conducted by the Army at Ft. Sill, Oklahoma and in FDT&E record flights conducted by the Army at Ft. Hood, Texas. Target detection rates for both moving and stationary targets averaged over the 60 training flights at Ft. Sill, and 17 record flights at Ft. Hood showed a significant improvement in detection rates over previous trials conducted without the enhanced autosearch capability. In fact, all detection, recognition, identification, and location requirements were surpassed by a significant margin (Table 2).

	INDIVIDUAL		ARRAYS	
	REQUIRED	ACHIEVED	REQUIRED	ACHIEVED
STATIONARY		39%		12%
Open Light Cover		89%	30%	91%
MOVING		99%	50%	98%

Means no Requirement

Table 2: FDT&E Results

The soldier's workload has been reduced significantly, both during mission planning and inflight. Additionally, because of the improved search geometry, the passive target location algorithms converge rapidly and, as a result, stabilized payloads without a laser rangefinder capability can be used for precision target location with a minimum impact on mission time.

These results demonstrate an improved target acquisition capability that augments the multimission role of the Aquila unmanned air vehicle. Coupling this improved target acquisition capability with Aquila's laser designation and fire direction capabilities demonstrated during Developmental and Operational Testing results in an extremely effective battlefield asset that is available now.

## References

1. Johnson, J., *Analysis of Image Forming Systems*, Image Intensifier Symposium, Fort Belvoir, Va., October 1958.
2. Bates, H., *Recommended Aquila Target Search Techniques*, Advanced Sensors Directorate, Research, Development, and Engineering Center, Redstone Arsenal, AL, July, 1987.
3. Simon, C., *Rapid Acquisition of Radar Targets from Moving and Static Displays*, Human Factors, Vol 7, June, 1965.

## An Intelligence-driven RPV Mission Planner

Authors: Dr. Klaus Dannenberg, President, Merit Technology  
Mel Barney, Vice President, Merit Technology  
Chuck Kirklen, Program Manager, Merit Technology

### ABSTRACT

The time required to plan RPV missions can be greatly reduced by the application of technology currently available. Additionally, the effectiveness of these missions can be increased significantly. The application of expert system based processing of near real time intelligence, route planning techniques, and high resolution graphics to the RPV mission planning process can result in an integrated planning aid that accomplishes both a savings in planning time and an increase in mission effectiveness.

Expertise in RPV mission planning is acquired by the repetitive performance of planning and observing actual RPV missions. This expertise is primarily centered in those military personnel responsible for defining and directing the development of RPV systems. The requirements for these systems are driven by mission requirements, and are often heavily derived from the tools available. The new tools suggested in this paper will have a significant impact on the planning process. The development of a system such as the one suggested in this paper will require participation by these experts.

The most time consuming part of an RPV mission planning exercise is the collection and assimilation of relevant intelligence data. These data include enemy threat tactical, communication, and situation data, as well as friendly tactical, communication, and situation data. A system that collects and filters these data was demonstrated in a JCS exercise in Europe in April of 1987. The heart of this system, the Intelligence-driven Mission Planning Station (IMPS), successfully provided relevant intelligence data for the Wild Weasel defense suppression mission.

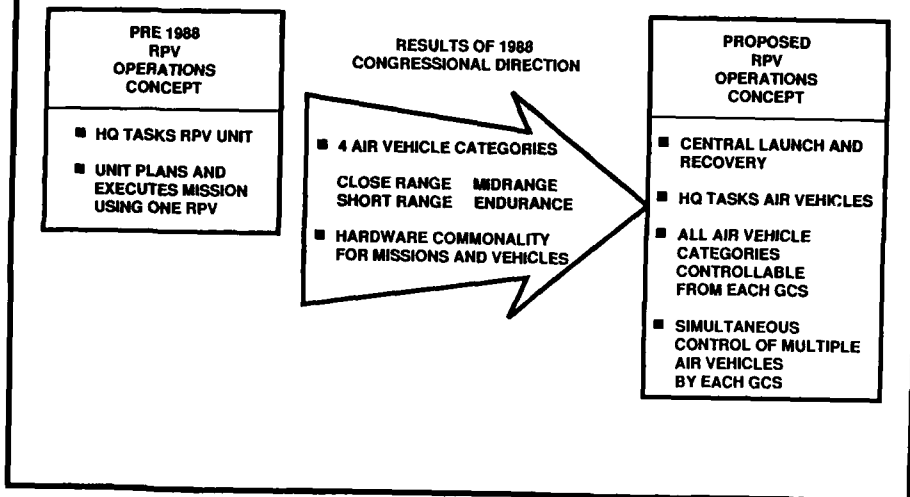
The combination of onboard sensors and stored terrain data bases have made possible the development of algorithms that select optimum routings for air-to-ground penetration missions. Merit Technology has provided more than a dozen other customers with guidance algorithms to accomplish this task. Optimal route generation can first be exercised in the ground based mission planner, and the resulting data can be used to provide onboard mission replanning.

The graphics required to plan an effective RPV mission quickly include plan view, God's-eye view, perspective view, and analytical statistical graphs. All these capabilities have been successfully developed, demonstrated, and delivered in the form of Merit Technology's Battle Area Tactical Simulation (BATS) software package.

This paper outlines how these elements may be combined in an RPV Mission Planner today.

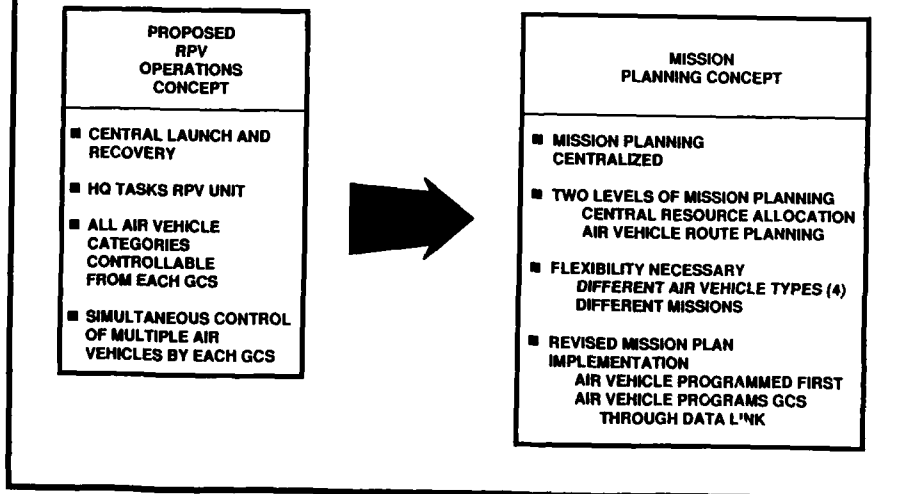
MERIT

## JOINT SERVICE RPV PROGRAM CONSOLIDATION WILL IMPACT RPV OPERATIONS



MERIT

## CENTRALIZED RPV OPERATIONS IMPACT MISSION PLANNING FUNCTIONS



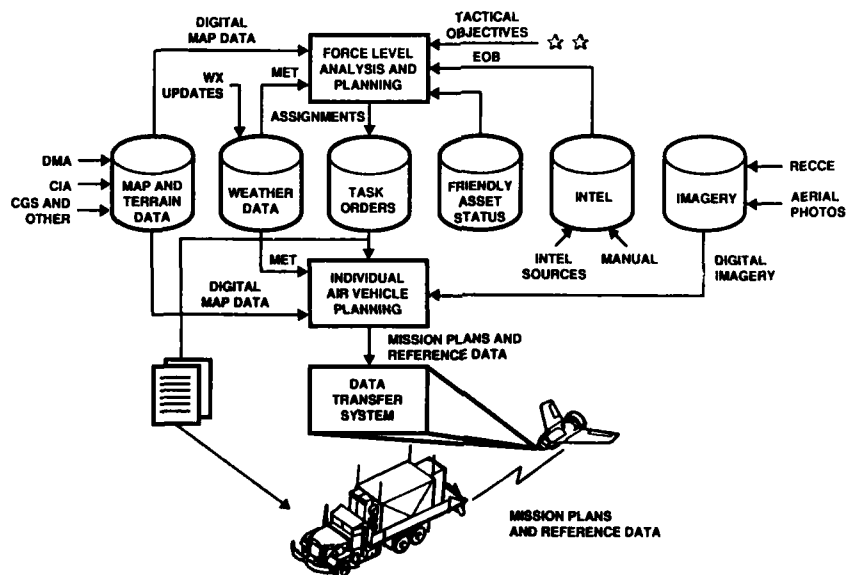
MERIT

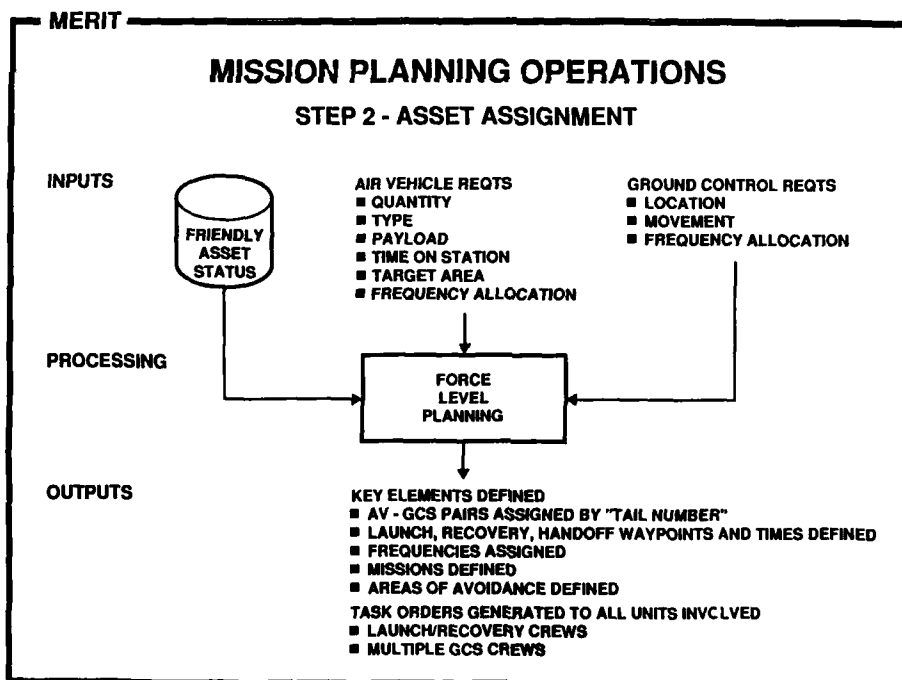
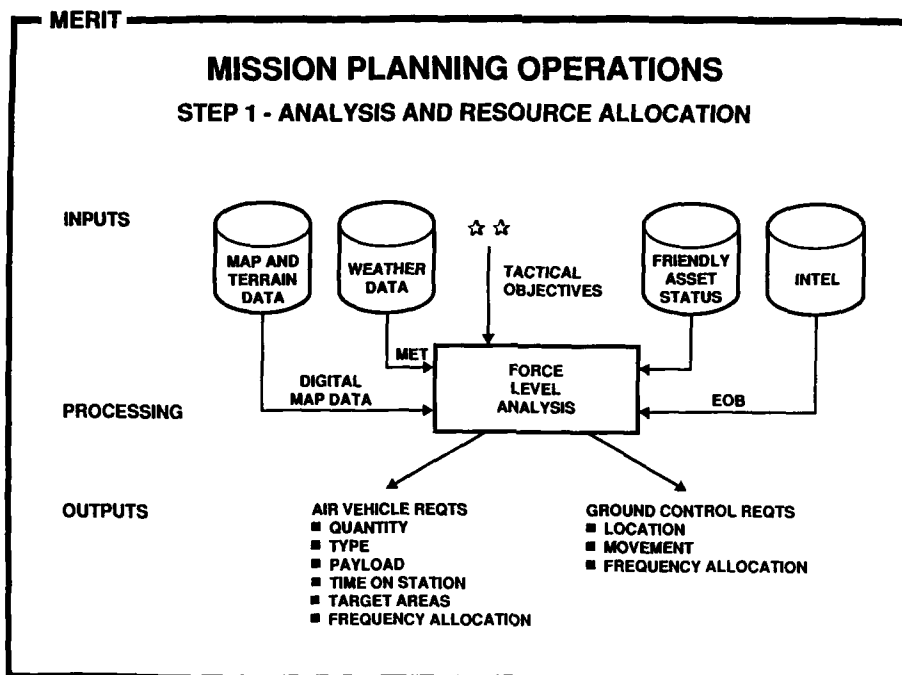
## MISSION PLANNING OPERATIONS OVERVIEW

STEP	LOCATION	CLASSIFICATION REQUIREMENT
1. ANALYSIS AND RESOURCE ALLOCATION	HQ	YES
2. ASSET ASSIGNMENT	HQ	YES
3. INDIVIDUAL AIR VEHICLE ROUTE PLANNING	HQ	NO
4. TRANSFER MISSION PLANS TO AIR/GROUND ELEMENTS	<ul style="list-style-type: none"> <li>■ AT LAUNCH SITE TO AV</li> <li>■ PRE FLIGHT/INFLIGHT TRANSFER FROM AV TO GCS</li> </ul>	NO

MERIT

## PROPOSED PLANNING SYSTEM ARCHITECTURE



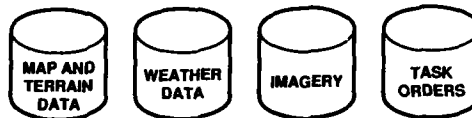


MERIT

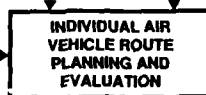
### MISSION PLANNING OPERATIONS

#### STEP 3 - INDIVIDUAL AIR VEHICLE ROUTE PLANNING

INPUTS



PROCESSING



OUTPUTS



DIGITAL TRANSFER MODULE CONTAINING

- WAYPOINTS - LAUNCH, RECOVERY, HANDOFF, FLIGHT
- CRITICAL IMAGERY INFORMATION
- EMERGENCY INSTRUCTIONS

MERIT

### MISSION PLANNING FUNCTIONS

- REVIEW AND ASSESS MISSION OBJECTIVE
  - TARGETS/WEAPONS
  - TIMING
  - PRIORITIES
  - CONTINGENCIES
- ASSESS THREAT
  - LOCATIONS (UNCERTAINTIES)
  - COVERAGE/CAPABILITIES
  - LETHALITY
- PLAN ROUTE
  - FRIENDLY REGION/INGRESS/WEAPON DELIVERY
  - TIMING, FUEL, ALTITUDES, VELOCITIES, G'S
  - NAVIGATION PLAN, CONTINGENCIES
- PLAN OFFENSIVE ACTIONS
  - REQUIRED TARGET ACQUISITION/SENSOR CONTROL
  - ACQUISITION AND SEARCH MANEUVERS
- DEFENSIVE PLAN
  - SIGNATURE/SENSOR CONTROL
  - THREAT AVOIDANCE PLANS (KNOWN AND POP - UP THREAT)
  - THREAT ASSESSMENT PLAN
  - THREAT REACTION AND ECM PLAN
- DATALINK COORDINATION PLAN
  - MAINTAIN LINE OF SIGHT
  - FREQUENCY UTILIZATION
  - REQUIRED DOWNLINK INFORMATION
  - LOST LINK CONTINGENCIES
  - ANTIJAM CAPABILITY UTILIZATION

## MERIT

## EVALUATION ALGORITHMS

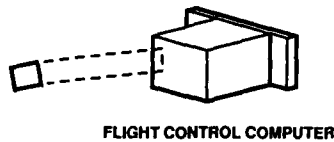
- NAVIGATION/ROUTE
  - CAPABILITY OF COMBINED NAV SENSORS
  - VELOCITY/TIMING EVALUATION
  - FUEL BURN EVALUATION
- SURVIVABILITY
  - THREAT EXPOSURE
  - EFFECTS OF THREAT ASSESSMENT, SIGNATURE CONTROL, ECM
  - THREAT ENCOUNTERS AND PROBABILITY OF SURVIVAL
  - EFFECTS OF LATERAL AND VERTICAL FLIGHT PATH MANEUVERS
- SENSOR UTILIZATION
  - PROBABILITY OF SUCCESSFUL SENSOR UTILIZATION CONSIDERING POSITION
  - TERRAIN, WEATHER, OBJECTIVE, TIME LINKS, SENSOR CAPABILITY
  - PREDICT WHAT SENSOR WILL SEE UNDER PLANNED CIRCUMSTANCES
- DATA LINK UTILIZATION
  - PROBABILITY OF ENEMY EXPLOITATION
  - PROBABILITY OF SUCCESSFUL COMMUNICATION CONSIDERING COM SYSTEM USED, LOCATIONS, TERRAIN, ENEMY EXPLOITATION CAPABILITIES
  - LINE OF SIGHT MAINTENANCE

## MERIT

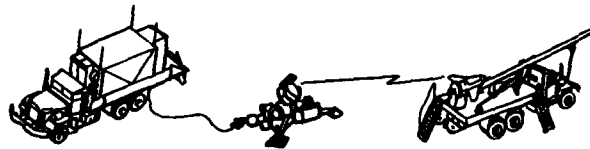
## MISSION PLANNING OPERATIONS

## STEP 4 - TRANSFER MISSION PLANS TO AIR/GROUND ELEMENTS

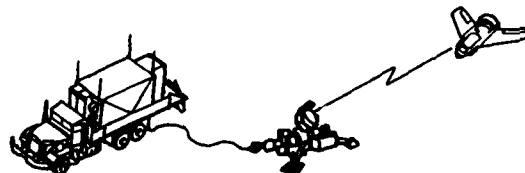
- A. PROGRAM AIR VEHICLE  
VIA DIGITAL TRANSFER  
MODULE INSERTED INTO  
FLIGHT CONTROL COMPUTER



- B. PRIOR TO LAUNCH,  
TRANSMIT FLIGHT PLAN  
TO GCS FOR LAUNCH/  
RECOVERY OPERATIONS  
AND HANDOFF

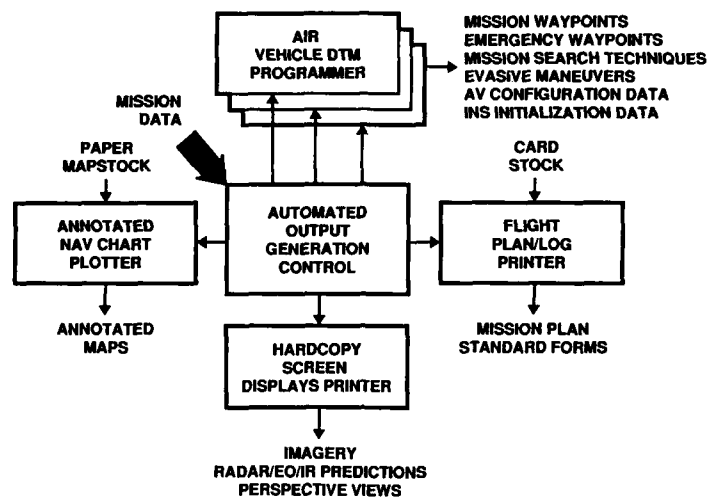


- C. AFTER INFLIGHT HANDOFF  
TRANSMIT FLIGHT PLAN AND  
CRITICAL IMAGERY INFORMATION  
TO FORWARD CONTROL STATION  
FOR MISSION EXECUTION



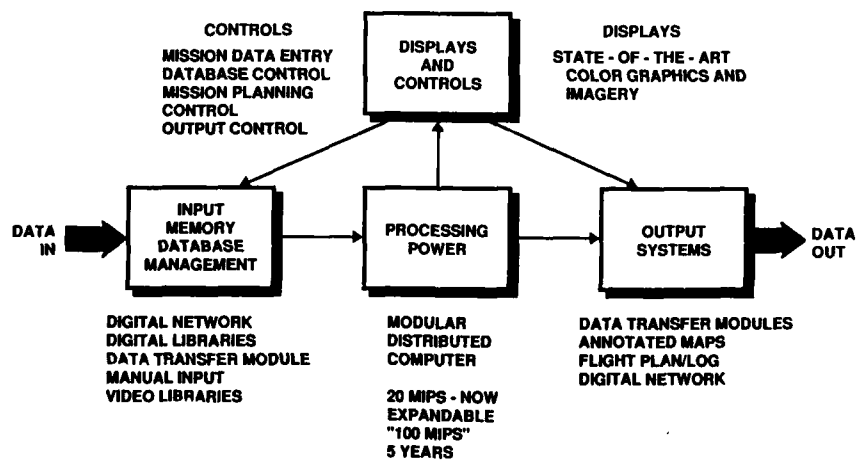
MERIT

### AMPS OUTPUT GENERATION



MERIT

### HARDWARE COMPONENTS OF ADVANCED MISSION PLANNING SYSTEM



**MERIT**

## **SUMMARY**

- **REVISED RPV PROGRAM STRUCTURE  
DRIVES REVISED OPERATING PROCEDURES  
AND MISSION PLANNING CONCEPTS**
- **PROPOSED MISSION PLANNING CONCEPT  
JUSTIFIES STANDALONE MISSION  
PLANNER FOR HQ UNIT**
- **TECHNOLOGY, ALGORITHM, HARDWARE,  
AND SOFTWARE IS AVAILABLE TO  
EXECUTE THESE CONCEPTS**

## DISTRIBUTION OF HARDWARE AND SOFTWARE ELEMENTS IN UNMANNED AIR VEHICLE SYSTEMS

Larry D. Sauvain  
Staff Engineer  
Lockheed Missiles & Space Company, Inc.  
O/T7-40, B/312  
6800 Burleson Rd.  
Austin, Texas 78744-1016

*Summary. Future unmanned air vehicle systems will be highly automated in order to accomplish their intended mission. These increased levels of automation are best achieved when the computer and man-machine interface elements are incorporated into the initial system design. Adequate capacity, growth capabilities and the maximum use of previously developed system elements are essential considerations in the computer hardware selection. The software structure must be modular, maintainable and have adequate configuration management tools to assure that the correct software is in use at all times. Since additional unplanned mission requirements may evolve, it is important that the man-machine interface elements be easily reconfigured. The basis for these assertions and how they were achieved within the ground control station portion of the Lockheed Demonstration and Research Test System will be addressed within this paper.*

### Introduction

Many aspects of unmanned air vehicle (UAV) operations require that distributed methods of command, control, data analysis and fusion be employed for the successful UAV system. The determination of what task should be performed by which subsystem, whether it should be conducted on the ground or in the air, and the level of automation of these tasks should be the result of careful analysis of the mission requirements. Future unmanned air vehicle mission requirements may also arise which the customer or system designer has not specifically anticipated. Therefore, the unmanned air vehicle system design should not only carefully address the immediate customer needs but permit the system to gracefully incorporate different sensor packages, datalinks, air vehicles or operational scenarios.

In order to achieve these objectives, it is necessary that the unmanned air vehicle system have a flexible distributed computer hardware and software architecture. The experience Lockheed has gained in developing and flight testing the Aquila and six other unmanned air vehicles, and in particular the most recent knowledge obtained during the Demonstration and Research Test System (DARTS) program, has resulted in a computer architecture that is suitable for current mission requirements and expandable to meet future needs.

This paper will describe some of the hardware and software tradeoffs necessary in unmanned air vehicle system design and their implementations within the DARTS system.

### Level of Automation

An important design and procurement consideration for unmanned air vehicle systems is the determination of what level of automation is necessary to support the intended unmanned air vehicle system operations. Typically, the greater the level of automation, the higher the initial procurement price but the lower the life cycle cost. Automated systems may require additional equipment when compared to a nonautomated alternative but often result in lower initial training and required skill levels from the operators. Proficiency training is less of an issue in an automated system since the typical operation may only require that a button be depressed. In a nonautomated system considerable eye/hand coordination can be necessary and periodic "flying" is mandatory. The nonautomated approach works only in those situations where the operators are available for considerable time after the initial training and can periodically have actual operational exposure to avoid loss of proficiency.

In a nonautomated system, the system's performance characteristics are dependent on the skills of the operator which can vary appreciably between personnel. Factors such as operator fatigue can also affect system performance more adversely in a nonautomated than in an automated system. In a properly designed automated system, software changes can be made to improve the system performance levels consistently better than the best skilled human operators can achieve. This was demonstrated three years ago with the automation of the Aquila recovery system, which has resulted in one of the most consistent and reliable recovery systems within the unmanned air vehicle industry today.

Other areas where automated systems have an important advantage are those situations that are tedious or lengthy in duration and where operations personnel may become inattentive or disoriented. This was observed by U. S. Army personnel during systematic area searches for optical targets using the Aquila system. A systematic target search over large land areas

is one of the most difficult missions to be performed by a short-range unmanned air vehicle. This mission requires that the air vehicle must be flown at proper attitude and search ranges while the payload optics are controlled to uniformly observe all necessary surface areas. A partially automated area search capability was available during Aquila Operational Test (OT) II which resulted in a moving target detection rate of 31 percent. This was improved to a notable 98 percent detection rate during U. S. Army-conducted Aquila Force Development Test & Experimentation testing by automating the guidance and payload operations. Only an automated system has demonstrated the capability to consistently search all key areas for targets while also optimizing total search time.

Automation can also result in improvements for other mission phases such as launch, mission planning, self-testing, data acquisition, emergency operations, and data link control. It is possible to characterize an unmanned air vehicle system by its level of automation in its functional areas and thus provide a good benchmark for comparison of systems. To illustrate this, a review of public domain literature on two unmanned air vehicle systems was conducted to provide a basis of comparison with the Aquila system. A chart was then produced to compare the levels of guidance automation available from these three systems (see Figure 1). The prospective unmanned air vehicle system purchaser can gain considerable operational insights into life cycle and operational capabilities by performing such a comparison of all mission phases.

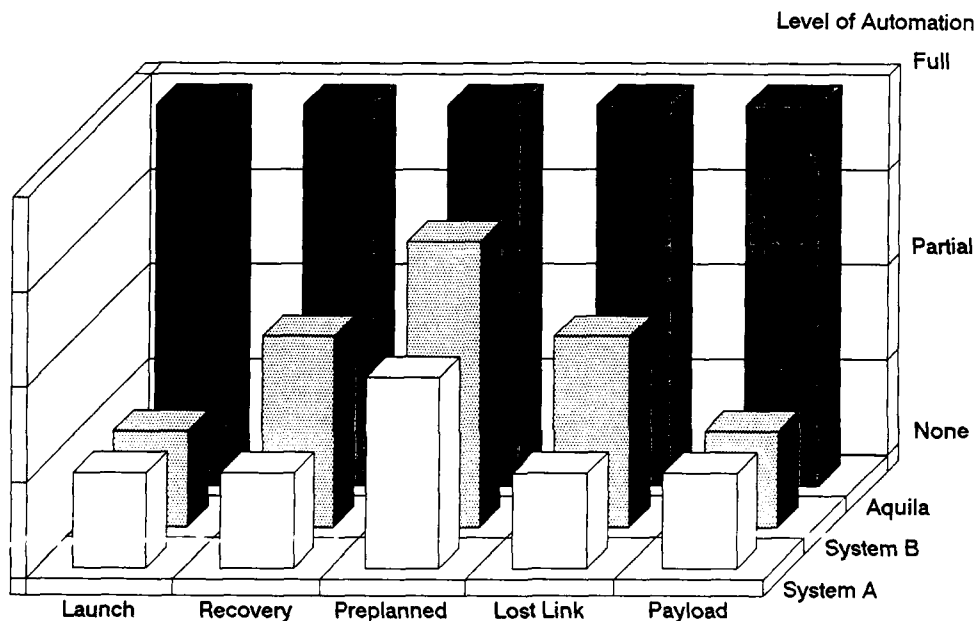


Figure 1: Level of Guidance Automation

The ability to achieve a high level of automation requires that careful attention be given during the design phase of the computer hardware, software, and man-machine interfaces. Automation should be an integrated part of the system and not just an afterthought.

#### Computer Hardware Selection

The computer hardware architecture selected will have a direct bearing on the ability of the unmanned air vehicle system to perform current as well as future missions. Unmanned air vehicle computer hardware selection should be based not only on the pricing, capacity, and the physical constraints of the system but also on such things as:

- The existence of adequate software development tools
- The availability of hardware maintenance features
- Maximum use of a single standard microprocessor family
- Maximum use of nondevelopmental items (NDI)
- Use of standard computer bus architectures designed for real-time applications
- Availability of the hardware elements in fully militarized and commercial versions

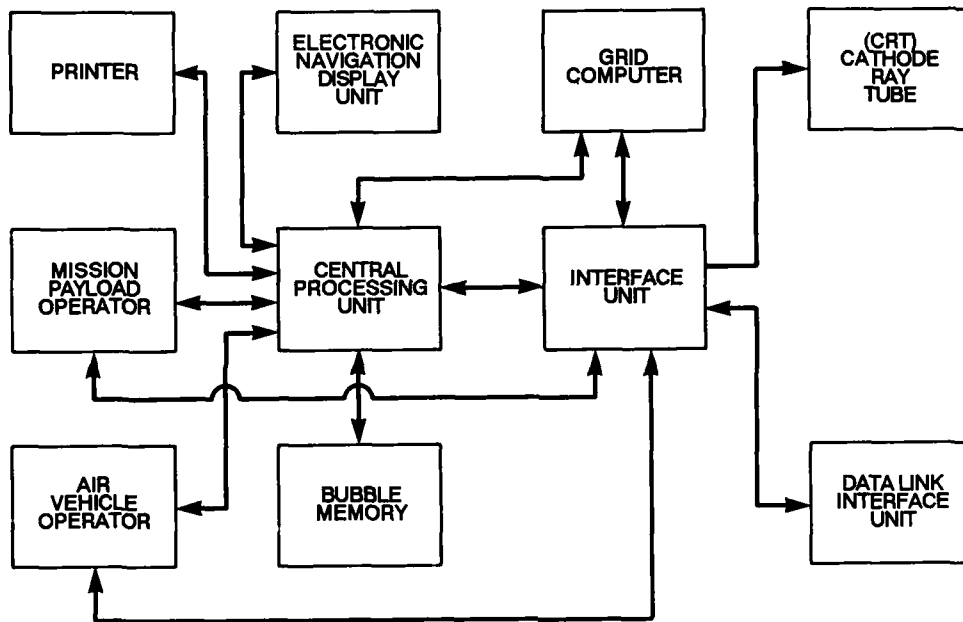


Figure 2: DARTS Ground Control Station System Block Diagram

- Throughput, memory, and I/O growth capabilities for future system requirements
- Adaptability to a variety of local and remote communications networks.

Lockheed has developed a ground control station consistent with these features for its Demonstration and Research Test System (DARTS). This network of computers is illustrated in Figure 2 and is based on the Intel family of microprocessors operating in a standard Intel Multibus. All computer chassis, memory, and processor boards are available as standard products from computer suppliers in militarized (Figure 3), ruggedized, and commercial versions.

The DARTS computer architecture as shown in Figure 4, permits the use of special Lockheed-developed interface boards for data link, video signal manipulation, and test purposes. By replacing the datalink interface board, the ground system hardware can interface with any of the currently available unmanned air vehicle data link systems. This has been accomplished for the VEGA datalink system. Also of considerable significance is the ability to incorporate interface boards with their own dedicated microprocessor. This relieves the main processor of much of the interrupt processing and permits expansion to an almost unlimited number of interface channels.

The processor speeds and memory capacities can be readily upgraded by replacing individual boards within the computer systems. Although the current DARTS configuration has adequate computational capacity, its capacity can be increased by upgrading the processor to an Intel 80386. This processor computes 6200 Drystones per second, which is over three times faster than the industry standard VAX 11/780.

The Multibus was selected because of the availability of a large number of commercial and military nondevelopmental item boards for this architecture. The Multibus has had years of refinement by industry and IEEE committees, and there are currently over 240 manufacturers of Multibus products. Data transfer rates for the Multibus are quite adequate for existing, as well as projected, unmanned air vehicle ground station needs.

### Software

Software is a critical element in the overall capabilities and performance levels of the unmanned air vehicle system. Software failures have the potential not only of resulting in poor mission performance, but also of causing catastrophic flight incidents. Properly developed software will rarely result in situations where a seemingly "safe" software change to correct one problem results in a new, unexpected problem. A good software architecture is essential in avoiding such problems and

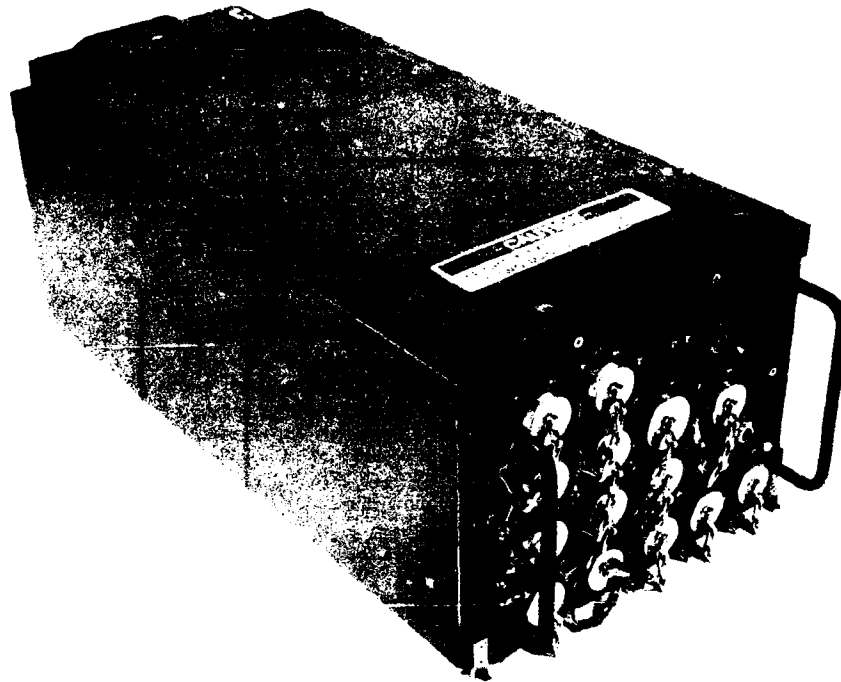


Figure 3: Militarized Configuration of Ground Station Main Computer

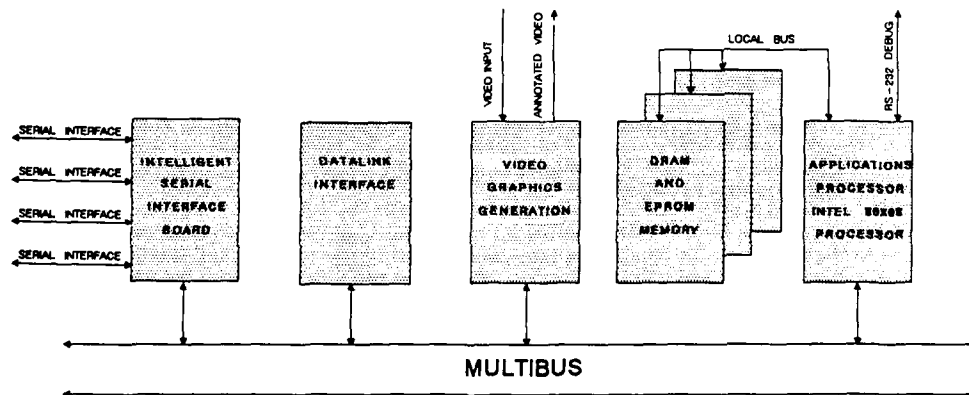


Figure 4: Ground Station Main Computer Internal Architecture

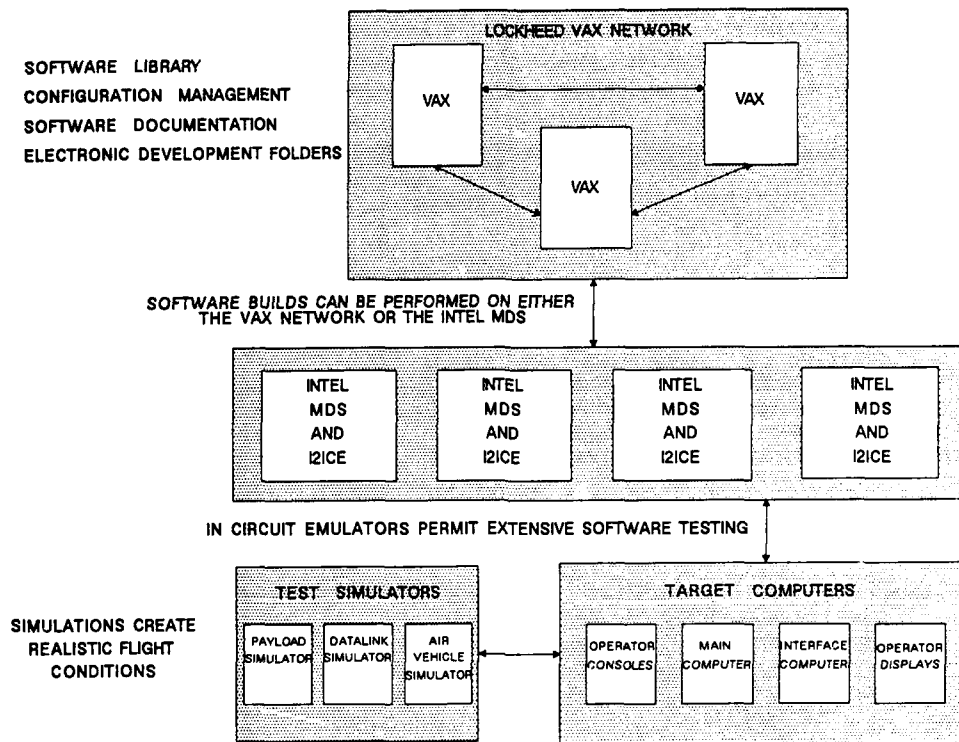


Figure 5: DARTS Software Development Environment

producing reliable and maintainable computer programs.

The implementation of software on a distributed computer system can put additional strain on an improper software design. One such example is an unmanned air vehicle guidance system that may have portions of this function distributed over numerous ground and airborne computer systems. If one software or hardware element fails, it may have adverse effects on the entire guidance system. Operational considerations may require that the software aboard the air vehicle be capable of commanding more than just a simple return home by flying on a heading for a particular period of time. The air vehicle may have to fly sophisticated predesignated flight corridors to enhance survivability and to avoid endangering friendly air forces. Additionally, a properly designed software system will inform ground personnel of the air vehicle's estimated position and activities by simulating air vehicle performance during these lost link operations. The Lockheed DARTS software unmanned air vehicle architecture is designed to meet these kinds of existing challenges and meet the future needs of the unmanned air vehicle community.

Modern software library configuration management schemes have been utilized and appropriate programming standards developed and enforced. The DARTS software development environment (see Figure 5) includes a network of VAX computers, Intel development systems, target computers, and simulation systems. This permits the exercise of proper management control of the software development and maintenance cycles. All software used in flight is traceable to the VAX software library and cannot be changed without proper authorization.

Some of the features of this software include the use of high-level languages, a considerable degree of modularity, the ability to operate in a multiprocessor environment, and extensive built-in-test capabilities. Programming development standards have been implemented that include restrictions on software module size, standardization of naming conventions and formalization of module internal documentation.

Rigorous software control processes ensure that all software changes are thoroughly tested prior to actual air vehicle flights by testing with simulated and actual data link, payload, and air vehicle hardware. The final test phase prior to actual air vehicle flight includes captive air vehicle flights. This is accomplished by mounting a DARTS unmanned air vehicle

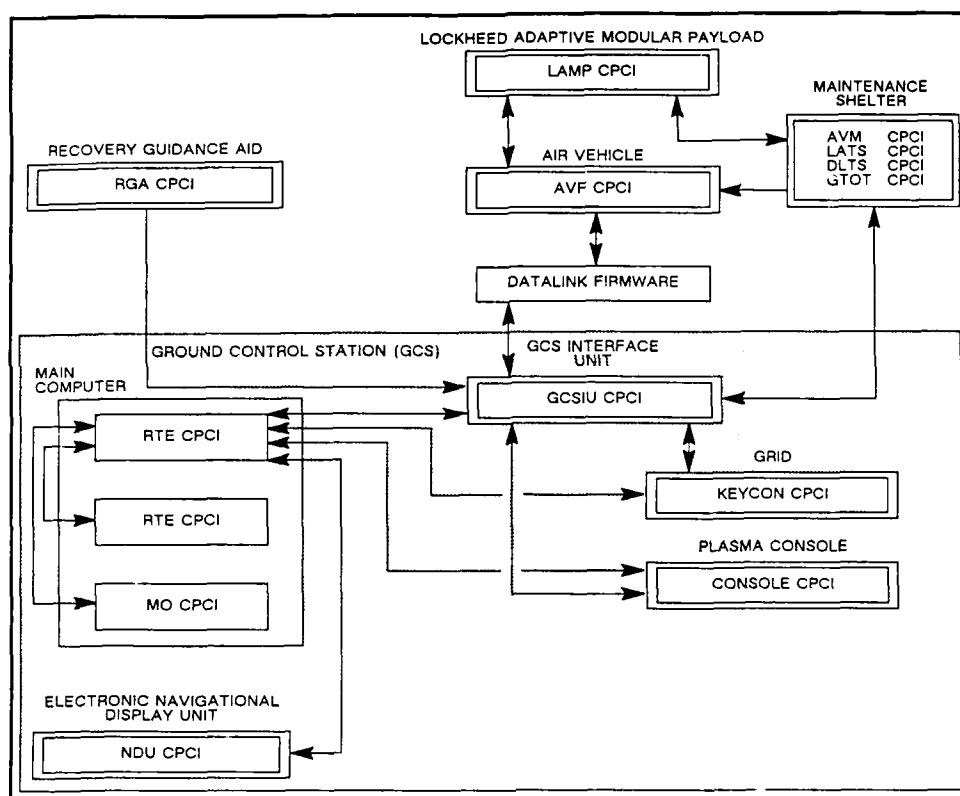


Figure 6: DARTS Software is Modular With Well Defined Interfaces

underneath a manned aircraft and having the manned aircraft respond to the commands given by the unmanned air vehicle to its flight control surfaces.

Software nondevelopmental item documentation for the system includes a system level interface specification, electronically maintained unit development notebooks and requirements documentation for each software configuration item. This documentation is electronically stored and the informational contents are available for reformatting to a variety of military standards.

All software, except for the air vehicle flight software which employs a special bit slice processor, executes on Intel microprocessors. Figure 6 provides a representation of the DARTS software configuration.

### Man-Machine Interface

Man-machine interface (MMI) elements with embedded computer systems or computer interfaces are often included as part of the unmanned air vehicle computer system. Common examples of these man-machine interface elements include programmable displays, touch sensitive screens, computer enhanced video displays, and computer monitored knobs, buttons, and switches. These man-machine interface elements often require as much software and interface design as stand alone computer systems, and proper hardware and software controls should be applied. Additionally, it is important for these man-machine interface elements to be adaptable to future mission requirements. The man-machine interfaces in the DARTS ground control station are the result of extensive human factors studies as well as the introduction of new technologies into unmanned air vehicle systems.

These human factors studies included not only design recommendations for the physical equipment arrangement to ease operational activities (Figure 7) but also the proper display of command and status information. The arrangement of information on the operator displays resulted from:

- Detailed studies of the existing man-machine interface for the Aquila system and functional allocations between that system's operators

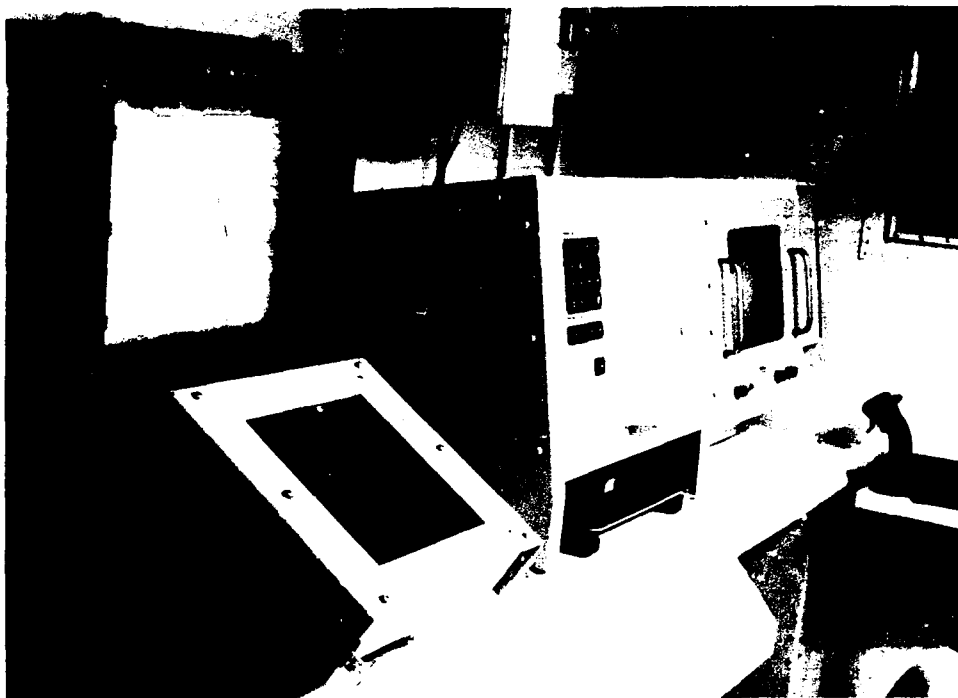


Figure 7: Equipment arrangement must be optimized for proper man-machine interface

- Preliminary designs of operator displays based on proposed integration of new technology
- Rapid prototyping of the proposed man-machine interface using a Lockheed proprietary user interface system (Figure 8)
- Performance studies and modifications of the prototype man-machine interface in response to simulated use by Lockheed and potential customer operations personnel
- Implementation of the man-machine interface on the target equipment (Figure 9)
- Testing and fine tuning of the man-machine interface with the target system using realistic simulations and captive air vehicle flights.

One important consideration in this process was the extensive use of operator menus. Unlike a panel of hardware switches and knobs which are always visible to the operator, only those functions available for use by the operators are displayed in the DARTS ground control station. Functions not available for the current mission phase are removed from the display, thus aiding the operator's decision process.

Operator displays consist of touch-sensitive plasma displays, an electroluminescent display with keyboard entry, a plasma navigation position display, and video display monitor.

Data entry for mission planning purposes is performed on a GRID keyboard. During this mission phase the operator enters the location of key ground elements, weather conditions, and the desired flight profile, which includes position, altitude, level of jinking, air speed, loiter type, and loiter time of the air vehicle. The operator can also preprogram mission payload operations by entering a list of cued targets and designate those areas for which an autosearch is desired. The operator can request a printout of the mission plan profile and an estimate of the fuel usage on the printer. He can also request a plot on the electronic navigation display unit (ENDU), which will result in a computer-generated plasma display plot of the air vehicle flight plan and target autosearch areas overlaid on a paper map of the region (Figure 10). During a mission, the operators have the capability of using the GRID to modify or develop a new mission plan.

The payload operator position has a video display, a joystick for payload control, and an operator plasma console. The video display can show sensor data in real time or it can display previously recorded video data. This video display can overlay alphanumeric as well as graphical data on the downlinked video sensor data. This overlaid data includes air vehicle position, air vehicle heading, target location, time, and a north pointing vector. The air vehicle operator gets continuous

MP TRACKING DATA		MISSION PAYLOAD		LASER STATUS	
AZI _____ mls DEPRESSION _____ mls TARGET _____ BURST _____ ALTITUDE _____ meters RNG _____ meters SHFT _____		<div>MAIN</div> <div>VIDEO</div> <div>LASER CUED TARGET</div>		LASER: <div>OFF</div> PULSE STATE: <div>SINGLE SHOT</div>  "MULTI-REFLECT" MSG.	
<b>TARGET/BURST LOCATION</b> EASTING <div></div> NORTHING <div></div>		<b>LINE OF SIGHT</b> RANGE <div></div> AZIMUTH <div></div> DEPRESSION <div></div>			
<b>PAYLOAD</b> <div>POWER ON</div> <div>POWER OFF</div> <div>UNLOCK</div> <div>LOCK</div>		<b>MISSION</b> <div>SEARCH</div> <div>SCENE</div> <div>FEATURE</div> <div>OFFSET TRACK</div> <div>SURVEY UPDATE</div> <div>TARGET</div> <div>AUTO RETURN</div> <div>BURST</div>			

Figure 8: Rapid prototyping of operator displays ensures correction of MMI problems early in the development cycle

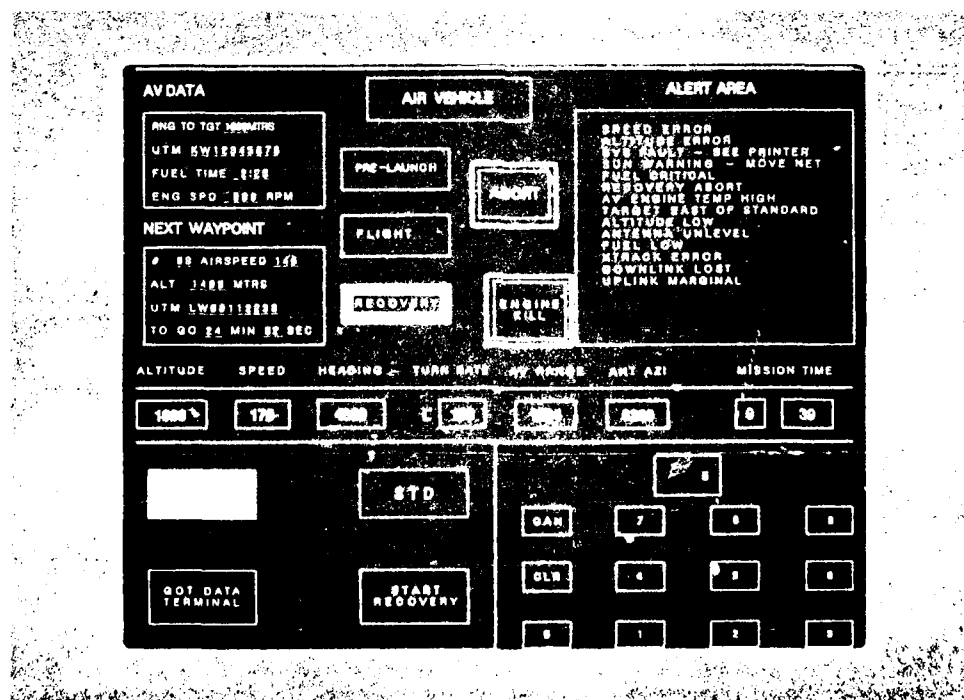


Figure 9: Prototype displays are then implemented on the actual hardware

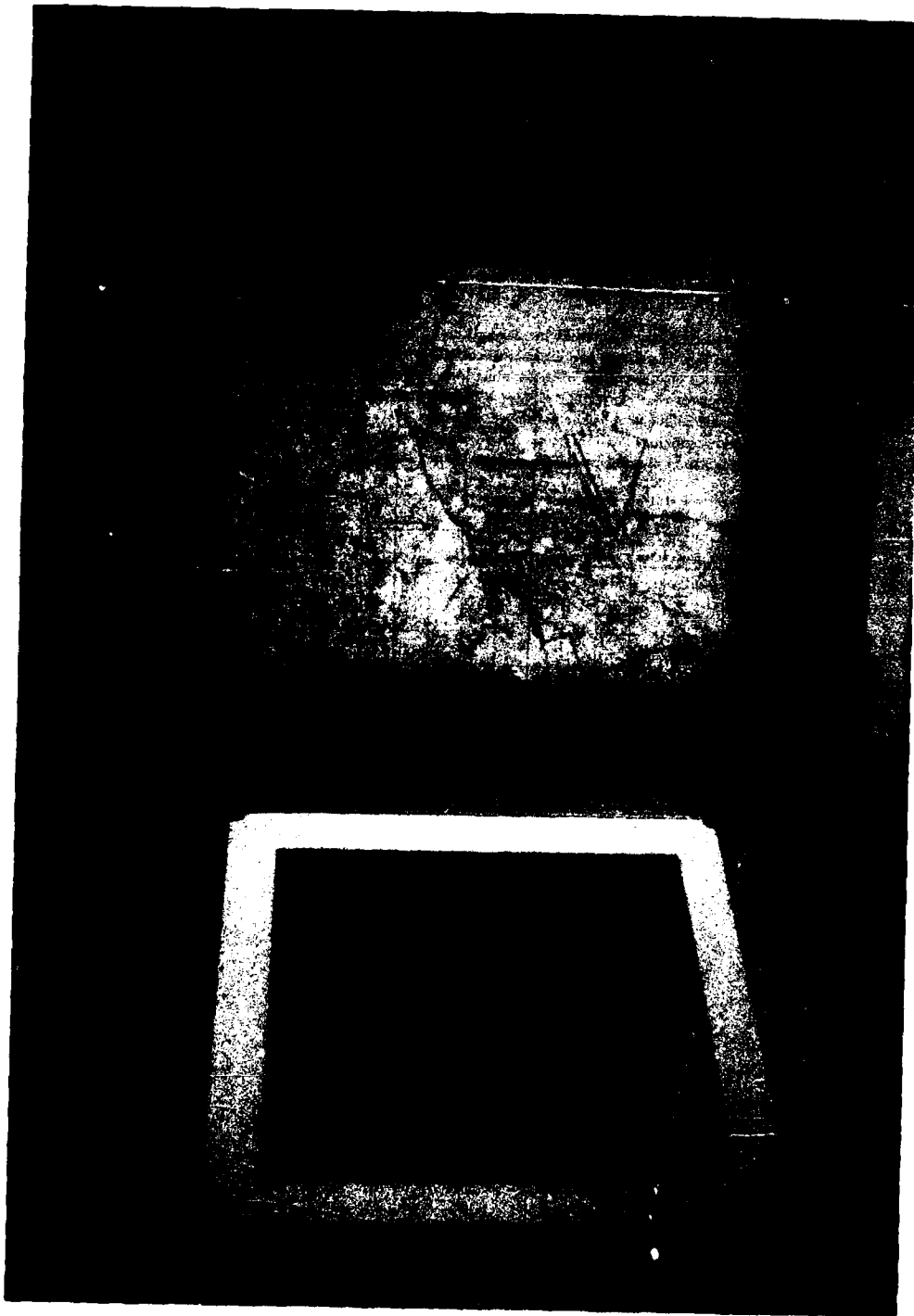


Figure 10: Flight planning data and actual flight path data are displayed on a paper map-plasma display system.

updates on air vehicle position, fuel usage, and air vehicle fault conditions, if any. Both operator consoles have a series of programmable buttons which allow the operators to control the air vehicle and operate the payload. Since the same hardware and software exists in both consoles, it is possible to change the crew member functions dynamically during a mission, thus making it possible for either crew member to become an air vehicle or payload operator. This feature is particularly useful in providing redundancy in the event that one of the plasma consoles should fail. Because the displays are programmable, it is also a straightforward process to change the labels into a language other than English or to add new display formats to support new data links or payloads. In addition to providing a means of control, these consoles also provide numeric display of all key operational data values.

While in flight, the electronic navigation display unit provides a plasma plot of actual air vehicle position and payload autosearch activities overlaid on the planned mission profile developed during mission planning. The printer also provides a printout of run time faults detected by the system during the flight. This includes faults occurring on the ground as well as in the air.

### **Conclusion**

As the unmanned air vehicle mission becomes increasingly more sophisticated and life cycle costs continue to gain in significance, it is imperative that the unmanned air vehicle computer system address these issues with increased levels of automation. The unmanned air vehicle system of today must look forward to these future requirements by implementing a distributed network of computers that can satisfy greater computer throughput, memory, and I/O needs. Proper software development and control methodologies must be employed, or unnecessary schedule and asset risks will occur. The man-machine interfaces must have sufficient flexibility to adapt to these new mission and automation requirements by providing the ability to change through software, not hardware modifications.

The DARTS ground control station has just such an architecture and has demonstrated its flexibility by interfacing with six different sensor packages and two major data links. It is not just a paper system but has been used in support of unmanned air vehicle test flights since October 1987 at Lockheed's South Texas Test Facility. Development continues in integrating the ground control station with new sensor packages, data links and air vehicles. The DARTS ground control station's modular hardware, software, and man-machine interface make it an excellent candidate for the next generation of unmanned air vehicles.

## TECHNOLOGY AND EVALUATION OF UNMANNED AIR VEHICLES

GEORGE R SEYFANG  
PRINCIPAL PROJECTS ENGINEER  
BRITISH AEROSPACE PLC  
MILITARY AIRCRAFT DIVISION  
WARTON AERODROME  
PRESTON  
LANCASHIRE PR4 1AX  
ENGLAND

### SUMMARY

The 15 years of UMA studies and experimental work done at BAe indicate that all of the technologies required to allow UMA to fulfil the air-to-ground roles in increasingly dangerous scenarios now exist. There appears to be the potential for significant savings in peacetime operating costs with UMA, although there would have to be changes to the services' infrastructure to gain all of these potential savings.

### 1.0 INTRODUCTION

This paper, Fig. 1, will present a wide-ranging view of various UMA concepts which have been studied over the past 15 years by British Aerospace, Military Aircraft Division, it will describe work on those technologies appropriate and specific to UMA and finally, by means of evaluation examples, it will show areas where UMAs might be a part of future weapon systems.

BAe at Warton have studied an evolving range of unmanned air vehicles under titles such as RPV, Drone, ASM, UMA, MSOW etc as shown in Fig. 2. The evolution has been driven by the increasing awareness of the limitations and lack of operational robustness of the early man-in-the-loop RPV. Even during the mid 1970's it was apparent that the 'useful' UMA would have to have many of the autonomous characteristics of the manned aircraft if it was to be widely accepted.

### 1.1 WHY UMA NOW?

The reasons which can make UMA attractive to both services and treasury are the well-documented ones of allowing effective air operations to be made against heavily defended targets and the potential for significant cost savings, Fig. 3. There have been several 'false-starts' in UMA incorporation into air forces - in particular in the UK it was stated that 'no more manned combat aircraft were necessary' as long ago as 1957! However, the technologies to enable UMA to be effective across a wide range of roles did not then exist.

It is now 30 years on from that particular 'false-start' and we believe that substantial progress has been made and that the technologies to allow a significant range of air-to-ground roles to be undertaken by UMA do now exist. Finally, the general world-wide trends to automation and robotics are likely to make acceptance of UMA less of a difficult 'pill-to-swallow' by the more conservative elements.

### 1.2 UMA CONCEPTS

There appear to be 3 main classes of UMA differing mainly by their degree of autonomy, Fig. 4.

The Remotely Piloted Vehicle which relies on a data/command link to allow manned (possibly multiple) intervention in various phases of the mission. This intervention might range from attempting to 'fly' the complete mission as if in a simulator, to making navigation updates/corrections, to searching for and attacking the targets. Depending on which level of involvement is chosen, there is a different sensor and data-link combination, however in each case there is a need at critical times for a real-time link and a total reliance upon it. We made several studies of data-links, relay stations etc, their vulnerability to both electronic and physical attack, and concluded that systems relying on such a vital link were unlikely to be adequately robust in the long term.

The Drone, which flies a pre-programmed mission such as Reconnaissance or Electronic data gathering, clearly has a part to play in the UMA field. It may operate in a totally independent manner and even if it uses data-links to speed the return of information, these may be arranged to repeat and/or alter important signals so as to penetrate the electronic jamming screen. In other words there is no total dependence on real-time data links, rather a potential benefit from them for drones.

The 'true' UMA which we see as having the widest applicability, certainly in the air-to-ground attack roles, is one which is able to operate autonomously. This autonomy must encompass the whole mission of flying to a designated area, searching for targets, attacking them and either returning to base or signalling the outcome of the mission - i.e. just as a manned aircraft sortie would be operated. The ultimate UMA would, of

course, be able to tackle several types of target, i.e. it would be a multi-role vehicle, able to offer the commander flexibility of operations depending on the run of battle.

### 1.3 UMA TASKS

The air-to-ground tasks may be divided into 4 main categories of increasing difficulty, Fig. 5. Even 15 years ago it was clear that Recce and Defence Suppression (by Anti-Radar Missiles) could be tackled. The attack of known, Fixed Targets was also then becoming feasible with the development of improved inertial navigation systems. These could be further improved in their effective accuracy if several UMA, each with an IN system, were to fly in close formation and pool their estimated positions. Modern short range microwave links would be adequate to facilitate this exchange of information and also to control the formation pattern. Also being developed in the 1970s were the various terrain - referenced and satellite navigation systems which offered semi-continuous position fixing of adequate accuracy for a wide range of fixed target attacks.

The most difficult task in air-to-ground operations is the location and subsequent attack of Mobile Targets such as tanks etc. It was this task which we at BAe started to tackle in the mid 1970s since we saw that the outcome of whether this challenging task could be met by a fully autonomous UMA would have a great bearing on whether the UMA could have a significant part to play alongside, or even partially replacing, the conventional manned ground attack aircraft.

### 1.4 ANTI-ARMOUR UMA - CONCEPT OF OPERATIONS

In order to structure our examination of the design and technology of UMAs to locate and attack mobile targets, we postulated a concept of operations as shown in Fig. 6 and Fig. 7. In each case it will be seen that the operation is to be carried out in the same manner as it would be with manned aircraft in the anti-armour role.

In Fig. 6 the general scenario is shown with C<sup>3</sup>I indicating an area of enemy territory inside which it is believed that substantial numbers of enemy armoured vehicles are 'on the move'. There are two reasons for choosing to attack when armoured vehicles are 'on the move', exposure and distinctiveness. Only when vehicles are stationary and hiding can they deploy effective camouflage and decoys which make detection and recognition difficult for manned and unmanned aircraft. Once the movement of an enemy force has been observed by intelligence assets then an attack must be made within a period of a few hours - before the vehicles reach their new positions and hide. During these few hours the attack is made by air vehicles from either ground or air-launch positions. These vehicles fly in groups to the designated area using moderate quality navigation and terrain following/avoidance systems and commence to search.

The search phase, Fig. 7, will be optimised to maximise the probability of finding targets and will take a form depending on the likely routes of the enemy vehicle formations. In rear areas, vehicles are likely to be on roads and hence a typical search pattern would be to fly so as to maximise the length of roads searched. In forward areas the vehicles may be off-road and so an area search, possibly involving box or raster flight patterns, is typical. It should be mentioned here that the UMA range or radius of action requirement specifications should make adequate allowance for the distance flown during searching - in addition to that required merely for penetration to the designated search areas. Once a group of vehicles has been detected and recognised as such, the UMA should fly so as to put the maximum number of sub-munitions over the maximum number of targets in a first pass attack manoeuvre.

This then is the task we saw as necessary for a useful UMA to be able to carry-out. The technologies to complete the various phases of the UMA mission will now be discussed.

## 2.0 UMA TECHNOLOGIES

The major technology classes for a UMA are shown in Fig. 8. These comprise those relating to the operation of the air vehicle as a flying machine, those relating to the 'intelligence' of the UMA to enable it to 'choose' what to do and when, and finally those relating to the munitions payload.

### 2.1 AIR VEHICLE TECHNOLOGY

The various aspects of the air vehicle as a flying machine are shown in Fig. 9. As a result of several studies made at BAe over the past 15 years, and done to different levels of detail, some general observations may be made. The size of a UMA is governed, as is that of a manned aircraft, by the payload/range/speed requirements of the design mission(s). The level of technology applied to the airframe structure, the propulsion system and the payload dispenser must be assessed in the light of the overall system cost-effectiveness. However, early studies did indicate that Expendable UMA, i.e. those designed for a single short life sortie, have no need for multiplexed, redundant flight-control systems, electrical power systems etc. In the case of Recoverable UMA, i.e. those designed for several or many sorties in peace and war, the same rules of redundancy for cost-effectiveness apply as for manned aircraft. There may be subtle differences between requirements for safety of the aircrew of manned aircraft and the perceived safety of ground-based civilians from 'robot aircraft', and these latter may have significant legal/political implications.

The whole topic of launch and recovery of UMA has received possibly too much

attention in the minds of the community. In the case of expendable UMA then the two options of ground launch and air launch are available and the choice of one or both may be made depending on the perception of their relative advantages. The technology has existed for either for many years. In the case of recoverable UMA we reached the conclusion that the cost of sustained operations precluded the more exotic take-off and landing methods and that it is difficult to improve upon the wheel as a means of travelling over the ground!

The major difference between manned and unmanned aircraft is likely to be their frequency of peacetime flying - if any. There are means of storing UMA, either as a 'wooden-round' in a sealed container from the manufacturer, or in some form of protective bag which may be re-sealed by the Services between infrequent flights. The former has been evolved in the case of cruise missiles whilst the latter has evolved where air forces have wished to store manned aircraft for periods of years either as reserve fleets or, more likely, as spare aircraft to make up attrition during peacetime.

In general all these air-vehicle technologies exist and may be used with little or no modification for UMA.

## 2.2 NAVIGATION TECHNOLOGIES

There are several technologies which are appropriate to different classes of UMA ranging from simple air data types, through inertial and terrain-referenced types to satellite-based, Fig. 10. Each type has its place and by the end of the 1970's it was clear that no bar to the use of UMA would come from a lack of navigation accuracy. Rather the opposite, the cruise missile navigation systems were likely to be put into manned aircraft to improve their capability!

## 2.3 TARGET FINDING TECHNOLOGY

This area appeared to be the one in which there had to be advances if a useful UMA was to be derived. Whereas many fixed, known targets could be attacked once the navigation accuracy (and the map accuracy) had been brought to a level appropriate to the types of munition to be delivered; the class of mobile targets is a completely different matter, Fig. 11.

As postulated in Fig. 6 & 7 there is a need for sensor(s) to search for, locate and recognise mobile targets such as tanks, trucks etc at a range sufficient to enable a 1st pass attack to be made. This was the critical technology which was missing in the 1970's and in which BAe has invested significant effort and money to examine and develop.

### MOBILE TARGET SEARCH SENSORS

The task for the search sensor is to detect and recognise valid target groups at a range of 2-3Km whilst the UMA is flying at high subsonic speed and low altitude to minimise threats from ground and air defences. This task is not too difficult in an open desert terrain but is considerably more difficult in the European scenario where the weather can be foul and there is a considerable amount of wooded and urban development, Fig. 12. In addition to all of the 'natural' difficulties, the 'fog-of-war' generated incidentally, or deliberately by the enemy in the form of camouflage and decoys, must be overcome.

### COMPARISON OF MOBILE TARGET SENSORS

An initial study of the task and the sensor physics suggested that only 2 classes of sensor might meet the demanding objectives of detecting individual vehicles, locating them accurately relative to each other, and recognising at least the class of vehicle - armoured or soft skinned. All this is to be done in European weather and the European cultural scene. These 2 sensors are passive Infra-Red of the forward looking variety FLIR and Millimetric Radar - the latter offering several potential advantages.

At the time of our initial investigations there was considerable world-wide activity on IR sensors of various types and we believed that IR sensors would be developed to their best capability. In stark contrast we found that very little was being done on Millimetric Radar despite its apparent advantages for the mobile target task. Strangely, the rapid development of radar during WW2 from metric, through decimetric to centimetric wavebands had stagnated, and despite our efforts to interest radar companies, there was no real movement into the millimetric band.

The advantage of millimetric radar as we perceived them in the mid 1970s are shown in Fig. 13 as a substantial increase in search swathe and a robustness against poor weather. Both these improvements could apparently be achieved plus accurate target location in range and bearing from an antenna sized to fit comfortably inside a UMA. In the lack of any other way of 'proving' these perceptions we were forced to start our own company-funded millimetric radar experimental programme which has evolved into a system development programme following the successful results obtained.

### MILLIMETRIC EXPERIMENTAL PROGRAMME

In order to gather data which would lead to knowledge of the usefulness of millimetric radar, BAe initially specified and purchased simple measurement radar systems. In due course we modified them in-house to extend the capability from ground-based,

staring, bistatic, low-powered systems to airborne, scanning, monostatic, high-powered systems, Fig. 14. Over the period of 10 years a large data-bank of both target and background clutter has been accumulated.

Initial testing demonstrated the simple sensor physics extrapolations from centimetric radar to be generally true. The mapping advantages of narrow ( $\frac{1}{2}^\circ$ ) beams from moderate-sized antennae and the powerful MTI signature of moving targets were both demonstrated. At an early stage in our experimental programme we confirmed that moving vehicle targets could be detected and recognised fairly easily but that stationary vehicle targets were more difficult to differentiate from the background clutter of Europe. However, this latter result had been expected and the several radar variables incorporated in our experimental radars were exercised to achieve an optimum radar signal and derive robust signal processing algorithms.

Following the 10 year period of our experimental programme, and in many cases as a direct fall-out from it, there is now a wide variety of millimetric radar components, systems and associated test equipment available. The combination of our data-gathering measurements and evolution of target acceptance/clutter rejection algorithms allows us to say that military vehicles of interest can be detected, recognised and classified autonomously by millimetric radar, Fig. 15. This conclusion has been tested in European weather and with European terrain. The result is enhanced when groups of vehicles are the target rather than single vehicles. Thus millimetric radar together with target discrimination signal processing has been shown to be a powerful sensor for UMAs (and also for manned aircraft as a searching aid for the pilot).

#### RECONNAISSANCE SENSORS

One of the roles which UMA already carry out is that of Recce Drone. Currently the sensors in such vehicles comprise Photographic and Linescan techniques in the visible and infra-red region of the spectrum. The encouraging results being gathered in the BAE millimetric radar experimental programme suggest that such a sensor would make a useful additional recce sensor since it has performance features which can complement those of the existing sensors, Fig. 16.

#### 2.4 REPORTING TECHNOLOGY

The UMA has one potential weakness relative to the manned aircraft - it is not obvious how the commander will know whether it has done its job properly and whether it has fortuitously gathered recce information, Fig. 17. To overcome this problem it is possible to make the UMA transmit a short message to base about its success, or lack of it. Such a message could have a very low data rate so that it would penetrate hostile jamming even at low frequencies which permit direct broadcast. In the case of an expendable UMA then a post-attack terminal climb to signal from a line-of-sight altitude would permit a high frequency directed communication to be made. Other applications of reporting discovered targets to following vehicles in a master-slave or a wolf-pack formation can be considered for UMA just as for manned aircraft.

#### 2.5 PAYLOAD TECHNOLOGY

The final link in the UMA chain of effectiveness is that of the payload - which is likely for most targets to comprise multiple submunitions, each able to attack an individual target. The designed size of each submunition is dependent on the kill mechanism, the homing/fuzing sensor accuracy and the delivery pattern and accuracy. In general the size and mass of the munition depend on the target hardness/armour type, the cost and volume depend on the target size and dispensing range. These factors can be exchanged to some extent but the warhead size cannot be reduced below that which will inflict adequate damage, Fig. 18. Unfortunately, an adequate description of the current and future target armour characteristics is not always available and so a conservative, oversized munition has to be selected. This in turn feeds back as a reduced number of munitions which each UMA can carry and/or an increased UMA size and cost.

#### 2.6 STAGING TECHNOLOGY

It is not always optimum to make the mission a 2-stage mission i.e. UMA bomber dropping bombs. There are occasions where a single-stage or a 3-stage mission can be the best solution both for flight performance and distribution of the expensive sensors between UMA and munitions, Fig. 19. The optimum arrangements can only be determined when a "design mission" and a given level of technology are defined.

#### 3.0 EVALUATION

Many studies have been made of all aspects of UMA operation and several examples are presented to show indicative trends.

##### 3.1 EVALUATION OF SEARCH CAPABILITY

To aid the selection of the critical technology for UMA, the search sensor for finding mobile targets, a substantial evaluation exercise of these has been pursued. Sample results are shown in Fig. 20 and Fig. 21. In Fig. 20 is shown the accumulated probability of finding an attackable target as a function of distance flown whilst searching. Clearly the wider search swathe of a millimetric radar reduces the time-at-risk considerably compared to the lesser search swathe of an infra-red system. To a

first order, the effect of enemy defences is directly proportional to the time-at-risk and hence the mission success and/or survival of the mission are relateable to search swathe. Fig. 21 shows the effect of a search sensor which has the capability of 'mapping' a group of target vehicles - as is possible for instance with a millimetric radar and not with passive infra-red. If the group is mapped at sufficient range that an optimum attack manoeuvre rather than a non-optimum manoeuvre is made, there is a doubling or more of the number of targets engaged by the submunition pattern. The combined advantage of an autonomous millimetric radar is a several-fold improvement in mobile target attack effectiveness - for UMA or manned aircraft.

### 3.2 EVALUATION OF UMA RECOVERABILITY

In the case of manned aircraft it is not allowable to consider whether the system should be recoverable or expendable. For UMA however this is a real issue which can be studied and optimised. Fig. 22 shows the UMA design and operations features which can affect the choice of recoverability. The effect on R&D cost and Production Unit Cost are primarily via the increased size and complexity of the UMA to make it recoverable, Fig. 23. The effects on peacetime operational costs are related to the number of maintenance and base personnel required to operate the complete system in peace and war.

Perhaps the most important factor affecting the choice of expendable or recoverable UMA is the level of attrition it is likely to face in wartime. A typical result from many studies of the total life cost of a fleet of UMA to complete a wartime task is shown in Fig. 24. The major variable is the greatest unknown - the actual loss rate per sortie, which can be estimated but will not be known for certain. Again it is unfortunate that estimates made by many organisations disagree on the likely value of the loss rate - and disagree over an order of magnitude! Clearly then it is important to look at Fig. 24 with a view to selecting a system having a low sensitivity of cost to variations of the defence effectiveness. The result is further subject to unknown factors due to applications of stealth and defence suppression!

### 3.3 EVALUATION OF UMA OPERATIONS

Studies of the relative advantages of ground-launching and air-launching expendable UMA have been made, and whilst it is not easy to assign numerical values to the advantages, they are worth listing, Fig. 25. The recent INF treaty may influence the optimum towards air-launch.

It is tempting to believe that any cost savings which might be made by the introduction of UMA in certain roles will be significant in reducing overall service costs. The limited information available suggests that this may not be wholly true, especially in the case of small UMAs. The indications are that peacetime operating costs of various sized air vehicles may not be pro-rata with their size and purchase cost, Fig. 26. There may well be a large 'fixed' infrastructure cost associated with the way the services operate manned aircraft and it may take re-thinking of this aspect if all the potential cost savings due to UMA are to be passed on.

### 3.4 EVALUATION OF UMA VS MANNED AIRCRAFT

BAe have made several attempts to try to compare the total life costs of manned and unmanned aircraft. It is very difficult to reach firm conclusions since so many of the variables are not calculable, however Fig. 27 is a summary of the general impression gained so far. The prime cost driver is the Military Task and to a first order there does not seem to be an enormous cost associated with having a man or a robot conducting the carrying-out of this task in wartime. There does seem to be a significant potential for the reduction of peacetime operating costs by the virtual elimination of 'training flights' and the associated maintenance and attrition through accidents over a period of up to 20 years, however this would require a change to the way the Services operate.

A notional study of the 20 year life costs of 3 different fleet concepts has been made and is illustrated in Fig. 28. The common factor was the military task of delivering a specified payload in a specified time against defences of a specified level of effectiveness. The conventional manned fleet of aircraft incur a peacetime operating cost comparable with their total R&D and Production costs. A fleet of recoverable UMA would have similar R&D and Production costs but could have a significantly lower peacetime operating cost. The expendable UMA fleet would have a lower R&D cost (smaller vehicle) but a higher Production cost (many more vehicles) possibly giving a similar total cost. These figures can only be approximate but do serve to illustrate differences in where the costs might be incurred, and when the costs might be incurred.

### 4.0 SUMMARY

The 15 years of UMA studies and experimental work done at BAe indicate that all of the technologies required to allow UMA to fulfil the air-to-ground roles in increasingly dangerous scenarios now exist. There appears to be the potential for significant savings in peacetime operating costs with UMA, although there would have to be changes to the services' infrastructure to gain all of these potential savings.

### ACKNOWLEDGEMENTS

A small, dedicated team of project engineers at BAe Warton has done the pioneering work over the past 15 years which has allowed the substance of this paper to be written.

## NAVIGATION AND GUIDANCE TESTING OF THE LOCKHEED/U. S. ARMY AQUILA REMOTELY PILOTED VEHICLE

Steven L. Ferguson  
Flight Test Analysis Engineer, Sr.  
O/T7-43, B/312  
Lockheed Missiles & Space Company, Inc.  
6800 Burleson Rd.  
Austin, Texas 78744-1016

*Summary. This paper describes the Lockheed/U. S. Army Aquila Remotely Piloted Vehicle test program. The Aquila system is described, the data collection system discussed, and then particular tests required for testing the various navigation and guidance functions of the Aquila are described.*

### Introduction

The navigation and guidance testing of a remotely piloted vehicle has always represented a challenge to the test engineer. With the introduction of jam-resistant data links and the requirement for pinpoint accuracy, this task has become extremely difficult, yet has become the focal point of most testing. The Lockheed/U. S. Army Aquila Remotely Piloted Vehicle (RPV) developed to satisfy the Target Acquisition, Designation, and Reconnaissance (TADAR) mission presented an especially challenging task for all involved. It was imperative that the air vehicle, using steerable airborne datalink antennas with a narrow beam width, know its position in space at all times.

This paper will describe the Aquila system and then discuss the testing aspects of the Aquila test programs. Special range requirements, flying test bed development, and specialized test planning required to satisfy the requirements placed on the Aquila system will also be discussed.

### The Aquila System

The Aquila system (Figure 1) consists primarily of five subsystems: the ground control system, the air vehicle, the datalink system, the launcher system, and the recovery system.

Although all of these systems are required for a complete mission, for the purposes of this paper only the first two of these systems will be discussed in detail. The datalink system will be described as it interfaces with the rest of the system.

#### Ground Control Station

The ground control station is the control center for all Aquila RPV activities. Three consoles provide operator interface with the air vehicle, mission payload system, and the remote ground terminal (RGT). A fourth console is provided for the mission commander.

All commands for direction of the air vehicle in flight are initiated at the air vehicle operator's console. A data terminal is provided for preflight mission entry and inflight mission plan and site setup changes. Inflight mission changes available from the air vehicle operator's console consist of immediate loiter maneuvers, immediate waypoint commands, and manual guidance by airspeed, altitude, and heading. If required, an entire or partial mission plan can be changed in flight without interrupting the flight of the air vehicle. The air vehicle operator is also responsible for entering the system site setup data, which includes location and orientation of the datalink remote ground terminal, the launcher system, the recovery system, current weather conditions, and air vehicle fuel load.

#### Air Vehicle System

The Aquila air vehicle is a delta-wing aircraft with a shrouded propeller. The air vehicle is powered by a 25-horsepower, two-cycle gasoline engine driving a two-bladed propeller. The major systems carried by the air vehicle include the attitude reference assembly, the mission payload system, the airborne data terminal (ADT), the engine module, and the flight control electronics package (FCEP). These systems in conjunction with other subsystems allow the air vehicle to fly for up to 3 hours with approximately 15 kilograms of gasoline.

The FCEP is the heart of the air vehicle. It controls flight of the aircraft and communications with the ground. The FCEP communicates directly to the attitude reference assembly, which is the inertial sensor for the air vehicle. The FCEP reads data from all systems on board and issues commands appropriate to the current mode of operation. The mission payload system provides near real-time imagery directly to the ground and is under direct control of the mission payload operator in the ground control station. The mission payload system provides two modes of automatic tracking, which

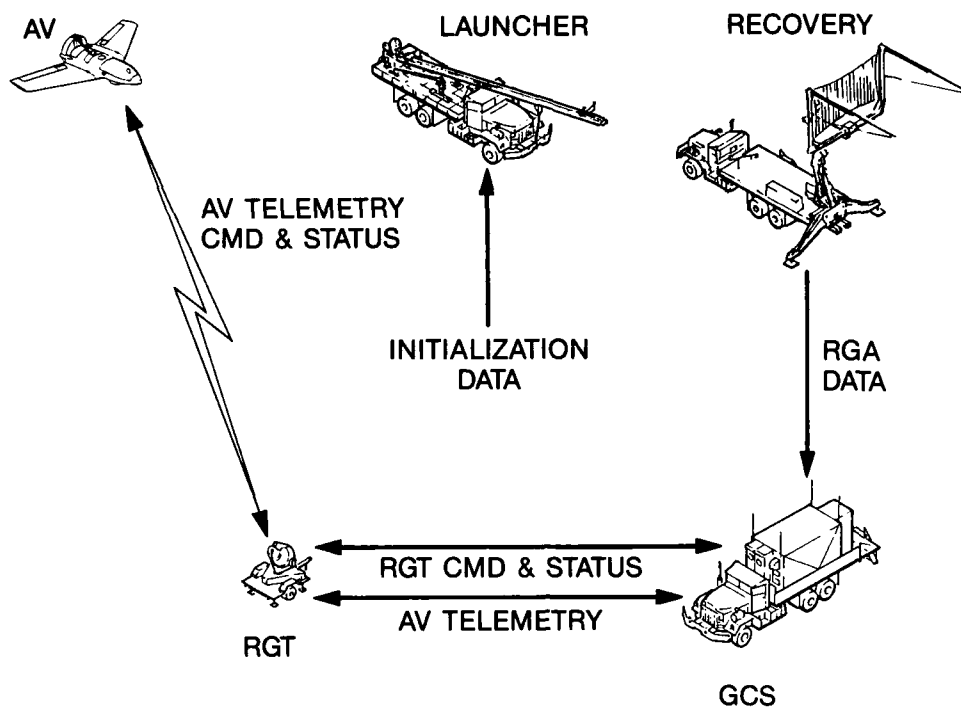


Figure 1: Aquila System Components

stabilize the payload through the use of correlation trackers. A boresighted laser rangefinder provides accurate range-to-target information and laser designation for laser-guided munitions. Payload azimuth and elevation angles are sent directly to the FCEP.

The airborne data terminal is the center for airborne communications through the Harris Corporation Modular Integrated Communication and Navigation System (MICNS). The airborne data terminal contains steerable antennas on the top and bottom of the unit. These antennas are pointed at the remote ground terminal using commands from the FCEP.

### The Aquila Navigation Process

The Aquila system was designed to be operated by an Army soldier with a minimal amount of training, be capable of locating a tank-size target at long ranges, have a jam-resistant datalink system requiring narrow-beam steerable airborne antennas, and be able to return to be recovered in a 4.3 x 6.1 meter net. These factors taken together require that the system be able to navigate with precision. The following paragraphs will discuss briefly the process used by the Aquila system for obtaining precise navigation.

The navigation process begins with obtaining survey data for initializing the system. The essential measurements for site setup are: datalink remote ground terminal location and altitude; launcher system location, altitude, and heading; recovery system location, altitude, and heading; orienting station location, and altitude; and orienting station to end of orienting line angle.

All guidance locations are required to be in the Universal Transverse Mercator (UTM) system. Altitudes are entered in meters above sea level. Angles are measured from true north. Other data are required for the system to determine grid convergence, grid magnetic angle, the current map year, grid zone, and spheroid model used.

Prior to launch the operator at the launcher system inputs codes for the MICNS datalink system and initial pointing angles for the airborne data terminal. These data are transmitted to the air vehicle during powerup for pointing and initialization of the airborne data terminal antennas. Without this data the FCEP would not be able to point the antennas accurately enough to obtain links with the ground.

During the prelaunch phases, the remote ground terminal antenna is pointed at the air vehicle, the airborne data terminal antennas are pointed at the remote ground terminal, and the data link is established. Once both up link and down link are established, the ground control station transmits information about air vehicle location, remote ground terminal location, recovery system and launcher system location and orientation. Checks are performed to verify system and datalink integrity.

and antenna operation. The inertial navigation system in the air vehicle is initialized to the current launcher system location and altitude. The first six mission plan instructions are transmitted to the air vehicle and stored in the FCEP. Navigation updates are processed using the remote ground terminal pointing angle and range to remove inertial system drift. Other processes initialize navigation filters and prepare the air vehicle to start the engine.

Once navigation initialization is complete, calculations are made to determine a waypoint (Waypoint 0, or WP 0) that is 1 kilometer straight out and 100 meters above the launcher system altitude. The engine then is started, and a series of tests are performed to verify engine operation. When the system has passed all prelaunch phases without any failures, the "OK to Launch" light is illuminated. Launch must be initiated within 70 seconds after the "OK to Launch" light is lit, or the air vehicle will automatically abort the launch sequence. The FCEP continues to monitor status of key parameters in the air vehicle for any sign of failure and will abort the launch automatically if such a failure is detected prior to leaving the launch rail.

In-flight navigation is performed by the attitude reference assembly inertial guidance system. Air vehicle position is calculated in terms of delta latitude and longitude from the remote ground terminal location. The air vehicle position in conjunction with the remote ground terminal position is used to calculate pointing angles for the airborne data terminal antennas. Attitude reference assembly drift is minimized by using periodic range and azimuth updates from the remote ground terminal antenna. The navigation update data can be rejected if they fall outside of pre-set bounds. If a navigation update is not received for any reason, the FCEP will use an integrated true airspeed (TAS) to calculate the air vehicle position for updating navigation filters.

If for any reason the datalink does not function for a preset period of time, the FCEP will fly the air vehicle to a previously-set, lost-link waypoint and orbit at that location. The ground control station, on detecting a lost-link condition, will take direct control of the remote ground terminal and continue to point it at the predicted air vehicle position based on the last known guidance mode. When the lost-link timer has decremented below zero, the air vehicle navigates to the first lost-link waypoint, and the remote ground terminal is commanded to follow the predicted air vehicle position. Several modes of link reacquisition are used. If link is not reacquired after the time allotted for the first lost-link waypoint, the air vehicle will proceed to the next lost link waypoint and await reacquisition. Eight lost-link waypoints can be entered into the mission plan. If link is not reacquired after completing all lost-link waypoints, the air vehicle will execute whatever instruction has been entered into the mission plan for the emergency instruction designated as WP 99. At completion of WP 99, the air vehicle will either deploy the parachute if in friendly territory or dive into the ground if in unfriendly territory. The designation of friendly or unfriendly territory is entered when the system is started and can be changed anytime during the flight.

Final approach guidance into the recovery net is accomplished with the Lockheed-developed recovery guidance aid. This system uses infrared detectors to track the near-infrared beacon that is located on the nose of the air vehicle. Horizontal and vertical offsets from the preset glide slope are transmitted to the air vehicle, and appropriate corrections are performed to bring the air vehicle back onto the desired glide path.

### **The Lockheed Manned Aircraft Flying Testbed**

To test all aspects of the Aquila RPV system, Lockheed has developed a flying testbed that can test system integration without endangering hardware. The Lockheed Manned Aircraft (MAC) system has grown from using a Piper Seneca aircraft (Figure 2) with all essential air vehicle systems mounted onboard (MAC I and MAC II) to the current configuration (Figure 3), which uses a de Havilland Twin Otter to carry an entire air vehicle mounted on a trapeze below the aircraft (MAC III).

The use of a flying testbed allows the accomplishment of high risk development tests which could otherwise cause the loss of an air vehicle. With the capability to mount an entire air vehicle under the MAC III, it is possible to test the capability of an air vehicle as a unit prior to delivering the unit to the customer and to perform tests in airspace that would normally be off-limits to an unmanned aircraft. Lockheed now routinely tests air vehicles with the MAC III aircraft in controlled airspace in the Austin area.

The Aquila air vehicle is mounted on a trapeze below the MAC III aircraft. Umbilicals connect the air vehicle to a computer inside the MAC III. The onboard computer acts as a "ground" control station and launcher system until links are acquired with the ground control station after takeoff. The air vehicle is commanded through the same launch sequence that is used in a real flight. When the air vehicle is "launched," the onboard computer tricks the FCEP into "thinking" that it is in flight, and the air vehicle begins navigating toward WP 0. A fictitious waypoint is sent to the air vehicle to bring the engine speed down until the ground control station can obtain links with the air vehicle. When the MAC III is safely airborne, the trapeze is lowered to approximately 2.5 meters below the MAC aircraft so that the airspeed sensor will be unobstructed by flow around the MAC and the datalink antennas will not be shaded by the MAC wings. Once the ground control station acquires links with the air vehicle, any maneuver that can be done with the air vehicle can be performed with the MAC III.

Air vehicle guidance commands are relayed to the pilot of the MAC via the onboard computer system. The computer accepts the digital roll command error and altitude error data directly from the FCEP and converts them to analog signals. These signals are used to drive two needle gauges on the pilot's display indicator (PDI) panel. When links are established

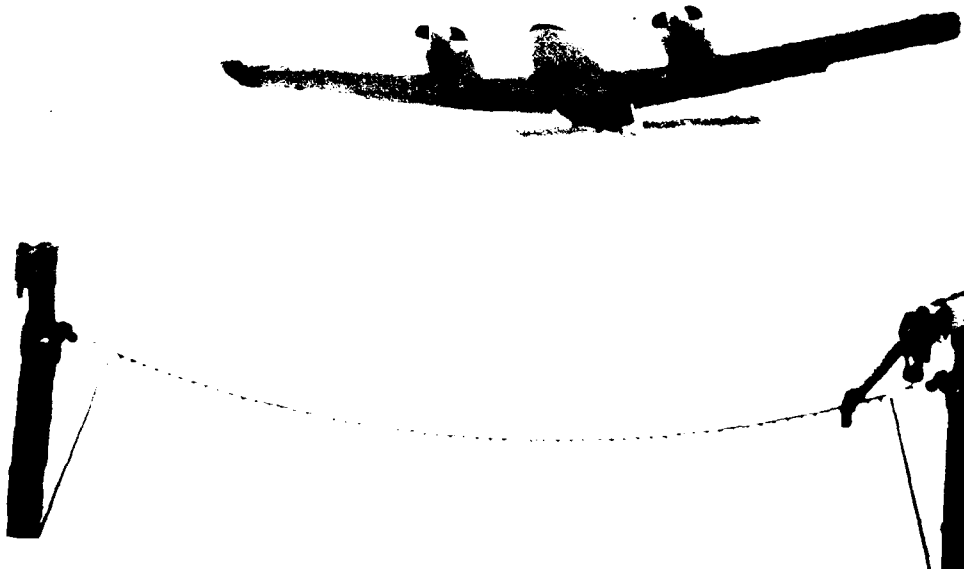


Figure 2: MAC II

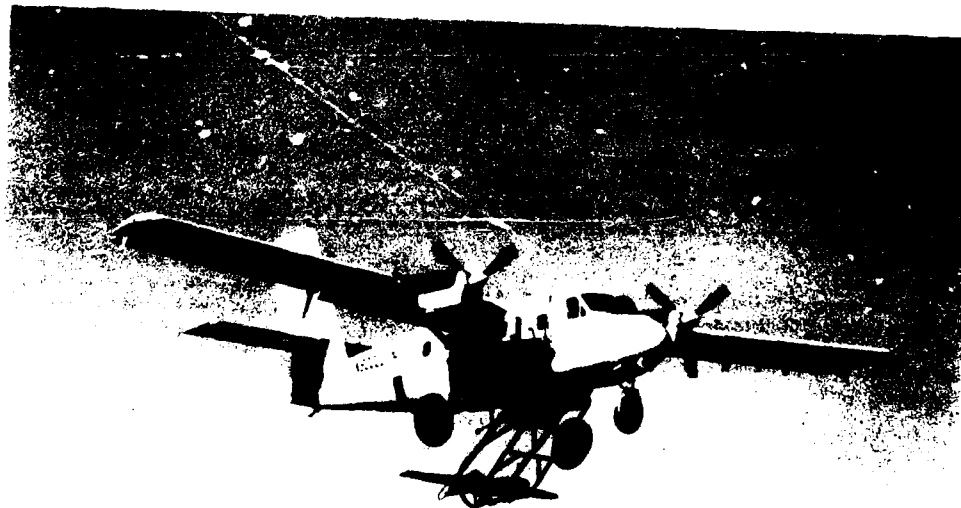


Figure 3: MAC III

with the air vehicle, the pilot is informed via radio that he is cleared to follow PDI steering commands. The task of the pilot is to change his roll angle and altitude in order to maintain the PDI needles in the null position. This method has proven to be the easiest and best way to present the air vehicle guidance commands to the MAC pilot.

As mentioned previously, the MAC III was invaluable in testing system integration and navigation performance of the Aquila system. Features of the Aquila system such as dead reckoning (navigation without the benefit of ground updates), lost-link guidance, recovery guidance, handoff, maximum datalink range, and emergency waypoint execution could not have been tested and perfected without the use of a system such as the MAC aircraft. The MAC III alone paid for itself in the first three months of operation when several flaws were detected in air vehicles during a MAC flight that would have resulted in loss of an air vehicle if they occurred during a free flight. With the MAC III aircraft new methods and system software can be tried without fear of losing an air vehicle.

### Data Acquisition System

Testing of any complicated system requires the ability to collect data to verify system performance. The Aquila remotely piloted vehicle system requires collection of a wide variety of data, ranging from aerodynamic performance data to the hydraulic pressure on the launcher system. The Lockheed Data Acquisition System (DAS) will be discussed briefly below, and then emphasis will be placed on data collected to verify system navigation and guidance performance.

The Aquila data acquisition system was designed to collect and store all data transmitted between all subsystems. In addition to the system data, environmental data were collected in order to verify the operating environment of the system. These data were collected in the field with the Data Acquisition System van (DAS van). Figure 1 shows the interfaces between the Aquila system and the DAS van and presents a list of the various data sources. Each source of data was assigned a link number to distinguish it for data collection and processing purposes. The table at the bottom of Figure 1 shows the various link numbers and the source of the data.

Ground system data is tapped directly out of the ground control station and transmitted directly via hard line to the DAS van. Air vehicle data is sent by telemetry to the ground via a C-Band telemetry link completely separated from the MICNS datalink system. Data transmitted to the ground included data tapped directly from the FCEP and other temperature, pressure, voltage, and vibration data taken from various locations throughout the air vehicle. Vibration data is transmitted in an FM-FM format. All other air vehicle data is transmitted in a pulse code modulation (PCM) format. These data are recorded simultaneously, with the ground system data and time code onto magnetic tape. Selected data items were used for real time monitoring during air vehicle and MAC flights.

To validate Aquila system navigation performance, it was necessary to collect data from independent sources for target locations, target illumination and reflectance, and air vehicle location. Target location was determined directly by conventional surveying techniques. Target reflectance and illumination was measured directly and recorded manually on each day of testing. Each air vehicle was equipped with a transponder for radar tracking. All air vehicle flights were tracked using an FPS-16 radar system. These data were recorded onto magnetic tape and sent to the Lockheed Data Analysis Facility (DAF) in Austin, Texas for analysis.

A partial list of data that was collected from the various data sources is shown below. Although not a complete list, the most important data items used for evaluating navigation and guidance performance are shown in Table 1.

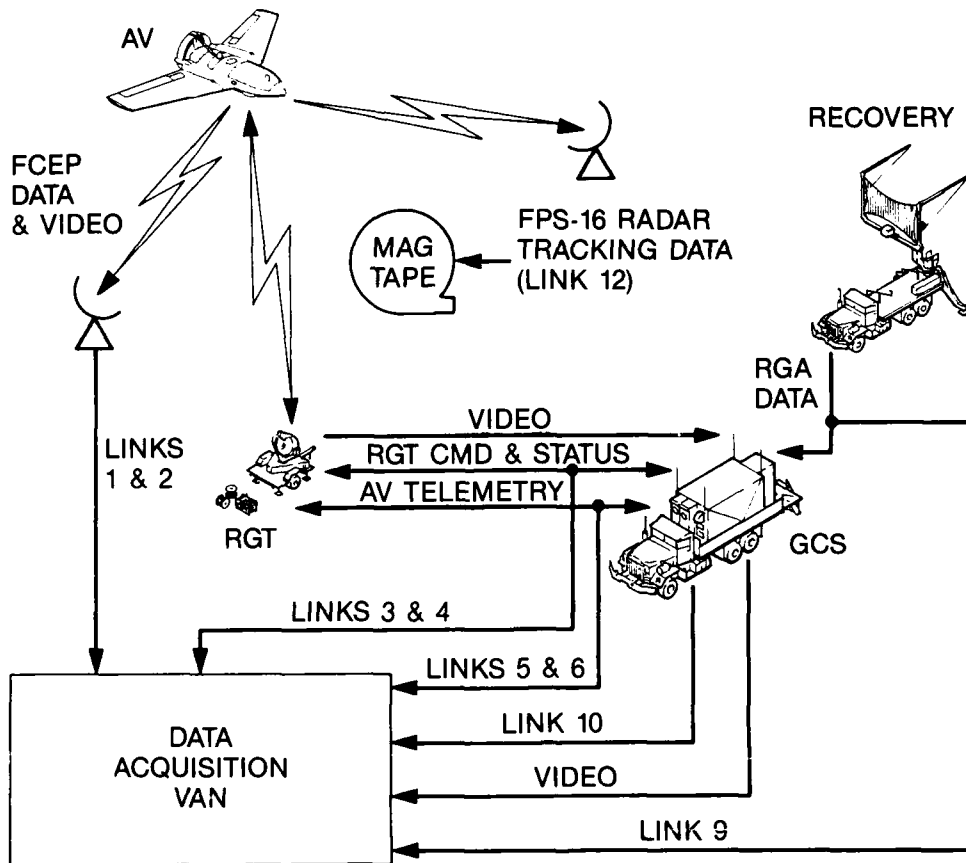
### Data Reduction and Analysis

This section will describe the data reduction capabilities of the Lockheed DAS van and Data Analysis Facility and discuss the specific ways in which these data were used to evaluate system performance.

To evaluate the masses of data collected during the testing of the Lockheed Aquila System, a dedicated data reduction facility was developed. The Data Analysis Facility contains the equipment necessary to reduce all forms of data collected during the testing of the Aquila. Figure 5 is a block diagram representation of the Data Analysis Facility. The DAS van discussed in the previous section and the Data Analysis Facility are functionally equal. The Data Analysis Facility, however, contains a larger, faster computer for quicker processing of data and provides software development and data archiving for both itself and the DAS van.

Data products of the Data Analysis Facility include printed tabular listings of data, plotted data, ASCII encoded data on magnetic tape, and specialized data processing. The Data Analysis Facility uses Data General MV15000 and Eclipse C350 computers to process data. Specially written device drivers provide the interfaces for acquiring data from all data sources in the Aquila Data Analysis System. Over 1000 mega-bytes of disk storage provide access to most data for flights on disk. Other flights not currently on disk can be loaded as they are required for processing.

To evaluate navigation and guidance performance of the Aquila system, a specialized program was written to compare various sources of data. The navigation error program provides error in velocities and position of the air vehicle by using other independent data as a reference. The independent data used to produce navigation error data for the Aquila system were the remote ground terminal range and azimuth data and the FPS-16 radar data. The remote ground terminal pointing data is actually not independent of the air vehicle navigation data because the air vehicle uses remote ground terminal pointing data to update navigation filters while in flight. The comparison of remote ground terminal pointing and air



### DAS DATA LINK DEFINITIONS:

- LINK 1 - AV ENVIRONMENTAL DATA
- LINK 2 - FCEP DATA
- LINK 3 - RGT COMMAND DATA
- LINK 4 - RGT STATUS DATA
- LINK 5 - AV COMMAND TELEMETRY DATA
- LINK 6 - AV STATUS DATA (DOWNLINK)
- LINK 9 - RGA CAMERA DATA
- LINK 10 - GCS COMPUTER DATA
- LINK 12 - FPS-16 RADAR TRACKING DATA

Figure 1. Data Acquisition System

RGT Status	RGT azimuth and elevation angles
RGT Command Data	RGT range to AV
AV Command Data	Commanded RGT azimuth and elevation angles
	Initialization data
	RGT azimuth
	RGT range to AV
	RGT location
	Second RGT location (for handoff)
AV Status Data (downlink data)	AV delta latitude
	AV delta longitude
	Target delta latitude
	Target delta longitude
	Lost Link Timer
FCEP Telemetry Data	Navigation Update Requested discrete
	AV delta latitude
	AV delta longitude
	States Updates discrete
	Navigation Update Rejected discrete
	True Airspeed Update Used discrete
	Lost Link discrete
	Observation Residuals
	ADT antenna pointing angles
	Easting and Northing Velocities
	True Airspeed
	Ground Speed
	Heading Angle
	Altitude
	Payload Pointing angles

Table 1: Data Items

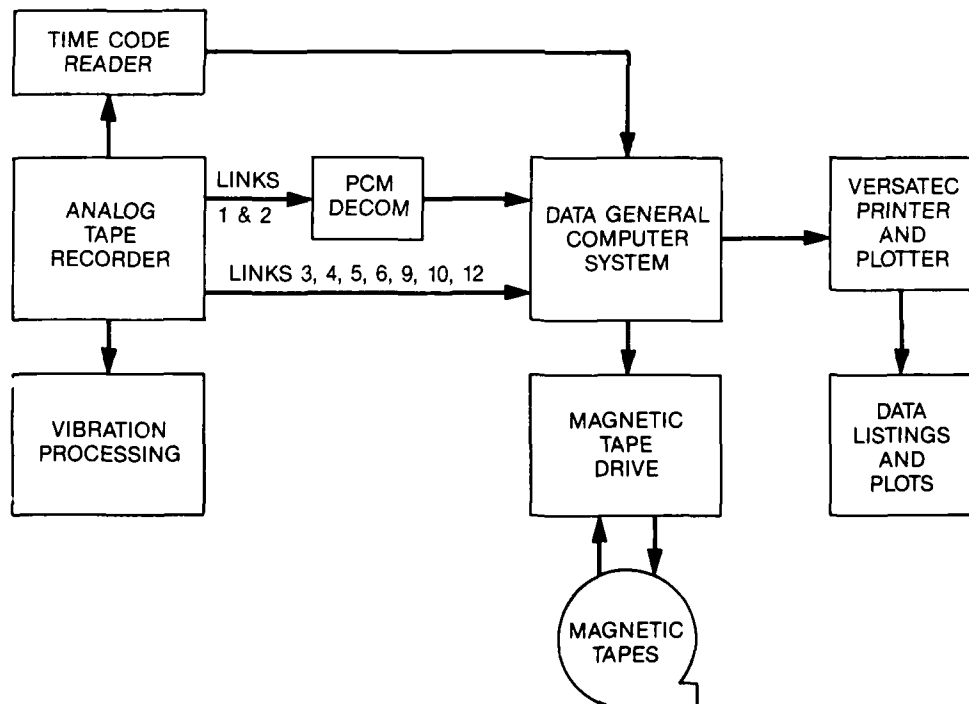


Figure 5: Data Analysis Facility

vehicle location and velocity data does provide insight into how well the system is integrated and whether the navigation updates used by the air vehicle are being used properly. Comparison of FPS-16 data with air vehicle position and velocity data provides an absolute measure of how accurately the air vehicle is navigating.

Figure 6 shows a navigation error plot using the remote ground terminal for reference data. Navigation updates which occur every 20 seconds can be seen in the data as large changes in the position errors. Long-term oscillations about zero error are a function of many factors and cannot be traced to any one cause. The steady drift in navigation updates near the end of the plot is due to the continuous use of true airspeed updates during a handoff operation when neither ground control station has control of the air vehicle.

### Mission Planning and Flight Testing

The flight testing of the Aquila system navigation and guidance functions includes the following areas:

1. Waypoint guidance
2. Loiter guidance
3. Manual mode guidance
4. Dead reckoning navigation
5. Recovery guidance
6. Target location
7. Survey update
8. Handoff
9. Lost-link navigation.

Each of these topics will be discussed with respect to special mission planning and range requirements needed to test these areas during an air vehicle flight.

#### Waypoint and Loiter Guidance

The Aquila air vehicle essentially flies itself without constant external input from the operator. The system is capable of flying an entire mission under waypoint guidance. Waypoint guidance is a point-to-point type of guidance using UTM coordinates, altitude, and airspeed to specify the desired flight path. Each point in space is called a waypoint. Any waypoint can include loiter maneuvers such as circles, racetracks, or figure eights with radii varying from 0.25 to 3.12 kilometers. Figure 7 illustrates the requirements placed on each type of loiter maneuver. Loiter maneuvers require two waypoints for definition. The first waypoint defines the location to start the maneuver and the second defines the loiter orientation and radius. In the case of the figure eight, the orientation waypoint indicates the direction that the air vehicle will turn at each end of the figure eight. The racetrack orientation waypoint defines the opposite end of the racetrack. The circle requires no orientation and hence the orientation waypoint for the circle defines only the radius.

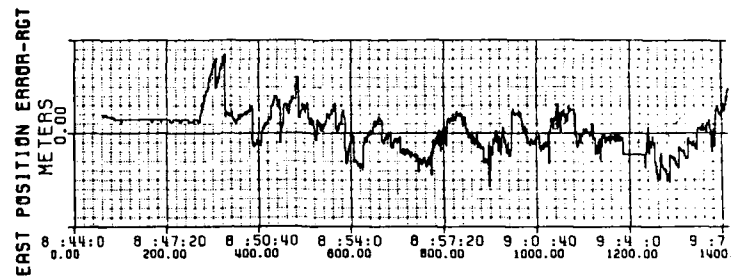
The testing of waypoint guidance was the easiest execute. Every flight that was performed contained waypoint guidance, and hence there was little need to plan specific tests for this type of guidance. Guidance in waypoint mode was routinely verified using navigation error plots from the Data Analysis Facility. The "Go There" function of the Aquila system allows the operator to send the air vehicle in the direction that the payload is pointing. This function of waypoint guidance mode can be verified easily by comparing the payload true azimuth at the time that the "Go There" is executed with the air vehicle course after stabilization.

It was necessary to verify that loiter maneuvers would navigate properly at all radii from the minimum to the maximum. The smaller radius maneuvers were tested routinely during most air vehicle flights. The large radius (3.12 kilometer) was not tested until later in the test program using the MAC III. These tests resulted in egg shaped circles and odd shaped figure eights. Tests with the air vehicle produced similar results. An investigation revealed that there was a component of lateral acceleration that was not being corrected when shallow bank maneuvers were performed. After correcting this problem, loiter maneuvers of all radii were performed without error. In addition to the problem discovered with the lateral acceleration component, it was discovered that the MAC III was unable to perform perfect loiter maneuvers in excess of 2 kilometers due to a scaling problem in the PDI display.

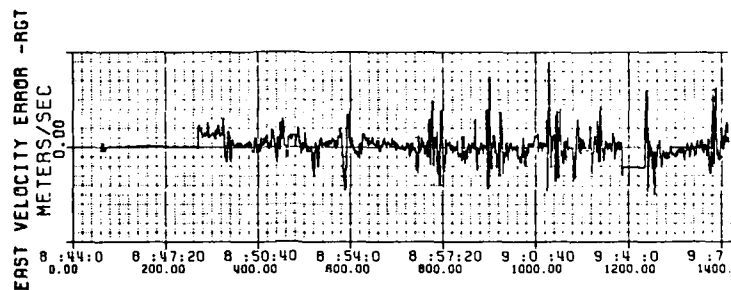
#### Manual Mode Guidance

In addition to waypoint guidance mode it is also possible to control the air vehicle directly in manual guidance mode. Manual guidance mode is a bit of a misnomer in that one does not actually control the air vehicle manually as one would an airplane. Manual guidance mode is much like changing heading, airspeed, and altitude on an aircraft that is on automatic pilot. Commands, which are issued from the air vehicle operator's console, specify a given altitude, airspeed and heading.

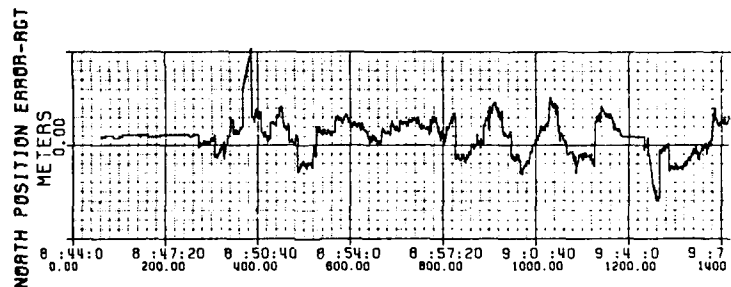
A410 - F017

SOURCE 11  
PARAMETER 8 6 4START 067:08:44:0 .000  
STOP 067:09:49:0 .000NAV TIME/HR:MIN:SEC  
SECONDS FROM START

A410 - F017

SOURCE 11  
PARAMETER 8 6 2START 067:08:44:0 .000  
STOP 067:09:49:0 .000NAV TIME/HR:MIN:SEC  
SECONDS FROM START

A410 - F017

SOURCE 11  
PARAMETER 8 6 3START 067:08:44:0 .000  
STOP 067:09:49:0 .000NAV TIME/HR:MIN:SEC  
SECONDS FROM START

A410 - F017

SOURCE 11  
PARAMETER 8 6 1START 067:08:44:0 .000  
STOP 067:09:49:0 .000

▲ LAST LINE \* CHECKOUT ERROR  
NAV TIME/HR:MIN:SEC  
SECONDS FROM START

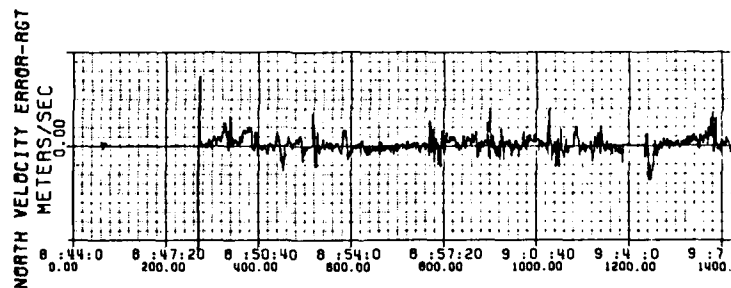


Figure 6: Navigation Error Plot

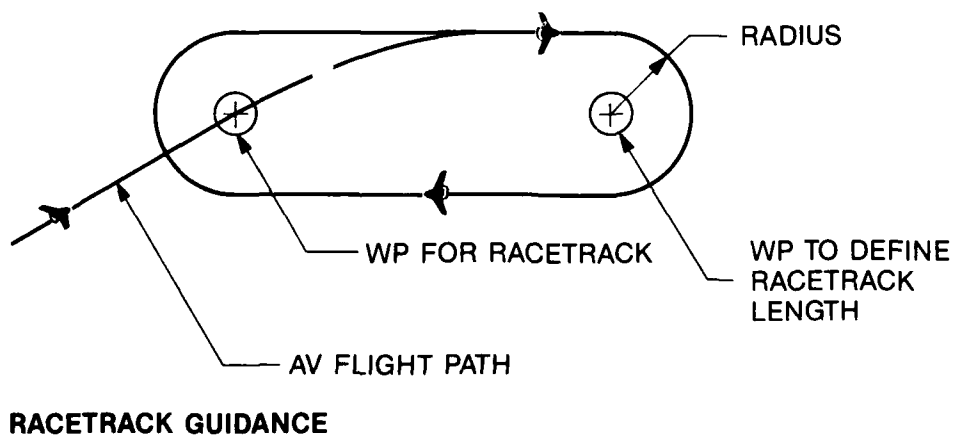
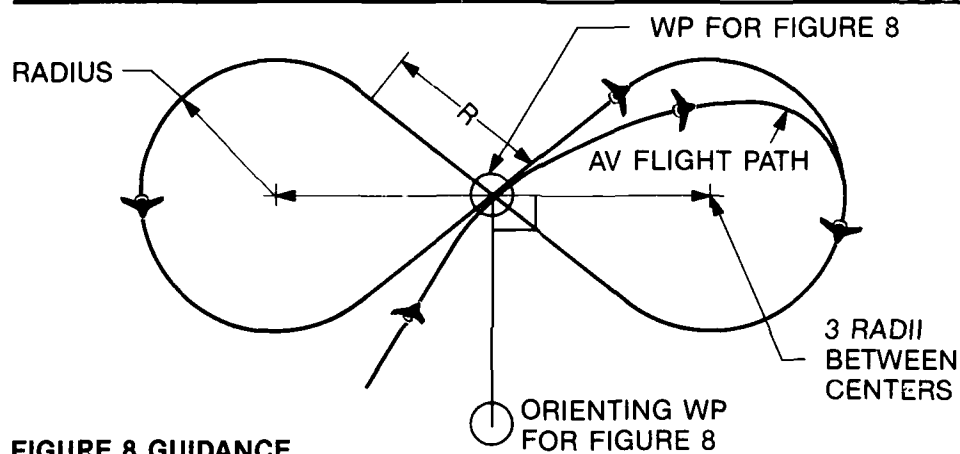
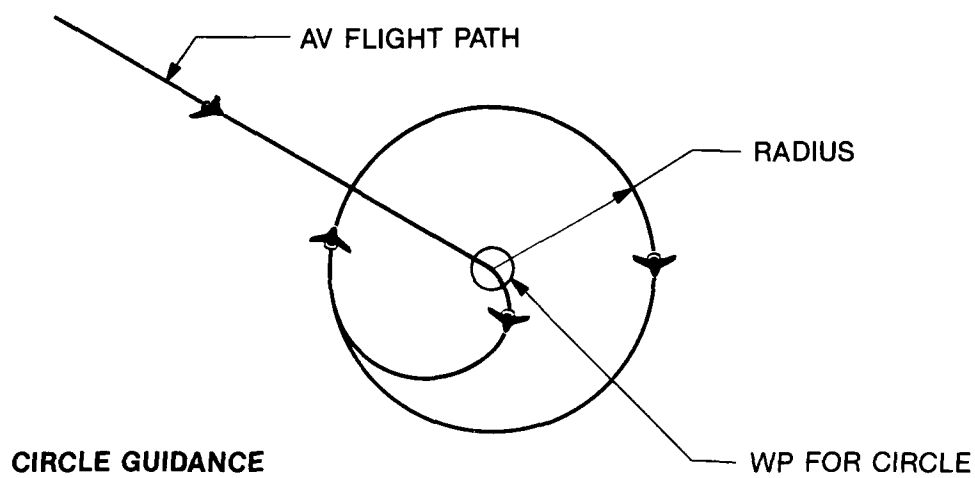


Figure 7: Loiter Guidance

A separate function in manual mode is the ability to command a fixed turn rate varying from 50 mil/second ( $\approx 3^\circ/\text{second}$ ) up to 200 mil/second ( $\approx 12^\circ/\text{second}$ ).

To verify heading, altitude, and airspeed data during manual mode maneuvers, air vehicle data was compared with radar data. In all cases manual mode worked as designed. Turn rate commands were entered for a specified amount of time, and the rate of turn from radar data was compared with air vehicle data over the same time period. All turn rate commands functioned properly.

#### **Dead Reckoning Guidance**

The Aquila system can also be commanded to fly without navigation updates from the ground during portions of the mission either because of remote ground terminal line-of-sight interruptions or to keep the ground control station radio frequency emissions to a minimum during portions of the mission. A special waypoint guidance instruction in the mission plan is used to designate dead reckoning navigation. During periods of dead reckoning, the time that the air vehicle will continue to navigate before flying to the lost-link waypoint is extended to 2500 seconds. At the end of a dead reckoning segment in the mission plan, a reacquisition circle of 0.25 kilometers is performed while the ground control station reacquires the air vehicle. This type of testing contains an element of risk because if the inertial navigation system drifts too far off, the airborne data terminal antennas will not be pointed in the right direction to reacquire links with the remote ground terminal on the ground. Many MAC flights were performed prior to actually trying this test with an air vehicle free flight.

To test the system without the aid of ground navigation updates, it was necessary to disable the uplink to the air vehicle to prevent data being sent to the air vehicle. The downlink was maintained in order to monitor air vehicle status. Real-time radar plots were used to verify that the air vehicle was not drifting out of a predefined corridor around the planned flight path. During this time the air vehicle continued to fly the box pattern that had been put in the mission plan. A maximum of 20 minutes of dead reckoning navigation was required to meet system performance. At the end of the 20 minutes, the air vehicle had drifted approximately 1.8 kilometers from its actual position. At the end of the dead reckoning segment uplink was reacquired and the flight continued.

#### **Recovery Guidance**

Final approach guidance into the recovery net is accomplished with the recovery guidance aid. This system uses infrared detectors to track the near infra-Red (NIR) beacon that is located on the nose of the air vehicle. The Aquila system creates a set of recovery pattern waypoints based on the recovery system location and orientation. These waypoints set the air vehicle up for final approach into the net and for abort go-around waypoints in the event of an aborted recovery. Prior to completing the second recovery waypoint (WP 80) the air vehicle operator in the ground control station presses the "Start Recovery" button. At this point the NIR beacon is illuminated, and the recovery guidance aid begins tracking the air vehicle. On completion of WP 80, the ground control station automatically begins transmitting data received from the recovery guidance aid cameras to the air vehicle. When the air vehicle crosses the  $5^\circ$  glide slope of the recovery guidance aid camera line of sight, it enters the glide slope and begins using the data sent up from the ground control station for guidance. The engine speed is varied to control ground speed to 36 meters/second. At 100 meters out from the net, the air vehicle stops using guidance aid data and inertially maintains its current glide slope into the net.

Testing of the recovery guidance aid system required many hours of MAC flight testing doing approach after approach to the net. Aligning the recovery system and determining the true heading of the recovery net were at first thought to be extremely critical; but after many tests, it was found that the recovery system orientation could be off by as much as  $8^\circ$ – $10^\circ$  without endangering a safe recovery. As a result of MAC testing it was determined that an additional waypoint should be added to the recovery system pattern in order to provide better alignment with the recovery system.

The abort criteria built into the air vehicle were designed to cause the air vehicle to abort recovery if it was outside predetermined limits in offset from the glide slope. To determine what these bounds should be, special tests were performed to determine how far off laterally the air vehicle could be and still enter the glide slope and be recovered safely. These tests were designed to intentionally misalign the approach of the MAC with the recovery system. Tests with the MAC simulated late and early entry onto the glide slope, lateral misalignments, various sun angles, and drifting off of the glide slope after starting recovery. These tests resulted in many design modifications in order to achieve a smooth transition onto the glide slope and realistic abort criteria. After many air vehicle flights, the recovery guidance aid system has proven itself to be virtually 100 percent reliable in accomplishing a safe recovery of the air vehicle.

#### **Target Detection, Recognition, and Identification**

The mission of the Aquila air vehicle is to locate targets in a tactical battlefield. Target location can be determined using either passive target location or active laser range-finding. Passive target location is accomplished by successive triangulations on a fixed point. Using the air vehicle position, mission payload system depression, and mission payload system azimuth angle, it is possible to converge onto a solution for the target location if the payload is held on a fixed location. Active laser range-finding requires only a single observation in order to determine target location.

To test target detection, recognition, and identification with the Aquila system, it was first necessary to have targets with a fifth order survey. Targets included vehicles, buildings, and specially built target boards. To plan missions for detection, recognition, and identification, it was necessary to consider range restrictions for laser operations, loiter maneuver location

for a given sun angle and time of day, and special loiter patterns for using the specially designed detection, recognition, and identification target boards. The detection, recognition, and identification targets were designed so that a set of either vertical or horizontal bars could be presented to the air vehicle on each approach. The task of the operator was to determine the point in time at which he could determine whether the bars were horizontal or vertical. This time was then used to calculate the range-to-target at which the target was discerned. Three target boards were used. One for detection, one for recognition, and one for identification.

#### Survey Update

The survey update function of the Aquila system provides a method for improving the accuracy of site setup data using known targets on the ground to calculate the location of the air vehicle and hence the remote ground terminal location. This situation might exist in a tactical scenario where the remotely piloted vehicle battery has emplaced the system with limited survey data on that location. The crew would launch the air vehicle, and then after the air vehicle was in flight, do a survey update to determine more accurately the remote ground terminal location. A survey update will give data accurate to the same degree as the known target locations. It is desirable to have three targets for the survey update, but the update can be performed with two targets. Additional targets used for the survey update will be averaged with the previous data obtained with the survey update function.

Testing of the survey update function was performed many times with the MAC prior to performing an actual free flight. The method for testing the survey update function was to intentionally change the alignment of the remote ground terminal before launch. During the flight, several survey updates would be performed and the resulting remote ground terminal position compared with the actual surveyed position. It was necessary for the first target to be a minimum of 10 kilometers away from the remote ground terminal and the second target a minimum of 20 kilometers away from the first target. The third and successive targets could be at any location with an accurate known location. Survey update testing validated the capability to launch an air vehicle with an inaccurate starting location, correct the survey location after performing a survey update, perform a mission, and return for a safe recovery.

#### Handoff

The capability to transfer control of an air vehicle while in flight was necessary to implement the central launch and recovery site mode of operation for the Army. This operational concept provided for several forward control stations consisting of a ground control station and a remote ground terminal and only one central site for launching and recovering air vehicles. In this operational mode an air vehicle with a defined mission would be launched and handed off to a forward control station in the area where the mission was to be performed. After handing the air vehicle off to a forward control station, the central launch and recovery site could either launch another air vehicle and hand off to a different forward control station or receive an air vehicle coming back from a different mission from another forward control station, or conduct a mission directly from the central launch and recovery site.

The process of performing a handoff requires that the air vehicle be told where the second remote ground terminal is located so the airborne data terminal antennas can be pointed properly for link acquisition. When the handoff is actually executed, the air vehicle is put into a holding circle and commanded to point the airborne data terminal antennas at the second remote ground terminal. Then the central launch and recovery site disables the remote ground terminal transmitter so that the central launch and recovery site uplink signal will not interfere with the forward control station acquisition process. At this point the forward ground control station executes a handoff receive and begins attempting to acquire the air vehicle at the acquisition circle location. After links are acquired, data blocks are sent to the air vehicle to reinitialize navigation filters; the air vehicle is then under complete control of the forward control station. If links are not acquired by the forward control station within 5 minutes after the last uplink message from the central launch and recovery site, the FCEP in the air vehicle will point the airborne data terminal antennas back toward the central launch and recovery site remote ground terminal and attempt to reacquire links with the central launch and recovery site.

Testing of the handoff capability was done in three phases. The first handoffs were performed with both the central launch and recovery site and the forward control station co located. The second phase was performed with the two remote ground terminals located approximately 2.5 kilometers apart. The third phase was long range handoffs with the forward control station approximately 50 kilometers from the central launch and recovery site. In all cases, handoffs were performed with the MAC many times prior to performing an actual air vehicle flight. The U. S. Army now uses the central launch and recovery site operational concept routinely in its operations with the Aquila system.

#### Lost-Link Guidance

If the Aquila air vehicle does not receive a message from the ground control station within a preprogrammed time period, the FCEP will enter lost link guidance mode. The time that the air vehicle will fly without uplink before entering lost link mode is referred to as the lost link timer. The FCEP keeps the lost-link timer internally and will decrement this number until a valid uplink message is received. When a valid message is received, the FCEP resets the lost link timer to the maximum value allowed. The maximum lost-link timer value is set by the ground control station. This maximum value can range from 50 to 150 seconds during normal flight and is set to 2500 seconds during dead reckoning.

When lost link mode is entered, the air vehicle navigates to the first lost link waypoint designated WP 91. WP 91 can be any valid waypoint instruction, but is normally a 0.25 km circle at a pre-determined location. The ground control

station, which maintains a duplicate of the air vehicle lost-link timer and mission instructions, commands the remote ground terminal antenna to point at the predicted location of the air vehicle when the lost-link timer reaches zero. The air vehicle location is estimated based on the last known flight mode and next waypoint. If links are not reacquired after completion of WP 91, the air vehicle begins navigating to WP 92, 93, 94 and so on until completion of WP 99. The ground computer, in turn, steers the remote ground terminal antenna toward each waypoint and attempts to reacquire links. If links are not reacquired by the time the air vehicle completes WP 99, either the parachute is deployed or the air vehicle dives into the ground. The dive instruction is executed if the territory at the end of the lost-link file has been set to unfriendly, otherwise the parachute is deployed if the parachute is present. If no parachute is present and the territory is friendly, then the air vehicle will attempt a gentle glide to the ground.

All intentional testing of lost-link guidance was performed with the MAC. Lost-link guidance was never tested intentionally with the air vehicle in free flight. There were, of course, several times when lost-link mode was unintentionally tested with the air vehicle in free flight. All combinations of lost link were tested using the MAC, including WP 99 completion in both friendly and unfriendly territory.

REPORT DOCUMENTATION PAGE											
1. Recipient's Reference	2. Originator's Reference	3. Further Reference	4. Security Classification of Document								
	AGARD-CP-436	ISBN 92-835-0523-9	UNCLASSIFIED								
5. Originator	Advisory Group for Aerospace Research and Development North Atlantic Treaty Organization 7 rue Ancelle, 92200 Neuilly sur Seine, France										
6. Title	GUIDANCE AND CONTROL OF UNMANNED AIR VEHICLES										
7. Presented at	the Guidance and Control Panel 47th Symposium held at the Letterman Army Institute of Research, Presidio of San Francisco, California, USA from 4 to 7 October 1988.										
8. Author(s)/Editor(s)	Various		9. Date August 1989								
10. Author's/Editor's Address	Various		11. Pages 194								
12. Distribution Statement	This document is distributed in accordance with AGARD policies and regulations, which are outlined on the Outside Back Covers of all AGARD publications.										
13. Keywords/Descriptors	<table border="0"> <tr> <td>Dilemma cost efficiency</td> <td>RPVs</td> </tr> <tr> <td>Drones</td> <td>Target acquisition and identification</td> </tr> <tr> <td>Inertial guidance</td> <td>Target reconnaissance</td> </tr> <tr> <td>Infrared guidance</td> <td>Unmanned vehicles</td> </tr> </table>			Dilemma cost efficiency	RPVs	Drones	Target acquisition and identification	Inertial guidance	Target reconnaissance	Infrared guidance	Unmanned vehicles
Dilemma cost efficiency	RPVs										
Drones	Target acquisition and identification										
Inertial guidance	Target reconnaissance										
Infrared guidance	Unmanned vehicles										
14. Abstract	<p>This volume contains the Keynote Address and 15 unclassified papers out of the 25 presented at the Guidance and Control Symposium, held in San Francisco from 4 to 7 October 1988. The remainder of the papers (except paper Nos 12, 41, 42 and 53, not available at time of printing) are included in the classified supplement CP436.</p> <p>The papers were presented under the following topics: Operational concepts, Requirements and systems, Vehicle guidance and control, Optical systems, Systems external to the vehicle, Evaluation and test.</p>										

<p>AGARD Conference Proceedings No.436 Advisory Group for Aerospace Research and Development, NATO GUIDANCE AND CONTROL OF UNMANNED AIR VEHICLES Published August 1989 194 pages</p> <p>This volume contains the Keynote Address and 15 unclassified papers out of the 25 presented at the Guidance and Control Symposium, held in San Francisco from 4 to 7 October 1988. The remainder of the papers (except paper Nos 12, 41, 42 and 53, not available at time of printing) are included in the classified supplement CP436.</p> <p>P.T.O.</p>	<p>AGARD-CP-436</p> <p>Dilemma cost efficiency Drones Inertial guidance Infrared guidance RPVs Target acquisition and identification Target reconnaissance Unmanned vehicles</p>	<p>AGARD Conference Proceedings No.436 Advisory Group for Aerospace Research and Development, NATO GUIDANCE AND CONTROL OF UNMANNED AIR VEHICLES Published August 1989 194 pages</p> <p>This volume contains the Keynote Address and 15 unclassified papers out of the 25 presented at the Guidance and Control Symposium, held in San Francisco from 4 to 7 October 1988. The remainder of the papers (except paper Nos 12, 41, 42 and 53, not available at time of printing) are included in the classified supplement CP436.</p> <p>P.T.O.</p>	<p>AGARD-CP-436</p> <p>Dilemma cost efficiency Drones Inertial guidance Infrared guidance RPVs Target acquisition and identification Target reconnaissance Unmanned vehicles</p>
<p>AGARD Conference Proceedings No.436 Advisory Group for Aerospace Research and Development, NATO GUIDANCE AND CONTROL OF UNMANNED AIR VEHICLES Published August 1989 194 pages</p> <p>This volume contains the Keynote Address and 15 unclassified papers out of the 25 presented at the Guidance and Control Symposium, held in San Francisco from 4 to 7 October 1988. The remainder of the papers (except paper Nos 12, 41, 42 and 53, not available at time of printing) are included in the classified supplement CP436.</p> <p>P.T.O.</p>	<p>AGARD-CP-436</p> <p>Dilemma cost efficiency Drones Inertial guidance Infrared guidance RPVs Target acquisition and identification Target reconnaissance Unmanned vehicles</p>	<p>AGARD Conference Proceedings No.436 Advisory Group for Aerospace Research and Development, NATO GUIDANCE AND CONTROL OF UNMANNED AIR VEHICLES Published August 1989 194 pages</p> <p>This volume contains the Keynote Address and 15 unclassified papers out of the 25 presented at the Guidance and Control Symposium, held in San Francisco from 4 to 7 October 1988. The remainder of the papers (except paper Nos 12, 41, 42 and 53, not available at time of printing) are included in the classified supplement CP436.</p> <p>P.T.O.</p>	<p>AGARD-CP-436</p> <p>Dilemma cost efficiency Drones Inertial guidance Infrared guidance RPVs Target acquisition and identification Target reconnaissance Unmanned vehicles</p>

<p>The papers were presented under the following topics: Operational concepts, Requirements and systems, Vehicle guidance and control , Optical systems, Systems external to the vehicle, Evaluation and test.</p> <p>Papers presented at the Guidance and Control Panel 47th Symposium held at the Letterman Army Institute of Research, Presidio of San Francisco, California, USA from 4 to 7 October 1988.</p> <p>ISBN 92835-0523-9</p>	<p>The papers were presented under the following topics: Operational concepts, Requirements and systems, Vehicle guidance and control , Optical systems, Systems external to the vehicle, Evaluation and test.</p> <p>Papers presented at the Guidance and Control Panel 47th Symposium held at the Letterman Army Institute of Research, Presidio of San Francisco, California, USA from 4 to 7 October 1988.</p> <p>ISBN 92835-0523-9</p>
<p>The papers were presented under the following topics: Operational concepts, Requirements and systems, Vehicle guidance and control , Optical systems, Systems external to the vehicle, Evaluation and test.</p> <p>Papers presented at the Guidance and Control Panel 47th Symposium held at the Letterman Army Institute of Research, Presidio of San Francisco, California, USA from 4 to 7 October 1988.</p> <p>ISBN 92835-0523-9</p>	<p>The papers were presented under the following topics: Operational concepts, Requirements and systems, Vehicle guidance and control , Optical systems, Systems external to the vehicle, Evaluation and test.</p> <p>Papers presented at the Guidance and Control Panel 47th Symposium held at the Letterman Army Institute of Research, Presidio of San Francisco, California, USA from 4 to 7 October 1988.</p> <p>ISBN 92835-0523-9</p>

AGARD

NATO OTAN

7 rue Ancelle • 92200 NEUILLY-SUR-SEINE  
FRANCE

Telephone (1)47.38.57.00 • Telex 610 176

**DISTRIBUTION OF UNCLASSIFIED  
AGARD PUBLICATIONS**

AGARD does NOT hold stocks of AGARD publications at the above address for general distribution. Initial distribution of AGARD publications is made to AGARD Member Nations through the following National Distribution Centres. Further copies are sometimes available from these Centres, but if not may be purchased in Microfiche or Photocopy form from the Purchase Agencies listed below.

**NATIONAL DISTRIBUTION CENTRES**

**BELGIUM**

Coordonnateur AGARD – VSL  
Etat-Major de la Force Aérienne  
Quartier Reine Elisabeth  
Rue d'Evere, 1140 Bruxelles

**LUXEMBOURG**

See Belgium

**NETHERLANDS**

Netherlands Delegation to AGARD  
National Aerospace Laboratory, NLR  
P.O. Box 126  
3400 AC Delft

**CANADA**

Director of Science and Technology  
Dept of  
Ottawa



National Aeronautics and  
Space Administration

Washington, D.C. SPECIAL FOURTH CLASS MAIL  
20546 BOOK

Postage and Fees Paid  
National Aeronautics and  
Space Administration  
NASA-451



Official Business  
Penalty for Private Use \$300

**DENMARK**

Danish  
Ved Idt  
2100 C

**FRANCE**

O.N.E.I.  
29 Ave  
92320

**GERMANY**

Fachinf  
Physik.  
Karlsruhe  
D-7514

**GREECE**

Hellenic  
Aircraft  
Depart  
Holargos

**ICELAND**

Director of Aviation  
c/o Flugrad  
Reykjavik

**ITALY**

Aeronautica Militare  
Ufficio del Delegato Nazionale all'AGARD  
3 Piazzale Adenauer  
00144 Roma/EUR

**UNITED KINGDOM**

Defence Research Information Centre  
Kentigern House  
65 Brown Street  
Glasgow G2 8EX

**UNITED STATES**

National Aeronautics and Space Administration (NASA)  
Langley Research Center  
M/S 180  
Hampton, Virginia 23665

THE UNITED STATES NATIONAL DISTRIBUTION CENTRE (NASA) DOES NOT HOLD STOCKS OF AGARD PUBLICATIONS, AND APPLICATIONS FOR COPIES SHOULD BE MADE DIRECT TO THE NATIONAL TECHNICAL INFORMATION SERVICE (NTIS) AT THE ADDRESS BELOW.

**PURCHASE AGENCIES**

National Technical  
Information Service (NTIS)  
5285 Port Royal Road  
Springfield  
Virginia 22161, USA

ESA/Information Retrieval Service  
European Space Agency  
10, rue Mario Nikis  
75015 Paris, France

The British Library  
Document Supply Centre  
Boston Spa, Wetherby  
West Yorkshire LS23 7BQ  
England

Requests for microfiche or photocopies of AGARD documents should include the AGARD serial number, title, author or editor, and publication date. Requests to NTIS should include the NASA accession report number. Full bibliographical references and abstracts of AGARD publications are given in the following journals:

Scientific and Technical Aerospace Reports (STAR)  
published by NASA Scientific and Technical  
Information Branch  
NASA Headquarters (NIT-40)  
Washington D.C. 20546, USA

Government Reports Announcements (GRA)  
published by the National Technical  
Information Services, Springfield  
Virginia 22161, USA



Printed by Specialised Printing Services Limited  
40 Chigwell Lane, Loughton, Essex IG10 3TZ

ISBN 92-835-0523-9